Stress and Rab35 modulate Alzheimer's disease-related protein trafficking

Viktoriya Zhuravleva

Submitted in partial fulfillment of the
requirements for the degree of
Doctor of Philosophy
under the Executive Committee
of the Graduate School of Arts and Sciences

COLUMBIA UNIVERSITY

2021

© 2021

Viktoriya Zhuravleva

All Rights Reserved

Abstract

Stress and Rab35 modulate Alzheimer's disease-related protein trafficking

Viktoriya Zhuravleva

Chronic stress and elevated glucocorticoids (GCs), the major stress hormones, are risk factors for Alzheimer's disease (AD) and promote AD pathomechanisms in animal models. These include overproduction of synaptotoxic amyloid-β (Aβ) peptides and intraneuronal accumulation of microtubule-associated protein Tau. Tau accumulation is linked to downregulation of the small GTPase Rab35, which mediates Tau degradation via the endolysosomal pathway. Whether Rab35 is also involved in stress/GC-induced Aβ overproduction remains an open question. Here, I find that hippocampal Rab35 levels are decreased not only by stress/GCs, but also by aging, another AD risk factor. Moreover, I show that Rab35 negatively regulates Aβ production by sorting amyloid precursor protein (APP) and β-secretase (BACE1) out of the endosomal network, where they interact to produce Aβ. Interestingly, Rab35 coordinates distinct intracellular trafficking events for BACE1 and APP, mediated by its effectors OCRL and ACAP2, respectively. Additionally, I show that Rab35 overexpression prevents the amyloidogenic trafficking of APP and BACE1 induced by GCs. Finally, I begin to investigate how GCs and/or Rab35 affect the intercellular spread of Aβ and Tau through exosomes. I describe methods for purifying exosomes and measuring their secretion from neurons, astrocytes, and microglial cells in order to determine the effects of stress/GCs and Rab35 on this process. These studies identify Rab35 as a key regulator of Alzheimer's disease-related protein trafficking, and suggest that its downregulation contributes to stress- and AD-related pathomechanisms.

Table of Contents

List of Figures

Chapter 1

Chapter 3

Chapter 4

Chapter 5

Chapter 6

List of Tables

Chapter 2

Acknowledgments

I could never have completed my Ph.D. without the support and constant mentorship from Dr. Clarissa Waites. Thank you for always being available to help with anything, from troubleshooting experiments to writing grants and preparing me for the next step in my career.

I would like to thank Dr. João Vaz-Silva for beginning this project, being available for advice years after graduating, and always sending me files from experiments completed years ago so that I could pick representative images. I am also grateful for the collaboration with Dr. Ioannis Sotiropoulos and his lab, which contributed several experiments to this work, and aided in writing our manuscript.

I would also like to thank the Neurobiology and Behavior program co-directors for helping me navigate the Ph.D, and my thesis committee members, Drs. Franck Polleux, Ai Yamamoto, and Ulrich Hengst, for the insightful questions that guided my research, and for telling me that I'm ready to graduate when I wasn't even sure myself.

To past and present members of the Waites, Hengst, and Israely Labs, thank you for everything I've learned from you, for the help you have provided, and for making our lab space a pleasant work environment over the years.

Finally, a profound thank you to my friends and family for supporting me during my Ph.D. and not asking when I will be finishing my degree or what I'm planning to do with my life afterward. In particular, I would like to thank Lilian Coie, Remery A. Camacho, Eren Cameron, and Lisa Randolph for being my New York family throughout this journey, and especially during the past year, when we were unable to spend holidays with our families at home.

Financial support for the work presented in this thesis was provided by NIH grants R01NS080967 and R56AG057560 to Dr. Waites, and NIH/NINDS research supplement grant NS080967-2 to Viktoriya Zhuravleva. All animal treatments and preparations were conducted with grant support from Portuguese and European sources for Dr. Ioannis Sotiropoulos's lab (University of Minho, Portugal). Drs. Cristina Mota, João Cerqueira and Fernanda Marques (University of Minho) provided hippocampal tissue. Dr. Subhojit Roy (University of California, San Diego, USA) provided APP:VN and BACE1:VC plasmids, and Dr. Andrew Sproul (Stem Cell and Cellular Models Platform, Taub Institute for Research on Alzheimer's Disease, and the Aging Brain, Columbia University) provided iPSC-derived cortical neurons. The human aging RNAseq data were obtained from the Genotype-Tissue Expression (GTEx) Project, supported by the Common Fund of the Office of the Director of the National Institutes of Health, and by NCI, NHGRI, NHLBI, NIDA, NIMH, and NINDS. The data used in this manuscript were obtained from the GTEx Portal on 04/15/20 (dbGaP accession number phs000424.vN.pN). The human control vs. AD RNAseq data were obtained using a search of the NCBI GEO DataSets database (GEO accession number GSE159699; Nativio *et al.*, 2020). Images for APP/BACE1 trafficking studies were collected on the confocal microscope in the Taub Institute Shared Resource microscopy center (Taub Institute for Research on Alzheimer's Disease, and the Aging Brain, Columbia University), and TIRF images for exosome studies were collected in the Confocal and Specialized Microscopy Shared Resource Center of the Herbert Irving Comprehensive Cancer Center at Columbia University, supported by NIH grant #P30 CA013696 (National Cancer Institute). Schematics in figures 1-4, 7, 33, 34, 36-40, and 42 were made with BioRender.

Chapter 1: General Introduction

1.1. Stress and organismal homeostasis

1.1.1. Stress and glucocorticoid signaling

Stress is an adaptive response to events that disrupt organismal homeostasis. In response to a stressor, glucocorticoids (GCs), the major stress hormones, are released by the adrenal glands. This process is regulated by the hypothalamic-pituitary-adrenal axis (McEwen, 2007), in which corticotropin-releasing hormone is released from the paraventricular nucleus of the hypothalamus, leading to adrenocorticotropic hormone release from the pituitary, and resulting in the release of GCs from adrenal gland cortices (Lupien *et al.*, 2009). When GCs bind to receptors in the hypothalamus and pituitary, they inhibit the HPA axis, producing a negative feedback loop to prevent the continuous release of stress hormones (Lupien *et al.*, 2009).

In the brain, GCs are recognized by the glucocorticoid receptor (GR), which is expressed ubiquitously, and the mineralocorticoid receptor (MR), which is expressed in the hippocampus, prefrontal cortex, and amygdala, along with a few other select areas (Sotiropoulos *et al.*, 2019). GCs have a ten-fold higher affinity for the MR, activating it at low concentrations, whereas the GR becomes increasingly activated with increasing levels of GCs (Joels & Baram, 2009; Sotiropoulos *et al.*, 2019). MRs are therefore primarily responsible for initiation of the stress response and the immediate, non-genomic effects of GCs, as well as some gene-mediated processes. GRs, on the other hand, primarily contribute to slower, gene-mediated stress responses and to the termination of the stress response. They are involved in stress regulation and chronic stress response through their negative feedback on the HPA axis (De Kloet *et al.*, 2008). The GR also serves as a transcription factor, activating or repressing genes by binding to DNA directly through glucocorticoid response elements, or indirectly through tethered binding by

other transcription factors (Meijsing, 2015). GRs are most densely expressed in the hippocampus (Ruel & De Kloet, 1985), and their prolonged activation under chronic stress dysregulates cellular processes, which can lead to synapse loss, altered glial function, and the progression of neurodegenerative diseases (Harris & Seckl, 2011; McEwen *et al.*, 1986; McEwen *et al.*, 2016; Sousa & Almeida, 2012; Veldhuis *et al.*, 1982; Vyas *et al.*, 2016).

In the short term, stress responses are beneficial for modulating the transcription, translation, and degradation of specific proteins in cells, allowing organisms to deal with stressors and quickly return to homeostasis. However, long-term stress can disrupt cellular protein trafficking and maintenance processes (De Kloet *et al.* 2005). In neurons, proteins are primarily synthesized in the cell body and trafficked to the destinations where they perform their functions. Because neurons are morphologically complex, long-lived cells, it is of utmost importance that the protein trafficking machinery, itself made of proteins, works efficiently to transport each protein to its proper destination. Healthy cells are able to maintain their trafficking networks, but under stress, they must shut down or activate specific pathways to adapt and survive (Gundamaraju *et al.*, 2018). For example, glucocorticoids regulate the transcription of genes encoding key proteins for synaptic vesicle recycling, such as synaptosomal-associated protein 25 (SNAP-25) (Datson *et al.*, 2008). These processes allow cells to appropriately modulate neurotransmitter release at synapses under stress. Modifications to cellular pathways protect the brain in the short-term, but they can become dysregulated by chronic stress (De Kloet *et al.*, 2005), though at the level of individual organisms, responses to stress challenges vary in their severity and duration (Koolhaas *et al.*, 2011).

1.1.2. Chronic stress contributes to brain pathology

Chronic stress elevates GC levels and generates maladaptive cellular coping mechanisms that can produce neuronal damage. GR expression has been linked to stress susceptibility, indicating that brain GRs drive neuronal changes in response to chronic stress (Molteni *et al.*, 2010; Ridder *et al.*, 2005). For example, reduced GR expression was found to dysregulate the HPA axis and to increase helplessness following stress exposure in mice (Ridder *et al.*, 2005). Decreased GR levels also reduced the effects of stress on the expression of Brain-Derived Neurotrophic Factor (BDNF) and Arc (Molteni *et al.*, 2010), proteins essential for synaptic plasticity. These data suggest that GRs drive stress-induced changes in the brain, and that stress affects synaptic plasticity. Indeed, neuronal remodeling under stress has been well-documented, with acute and chronic stress producing opposite effects in the hippocampus and pre-frontal cortex (McEwen *et al.*, 2016). In the hippocampus, acute stress was found to enhance long-term potentiation and to be reversible, while repeated stress lead to dendritic atrophy and memory deficits (Brunson *et al.*, 2005; McEwen, 1999). In the pre-frontal cortex, acute stress induced the expression of cell-surface NMDA and AMPA receptors, while chronic stress reduced their expression (Yuen *et al.*, 2011). Chronic stress and high GC levels were also shown to promote dendritic shrinkage in the medial pre-frontal cortex of rodents (Cook & Wellman, 2004; Liston *et al.*, 2006; Radley *et al.*, 2004; Radley *et al.*, 2005). This shrinkage was reversible in young animals, but less so in middle aged and older animals (Bloss *et al.*, 2010), suggesting that aging limits the ability to recover from stress-induced synaptic changes. The combination of greater density of GRs in the hippocampus (Ruel & De Kloet, 1985) and reduced stress recovery in aged neurons (Bloss *et al.*, 2010) suggests that the hippocampus is particularly susceptible to stress-induced pathology during aging. These findings also indicate that stress may accelerate the

progression of age-related neurodegenerative diseases such as Alzheimer's disease, whose onset is characterized by hippocampal synapse loss.

1.2. Alzheimer's Disease

1.2.1. Alzheimer's disease pathology

Alzheimer's disease (AD) is a progressive neurodegenerative disease that currently affects 55 million people worldwide, and is projected to affect 152 million by 2050 (Livingston *et al.*, 2020; Yiannopoulou & Papageorgiou, 2020). Globally, the societal cost of AD and dementia is over $800 billion (www.who.int, 2020), and there are currently no cures or methods to slow AD progression (Yiannopoulou & Papageorgiou, 2020). AD is characterized neuropathologically by amyloid plaques, extracellular aggregates composed of amyloid-beta (Aβ) peptides, as well as neurofibrillary tangles, intracellular aggregates composed of Tau protein. The symptoms associated with AD, including memory loss, sleep disturbance, difficulty completing daily tasks, and changes in mood or behavior, are due to the progressive loss of synapses between neurons in the hippocampus, entorhinal cortex, and frontal cortex (Breijyeh & Karaman, 2020; Kashyap *et al.*, 2019; Nelson *et al.*, 2012; Scheff *et al.*, 2006; Selkoe, 2002). The causes of AD are multifactorial, including age, genetics, and environmental risk factors, though the single greatest AD risk factor is age. Ten percent of people aged 65 and older have AD, and the risk of developing AD doubles every five years thereafter (nia.nih.gov, 2019). These data indicate that aging renders our brains less capable of protein clearance through normal trafficking and degradative pathways, resulting in Aβ and Tau accumulation. Environmental factors and genetics further increase the risk of developing AD.

1.2.2. Environmental risk factors for AD

Lifetime stress and high circulating levels of glucocorticoids have been suggested as critical precipitating factors of AD (Csernansky *et al.*, 2006; Elgh *et al.*, 2006; Silva *et al.*, 2019; Vyas *et al.*, 2016). AD risk increases with mid-life stress (Johansson *et al.*, 2010), as well as with high stress-associated factors like depression, anxiety, and sleep disturbance (Burke *et al.*, 2018; Mejia *et al.*, 2003). Stress may also accelerate AD progression, as higher plasma cortisol levels correlate with more rapidly progressing dementia in humans (Csernansky *et al.*, 2006). Mechanistically, stress/GCs have been shown to induce Tau accumulation, amyloid precursor protein (APP) processing into Aβ, and Aβ production in cell culture and animal models (Catania *et al.*, 2009; Green *et al.*, 2006; Jeong *et al.*, 2006; Sotiropoulos *et al.*, 2011; Srivareerat *et al.*, 2009), suggesting that stress promotes the cellular pathomechanisms that drive AD. In rodents, GC administration increases Aβ production by inducing the expression of APP and its protease β-site APP cleaving enzyme-1 (BACE1) (Green *et al.*, 2006), as well as by shifting APP metabolism towards the amyloidogenic pathway (Sotiropoulos *et al.*, 2008). In a triple-transgenic rodent model of AD (3xTg-AD), even short-term stress increased Aβ generation and synapse loss (Baglietto-Vargas *et al.*, 2015), indicating that stress exacerbates AD pathology. Interestingly, blocking GRs reduced hippocampal Aβ40, Aβ42, and BACE1 levels in an APP/presenilin double transgenic AD mouse model (APPswe/PS1) subjected to early life stress (Lesuis *et al.*, 2018). These studies indicate that stress promotes cellular pathways associated with AD, and that these effects are largely driven by the effects of GRs.

Viral infections and brain trauma, including ischemic stroke or traumatic brain injury, can also increase the risk of developing AD (Mckee & Daneshvar, 2015; Sochocka *et al.*, 2017; Vijayan & Reddy, 2016). Recent studies have found that Aβ acts as an antimicrobial agent in the

brain by aggregating around microbes (Gosztyla *et al.*, 2018; Sochocka *et al.*, 2017), which can lead to increased Aβ generation following infection. Furthermore, both brain trauma and infection activate the immune cells of the brain to repair damage and rid the brain of microbes. This immune system activity increases the likelihood of neuroinflammation, which has been identified as a major contributor to AD progression (Kinney *et al.*, 2018; Ni Chasaide & Lynch, 2020) and a primary driver of Tau fibril formation (Newcombe *et al.*, 2018). Interestingly, stress and GCs can stimulate the immune system in the brain (Bellezza *et al.*, 2014; Drake, 2015; Logsdon *et al.*, 2016; Sprenkle, *et al.*, 2017), providing another avenue by which stress acts as a precipitating factor for AD.

1.2.3. Genetic risk factors for AD: Early-Onset Alzheimer's Disease

Several genes have been identified as determinants of familial, early-onset AD (EOAD; developing in patients in their 40s through mid-50s). Although mutations in these genes are rare, accounting for only one percent of Alzheimer's cases, they have revealed some of the causes of AD. AD-causative mutations in the *APP* gene surround its secretase cleavage site and increase Aβ generation; conversely, a mutation that reduces Aβ production is protective against AD (Li *et al.*, 2019; Tcw & Goate, 2017). Additionally, mutations in the γ-secretase subunits presenilin-1 (*PSEN-1*) and presenilin-2 (*PSEN-2*) are also linked to EOAD. These mutations increase the ratio of Aβ42/Aβ40, producing more hydrophobic, aggregate-prone Aβ42 monomers (Bi *et al.*, 2019; Breijyeh & Karaman, 2020; Dai *et al.*, 2018; Zhao *et al.*, 2020). All of these AD-causative genes affect APP processing and the production of Aβ, providing evidence that Aβ is a major factor in this disease.

1.2.4. Genetic risk factors for AD: Late-Onset Alzheimer's Disease

The majority of AD cases are late-onset and sporadic, and many of the risk genes associated with late-onset AD (LOAD) encode proteins that drive cellular trafficking mechanisms. Around 40-65% of people diagnosed with AD have the *APOEε4* gene, encoding a protein that serves as a ligand for receptor-mediated endocytosis of lipoproteins such as cholesterol, which are essential for normal brain function (Kim *et al.*, 2009; Liu *et al.*, 2013). The gene encoding the sorting protein-related receptor-1 (*SORL1*) has also been linked to AD (Yin *et al.*, 2015). SORL1 is a member of the APOE receptor family, mediating the uptake of APOE-rich lipoproteins (Taira *et al.*, 2001; Yin *et al.*, 2015), further underscoring the importance of lipoprotein trafficking in AD. Additionally, SORL1 has been implicated in the retention of APP in the Trans-Golgi Network, and the trafficking of Aβ toward lysosomes (Yin *et al.*, 2015), suggesting that disrupted endosomal trafficking of APP and Aβ can lead to AD.

Bridging integrator 1 (*BIN1*) is the second-most significant locus associated with LOAD, and it functions in clathrin-mediated endocytic pathways (Andrew *et al.*, 2019; Holler *et al.*, 2014), and extracellular vesicle secretion (Crotti *et al.*, 2019). Interestingly, large genome-wide association studies have identified another clathrin-associated gene as a risk factor for AD: phosphatidylinositol-binding clathrin assembly protein (*PICALM*) (Xu *et al.*, 2015). It is yet unclear precisely which PICALM-mediated processes are responsible for AD risk, but it has been implicated in the endocytosis of APP (Xu *et al.*, 2015). Both BIN1 and PICALM are linked to clathrin-mediated endocytosis, suggesting the importance of this pathway in AD.

The third most significant genetic risk factor for LOAD is the gene encoding clusterin (*CLU)*. Clusterin is an extracellular chaperone protein, which has been found intracellularly under stress and Aβ treatment (Humphreys *et al.*, 1999; Killick *et al.*, 2014; Nizard *et al.*, 2007;

Foster *et al.*, 2019), suggesting a relationship between cellular stressors and clusterin trafficking. Clusterin's role in Aβ accumulation is yet unclear, as it has been shown to both increase and decrease Aβ clearance (Foster *et al.*, 2019); however, the relationship between clusterin and Aβ may be dependent on the clusterin/Aβ ratio (Yerbury *et al.*, 2007). Clusterin is primarily generated by astrocytes, and while its expression increases with injury, inflammation, and AD (Foster *et al.*, 2019), recent research indicates that this may be protective rather than pathological (Chen *et al.*, 2021). Though the underlying mechanisms of these AD risk factors have yet to be identified, they indicate that dysregulated trafficking pathways contribute to AD.

Many of the genetic risk factors associated with LOAD lead to malfunctions in the endosomal pathway, which transports proteins to the plasma membrane and functions in protein internalization and recycling. The endosomal pathway is disrupted early in AD, suggesting that buildup of Aβ and/or Tau clogs these trafficking mechanisms, further contributing to protein aggregation (Xu *et al.*, 2016). Indeed, Aβ can accumulate in multivesicular bodies as it is taken up by neurons. This impairs the endolysosomal pathway, reducing degradation of other proteins (Almeida *et al.*, 2006). Similarly, APP and PSEN1 mutant neurons, which enhance amyloidogenic cleavage of APP, have deficits in lysosome proteolysis, which can be rescued by BACE1 inhibition, indicating that increased Aβ generation is driving these defects (Hung & Livesey, 2018). APP mutations increase total and phosphorylated Tau as well (Moore *et al.*, 2015), further complicating the trafficking problem in AD.

1.3. Cellular mechanisms of Alzheimer's Disease

1.3.1. Aβ functions at the synapse

While the detrimental effects of amyloid plaques remain controversial, considerable evidence shows that elevated levels of Aβ peptides are synaptotoxic, supporting the 'amyloid

cascade' hypothesis that AD is initiated by Aβ production (Mucke & Selkoe, 2012). For instance, full-length APP promotes synapse formation (Hoe *et al.*, 2012), and its non-amyloidogenic cleavage into sAPPα modulates synaptic transmission in the hippocampus, rescuing synaptic defects in *APP* knockout mice (Rice *et al.*, 2019). However, increased amyloidogenic cleavage of APP into Aβ has deleterious effects on synapses (Rajmohan & Reddy, 2017). In APP transgenic mice, synapse loss was greatest near Aβ plaques and oligomers, and lessened in a radial fashion away from them (Koffie *et al.*, 2009; Spires-Jones *et al.*, 2007), suggesting that Aβ can disrupt synapses. Likewise, in rat hippocampal cultures, prolonged Aβ exposure reduced dendritic spine density and produced abnormal spines (Lacor *et al.*, 2007). Aβ has also been shown to weaken synaptic transmission by decreasing synaptic vesicle endocytosis and reducing presynaptic protein levels (Park *et al.*, 2013; Reddy *et al.*, 2005). Furthermore, Aβ blocks long-term potentiation and induces long-term depression, as well as dendritic spine pruning, through its effect on glutamate receptors, as it has been shown to block glutamate reuptake and hyperactivate type 5 metabotropic glutamate receptors (mGluR5) (Li *et al.*, 2009; Shankar *et al.*, 2008; Zhang *et al.*, 2015).

Surprisingly, one of the best-characterized roles of Aβ is promoting synaptic function and plasticity. Studies show that deletion of either APP or BACE1 in transgenic mice reduces long term potentiation in hippocampal slices (Dawson *et al.*, 1999; Laird *et al.*, 2005), and Aβ monomers promote the survival of developing cultured cortical neurons deprived of trophic factors (Giuffrida *et al.*, 2009), indicating Aβ's beneficial roles at the synapse. Indeed, Aβ has been shown to regulate the recycling of synaptic vesicles and promote long term potentiation when expressed at picomolar concentrations (Lazarevic *et al.*, 2017; Puzzo *et al.*, 2011, 2008), which have been characterized as endogenous, non-pathogenic levels of Aβ (Cirrito *et al.*, 2003;

Parihar & Brewer, 2010; Seubert *et al.*, 1992). In line with these findings, picomolar concentrations of Aβ were shown to enhance LTP and spatial learning, as well as fear memory formation and consolidation in rodents (Finnie & Nader, 2020; Garcia-Osta & Alberini, 2009; Gulisano *et al.*, 2018). On the other hand, nanomolar concentrations of Aβ reduced plasticity (Puzzo *et al.*, 2011), providing evidence that excessive Aβ production is harmful to synapses. Together, these data indicate that non-amyloidogenic APP cleavage, and endogenous levels of amyloidogenic APP cleavage, are beneficial to the synapse, but that increased APP processing into Aβ peptides leads to neuronal damage by reducing synaptic transmission and inducing synapse loss.

Interestingly, synaptic activity increases APP endocytosis and BACE1-mediated Aβ production to promote synaptic function (Cirrito *et al.*, 2008, 2003; Kamenetz *et al.*, 2003). Since high concentrations of Aβ induce LTD, it has been proposed that Aβ may control a tightly-regulated negative feedback loop modulating neuronal activity and preventing excess Aβ generation and subsequent neuronal hyperactivation (Kamenetz *et al.*, 2003). Mouse models and human patient data have revealed that neuronal circuits are hyperactive in the early stages of AD, suggesting a dysregulation of this feedback loop. In APP-PS1 double transgenic mice and human APP-expressing J20 mice, neurons in the hippocampus and frontal cortex were found to be hyperactive and to exhibit reduced dendritic spine density (Busche & Konnerth, 2015). Similarly, in humans monitored by blood-oxygen-level dependent (BOLD) fMRI, asymptomatic individuals with high Aβ burden exhibited increased activation in the medial prefrontal cortex, and patients in the pre-dementia stages of AD had elevated resting-state activity in the hippocampus (Busche & Konnerth, 2015). Together, these studies suggest that elevated neuronal

activity is a symptom of prodromal and early-stage AD, and indicate a dysregulation of the feedback loop between neuronal activity and Aβ generation.

1.3.2. Role of Tau in the neuron

The microtubule-binding protein Tau is primarily localized to axons, where it serves to stabilize microtubules and maintain axonal transport. Hyperphosphorylation of Tau under pathological conditions leads to its dissociation from microtubules, reducing their stability and disrupting transport mechanisms. Furthermore, hyperphosphorylated Tau becomes mislocalized at synapses and in the somatodendritic compartment, where it gains new functions (Hoover *et al.*, 2010). For instance, phosphorylated Tau is prone to aggregation, and these aggregates inhibit proteasome function (Myeku *et al.*, 2016) and autophagy (Caballero *et al.*, 2021; Feng *et al.*, 2020), thereby disrupting neuronal proteostasis. At presynaptic terminals, pathogenic Tau binds to synaptic vesicles and inhibits their release (Largo-Barrientos *et al.*, 2021; McInnes *et al.*, 2018; Zhou *et al.*, 2017), while in the postsynaptic compartment Tau impairs AMPA and NMDA receptor anchoring and signaling (Hoover *et al.*, 2010; Ittner *et al.*, 2010; Li *et al.*, 2019; Liao *et al.*, 2014; Miyamoto *et al.*, 2017; Pallas-Bazarra *et al.*, 2019). These studies reveal that Tau hyperphosphorylation leads to neuronal dysfunction as a result of reduced microtubule stability, impaired protein degradation, and altered synaptic transmission.

Hyperphosphorylated Tau also becomes misfolded and aggregates into fibrils, which can serve as “seeds” to recruit soluble Tau, inducing further aggregation and the formation of neurofibrillary tangles (NFTs) (Guo & Lee, 2011). Tau propagation in the AD patient brain closely matches symptomatic progression of the disease (Braak & Braak, 1991). This propagation requires the secretion and reuptake of pathogenic Tau species (Braak & Del Tredici,

2016) and is mediated by exosomes, extracellular vesicles derived from the endolysosomal system (DeLeo & Ikezu, 2018; Ledreux *et al.*, 2021; Perez *et al.*, 2019; Ruan *et al.*, 2021; Xiao *et al.*, 2017). Interestingly, the presence of NTFs correlates with cognitive decline and synapse loss in AD, implicating Tau as a critical driver of disease progression. However, Tau aggregation in the absence of Aβ pathology causes frontotemporal dementia, not AD (Goedert & Jakes, 2005; Mufson *et al.*, 2014; Vana *et al.*, 2011), indicating that AD is a result of both Tau aggregation/mislocalization and APP misprocessing. Because both of these processes are dependent on intracellular trafficking mechanisms, it is important to illuminate the cellular trafficking pathways responsible for Tau and Aβ accumulation.

1.3.3. APP and BACE1 trafficking pathways lead to Aβ production

Amyloid-beta (Aβ) is generated by the cleavage of Amyloid Precursor Protein (APP), which can undergo cleavage by two pathways: amyloidogenic and non-amyloidogenic (**Fig. 1**). In the amyloidogenic pathway, APP is cleaved first by the β-secretase BACE1, producing extracellular, soluble sAPPβ and the β C-terminal fragment (β-CTF; C99). Secondary cleavage by the γ-secretase produces an intracellular AICD (APP intracellular domain) fragment, which may function in nuclear signaling, as well as Aβ, which is prone to aggregation (Haass *et al.*, 2012). This cleavage produces Aβ monomers of varying peptide lengths: Aβ40 is the most common, and Aβ42 is the most prone to fibril formation. In the non-amyloidogenic cleavage pathway, APP is first cleaved by the α-secretase, metalloprotease ADAM10, producing extracellular, soluble sAPPα and the α-C-terminal fragment (α-CTF; C83). Secondary cleavage by the γ-secretase creates the intracellular AICD fragment, and non-aggregating, extracellular p3 (Haass *et al.*, 2012).

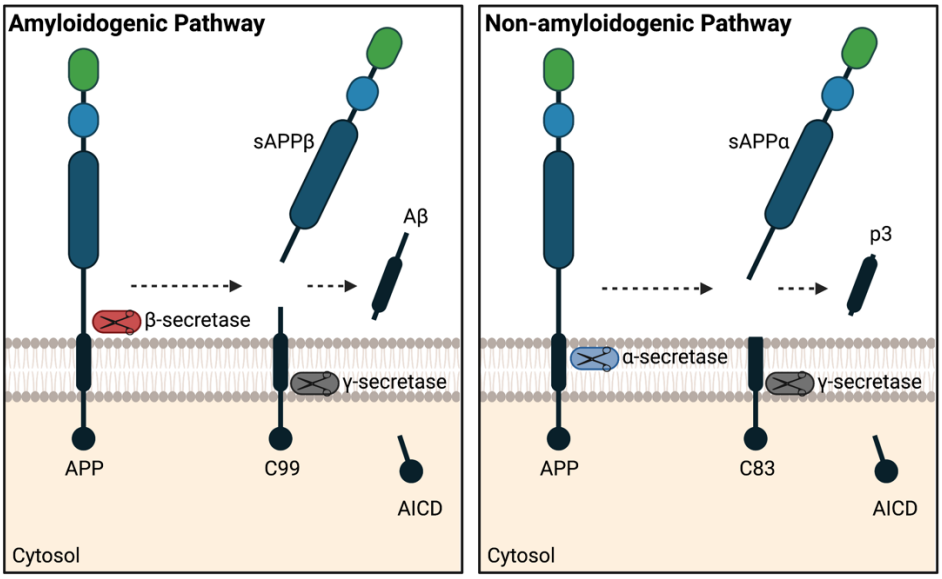

Figure 1. Cleavage of APP through the amyloidogenic and non-amyloidogenic pathways. In the amyloidogenic pathway, APP is cleaved by the β-secretase BACE1 and a γ-secretase, yielding the pathogenic β-C-terminal fragment (C99) and aggregate-prone Aβ. In the non-amyloidogenic pathway, APP is cleaved by α- and γ-secretases, yielding non-toxic, soluble products.

The generation of Aβ requires interaction between APP and BACE1, which is determined by their intracellular trafficking pathways. APP and BACE1 are membrane proteins that are transported from the endoplasmic reticulum (ER) through the trans-Golgi network (TGN), to the plasma membrane. From the plasma membrane, they can be internalized, entering the endosomal system. Either protein can then be recycled to the surface through recycling endosomes, trafficked back to the TGN through the retrograde pathway, degraded in lysosomes, or secreted through exosomes (**Fig 2.**).

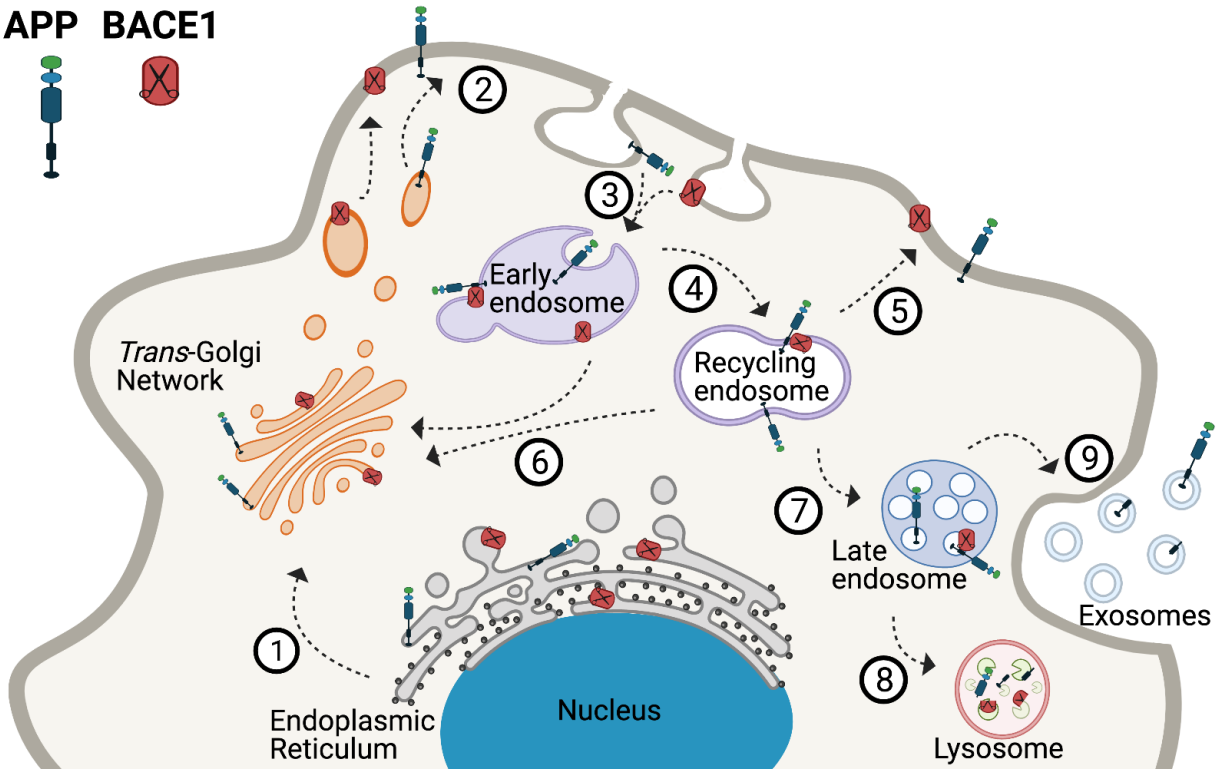

Figure 2. APP and BACE1 intracellular trafficking. Newly synthesized APP and BACE1 proteins travel from the endoplasmic reticulum to the Trans-Golgi Network (1) and to the plasma membrane (2). APP and BACE1 are internalized into endocytic compartments (endosomes) (3), where the acidic pH is optimal for BACE1 activity. Here, APP and BACE1 may interact to produce Aβ. From the early endosome, APP or BACE1 can be recycled (4) to the plasma membrane (5), or trafficked through the retrograde pathway to the Trans-Golgi Network (6). Alternatively, they can be sorted into late endosomes (7) and degraded when fused with lysosomes (8), or secreted as exosomes when fused with the plasma membrane (9).

1.3.4. Rab35 – a master regulator of intracellular trafficking

Intriguingly, many of the recently-identified genetic risk factors for late-onset AD (LOAD) are linked to endosomal protein trafficking, and have been shown to induce endosomal dysfunction and to prolong the residence times of APP and/or BACE1 in endosomes (Small *et al.*, 2017; Ubelmann *et al.*, 2017). Indeed, entry of APP and BACE1 into the endosomal network is an essential step in Aβ production (Cirrito *et al.*, 2005; Zou *et al.*, 2007), as endosomes contain the optimal acidic pH for BACE1 activity and have been identified as major sites of Aβ generation (Haass *et al.*, 2012).

Rab35 is a member of the Rab family of GTPases, which regulate endosomal protein trafficking by cycling between active (GTP-bound) and inactive (GDP-bound) states (**Fig. 3**), and recruiting effectors that catalyze downstream events such as membrane fusion and vesicle transport (Stenmark, 2009).

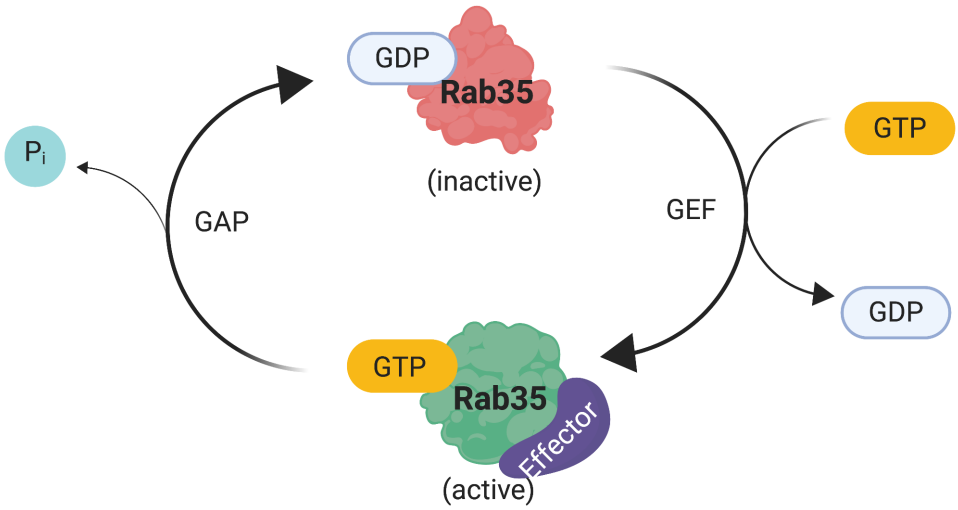

Figure 3. Rab35 activation cycle. Rab35 switches from an inactive (GDP-bound) state to an active (GTP-bound) state when a guanine exchange factor (GEF) exchanges GDP for GTP. Active Rab35 interacts with effectors, driving trafficking events. GTP-hydrolysis activating proteins (GAPs) return Rab35 to an inactive state by facilitating the removal of a phosphate group, generating GDP from GTP.

Rab35 is considered a 'master regulator' of endosomal protein trafficking due to its role in multiple cellular trafficking pathways (**Fig. 4**). These include an *e*ndosomal *s*orting *c*omplex *r*equired for *t*ransport (ESCRT)-mediated pathway for protein degradation (Sheehan *et al.*, 2016; Vaz-Silva *et al.*, 2018), the retrograde trafficking pathway to the trans-Golgi Network (Cauvin *et al.*, 2016), and a fast recycling pathway between endosomes and the plasma membrane (Kobayashi & Fukuda, 2013; Patino-Lopez *et al.*, 2008). Furthermore, Rab35 is a central regulator of phosphoinositide synthesis and F-actin dynamics during endocytic recycling (Klinkert & Echard, 2016), important for sorting cargo internalized by clathrin-mediated endocytosis (Dutta & Donaldson, 2015). Rab35 is also involved in neurite outgrowth and synapse formation (Kobayashi & Fukuda, 2012; Patino-Lopez *et al.*, 2008), as well as cell

adhesion and migration (Allaire *et al.*, 2013), and exosome secretion (Hsu *et al.*, 2010; Yang *et al.*, 2019). As a regulator of multiple cellular trafficking pathways, Rab35 is in a prime position to influence the trafficking of AD-related proteins.

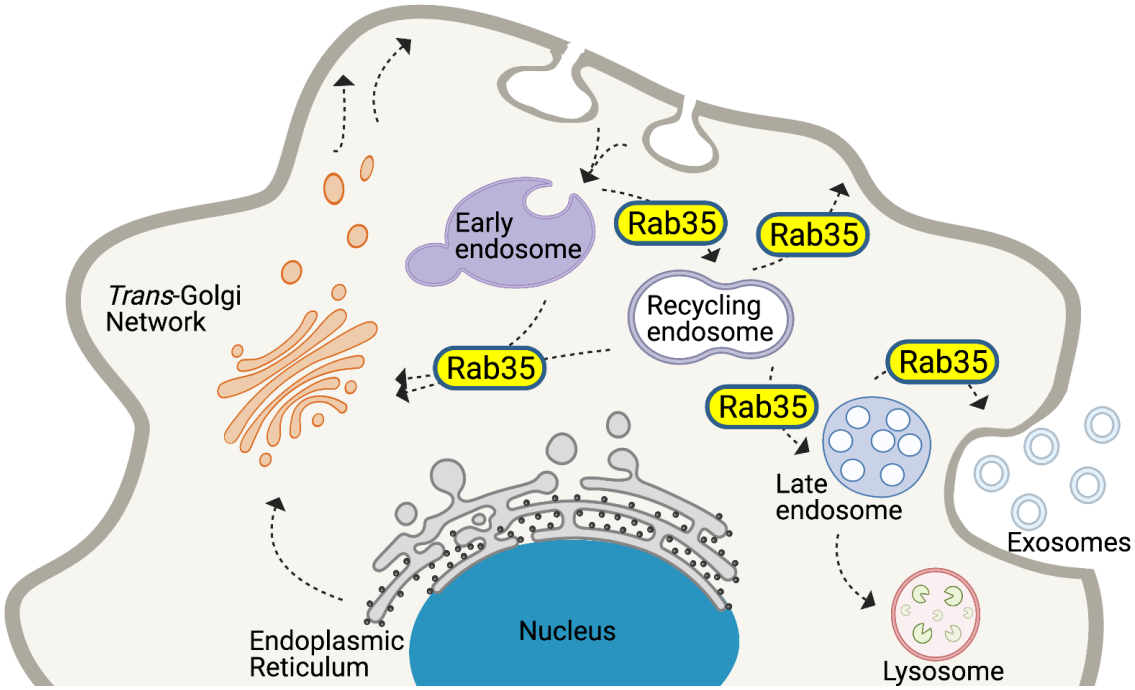

Figure 4. Rab35 mediates endosomal trafficking pathways. Rab35 has been shown to control protein sorting following clathrin-mediated endocytosis, as well as pathways involved in protein recycling, degradation, and retrograde trafficking, as well as exosome secretion.

Indeed, in our previous study, we demonstrated that Rab35 promotes the degradation of ubiquitylated Tau by sorting it into the ESCRT pathway. Interestingly, we found that glucocorticoids (GCs) downregulate Rab35, leading to intraneuronal Tau accumulation (**Fig. 5**) and downstream Tau-dependent pathology (i.e. synaptic and dendritic loss) in the rat hippocampus. AAV-mediated Rab35 overexpression rescued these deficits (Vaz-Silva *et al.*, 2018), underscoring its role in Tau trafficking and degradation in glutamatergic neurons. However, the role of Rab35 in stress/GC-mediated Aβ overproduction has not been explored,

although Rab35 has been identified as a negative regulator of Aβ production (Udayar *et al.*, 2013).

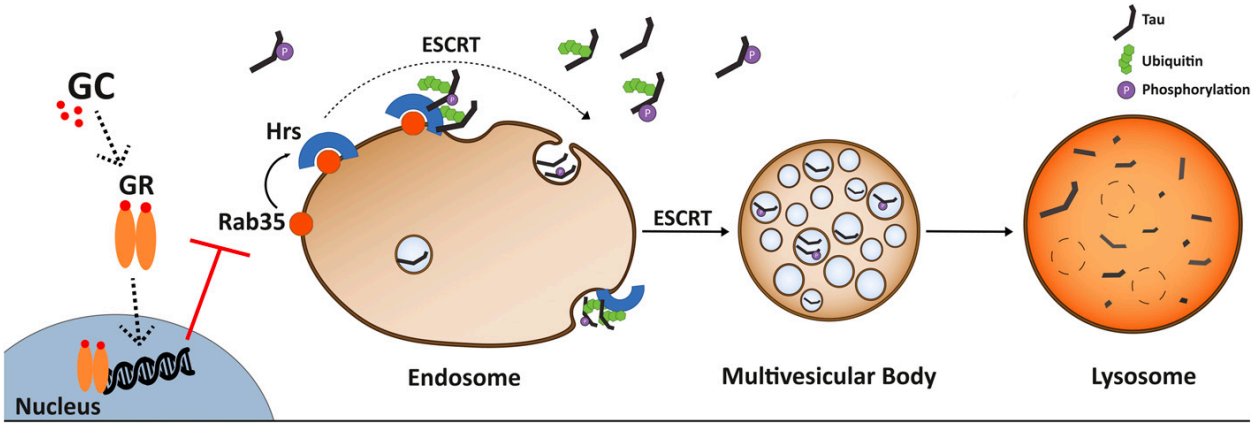

Figure 5. Working model of Tau degradation through the Rab35/ESCRT pathway, and its inhibition by glucocorticoids (GC). Rab35 mediates Tau clearance via the endolysosomal pathway by recruiting the initial ESCRT component Hrs, which recognizes and sorts ubiquitylated Tau into early endosomes for packaging into MVBs. GC suppress transcription of Rab35, which in turn decreases Tau sorting into MVBs and its subsequent degradation by lysosomes, leading to Tau accumulation and related neuronal atrophy. Copyright © 2018 The Authors, published by John Wiley & Sons, all rights reserved. Figure and caption reprinted from Vaz-Silva, *et al.*, 2018, with permission under the terms of the granted license, provided as-is with no warranties or liabilities concerning this material.

In this thesis, I identify Rab35 as a molecular substrate through which stress/GCs could increase Aβ production, a hallmark of AD. I show that Rab35 levels are significantly decreased with stress, Aβ infusion, and aging, all conditions associated with AD. Furthermore, I find that Rab35 is an important negative regulator of APP and BACE1 interaction in the endosomal network, promoting APP recycling to the cell surface and BACE1 retrograde trafficking to the TGN to reduce Aβ generation in endosomes. Finally, I describe methods for assessing exosome secretion in neurons, astrocytes, and microglia to determine how GCs and Rab35 affect exosome-mediated intercellular spreading of AD-associated proteins.

Chapter 2: Materials and Methods

2.1. Methods used for Rab35-mediated endosomal trafficking experiments in chapters 3 and 4

2.1.1. Primary neurons and cell lines

Primary neuronal cultures were prepared from E18 Sprague Dawley rat embryos and maintained in Neurobasal with GlutaMAX (Invitrogen) and N21 supplement (R&D systems) for 14 days *in vitro* (DIV) before use, as described previously (Sheehan *et al.*, 2016). Neuro2a (N2a) neuroblastoma cells (ATCC CCL-131) were grown in DMEM-GlutaMAX (ThermoFisher) with 10% FBS (Atlanta Biological) and 1% Anti-Anti (ThermoFisher) and kept at 37°C in 5% CO_2. During dexamethasone treatment in N2a cells, FBS in the growth media was reduced to 3%. Human iPSC-derived neuronal primary cultures were generated using manual rosette selection and maintained on Matrigel (Corning) (Topol *et al.*, 2015). Concentrated lentiviruses expressing control-sgRNA or hu-APP-sgRNA were made using Lenti-X concentrator (Clontech). The iPSC-derived neuronal cultures were transduced with either control-sgRNA or hu-APP-sgRNA after Accutase splitting, and were submitted to puromycin selection the subsequent day. Polyclonal lines were expanded and treated with puromycin for 5 more days before banking. Neuronal differentiations were carried out by plating 165,000 cells/well (12-well plate) in N2/B27 media (DMEM/F12 base) supplemented with BDNF (20 ng/ml) and laminin (1 µg/ml).

2.1.2. Pharmacological treatments

Pharmacological agents were used in the following concentrations and time courses: cycloheximide (Calbiochem, 0.2 µg/µl, 2, 4, 8, or 24h), dexamethasone (Invivogen, 10 µM, 24h).

2.1.3. Lentivirus production, transduction, and DNA transfection

DNA constructs were described previously (Sheehan *et al.*, 2016; Vaz-Silva *et al.*, 2018). APP:VN and BACE:VC constructs were a gift from Dr. Subhojit Roy (University of Wisconsin, USA). Briefly, Rab GTPases were subcloned into pKH3 vector at the EcoRI site to create HA-tagged Rabs. Lentivirus was produced as previously described (Sheehan *et al.*, 2016). Neurons were transduced with 50–150 µL of lentiviral supernatant per well (12-well plates) or 10–40 µL per coverslip (24-well plates) either at 3 DIV for shRNA transduction or 10 DIV in gain-of-function experiments. Respective controls were transduced on the same day for all experimental conditions. Primary neuronal cultures were collected for immunoblotting or immunocytochemistry at 14 DIV. N2a cells were transfected using Lipofectamine 3000 approximately 24h after plating, according to the manufacturer's instructions. For the bimolecular fluorescence complementation assay, double transfection of APP:VN and BACE1:VC constructs was performed 48h after transfection with HA-Rab GTPases, to allow longer expression of the Rabs. Cells were then fixed and analyzed 18h after the APP:VN and BACE1:VC transfection.

2.1.4. Flow cytometry

N2a cells were detached using TrypLE Express (Life Technologies) for 5 min at 37ºC, resuspended in culture medium, and centrifuged (3,000 rpm, 5 minutes, 4ºC). The pellet was washed once with 0.2 mM EDTA and 0.02% BSA in 1X PBS (Flow buffer), centrifuged again, resuspended in 100 µL of flow buffer, then fixed with 4% paraformaldehyde solution for 15 min at room temperature. Cells were washed (1X PBS) and resuspended in 1.5% FBS and 0.05%

saponin in 1X PBS (permeabilization solution), then placed on a shaker for 30 min at RT. Following centrifugation, the supernatant was discarded, and the cell pellet resuspended in permeabilization solution with anti-HA-tag Alexa(R)-647 (Cell Signaling Technologies) for immunostaining, then placed on a shaker for 90 minutes at 4ºC. After washing twice with flow buffer, cells were resuspended in ice-cold Flow Buffer (0.2% FBS, 0.5mM EDTA in 1X PBS), strained through a 35µm nylon mesh to promote single cell suspensions, and kept on ice. Cells and fluorescence were analyzed by BD Fortessa Cell Analyser and BD FACSDiva software (BD Biosciences). Unstained cells were used as a control for background fluorescence. Far-red (APC) and green (FITC) fluorescence were analyzed, as they marked the HA-tag and Venus fluorescence (APP-BACE1 interaction), respectively. 50,000 events were recorded for each sample, with two samples for each condition per experiment. Flow Cytometry data were analyzed using FCS Express 6 (DeNovo Software). Median fluorescence intensity of the Venus (APP-BACE1) signal was calculated for the HA+ cells only, thus in double positive cells. The median Venus fluorescence intensity of each sample was compared to the median Venus fluorescence of all samples, thus comparing each condition to the average of the whole population.

2.1.5. Immunofluorescence microscopy

Immunofluorescence staining in neurons and N2a cells was performed as previously described (Sheehan *et al.*, 2016). Briefly, cells were fixed with Lorene's Fix (60 mM PIPES, 25 mM HEPES, 10 mM EGTA, 2 mM MgCl2, 0.12 M sucrose, 4% formaldehyde) for 15 min, and primary and secondary antibody incubations were performed in blocking buffer (2% glycine, 2% BSA, 0.2% gelatin, 50 mM NH4Cl in 1X PBS) for 1h at room temperature. Coverslips were

mounted using Aqua Poly/Mount (Polysciences, Inc.). Images were acquired using a Zeiss LSM 800 confocal microscope equipped with Airyscan module, using a 63X objective (Plan-Apochromat, NA 1.4).

2.1.6. Proximity ligation assay

Proximity ligation assay (PLA) was performed in primary hippocampal neurons and N2a cells according to the manufacturer's instructions (Duolink, Sigma). Until the PLA probe incubation step, all manipulations were performed as detailed in the immunocytochemistry procedure. PLA probes were diluted in blocking solution. The primary antibody pairs used were C1/6.1 (anti-APP, Mouse; Biolegend) and anti-BACE1 (Rabbit, Cell Signaling Technology). All protocol steps were performed at 37°C in a humidity chamber, except for the washing steps. Coverslips were then mounted using Duolink In situ Mounting Media with DAPI, and imaged using a 40X objective (Plan-Apochromat, NA 1.4).

2.1.7. Neuronal image analysis

Images were analyzed and processed using Fiji/ImageJ software. PLA puncta were counted using the Multi-point tool, and cell area was measured with the Polygon selection tool. Colocalization analysis between APP (22C11, Millipore) or BACE1 (Cell Signaling) and intracellular compartments (Rab11, Cell Signaling; Syntaxin-6, Synaptic Systems) in neurons was determined using the JACoP plugin, in order to obtain the Mander's coefficient corresponding to the fraction of APP or BACE1 colocalized with each compartment.

2.1.8. Aβ Measurements

Human iPSC-derived neuronal cultures were kept for 3 days post-transduction, after which 50% of the media was changed. Then, conditioned media was collected after 72h, centrifuged at 2,000 rcf for 5 min and stored at –80ºC. Aβ42 and Aβ40 levels were measured using V-PLEX Aβ Peptide Panel 1 (4G8) Kit (MesoScaleDiscovery, MSD) following the manufacturer's protocol and their concentration was presented as percentage of control levels, after normalization to total protein in the conditioned media (measured using ThermoFisher Scientific BCA assay kit).

2.1.9. Animals

Male Wistar rats (Charles River Laboratories, France) were maintained under standard laboratory environmental conditions (lights on from 8 a.m to 8 p.m, room temperature 22°C, relative humidity 55%, *ad libitum* access to food and water). All experimental procedures were approved by the local ethical committee of the University of Minho and the national authority for animal experimentation (DGV9457); all experiments were in accordance with the guidelines for the care and handling of laboratory animals, as described in the Directive 2010/63/EU. Twelve-month-old animals were randomly divided into the below three groups: control, stressed, Aβ-infused animals (n = 8-10 per group). For stressed animals, the chronic unpredictable stress paradigm lasted for 4 weeks and consisted of random application of one of the following stressors (one stressor per day): (i) rocking platform, (ii) air dryer, (iii) cold water, and (iv) overcrowding, as previously described (Catania *et al.*, 2009). Control, non-stressed animals remained in their home cages during the stress period. At the end of the stress paradigm, all

animals were implanted with Alzet miniosmotic pumps for i.c.v. delivery of Aβ1-40 (Eurogentec; 25 µg/200 µl, 0.5µl per hour) or saline for 14 days (Prediger *et al.*, 2007). For the Aβ1-40 or saline infusion, mini-osmotic pumps (Alzet. Osmotic Pumps, DURECT, 2002 model) and cannulae (Alzet Brain Infusion Kit) were implanted in the left lateral ventricle using the following coordinates from Bregma: -0.6mm anteroposterior, -1.4mm mediolateral, -3.5mm dorsoventral according to Paxinos and Watson (Paxinos & Watson, 1986). Pump and cannula implantation were done under anaesthesia [75 mg/kg ketamine (Imalgene, Merial) and 1mg/kg medatomidine (Dorbene, Cymedica)]. For the aged rat study, young (4 month-old) and aged (22-24 month-old) male Wistar rats were used (n = 4-8 per group). For the Rab35 overexpression experiment, another set of male Wistar rats (17 month-old; Charles River Laboratories, Spain) were randomly divided into two groups (n = 2–6 per group) and were bilaterally injected into the dorsal hippocampus with AAV8-GFP or AAV8-Rab-GFP virus [coordinates from Bregma, according to Paxinos and Watson 50: -3.0 mm anteroposterior (AP), ±1.6 mm mediolateral (ML), and -3.3 mm dorsoventral (DV)] under anesthesia with 75 mg/ kg ketamine (Imalgene, Merial) and 0.5 mg/kg medetomidine (Dorbene, Cymedica), as previously described (Vaz-Silva, *et al.*, 2018).

2.1.10. Immunoblotting

For immunoblotting experiments, human iPSC-derived neuronal cultures were collected in Lysis Buffer (50 mm Tris-Base, 150 mm NaCl, 1% Triton X-100, 0.5% deoxycholic acid) with protease inhibitor (Roche) and phosphatase inhibitor cocktails II and III (Sigma) and clarified by centrifugation at high speed (10 min, 20,000 g). Rat hippocampi were homogenized in lysis buffer (50 mm Tris-Base, 150 mm NaCl, 1% Triton X-100, 0.5% deoxycholic acid) with

10mM $MgCl_2$ and clarified by centrifugation at high speed (15 min, 20,000 g). Protein concentration was determined using the BCA protein assay kit (ThermoFisher Scientific) and the same amount of protein was used for each condition, which was diluted and denatured in 2X SDS sample buffer with beta-mercaptoethanol (Bio-Rad; prepared per the manufacturer's instructions). N2a cells were collected in 2X SDS sample buffer with beta-mercaptoethanol. Samples were subject to SDS–PAGE, transferred to nitrocellulose membranes using wet transfer (Mini Trans-Blot Cell, Bio-Rad), and probed with primary antibody in 5% BSA/PBS + 0.1% Tween-20, followed by DyLight 680 or 800 anti-rabbit, anti-mouse (Thermo Scientific) or by HRP-conjugated secondaries (Bio-Rad). Primary antibodies used for western blotting are listed in **Table 1**. Membranes were imaged using an Odyssey Infrared Imager (model 9120, LI-COR Biosciences), and protein intensity was measured using Image Studio Lite software (LI-COR Biosciences).

Antibody	Manufacturer	Concentration
Actin	Abcam (#8224)	1:1000
ACAP2	ProteinTech (#14029-1-AP)	1:1000
APP & CTFs	Biolegend (APP C1/6.1; #802801)	1:1000
BACE1	Cell Signaling (D10E5; #5606)	1:1000
GFP	Invitrogen (#A6455)	1:1000
mCherry	Abcam (#ab125096) Biovision (#5993)	1:1000
OCRL	ProteinTech (#17695-1-AP)	1:1000
Rab5	Synaptic Systems (#108011)	1:1000
Rab7	Abcam (#ab50533)	1:1000
Rab8	ProteinTech (#55296-1-AP)	1:1000
Rab11	Cell Signaling (D4F5; #5589)	1:1000
Rab14	Santa Cruz (#sc-98610)	1:500
Rab35	ProteinTech (#11329-2-AP)	1:1000
Tubulin	Abcam (#ab4074) Sigma (#T9026)	1:5000

Table 1. List of primary antibodies used for western blotting.

2.1.11. Retrograde trafficking assay

N2a cells were co-transfected with APP-GFP or FLAG-BACE1 and HA or HA-Rab35 constructs. Approximately 48 hours after transfection, cells were starved in serum-free DMEM for 30 minutes. Cells were then incubated for 30 min at 4ºC with 22C11 antibody (anti-N-terminus of APP, Millipore) or anti-FLAG (Millipore). Antibodies were diluted 1:100 in complete medium + 1M HEPES. Following antibody incubation, cells were washed with complete medium + HEPES and either immediately fixed with Lorene's fixative for 15 min, or incubated at 37ºC for 10, 30, or 60 min and then fixed, followed by washing with 1X PBS. For immunostaining, cells were permeabilized using Triton X-100, and coverslips were immunostained with the following primary + secondary antibody pairs: internalized anti-22C11 or anti-FLAG + goat-anti-mouse Alexa(R)-568 to tag internalized APP or BACE1; anti-Syntaxin-6 (Synaptic Systems) + Alexa(R)-647 to tag the trans-Golgi network (TGN); and anti-BACE1 (for BACE1-transfected conditions only; Cell Signaling) + Alexa(R)-488 to tag total BACE1. Cells overexpressing Rab35 were detected using an anti-HA primary antibody (Rabbit, Cell Signaling; Mouse, Biolegend) + Alexa(R)-405 secondary antibody (data not shown). For analysis, Fiji/ImageJ was used to outline each transfected cell and clear the background. Colocalization between APP or BACE1 and the TGN was determined using the JACoP plugin, and the Mander's coefficient was used for reporting the fraction of APP or BACE1 colocalized with the TGN.

2.1.12. Recycling assay

N2a cells were co-transfected with APP-GFP or FLAG-BACE1 and HA or HA-Rab35 constructs. Approximately 48 hours after transfection, cells were starved in serum-free DMEM

for 30 minutes and then incubated for 30 min at 4ºC with 22C11 antibody (anti-N-terminus of APP, Millipore) or anti-FLAG (Millipore) as in the retrograde trafficking assay. Following antibody pulse, coverslips were washed with complete medium + HEPES and incubated with goat-anti-mouse unconjugated antibody (1:50; Invitrogen) for 30 min at 4ºC to allow for APP or BACE1 internalization while blocking any primary antibody on the surface that is not internalized. Antibodies were diluted in complete medium + 1M HEPES. Coverslips were washed with complete medium + HEPES and fixed with Lorene's fixative for 15 min or incubated at 37ºC for 10, 30, or 60 min and then fixed, followed by washing with 1X PBS. Coverslips were immunostained with goat-anti-mouse Alexa(R)-568 for 1hr at RT prior to cell permeabilization to mark recycled 22C11 or FLAG antibodies, and any remaining surface antibody was blocked using goat-anti-mouse unconjugated antibody (1:50, 30 min at RT). Following cell permeabilization, internalized 22C11 or FLAG was marked using goat-anti-mouse Alexa(R)-647 secondary antibody. Total BACE1 and HA were tagged as in the retrograde trafficking assay. Internalization and recycling of APP and BACE1 were determined using Fiji/ImageJ by outlining each cell and normalizing the fluorescence of (1) internalized APP or BACE1 and (2) recycled APP or BACE1 to total APP or BACE1. These values were then normalized to the first control timepoint for APP or BACE1 to determine change over time.

2.1.13. Steady-state surface protein measurement

N2a cells were co-transfected as in the retrograde trafficking and recycling assays. Approximately 48 hours after transfection, surface APP and BACE1 were labeled with anti-22C11 or anti-FLAG antibodies prior to cell permeabilization, as in the recycling assay. Following permeabilization, coverslips were immunostained for HA (APP-GFP transfected cells)

or HA and BACE1 as described for the retrograde trafficking assay. Fiji/ImageJ software was used to determine surface APP and BACE1 by outlining each transfected cell and normalizing the fluorescence of surface APP or BACE1 to total APP or BACE1.

2.1.14. Bioinformatics analysis

RNA sequencing data across age groups were collected and produced by the Genotype-Tissue Expression (GTEx) project (https://gtexportal.org/home/). Rab35 transcripts per million were normalized to IPO8 transcripts per million for each sample using Microsoft Excel. RNA sequencing data for Control vs. AD were collected and produced by Nativio, et. al. (Nativio *et al.*, 2020) by aligning RNA-seq reads with STAR v.e.3.0e and annotating them with FeatureCounts v.1.6.2. Data were processed using R to obtain Rab35 and IPO8 transcripts per million. Rab35 transcripts per million were normalized to IPO8 transcripts per million using Microsoft Excel. IPO8 was chosen as a refence gene because it was the most stable gene tested from the GTEx and Nativio *et al.* datasets, using RefFinder (Xie *et al.*, 2012).

2.1.15. Statistical analysis

Graphing and statistics analysis were performed using Prism (GraphPad). Shapiro–Wilk normality test was used to determine whether data sets were modeled by a normal distribution. Unpaired, two-tailed t-tests, one-way ANOVA, or two-way ANOVAs were used with values of $P < 0.05$ being considered as significantly different.

2.2. Methods used for exosome experiments in Chapter 5

2.2.1. Primary neurons and cell lines

Primary cortical neuron cultures were prepared from E18 C57/BL6 mouse embryos or E18 Sprague Dawley rat embryos of either sex using a modified Banker culture protocol (Banker & Goslin, 1998), as described above in the primary neurons and cell lines section for Chapters 3 and 4. Neurons were plated in Neurobasal medium with GlutaMAX (Invitrogen) and N21 supplement (R&D Systems) at a density of 3 million cells per 10 cm dish (dishes treated with Poly-L-Lysine, Sigma). Rat neurons were maintained for 14 DIV, undergoing half-media exchanges at 2 DIV and 7 DIV. Mouse neurons treated with dexamethasone were maintained for 14 DIV, undergoing a full media exchange and dexamethasone treatment at 12 DIV.

Primary cortical astrocyte cultures were prepared from P1-P3 C57/BL6 mouse pups or P1-P3 Sprague Dawley rat pups of either sex using the same dissection techniques as for cortical neurons. Glia were dissociated in TrypLE Express (Invitrogen) for 30 min, washed with Hanks Balanced Salt Solution (Sigma), and centrifuged at 1000 rcf for 15 min. Supernatant containing neurons was aspirated, and the remaining glia were resuspended in DMEM-GlutaMAX (ThermoFisher) with 10% FBS (Atlanta Biological) and 1% Anti-Anti (ThermoFisher). Glia were plated in T75 flasks pre-treated with Poly-L-Lysine (1.5 rat or 3 mouse pups' cortices per flask). Microglia were shaken off of the flask surface at 2 and 7 days after dissection by placing flasks on a vortex (Southwest Science) for 1 min at medium speed. Medium containing microglia was aspirated and replaced with fresh DMEM-GlutaMAX + 10% FBS + Anti/Anti. Rat and mouse embryos were used at separate times because our initial NTA studies were conducted with rat primary cultures, and our updated protocol using ExoView on-chip exosome analysis requires the use of anti-mouse antibodies, for which we use mouse primary cultures.

Neuro2a (N2a) neuroblastoma cells (ATCC CCL-131) and Immortalized mouse MicroGlial (IMG, Millipore) cells were grown and maintained as described above (Chapters 3 and 4 section). Immediately prior to dexamethasone treatment, medium was exchanged to DMEM-GlutaMAX with 10% Exosome-Depleted FBS (Gibco) and Anti-Anti.

2.2.2. DNA transfection

CD63 and CD81 tagged with pHluorin (**Table 2**) were subcloned from the pUC57-GW-Kan vector (Genewiz) into pmCherry-C2 vector (Addgene) at KpnI and BamHI sites to create mCh-pHluorin-CD63 and mCh-pHluorin-CD81. Approximately 1h after plating, N2a and IMG cells were transfected using Lipofectamine 3000, according to the manufacturer's instructions.

2.2.3. Dexamethasone treatments

Primary cortical neurons and astrocytes were treated with dexamethasone (Invivogen, 20uM) for 48h, starting on 12 DIV. N2a and IMG cells were treated with dexamethasone (Invivogen, 10μM) for 24h, starting at 48h after plating or DNA transfection.

Construct	Sequence
pHluorin-CD63	TCTAGAGGTACCAGAGCGGCGCCACCATGGCGGTGGAAGGAGGAATGAAATGTGTGAAGTTCT TGCTCTACGTCCTCCTGCTGGCCTTTTGCGCCTGTGCAGTGGGACTGATTGCCGTGGGTGTCG GGGCACAGAGATCTGGTGGAAGTAAAGGAGAAGAACTTTTCACTGGAGTTGTCCCAATTCTTG TTGAATTAGATGGTGATGTTAATGGGCACAAATTTTCTGTCAGTGGAGAGGGTGAAGGTGATG CAACATACGGAAAACTTACCCTTAAATTTATTTGCACTACTGGAAAACTACCTGTTCCTTGGC CAACACTTGTCACTACTTTAACTTATGGTGTTCAATGCTTTTCAAGATACCCAGATCATATGA AACGGCATGACTTTTTCAAGAGTGCCATGCCCGAAGGTTATGTTCAGGAAAGAACTATATTTT TCAAAGATGACGGGAACTACAAGACACGTGCTGAAGTCAAGTTTGAAGGTGATACCCTTGTTA ATAGAATCGAGTTAAAAGGTATTGATTTTAAAGAAGATGGAAACATTCTTGGACACAAATTGG AATACAACTATAACGATCACCAGGTCTACATCAGGGCAGACAAACAAAAGAATGGAATCAAAG CTAACTTCAAAATTAGACACAACATTGAAGATGGAGGCGTTCAACTAGCAGACCATTATCAAC AAAATACTCCTATTGGCGATGGGCCCGTCCTTTTACCAGACAACCATTACCTGTTTACAACTT CTACTCTTTCGAAAGATCCCAACGAAAAGAGAGACCACATGGTCCTTCTTGAGTTTGTAACAG CTGCTGGGATTACACATGGCATGGATGAACTATACAAAAGATCTCTTGTCCTGAGTCAGACCA TAATCCAGGGGGCTACCCCTGGCTCTCTGTTGCCAGTGGTCATCATCGCAGTGGGTGTCTTCC TCTTCCTGGTGGCTTTTGTGGGCTGCTGCGGGGCCTGCAAGGAGAACTATTGTCTTATGATCA CGTTTGCCATCTTTCTGTCTCTTATCATGTTGGTGGAGGTGGCCGCAGCCATTGCTGGCTATG TGTTTAGAGATAAGGTGATGTCAGAGTTTAATAACAACTTCCGGCAGCAGATGGAGAATTACC CGAAAAATAACCACACTGCTTCGATCCTGGACAGGATGCAGGCAGATTTTAAGTGCTGTGGGG CTGCTAACTACACAGATTGGGAGAAAATCCCTTCCATGTCGAAGAACCGAGTCCCCGACTCCT GCTGCATTAATGTTACTGTGGGCTGTGGGATTAATTTCAACGAGAAGGCGATCCATAAGGAGG GCTGTGTGGAGAAGATTGGGGGCTGGCTGAGGAAAAATGTGCTGGTGGTAGCTGCAGCAGCCC TTGGAATTGCTTTTGTCGAGGTTTTGGGAATTGTCTTTGCCTGCTGCCTCGTGAAGAGTATCA GAAGTGGCTACGAGGTGATGTAGCTCGAGGGATCC
pHluorin-CD81	TCTAGAGGTACCAGAGCGGCGCCACCATGGGAGTGGAGGGCTGCACCAAGTGCATCAAGTACC TGCTCTTCGTCTTCAATTTCGTCTTCTGGCTGGCTGGAGGCGTGATCCTGGGTGTGGCCCTGT GGCTCCGCCATGACCCGCAGAGATCTGGTGGAAGTAAAGGAGAAGAACTTTTCACTGGAGTTG TCCCAATTCTTGTTGAATTAGATGGTGATGTTAATGGGCACAAATTTTCTGTCAGTGGAGAGG GTGAAGGTGATGCAACATACGGAAAACTTACCCTTAAATTTATTTGCACTACTGGAAAACTAC CTGTTCCTTGGCCAACACTTGTCACTACTTTAACTTATGGTGTTCAATGCTTTTCAAGATACC CAGATCATATGAAACGGCATGACTTTTTCAAGAGTGCCATGCCCGAAGGTTATGTTCAGGAAA GAACTATATTTTTCAAAGATGACGGGAACTACAAGACACGTGCTGAAGTCAAGTTTGAAGGTG ATACCCTTGTTAATAGAATCGAGTTAAAAGGTATTGATTTTAAAGAAGATGGAAACATTCTTG GACACAAATTGGAATACAACTATAACGATCACCAGGTCTACATCAGGGCAGACAAACAAAAGA ATGGAATCAAAGCTAACTTCAAAATTAGACACAACATTGAAGATGGAGGCGTTCAACTAGCAG ACCATTATCAACAAAATACTCCTATTGGCGATGGGCCCGTCCTTTTACCAGACAACCATTACC TGTTTACAACTTCTACTCTTTCGAAAGATCCCAACGAAAAGAGAGACCACATGGTCCTTCTTG AGTTTGTAACAGCTGCTGGGATTACACATGGCATGGATGAACTATACAAAAGATCTACCACCA ACCTCCTGTATCTGGAGCTGGGAGACAAGCCCGCGCCCAACACCTTCTATGTAGGCATCTACA TCCTCATCGCTGTGGGCGCTGTCATGATGTTCGTTGGCTTCCTGGGCTGCTACGGGGCCATCC AGGAATCCCAGTGCCTGCTGGGGACGTTCTTCACCTGCCTGGTCATCCTGTTTGCCTGTGAGG TGGCCGCCGGCATCTGGGGCTTTGTCAACAAGGACCAGATCGCCAAGGATGTGAAGCAGTTCT ATGACCAGGCCCTACAGCAGGCCGTGGTGGATGATGACGCCAACAACGCCAAGGCTGTGGTGA AGACCTTCCACGAGACGCTTGACTGCTGTGGCTCCAGCACACTGACTGCTTTGACCACCTCAG TGCTCAAGAACAATTTGTGTCCCTCGGGCAGCAACATCATCAGCAACCTCTTCAAGGAGGACT GCCACCAGAAGATCGATGACCTCTTCTCCGGGAAGCTGTACCTCATCGGCATTGCTGCCATCG TGGTCGCTGTGATCATGATCTTCGAGATGATCCTGAGCATGGTGCTGTGCTGTGGCATCCGGA ACAGCTCCGTGTACTGACTCGAGGGATCC

Table 2. pHluorin-CD63 and pHluorin-CD81 sequences generated by GeneWiz. The tetraspanin proteins CD63 and CD81 were tagged with the pH-sensitive fluorophore pHluorin (highlighted in green) to detect exosome release by live imaging.

2.2.4. Exosome purification: Ultracentrifugation

Extracellular vesicles were isolated from conditioned medium by serial ultracentrifugation at 4ºC using an established protocol (Perez-Gonzalez *et al.*, 2017; Thery *et al.*, 2006). Medium was collected and centrifuged at 3220 x g for 20 min to discard any pelleted cell debris. The remaining medium was centrifuged at 20000 x g for 70 min to discard pelleted larger extracellular components. Medium was then centrifuged at 100000 x g for 70 min to pellet extracellular vesicles. Finally, pellets were washed with 1X PBS, centrifuged again at 100000 x g for 70 min, resuspended in 1 mL of 1X PBS, and stored at -80ºC.

2.2.5. Exosome purification: Size-exclusion chromatography

First, medium was collected and centrifuged at 3220 x g for 20 min to discard any pelleted cell debris. The remaining supernatant was concentrated to a volume of 0.50 – 1.0 mL by centrifugation (3220 x g for 10 min) in Amicon Ultra centrifugal filters (100,000 NMWL; Millipore). Extracellular vesicles were isolated from conditioned medium by size exclusion chromatography (Koh *et al.*, 2018; Lobb & Moller, 2017) using an IZON Automatic Fraction Collector and qEVoriginal columns (35nm; IZON), per the manufacturer's instructions. Extracellular vesicle fractions were collected in 1mL 1X PBS and stored at -80ºC.

2.2.6. Immunoblotting

For immunoblotting experiments, 3 ultracentrifugation-purified extracellular vesicle samples per cell type were concentrated to 15µL using Amicon Ultra centrifugal filters (100,000 NMWL; Millipore) by centrifuging at 3220 x g for 10 min. Samples were diluted and denatured in 2X SDS sample buffer with beta-mercaptoethanol (Bio-Rad) and subject to SDS–PAGE,

transferred to nitrocellulose membranes using wet transfer (Mini Trans-Blot Cell, Bio-Rad), and probed with primary antibody in 5% BSA/PBS + 0.1% Tween-20, followed by DyLight 680 or 800 (anti-rabbit, anti-mouse; Thermo Scientific). Primary antibodies used for western blotting were ALIX (ProteinTech) and TSG101 (Santa Cruz). Membranes were imaged using an Odyssey Infrared Imager (model 9120, LI-COR Biosciences).

2.2.7. Exosome measurements: Nanoparticle tracking analysis (NTA)

Concentrated extracellular vesicle samples were diluted 1:8 for samples collected from primary cultures, and 1:100 for samples collected from cell lines, for a total volume of 1.3mL per sample. Exosome size and concentration were measured by nanoparticle tracking of Brownian motion using ZetaView Nanoparticle Tracking Analyzer (ParticleMetrix). At the time of medium collection, cells were trypsinized and counted to estimate the number of exosomes per cell by dividing the total number of nanoparticles (determined by ZetaView) by the total number of cells.

2.2.8. Exosome measurements: ExoView on-chip interferometry and antibody-based tetraspanin detection

Microarray chips were pre-scanned for particles using ExoView R100 and ExoView Scanner software. Conditioned medium or purified exosome samples were diluted in Solution A (1:5 dilution for primary cultures, 1:100 for cell lines); 35µL of diluted samples were loaded onto microarray chips containing the tetraspanin antibodies CD9 and CD81, and incubated overnight (16h) at room temperature. After several washes with Solutions A and B, samples were incubated with anti-CD9 CF488a, anti-CD81 CF555, and anti-CD63 CF647 antibodies at a final

concentration of 1:1000. Following washes with solutions A and B, microarray chips were placed on a sample chuck and measured by interferometry and fluorescence imaging using ExoView R100 and ExoView Scanner software. Exosome size, number, and tetraspanin profiles were recorded for each sample using ExoView Analyzer; the RIgG and HIgG spots served as negative controls, and only fluorescence values exceeding the baseline RIgG and HIgG fluorescence were counted. All solutions, antibodies, microarray chips, and software were prepared and used per the manufacturer's instructions (ExoView Biosciences).

2.2.9. Live Total Internal Reflection Fluorescence (TIRF) imaging

N2a cells were plated on #1.5 (170μm) Poly-L-Lysine-treated glass-bottom MatTek dishes and maintained in complete medium at 37ºC with 5% CO_2. Cells were transfected with mCh-pHluorin-CD63 and mCh-pHluorin-CD81 approximately 1hr after plating, treated with dexamethasone 48hr after transfection, and imaged 24hr after dexamethasone treatment. Immediately prior to imaging, cell medium was exchanged to normal Tyrode's solution (2 mM $CaCl_2$, 2.5 mM KCl, 119 mM NaCl, 2 mM $MgCl_2$, 20 mM glucose, and 25 mM Hepes, pH 7.4). At least three fields of view were imaged per dish while cells were maintained in a humidity chamber (Tokai Hit) at 37ºC with 5% CO_2. Timelapse images were acquired at 500ms intervals for 3 min using an inverted Nikon Ti Eclipse microscope equipped with piezo Z and electron-multiplying charge-coupled device camera (Andor DU-897). A 100X CFI Apochromat TIRF objective (1.49/0.12 mm, a/0.17 differential interference contrast objective; Nikon) and NIS-Elements software (Nikon) were used for image capture.

2.2.10. Live imaging analysis

Exosome release was measured using Fiji/ImageJ Particle Tracker 2D/3D analysis (Mosaic plugin package) for images taken in the pHluorin channel. Total number of particles per imaging field detected by the plugin were normalized to the total number of cells in the imaging field using Microsoft Excel.

2.2.11. Statistical analysis

Graphing and statistics analyses were performed using Prism (GraphPad). Shapiro–Wilk normality test was used to determine whether data sets were modeled by a normal distribution. Unpaired, two-tailed t-tests, one-way ANOVA, or two-way ANOVAs were used with values of $P < 0.05$ being considered as significantly different.

Chapter 3: Glucocorticoids reduce Rab35 expression, which impacts Aβ production

3.1. Rationale

Chronic stress and elevated glucocorticoids (GCs) increase the risk for Alzheimer's disease (AD), and accelerate its progression (Burke *et al.*, 2018; Csernansky *et al.*, 2006; Johansson *et al.*, 2010; Mejia *et al.*, 2003; Sotiropoulos *et al.*, 2019; Vyas *et al.*, 2016). The pathological hallmarks of AD are the presence of cerebral Tau tangles and amyloid plaques, composed of aggregated amyloid-β (Aβ) peptides that accumulate following the proteolytic cleavage of amyloid precursor protein (APP) (Querfurth & LaFerla, 2010). Elevated levels of Aβ peptides are synaptotoxic, and AD may be initiated by Aβ production (Mucke & Selkoe, 2012). Indeed, familial early-onset forms of AD are caused by autosomal dominant mutations in APP or presenilin genes that promote amyloidogenic processing of APP into Aβ. However, 95% of AD cases are sporadic and late-onset, precipitated by a complex interplay of environmental and genetic risk factors.

In addition to aging, which constitutes the highest risk factor for AD, stress and glucocorticoids have been suggested as precipitating factors of disease (Csernansky *et al.*, 2006; Elgh *et al.*, 2006; Silva *et al.*, 2019; Vyas *et al.*, 2016), increasing Tau accumulation, APP misprocessing and Aβ production (Catania *et al.*, 2009; Green *et al.*, 2006; Sotiropoulos *et al.*, 2011). Interestingly, GC treatment can shift APP metabolism towards the amyloidogenic pathway (Sotiropoulos *et al.* 2008), suggesting that it promotes APP and BACE1 interaction.

Many of the genetic risk factors for late-onset AD (LOAD) are associated with endosomal protein trafficking dysfunction, prolonging the presence of APP and/or BACE1 in endosomes (Small *et al.*, 2017; Ubelmann *et al.*, 2017). The acidic pH of endosomes is optimal

for BACE1 activity (Haass *et al.*, 2012), which leads to Aβ production when APP and BACE1 interact in the endosomal network (Cirrito *et al.*, 2005; Lin Zou *et al.*, 2007).

The GTPase Rab35 is a master regulator of endosomal protein trafficking, and in a previous study, we showed that Rab35 recruits Hrs to initiate ESCRT pathway-mediated degradation of ubiquitylated Tau. We also found that high levels of glucocorticoids downregulated Rab35 in hippocampal neurons, leading to Tau accumulation (Vaz-Silva *et al.*, 2018). These findings demonstrate that GCs precipitate Tau pathology by disrupting Rab35-mediated endolysosomal trafficking. In addition to its role in Tau degradation, Rab35 has also been identified as a negative regulator of Aβ production in a loss-of-function screen of Rab GTPases (Udayar *et al.*, 2013), suggesting that it controls trafficking pathways involved in Aβ generation. However, the mechanisms by which Rab35 reduces Aβ production are yet unclear.

In this chapter, we discover that hippocampal Rab35 GTPase levels are decreased under conditions associated with amyloidogenesis in both rats and humans, and that Rab35 regulates Aβ production through its effects on APP and BACE1 interaction and their presence in endosomal compartments.

3.2. Results

3.2.1. Rab35 levels are decreased under conditions associated with Aβ overproduction

Our previous study showed that treatment with glucocorticoids (GCs) suppresses Rab35 expression in hippocampal neurons *in vivo* (Vaz-Silva *et al.*, 2018). To test whether chronic stress has a similar effect, I monitored the levels of Rabs associated with endocytic protein trafficking (Rabs 5, 7, 8, 11, 14, and 35), in the hippocampi of rats subjected to four weeks of a chronic unpredictable stress paradigm by our collaborators in the Sotiropoulos Lab. The chronic

unpredictable stress consisted of one randomly assigned stressor per day: air dryer, rocking platform, cold water, or overcrowding. I found that hippocampal Rab35 levels were decreased by ~60% in stressed rats compared to controls (**Fig. 6A-B**), and that this decrease was not observed for other Rabs associated with endocytic protein trafficking (**Fig. 6A-B**), in line with our previous findings (Vaz-Silva *et al.*, 2018). In parallel, I monitored hippocampal Rab levels in animals infused with Aβ peptides by our collaborators – a procedure that is widely used to model early AD neuropathology in rodents and primates (Fraustchy *et al.*, 1996; Geula *et al.*, 1998; Stephan & Phillips, 2005). Infused Aβ peptides interact with full-length APP to further stimulate Aβ production (Catania *et al.*, 2009; Davis-salinas *et al.*, 1995; Heredia *et al.*, 2004; Lorenzo *et al.*, 2000) and circumvent the need to overexpress human APP containing mutation(s) that impact its localization and trafficking. Importantly, levels of Rab14 and Rab35, but not most other endocytic Rabs, were similarly decreased in Aβ-infused hippocampi (**Fig. 6A-B**).

Since aging is the greatest risk factor for AD, and previous studies report increased APP misprocessing in the aged brain (Cisternas *et al.*, 2018; Jiang *et al.*, 2010; Kimura *et al.*, 2016), my colleague João Vaz-Silva also compared Rab35 expression levels in hippocampi of young (4 month old) versus aged (22-24 month old) rats. Again, we observed a significant (~25%) decrease in hippocampal Rab35 levels in the aged animals (**Fig. 6C-D**), suggesting downregulation of Rab35 expression with age.

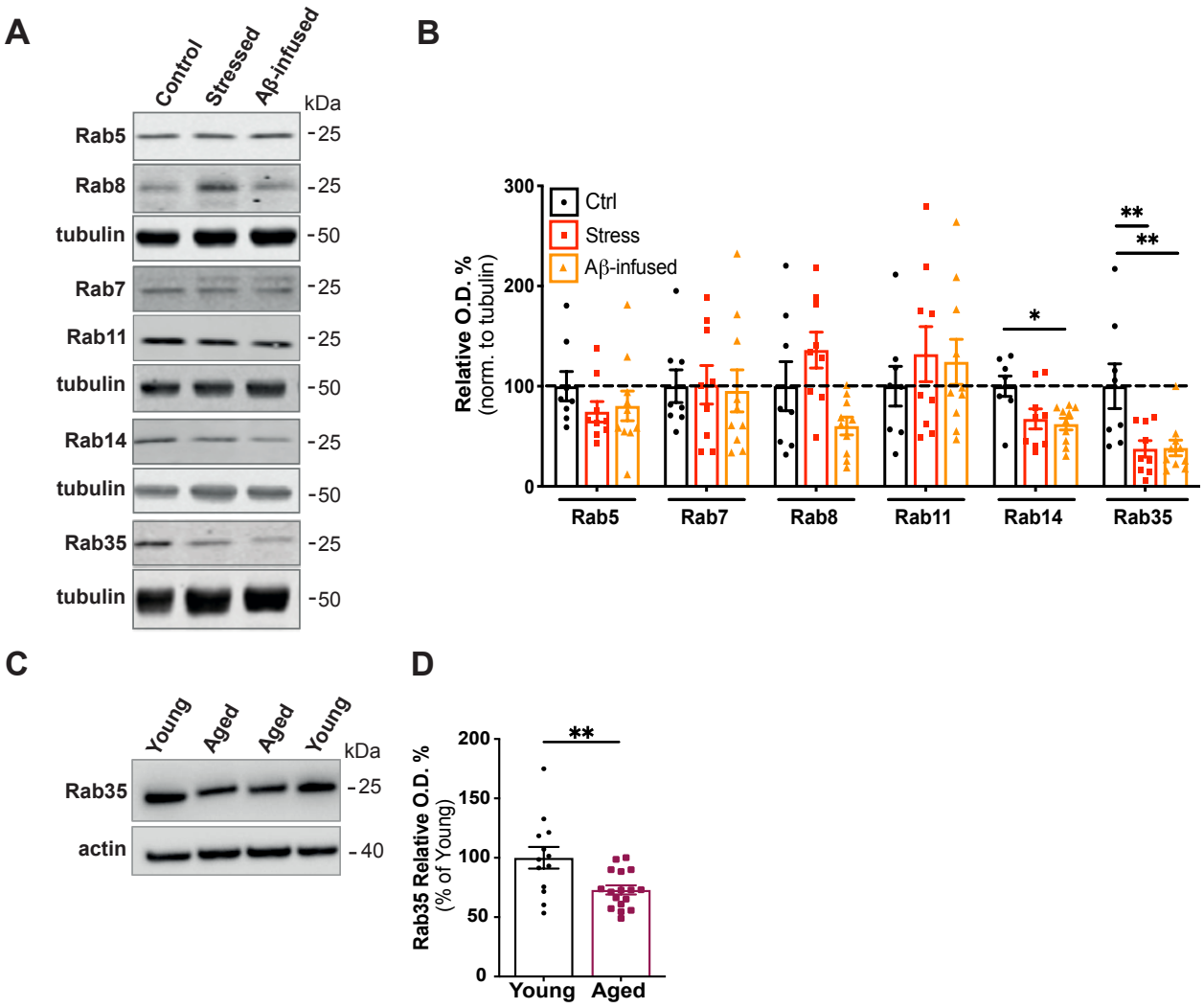

Figure 6. Hippocampal Rab35 levels decrease under stress, Aβ infusion, and aging in rats. A-B) Representative immunoblots and quantification of Rabs 5, 7, 8, 11, 14, and 35 levels in the hippocampus of control (Ctrl), stressed, and Aβ-infused rats. Blots were probed for the noted Rabs and tubulin, with values normalized to tubulin and expressed as percent of the control condition (dotted line). Rab14 and Rab35 levels are reduced by Aβ, but only Rab35 is significantly reduced by both chronic stress and Aβ (**$P_{CON\ vs.\ stressed}$=0.0075, *$P_{CON\ vs.\ Aβ\text{-}infused}$=0.0228, **$P_{CON\ vs.\ Aβ\text{-}infused}$=0.0069, one-way ANOVA with Dunnet's post hoc analysis, n=8–10/condition). **C-D)** Representative immunoblots and quantification of Rab35 levels in the hippocampus of young (4-month-old) and aged (22- to 24-month-old) rats. Blots were probed for Rab35 and actin, with values normalized to actin and expressed as percent of young animals. Rab35 levels are decreased in aged animals (**P=0.0056, unpaired t-test, n=13-17/condition).

To investigate whether aging similarly impacts Rab35 levels in humans, I analyzed gene expression data from the Genotype-Tissue Expression (GTEx) Portal, a collection of data from non-diseased human tissue (https://gtexportal.org/home/). Hippocampal mRNA transcript levels for Rabs 5, 7, 8, 11, 14, and 35 were normalized to those of IPO8, identified by RefFinder (Xie

et al., 2012) as the most stable gene across ages and brain regions of this data set. Intriguingly, I found that Rab11 and Rab35 transcripts were decreased in the hippocampi of individuals 60-79 years of age compared to those who are 20-39, while mRNA expression levels for Rabs 5, 7, 8, and 14 were not altered by aging (**Fig. 7A-B**). Among the endocytic Rab GTPases tested in our rat tissue and the human tissue database, Rab35 was the only Rab GTPase to show a consistent decrease in expression with stress, Aβ infusion, and aging. I therefore probed whether Rab35 levels decrease with age in various brain areas and found that Rab35 mRNA expression is reduced in the hippocampus and frontal cortex of aged individuals, but not in basal ganglia or cervical spinal cord, which are tissues less implicated in stress- and AD-related pathological changes (**Fig. 7C-D**). To determine whether Rab35 levels are similarly altered in the AD brain, my colleague Caroline Magalhaes de Toledo analyzed RNA-Seq data from high quality hippocampal tissue obtained from AD patients and age-matched controls (Nativio *et al.*, 2020). Transcript levels were again normalized to IPO8, and we found that Rab35 transcripts were reduced in the AD vs. control tissue (**Fig. 7E-F**). Together, these findings suggest that Rab35 expression decreases in brain regions impacted by stress, aging, and AD.

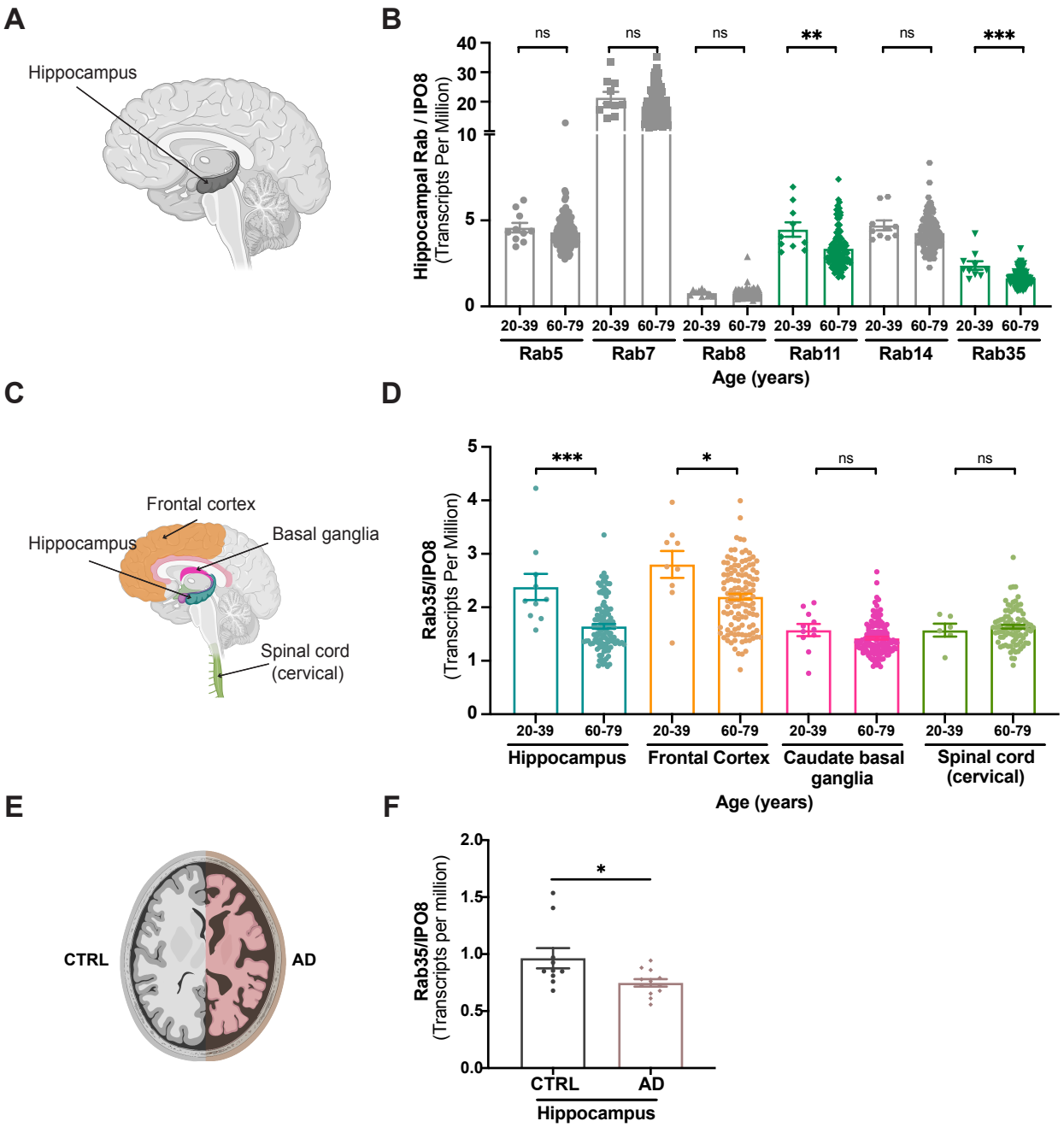

Figure 7. Hippocampal Rab35 levels decrease under conditions associated with amyloidogenesis in humans. A) Schematic diagram of human hippocampus, used for analysis of transcriptome data from the Genotype-Tissue Expression (GTEx) project. **B)** Quantification of hippocampal mRNA transcripts for Rabs 5, 7, 8, 11, 14, and 35 from individuals ages 20-39 years and 60-79 years, normalized to IPO8. Rab11 and Rab35 mRNA expression is decreased in the aged group (**P=0.0026; ***P=0.0003, Mann-Whitney test, n=10-114 samples/condition). **C)** Schematic diagram of human brain areas used for analysis of transcriptome data from the Genotype-Tissue Expression (GTEx) project: hippocampus, frontal cortex, caudate basal ganglia, and the cervical spinal cord. **D)** Quantification of Rab35 mRNA transcripts from individuals ages 20-39 years and 60-79 years, normalized to IPO8 (*P=0.0155, ***P=0.0003, Mann-Whitney test, n=6-135 samples/condition). **E)** Schematic of control and AD human brain. **F)** Rab35 hippocampal RNA expression in age-matched Control (CTRL) vs. Alzheimer's (AD) tissue samples, normalized against IPO8 and displayed as a fraction of control samples, from data collected by Nativio *et al.* (*P=0.03, Mann-Whitney test, n=10-12 samples/condition). All numeric data represent mean ± SEM.

3.2.2. Rab35 is a negative regulator of APP-BACE1 interaction and Aβ production

A previous study identified Rab35 as a negative regulator of Aβ production in a loss-of-function screen of Rab GTPases in non-neuronal cells (Udayar *et al.*, 2013), though the mechanism for this is yet unclear. To confirm these findings, I first determined whether boosting hippocampal Rab35 levels could inhibit APP processing in aged animals. Our collaborating lab injected 17-19 month-old rats with AAV8 to express GFP or GFP-Rab35 in the dorsal hippocampus (see **Fig. 8A**), and I measured the protein levels of APP C-terminal fragments (CTFs) compared to full-length APP. Intriguingly, I found that Rab35 overexpression decreased the levels of both α- and β- CTFs relative to full-length APP (**Fig. 8B-E**). These results suggest that Rab35 inhibits APP processing, and that its reduction during aging and/or stress could contribute to the increased Aβ production observed under these conditions.

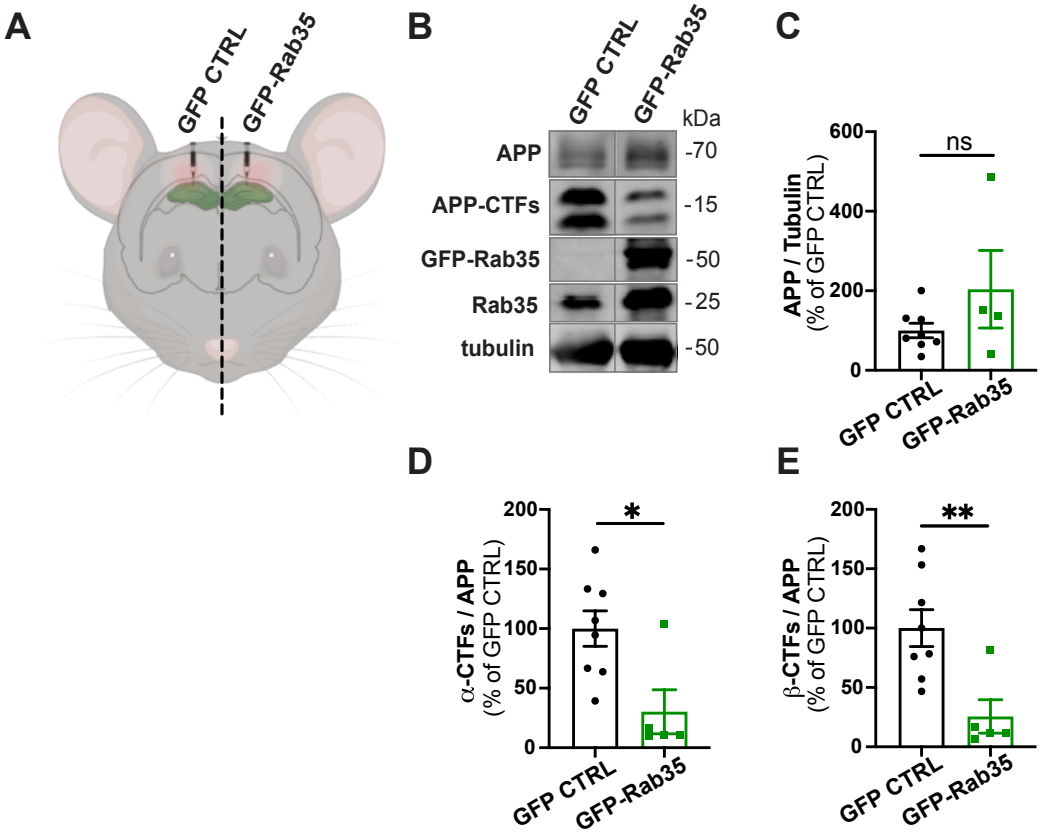

Figure 8. Rab35 overexpression in aged rat hippocampi reduces APP cleavage. A) Schematic of bilateral hippocampal injection of AAV-GFP control or AAV-GFP-Rab35 constructs into aged (22-24 months old) rats. Separate cohorts were used for each condition. **B-E)** Representative immunoblots and quantification of α- and β-APP C-terminal fragments (CTFs) relative to full-length APP in the dorsal hippocampus of aged rats. Blots were probed for APP, Rab35, and tubulin with values normalized to tubulin and expressed as percent of the GFP control condition. Rab35 expression significantly decreases the ratio of CTFs to full-length APP (*P=0.017, **P=0.0048; Welch's unpaired, two-tailed t-test, n=4-8 samples/condition). All numeric data represent mean ± SEM.

To verify that Rab35 impacts APP processing *in vitro*, I measured levels of APP cleavage products in N2a cells co-transfected with APP-GFP and either mCherry alone, mCh-Rab35, or mCh + siRNAs to knock down Rab35 (siRab35; see **Fig. 9A-B**). Here, overexpression of Rab35 significantly decreased (by ~70%) the levels of APP C-terminal fragments (CTFs) relative to total APP, while knockdown of Rab35 significantly increased CTFs (by ~300%; **Fig. 9C-D**).

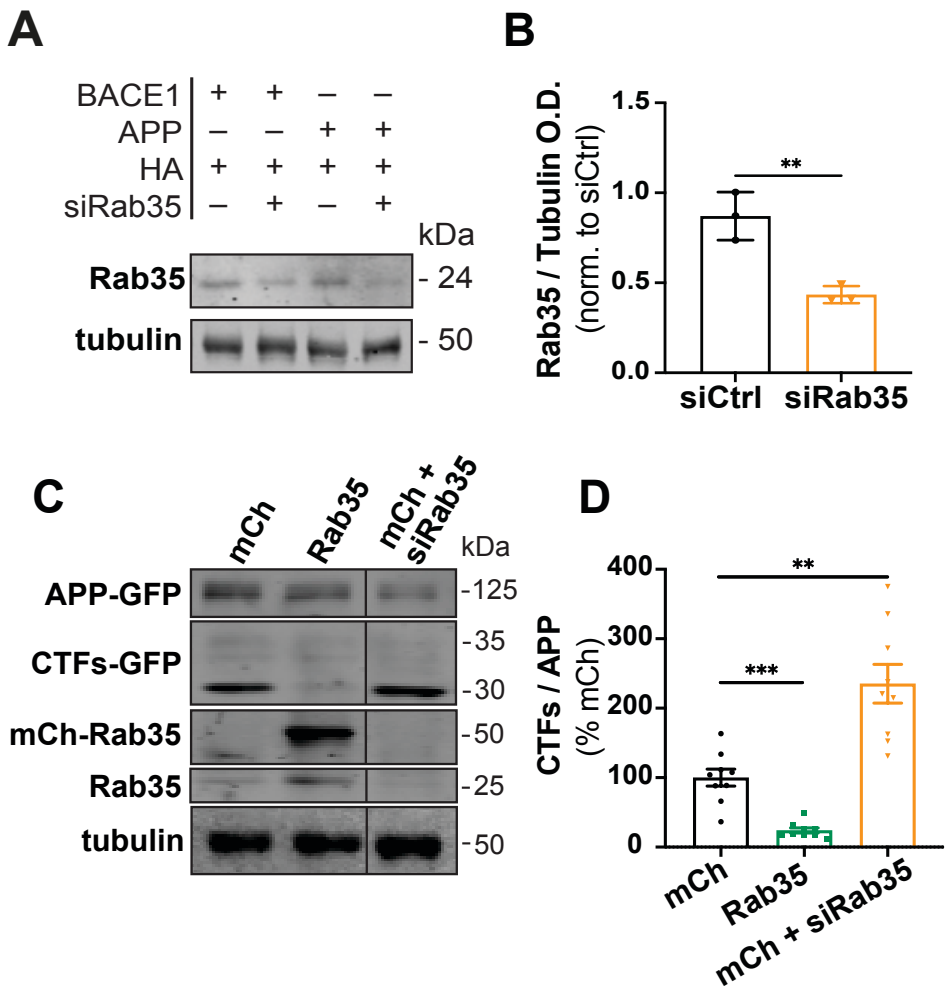

Figure 9. Rab35 overexpression reduces APP cleavage in N2a cells. A-B) Representative immunoblots and quantification of Rab35 knockdown in N2a cells expressing APP-GFP (APP) or FLAG-BACE1 (BACE1), HA control, and a control siRNA (siCtrl) or siRNA to knock down Rab35 (siRab35). Blots were probed for Rab35 and tubulin; values were normalized to tubulin and expressed as a fraction of the siCtrl condition. Cells transfected with siRab35 show a ~55% reduction in Rab35 expression, regardless of whether they co-express APP-GFP or FLAG-BACE1 (**P=0.0059, unpaired two-tailed t-test, n=3 samples/condition). **C-D)** Representative immunoblots and quantification of APP C-terminal fragments (CTFs) from N2a cells expressing mCherry, mCh-Rab35, or mCh + siRab35; blots were probed for GFP, tubulin, and Rab35, with values normalized to tubulin and expressed as percent of mCh control. Overexpression of Rab35 decreases CTFs relative to full-length APP (**P=0.0029, ***P =0.0006, Brown-Forsythe ANOVA with Welch's correction n=9 independent samples/condition). All numeric data represent mean ± SEM.

A decrease in CTFs was also observed in lysates from human induced pluripotent stem cell (iPSC)-derived cortical neurons lentivirally transduced with mCh or mCh-Rab35 (**Fig. 10A-B**). To determine whether levels of APP CTFs corresponded to Aβ production, we measured the concentration of Aβ40 and Aβ42 peptides in medium collected from these human-derived neurons. Indeed, Rab35 overexpression decreased the levels of both Aβ40 and Aβ42 by 20% (**Fig. 10C-D**). Together, these results indicate that Rab35 inhibits APP cleavage and the subsequent generation of Aβ peptides.

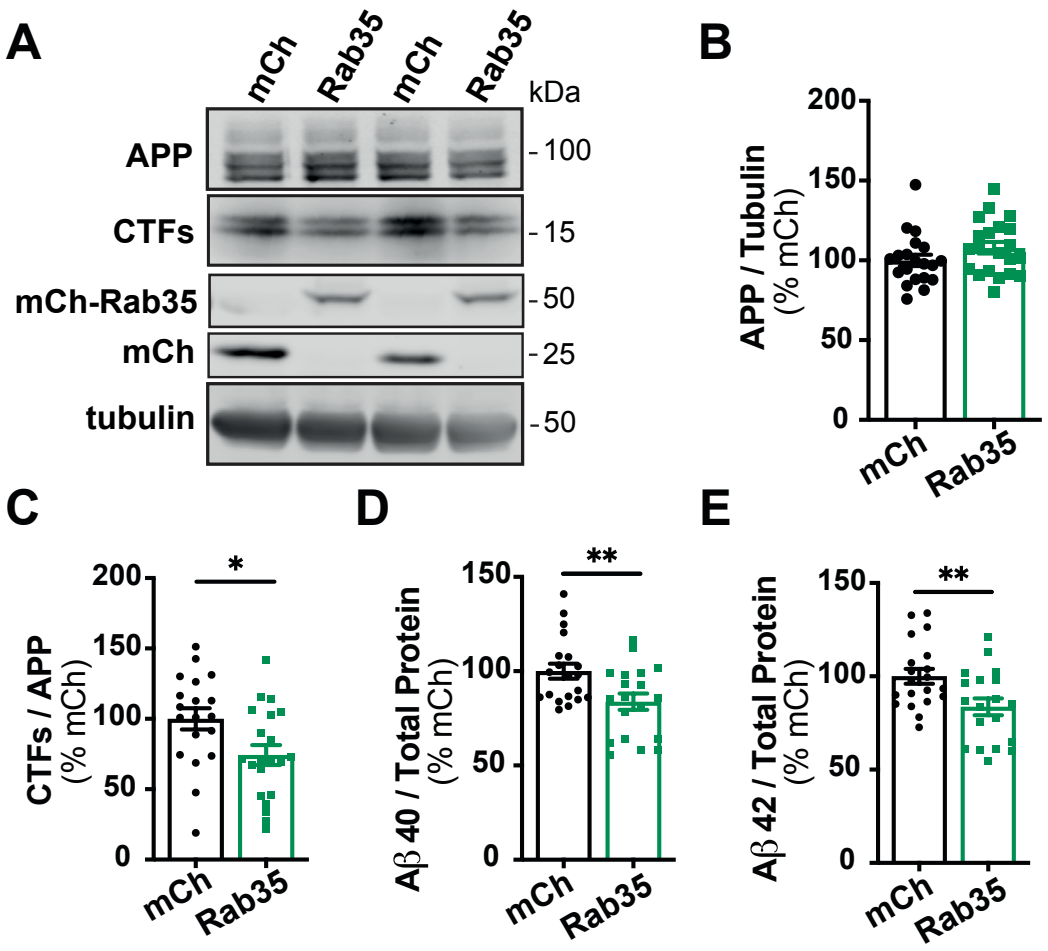

Figure 10. Rab35 overexpression suppresses amyloidogenic processing of APP in iPSC-derived cortical neurons. A-C) Representative immunoblots and quantification of APP C-terminal fragments (CTFs) from iPSC-derived cortical neurons expressing mCherry or mCh-Rab35. Blots were probed for APP/CTFs, tubulin, and mCherry, with values normalized to tubulin and expressed as percent of mCh control. Overexpression of Rab35 does not affect full-length APP expression but decreases CTFs relative to full-length APP (*P=0.017, unpaired t-test, n=19-21 samples/condition). **D-E)** Measurement of Aβ peptides secreted by iPSC-derived human neurons transduced with mCherry or mCh-Rab35. Values are normalized to total secreted protein and expressed as percent of mCh control. Rab35 overexpression decreases the levels of both Aβ40 (D) and Aβ42 peptides (E) (**$P_{A\beta40}$=0.008, **$P_{A\beta42}$=0.009, unpaired t-test, n=19-20 samples/condition, 4 independent cultures). All numeric data represent mean ± SEM.

To understand how Rab35 regulates APP processing at the subcellular level, we examined its effect on the interaction between APP and BACE1, required for the rate-limiting cleavage step of APP into Aβ. As a readout of APP-BACE1 interaction, we utilized a previously-published bimolecular fluorescence complementation (BiFC) assay in which APP is tagged with an N-terminal fragment of Venus fluorescent protein (APP:VN), and BACE1 with

the complementary C-terminal fragment (BACE:VC) (Das *et al.*, 2015) (see **Fig. 11A**). I used flow cytometry to analyze the mean Venus fluorescence intensity in mouse neuroblastoma (N2a) cells co-expressing APP:VN, BACE:VC, and HA-tagged Rab GTPases (for Rab gain-of-function), with Alexa(R)-647-labeled HA antibody identifying the Rab-expressing cells in which Venus fluorescence was measured (**Fig. 11B**). Compared to average Venus fluorescence across the 16 Rab GTPases investigated (**Fig. 11C**), I found that Rab35 gain-of-function decreased the Venus signal by 25% (**Fig. 11C**).

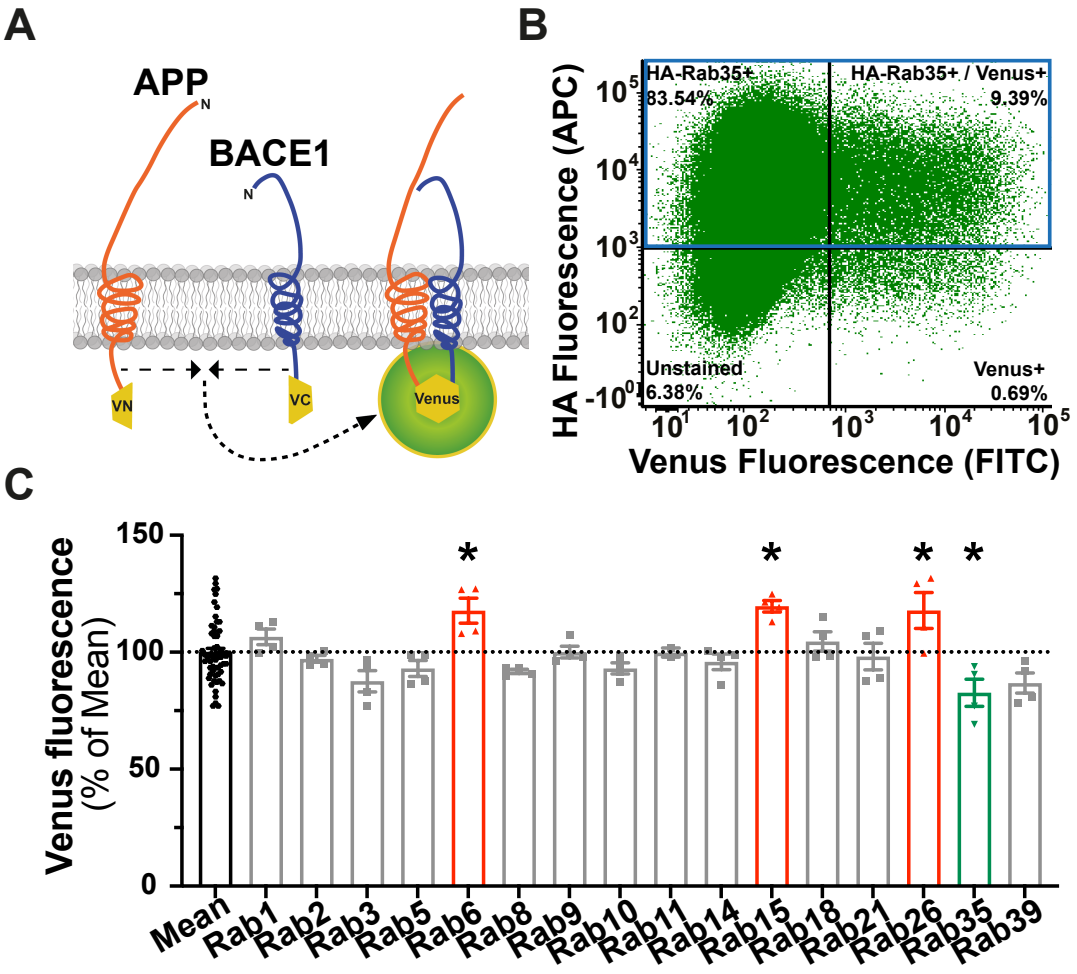

Figure 11. Rab35 reduces APP-BACE1 interaction in a screen using Venus Bi-Molecular Fluorescence complementation. A) Schematic diagram of bimolecular fluorescence complementation assay, in which APP and BACE1 are tagged with complementary fragments of Venus fluorescent protein (VN and VC, respectively). Reconstitution of Venus occurs upon close interaction between APP and BACE1, generating fluorescent signal. **B)**

Representative fluorescence activated cell sorting (FACS) plot of N2a cells co-expressing HA-Rab35 (HA-Rab35+), APP:VN, and BACE:VC (Venus+), as used for analyses in C. The number of HA-Rab35+ cells expressing low or no Venus fluorescence (top left quadrant) is greater than the number of HA-Rab35+ cells expressing high Venus fluorescence (top right quadrant). **C)** Quantification of Venus fluorescent protein (VFP) intensity in N2a cells overexpressing the indicated Rab GTPases. Venus fluorescence for each Rab is normalized to average VFP fluorescence of the entire Rab-expressing cell population (Mean). Rab35 is a negative regulator, and Rabs 6, 15, and 26 are positive regulators of APP-BACE1 interaction ($*P_{Rab6}$=0.0385, $*P_{Rab15}$=0.0135, $*P_{Rab26}$=0.0371, $*P_{Rab35}$=0.0468; one-way ANOVA, with Dunnet's post-hoc analysis; n=4 independent samples across 2 experiments, approximately 80,000 cells/condition). All numeric data represent mean ± SEM.

To confirm these findings, João Vaz-Silva performed quantitative fluorescence microscopy of N2a cells co-transfected with APP:VN and BACE:VC together with mCh, mCh-Rab35, or mCh co-expressed with an shRNA previously shown to knockdown Rab35 (shRab35; Sheehan *et al.*, 2016). Here, Rab35 overexpression again decreased Venus fluorescence by 70% compared to mCh control, suggesting reduced APP-BACE1 interaction, while Rab35 knockdown increased Venus fluorescence by 200% (**Fig. 12A-B**). Rab35 overexpression and knockdown had similar effects on the size of Venus puncta, with overexpression decreasing puncta size and knockdown increasing their size, magnifying the total fluorescence signal (**Fig. 12C**).

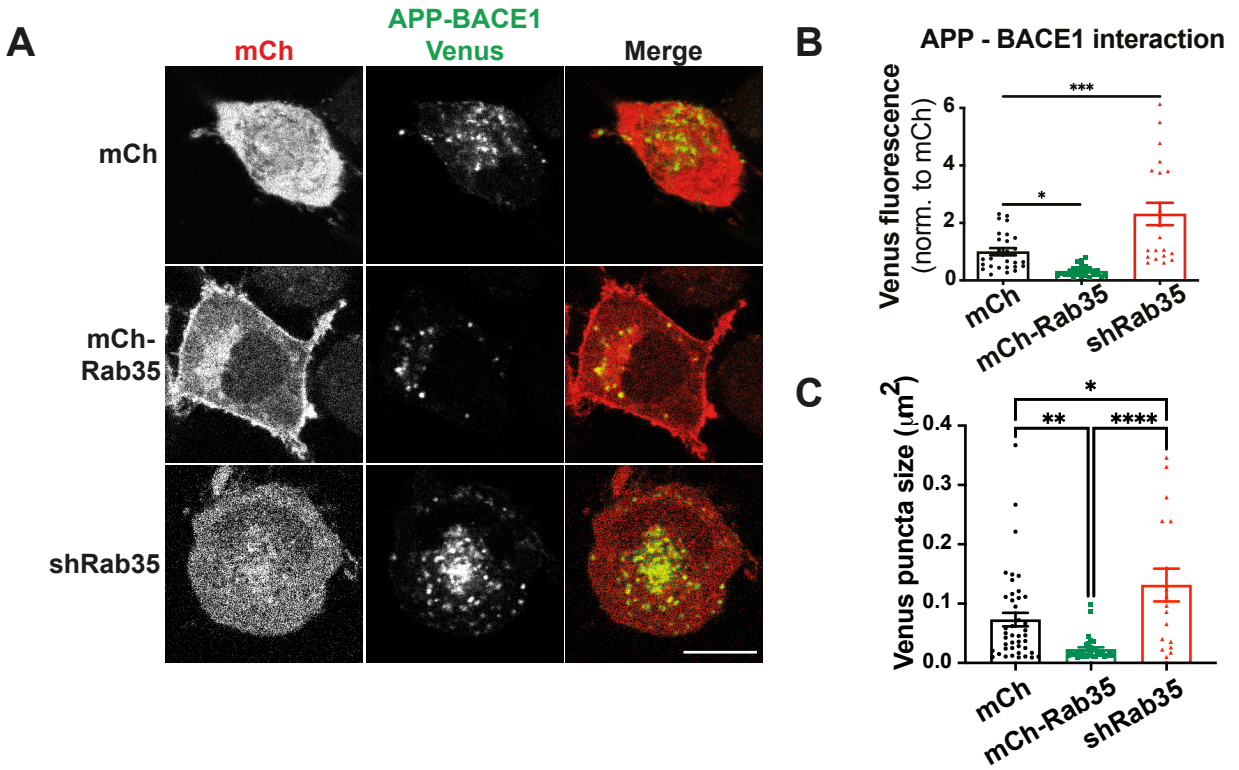

Figure 12. Rab35 is a negative regulator of APP-BACE1 interaction in N2a cells. A-C) Representative images and quantification of Venus fluorescence in N2a cells expressing APP:VN, BACE:VC, and either mCh, mCh-Rab35, or shRab35. **B)** Rab35 overexpression significantly decreases, and knockdown increases, Venus fluorescence intensity compared to mCh control (*P=0.042, ***P=0.0001, one-way ANOVA, with Dunnet's post-hoc analysis, n=21-27 cells/condition, 2 experiments). **C)** Venus puncta size in N2a cells expressing mCh, mCh-Rab35, or shRab35. Rab35 overexpression decreases, and knockdown increases, puncta size (*P=0.0142, **P=0.0077, ****P<0.0001, by one-way ANOVA with Tukey's multiple comparisons test, n=17-43 cells/condition, 2 experiments). Scale bar: 10 μm. All numeric data represent mean ± SEM.

We further assessed the impact of Rab35 on endogenous APP-BACE1 interaction in primary rat hippocampal neurons, using the proximity ligation assay (PLA) in neurons transduced either with mCh, mCh-Rab35, or mCh + shRab35 (see **Fig. 13A**). Though it is possible that Rab35 interferes with Venus reconstitution in the BiFC experiments in N2a cells, our PLA data was consistent with the BiFC experiments, revealing that Rab35 overexpression in primary hippocampal neurons significantly decreased the number of PLA puncta in cell bodies (from 6 to 4.5 puncta/250 μm^2), representing colocalized APP and BACE1 (**Fig. 13B-C**). Rab35 knockdown did not affect APP-BACE1 interaction, indicating that the PLA assay is not sensitive

enough to detect increases in this interaction (**Fig. 13B-C**). Overall, these findings demonstrate that Rab35 is an important regulator of APP-BACE1 interaction in neurons.

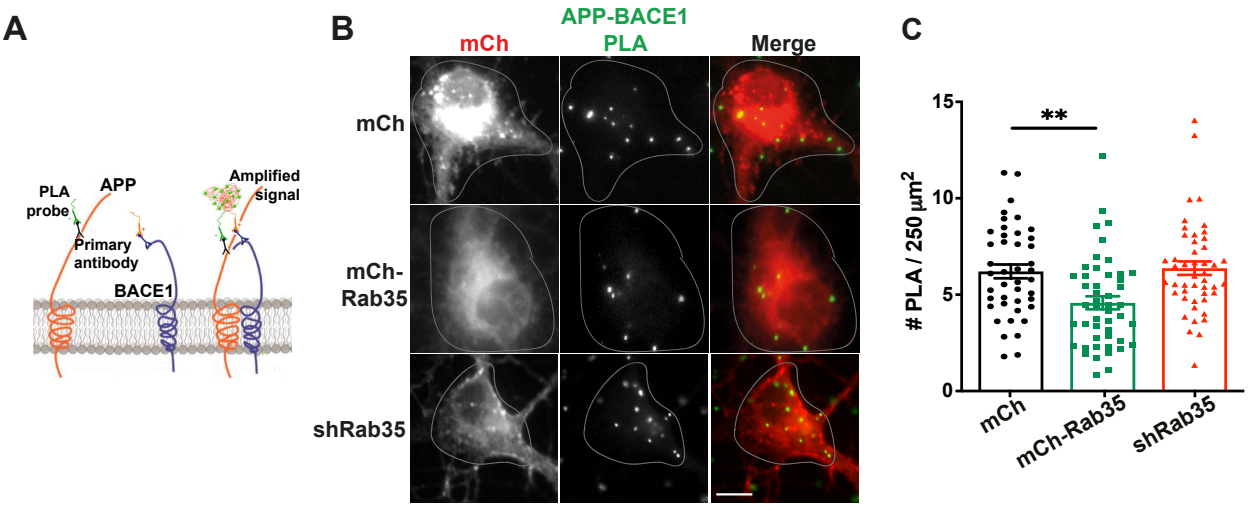

Figure 13. Rab35 is a negative regulator of APP-BACE1 interaction in hippocampal neurons. A) Schematic diagram of the proximity ligation assay (PLA). APP (orange) and BACE1 (purple) are tagged with primary antibodies, which are then recognized by anti-mouse and anti-rabbit PLA probes. When the probes are in close proximity, they produce a signal marking protein-protein interaction. **B-C)** Images and quantification for proximity ligation assay (PLA) to detect endogenous APP-BACE1 interaction in primary hippocampal neurons expressing mCh, mCh-Rab35, or shRab35. Overexpression of Rab35 decreases PLA puncta density in neuronal cell bodies compared to mCh control, while knockdown has no effect (**P=0.001, unpaired two-tailed t-test, n=43-44 cells/condition, 2 independent cultures). Scale bar: 10 µm. All numeric data represent mean ± SEM.

Given that APP is cleaved by BACE1 primarily in endosomes (Haass *et al.*, 2012), our findings suggest that Rab35 impacts APP and/or BACE1 trafficking and localization in the endosomal network. We therefore examined the effects of Rab35 overexpression and knockdown on endogenous APP and BACE1 colocalization with Rab11-positive recycling endosomes in hippocampal neurons (see **Fig. 14A, D**), a common site of APP cleavage by BACE1 (Bera *et al.*, 2020; Buggia-Prevot *et al.*, 2014; Chia *et al.*, 2013; Das *et al.*, 2015; Tan & Gleeson, 2019). Indeed, my colleague Mei Zhu found that Rab35 overexpression decreased both APP and BACE1 colocalization with Rab11 in the somatodendritic compartment by nearly one fourth (18% for APP and 25% for BACE1), while Rab35 knockdown increased colocalization by a similar amount (32% for APP and 21% for BACE1; **Fig. 14A-F**). Although Rab35

overexpression decreased the density of Rab11 endosomes (**Fig. 14H**), I found that its gain- and loss-of-function had no effect on endosome size (**Fig. 14H**), indicating that the observed changes in colocalization were not due to gross effects of Rab35 on the morphology of Rab11 endosomes. Rather, our findings suggest that Rab35 promotes APP and BACE1 sorting out of recycling endosomes.

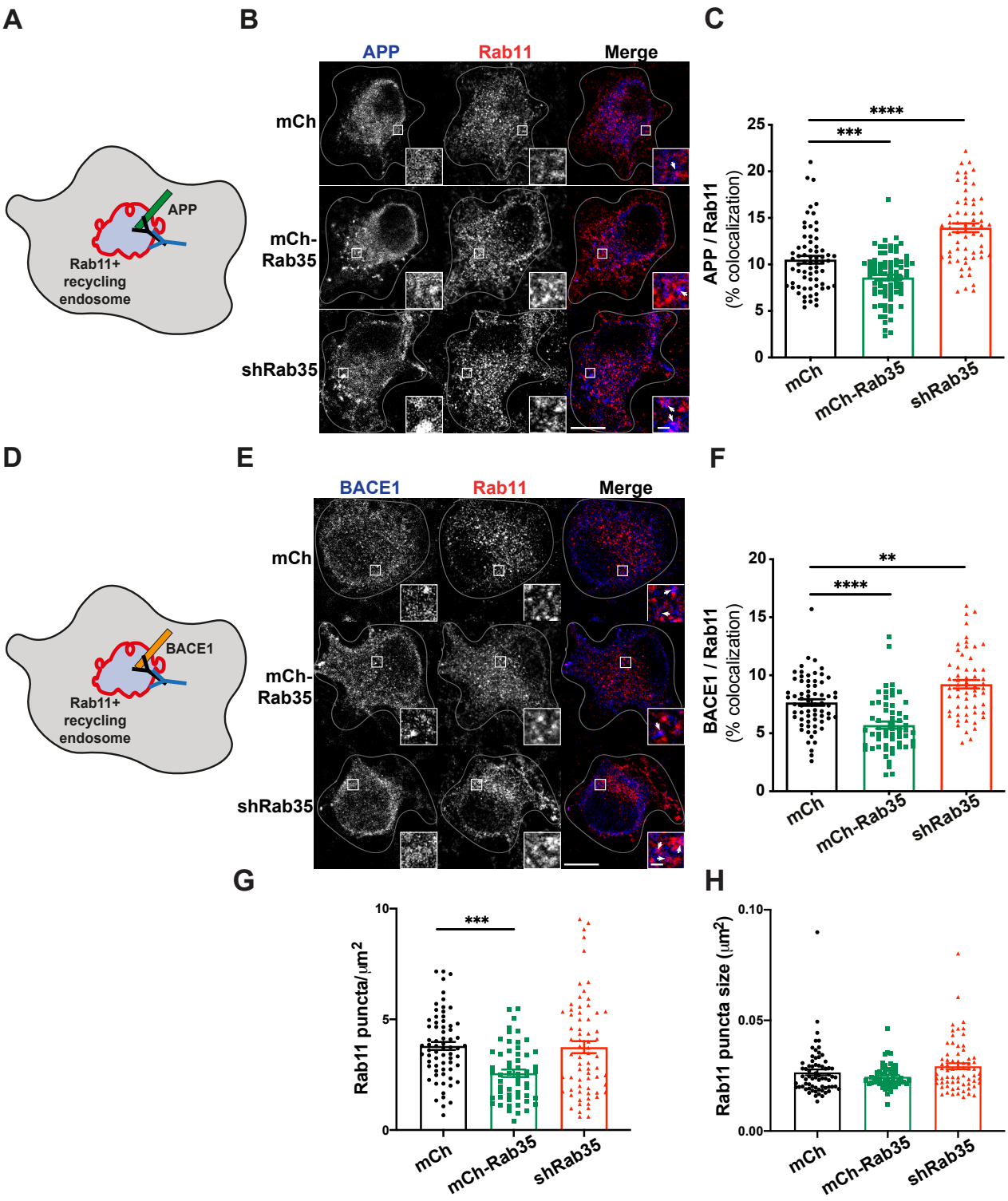

Figure 14. Rab35 regulates APP and BACE1 endosomal distribution in hippocampal neurons. A) Schematic representing colocalization between anti-APP antibody (blue) and Rab11-positive recycling endosomes (red) in primary hippocampal neurons. **B-C)** Representative images and quantification of APP colocalization with Rab11-positive recycling endosomes in 14 DIV hippocampal neurons expressing mCh, mCh-Rab35, or shRNA to knockdown Rab35 (shRab35). Compared to mCh control, Rab35 overexpression decreases APP colocalization with Rab11, while Rab35 knockdown has the opposite effect (***P=0.001, ****P<0.0001, one-way ANOVA, Dunnet post-hoc analysis,

n=62–78 cells/condition, 3 independent cultures). **D)** Schematic representing colocalization between anti-BACE1 antibody (blue) and Rab11-positive recycling endosomes (red) in primary hippocampal neurons. **E-F)** Representative images and quantification of BACE1 colocalization with Rab11 in 14 DIV hippocampal neurons. Rab35 overexpression decreases, and knockdown increases, BACE1 colocalization with Rab11 compared to mCh control (**P=0.001, ****P<0.0001, one-way ANOVA, Dunnett's post-hoc analysis, n=58-66 cells/condition, 3 independent cultures). Scale bars: 10 µm, 1 µm for zoomed insets. **G-H)** Quantification of Rab11 puncta density **(G)** and size **(H)**, showing that Rab35 overexpression reduces Rab11 puncta density but not size (**P=0.0002, one-way ANOVA with Dunnett's post hoc analysis, n=56-68 cells/condition, 3 independent cultures). All numeric data represent mean ± SEM.

3.3. Summary

Lifetime stress is a precipitating factor for AD, and can accelerate the disease. Stress has been shown to increase Aβ production, synaptic atrophy, and cognitive and mood deficits (Catania *et al.*, 2009; Lopes *et al.*, 2017; Sotiropoulos *et al.*, 2011). Aβ accumulation in AD and aging has been well-documented in humans (Fjell *et al.*, 2014; Rodrigue *et al.*, 2009) and rodents (Cisternas *et al.*, 2018; Kimura *et al.*, 2016), underscoring the need for investigating the molecular mechanisms of amyloidogenic APP processing. Previously, we showed that stress downregulates Rab35 and leads to increased Tau accumulation (Vaz-Silva *et al.*, 2018), but the roles of stress/GCs and Rab35 in APP amyloidogenic processing remain poorly understood.

In this chapter, I describe that Rab35 protein expression was reduced by stress, Aβ-infusion, and aging in the rat hippocampus. I also show that Rab35 RNA transcript levels were reduced in aged (60-79 years of age) vs. young (20-39 years of age) humans, and in AD patients vs. age-matched controls. Together, these data indicate that Rab35 levels are reduced by conditions associated with Aβ production in rodents and humans. Furthermore, our lab identified Rab35 as a negative regulator of APP-BACE1 interaction, which is necessary for Aβ production. I show that among 16 tested Rab GTPases, Rab35 most potently reduced APP-BACE1 interaction, and that Rab35 had these effects on endogenous APP-BACE1 interaction in hippocampal neurons. Moreover, we discover that this decrease in APP-BACE1 interaction has

functional consequences: Rab35 reduced APP CTFs in N2a cells and iPSC-derived cortical neurons. This is an intriguing result because β-C-terminal fragments (β-CTFs) have been shown to promote Tau hyperphosphorylation and accumulation (Moore *et al.*, 2015), and to impair endosomal protein sorting (Moore *et al.*, 2015; Willen *et al.*, 2017), further contributing to the dysregulation of intracellular trafficking in AD. We also show that this inhibition of APP cleavage also reduced secreted Aβ40 and Aβ42 in iPSC-derived neurons, indicating that Rab35-mediated decreases in APP-BACE1 interaction functionally reduce amyloidogenic cleavage and Aβ production.

Because Rab35 regulates intracellular protein trafficking through the endosomal network, I propose that Rab35 decreases APP-BACE1 interaction by limiting the presence of APP and BACE1 in endosomal compartments. Indeed, we show that Rab35 reduced both APP and BACE1 colocalization with Rab11-positive endosomes in hippocampal neurons. Together, the data presented in this chapter suggest that stress downregulates Rab35 expression, thereby enhancing Aβ generation through the increased interaction of APP and BACE1 in endosomal compartments.

Chapter 4: Rab35 sorts APP and BACE1 into distinct trafficking pathways, which may be disrupted by stress/GCs

4.1. Rationale

In chapter 3, we learned that Rab35 reduces APP-BACE1 interaction, Aβ production, and APP/BACE1 presence in endosomal compartments, where amyloidogenic cleavage of APP occurs. These results suggest that Rab35 either promotes the degradation of APP and/or BACE1, or that it mediates the sorting of these proteins into pathways that reduce their residence time in endosomes. In previous studies, we have shown that Rab35 recruits the ESCRT pathway, facilitating the degradation of synaptic vesicle proteins and Tau (Sheehan *et al.*, 2016; Vaz-Silva *et al.*, 2018). Rab35 also mediates protein retrograde trafficking from endosomes to the trans-Golgi network, such as that of the mannose-6-phosphate receptor (Cauvin *et al.*, 2016), and fast protein recycling to the plasma membrane, such as that of T-cell receptors and cell adhesion molecules (Allaire *et al.*, 2013; Argenzio *et al.*, 2014; Kouranti *et al.*, 2006; Patino-Lopez *et al.*, 2008). Given the multiple trafficking events regulated by Rab35, and its role in reducing APP-BACE1 interaction, it is possible that glucocorticoid (GC)-mediated downregulation of Rab35 impacts APP or BACE1 trafficking to modulate stress-induced Aβ production.

In this chapter, I investigate the role of Rab35 and GCs in APP and BACE1 trafficking pathways. I assess whether Rab35 mediates the degradation, retrograde trafficking, or fast recycling of APP and BACE1 and discover that Rab35 regulates BACE1 retrograde trafficking to the Trans-Golgi Network through the effector OCRL, and APP recycling to the plasma membrane through ACAP2. Furthermore, I test whether GC administration, which mimics stress in cells, dysregulates Rab35-mediated trafficking pathways of APP and/or BACE1. I find that GCs increase APP-BACE1 interaction and slow APP and BACE1 recycling, which can be

blocked by Rab35 overexpression. Together, these data reveal that Rab35 serves as a molecular link between stress and Aβ generation by mediating the intracellular trafficking pathways of APP and BACE1.

4.2. Results

4.2.1. Rab35 promotes BACE1 trafficking through the retrograde pathway

Given that Rab35 mediates protein degradation through the endolysosomal pathway (Sheehan *et al.*, 2016; Vaz-Silva *et al.*, 2018), we examined whether Rab35 decreases APP-BACE1 interaction and Aβ production by stimulating the degradation of APP and/or BACE1. Using a previously described cycloheximide (CHX)-chase assay to measure protein degradation by blocking the translation of new proteins (Miranda *et al.*, 2018; Sheehan *et al.*, 2016), João Vaz-Silva and I found that Rab35 gain- or loss-of-function did not alter the degradation rate of APP, APP CTFs, or BACE1 in hippocampal neurons (**Fig. 15**).

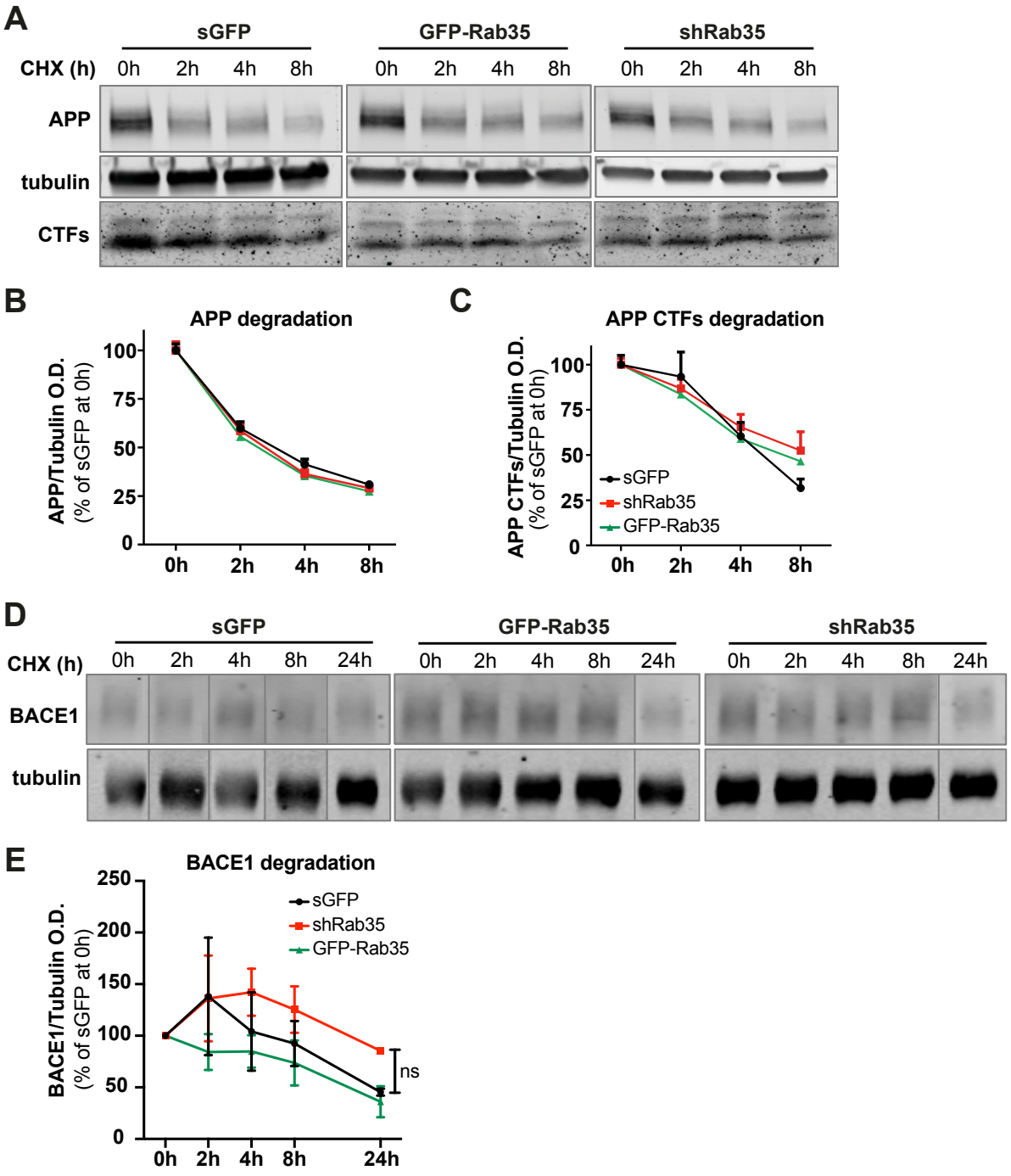

Figure 15. Rab35 does not alter degradation of APP, CTFs, or BACE1 in hippocampal neurons. A-C) Representative immunoblots and quantification of APP and APP CTF degradation in 14 DIV hippocampal neurons transduced with GFP, GFP-Rab35 or shRab35. Neurons were treated with cycloheximide (CHX) for 0, 2, 4 or 8 hours, and probed for APP and tubulin. Values were normalized to tubulin and expressed as percent of protein levels at 0h. Modulation of Rab35 levels does not alter APP and/or CTF degradation (n_{APP}=7-8 independent samples per condition/timepoint, n_{CTFs}=5-6 independent samples per condition/timepoint). **D-E)** Representative immunoblots and quantification of BACE1 degradation in 14 DIV hippocampal neurons transduced with GFP, GFP-Rab35 or shRab35, treated with CHX for 0, 2, 4, 8, or 24 hours, and probed for BACE1 and tubulin. Values were normalized to tubulin and expressed as percent of protein levels at 0h. Modulation of Rab35 levels does not alter BACE1 degradation (n=3-4 independent samples per condition/timepoint). All numeric data represent mean ± SEM.

Since Rab35 also regulates the retrograde trafficking of mannose-6-phosphate receptors from endosomes to the trans-Golgi network (TGN) (Cauvin *et al.*, 2016), I next examined whether Rab35 similarly promotes the retrograde trafficking of APP and/or BACE1. Here, I used a modified antibody feeding assay (Ubelmann *et al.*, 2017; Vieira *et al.*, 2010) in N2a cells, which are more amenable to trafficking assays than neurons. This assay was coupled with immunofluorescence microscopy to monitor the colocalization of internalized APP-GFP or FLAG-BACE1 with the TGN marker syntaxin-6 at several timepoints after antibody labeling (**Fig. 16**).

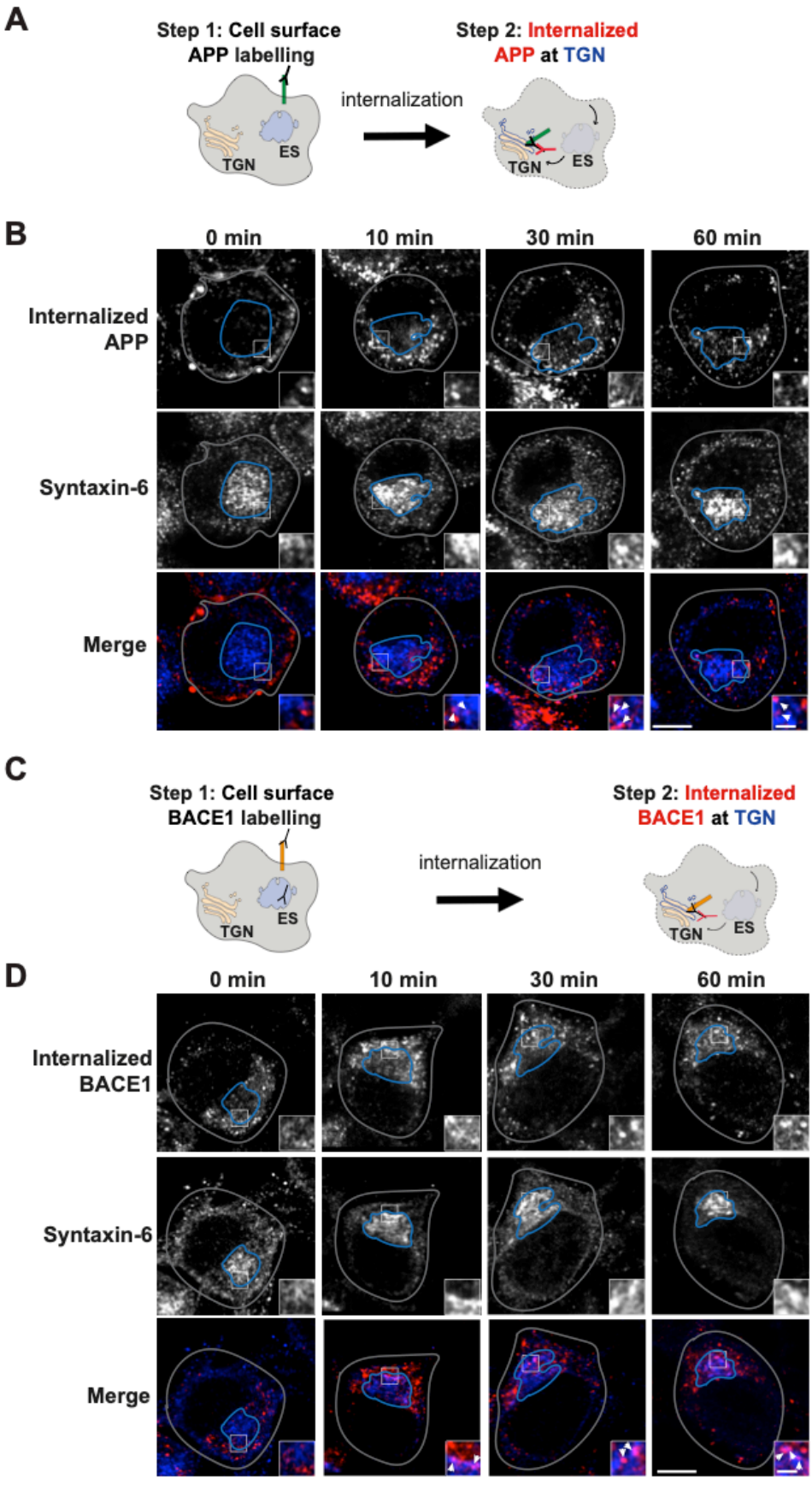
A
Step 1: Cell surface
APP labelling
internalization
Step 2: Internalized
APP at TGN
TGN
ES
B
0 min
10 min
30 min
60 min
Internalized
APP
Syntaxin-6
Merge
C
Step 1: Cell surface
BACE1 labelling
internalization
Step 2: Internalized
BACE1 at TGN
D
Internalized
BACE1

Figure 16. Retrograde trafficking assay timecourse for APP and BACE1. A) Schematic representation of APP retrograde trafficking assay, in which cell-surface APP was labeled with 22C11 antibody, cells were incubated for 0, 10, 30 or 60 minutes to allow for APP internalization, and finally, cells were immunostained with syntaxin-6 antibodies to label the TGN. **B)** Representative images of APP retrograde trafficking timecourse in control cells, with cells outlined in gray, the TGN area outlined in blue, and white arrowheads pointing to areas of colocalization in insets. APP colocalization with the TGN (insets) increases up to the 30 min chase timepoint and reduces at 60 min. **C)** Schematic representation of BACE1 retrograde trafficking assay. Surface FLAG-BACE1 was labeled with FLAG antibody. **D)** Representative images of BACE1 retrograde trafficking timecourse, showing BACE1 colocalization with the TGN (insets) increasing over the timecourse. Scale bars: 5 μm; 1 μm for zoomed insets. ES: Endosomal structure; TGN: trans-Golgi network.

In the case of APP, I found that Rab35 overexpression did not alter its colocalization with syntaxin-6 at any timepoint post-labeling compared to the control condition (**Fig. 17**). To verify that I was primarily tracking full-length APP vs. an N-terminal APP ectodomain fragment to which the APP antibody (22C11) is raised, I measured the colocalization between 22C11 and the C-terminal GFP tag of APP (**Fig. 18A-B**). While colocalization of these signals was ~50% (**Fig. 18B**), this measurement significantly underestimated the degree of colocalization due to saturating perinuclear levels of APP-GFP, which obscured dimmer puncta in the periphery where the majority of 22C11 signal was located (**Fig. 18A-B**). Moreover, shedding of the APP ectodomain is expected to occur at the plasma membrane, as evidenced by studies that enhanced APP ectodomain shedding by inhibiting APP internalization (Carey *et al.*, 2005; Haass *et al.*, 2012; Lichtenthaler, 2006). This APP ectodomain cleavage would lead to rapid diffusion of sAPP fragments into the medium rather than their recycling to the TGN. Together, these results indicate that Rab35 does not mediate the retrograde trafficking of APP.

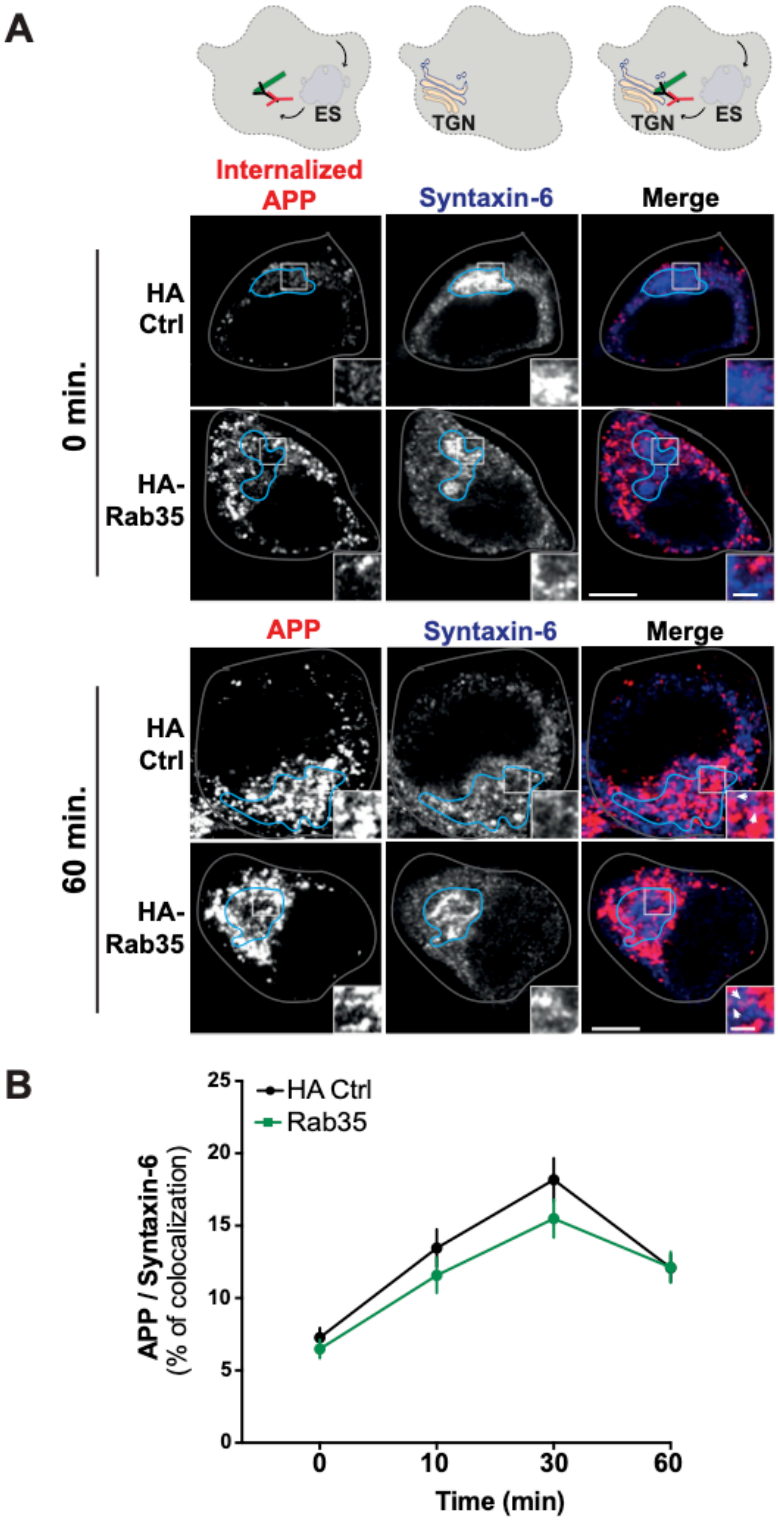

Figure 17. Rab35 does not affect APP retrograde trafficking in N2a cells. A-B) Representative images and quantification of N2a cells expressing APP-GFP and HA vector control or HA-Rab35. Internalized APP (red) and syntaxin-6 (blue) are shown at 0 and 60 min timepoints post-labeling. Overexpression of Rab35 does not significantly alter the colocalization of internalized APP with syntaxin-6 at any timepoint, indicating no change in retrograde trafficking (n=53-69 cells per condition/timepoint, 3 experiments). Scale bars: 5 µm, 1 µm for zoomed insets. All numeric data represent mean ± SEM. ES: Endosomal structure; TGN: trans-Golgi network.

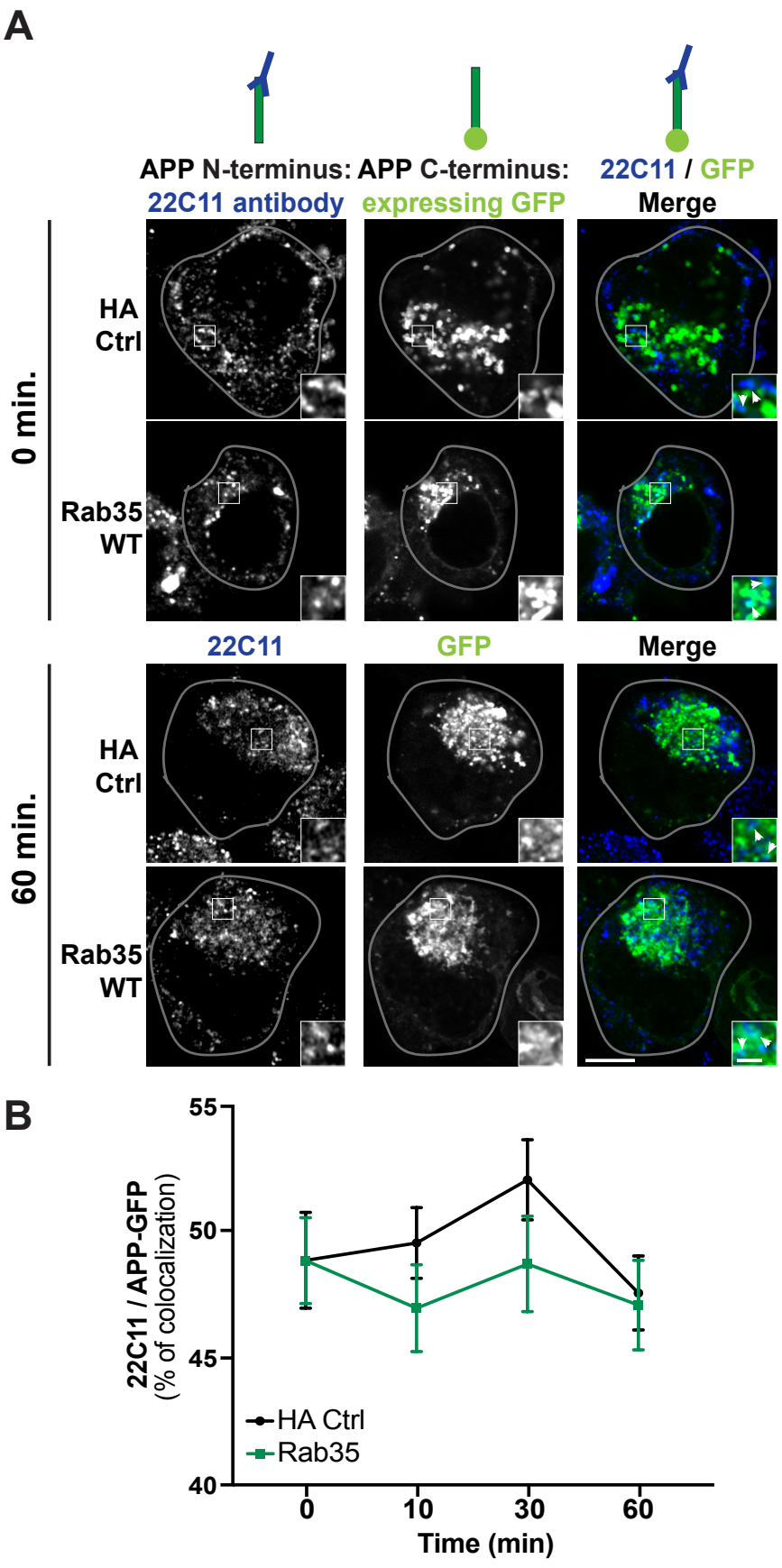
A
APP N-terminus:
22C11 antibody
APP C-terminus:
expressing GFP
22C11 / GFP
Merge
0 min.
HA Ctrl
Rab35 WT
22C11
GFP
Merge
60 min.
HA Ctrl
Rab35 WT
B
22C11 / APP-GFP
(% of colocalization)
55
50
45
40
HA Ctrl
Rab35
0
10
30
60
Time (min)

Figure 18. Colocalization between APP N- and C-terminus does not change throughout timecourse. A-B) Representative images and quantification of APP N- and C-terminus colocalization using 22C11 antibody to mark the N-terminus and GFP to mark the C-terminus in N2a cells expressing APP-GFP and HA control or HA-Rab35. 22C11 antibody (blue) colocalizes with GFP (green) approximately 50% of the time across timepoints and conditions (n=53-101 cells/condition, 4 experiments). White arrowheads in insets point to areas of colocalization. Scale bars: 5 μm; 1 μm for zoomed insets. All numeric data represent mean ± SEM.

I next performed the same assay with FLAG-BACE1 (see **Fig. 19A**). In contrast to its effect on APP, I found that Rab35 overexpression significantly increased the colocalization of internalized BACE1 with syntaxin-6 at the 30 and 60 min timepoints post-labeling, indicating that Rab35 regulates the retrograde trafficking of BACE1, but not APP. To determine whether this trafficking depends on Rab35 activation/GTP binding, I performed the same assay in N2a cells expressing dominant negative (DN) HA-Rab35. Expression of DN Rab35 either reduced or did not affect BACE1/syntaxin-6 colocalization at the majority of post-labeling timepoints compared to the control condition (**Fig. 19B-C**). However, DN Rab35 expression was lower than that of WT Rab35 (**Fig. 19D**), suggesting that the results likely underestimate the effects of Rab35 inactivation on BACE1 retrograde trafficking. Nevertheless, these results indicate that Rab35 activation is required for stimulating BACE1 retrograde trafficking.

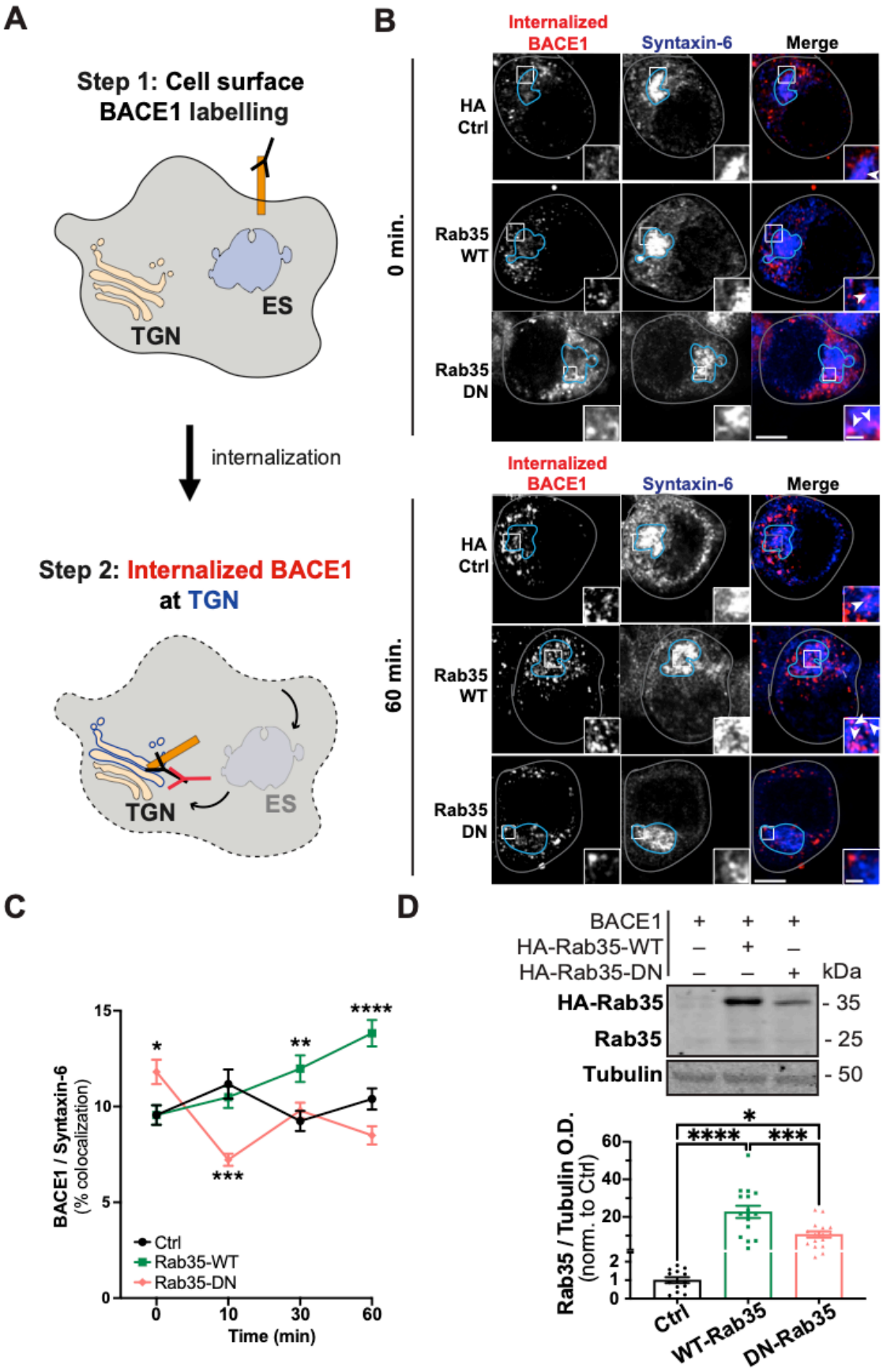
A
Step 1: Cell surface BACE1 labelling
TGN
ES
internalization
Step 2: Internalized BACE1 at TGN
TGN
ES
B
Internalized BACE1
Syntaxin-6
Merge
0 min.
HA Ctrl
Rab35 WT
Rab35 DN
60 min.
C
BACE1 / Syntaxin-6 (% colocalization)
Time (min)
Ctrl
Rab35-WT
Rab35-DN
D
BACE1
HA-Rab35-WT
HA-Rab35-DN
kDa
HA-Rab35
Rab35
Tubulin
- 35
- 25
- 50
Rab35 / Tubulin O.D. (norm. to Ctrl)
Ctrl
WT-Rab35
DN-Rab35

Figure 19. Rab35 stimulates the retrograde trafficking of BACE1. A) Schematic representation of BACE1 internalization assay, in which cell-surface BACE1 was labeled with FLAG antibody and cells were incubated for 0, 10, 30 or 60 minutes to allow for BACE1 internalization, followed by immunostaining with syntaxin-6 antibodies for TGN labeling. **B-C)** Representative images and quantification of BACE1 internalization in N2a cells expressing FLAG-BACE1 and either HA Control, HA-Rab35 wild-type (WT), or HA-Rab35 dominant negative (DN). Internalized BACE1 (red) and syntaxin-6 (blue) are shown at 0 and 60 min timepoints post-labeling. Compared to vector control, overexpression of WT Rab35 increases colocalization of internalized BACE1 with syntaxin-6 at both 30 and 60 min timepoints, and DN Rab35 prevents this effect (*$P_{DN\text{-}0\ min}$=0.0392, ** $P_{DN\text{-}10\ min}$=0.0011, ** $P_{WT\text{-}30}$ = 0.0025, **** $P_{WT\text{-}60\ min}$<0.0001, 2-way ANOVA and Sidak post hoc analysis, n=45-155 cells per condition/timepoint. 2-5 experiments. *Time* × *Rab35* interaction $F_{6,1253}$=8.002, P<0.0001, overall *Rab35* effect $F_{2,1253}$=10.43, P<0.0001). Scale bars: 5 μm; 1 μm for zoomed insets. **D)** Representative immunoblots and quantification of WT and DN Rab35 expression in N2a cells expressing FLAG-BACE1 with HA control, HA-Rab35 WT, or HA-Rab35 DN. Immunoblots were probed for Rab35 and tubulin. Rab35 levels are normalized to tubulin and expressed as a ratio of HA control condition. Cells express WT Rab35 at higher levels than DN Rab35 (*P=0.0131, ***P=0.0009, ****P<0.0001 by one-way ANOVA with Tukey's multiple comparisons test; n=14-16 independent samples/condition). All numeric data represent mean ± SEM. ES: Endosomal structure; TGN: trans-Golgi network.

The Rab35 effector and lipid phosphatase OCRL (Oculocerebrorenal Syndrome of Lowe Inositol Polyphosphate-5-Phosphatase) is required downstream of Rab35 for the retrograde trafficking of mannose-6-phosphate receptors (Cauvin *et al.*, 2016). To test whether Rab35-mediated retrograde trafficking of BACE1 also requires OCRL, I performed the same antibody feeding/TGN colocalization assay in the presence of siRNAs against OCRL (siOCRL; **Fig. 20A**). While OCRL knockdown alone did not affect BACE1 colocalization with syntaxin-6 compared to control siRNAs, it did prevent the Rab35-mediated increase in BACE1/syntaxin-6 colocalization (**Fig. 20B-C**), indicating that Rab35 stimulates the sorting of BACE1 into the retrograde pathway through its effector OCRL.

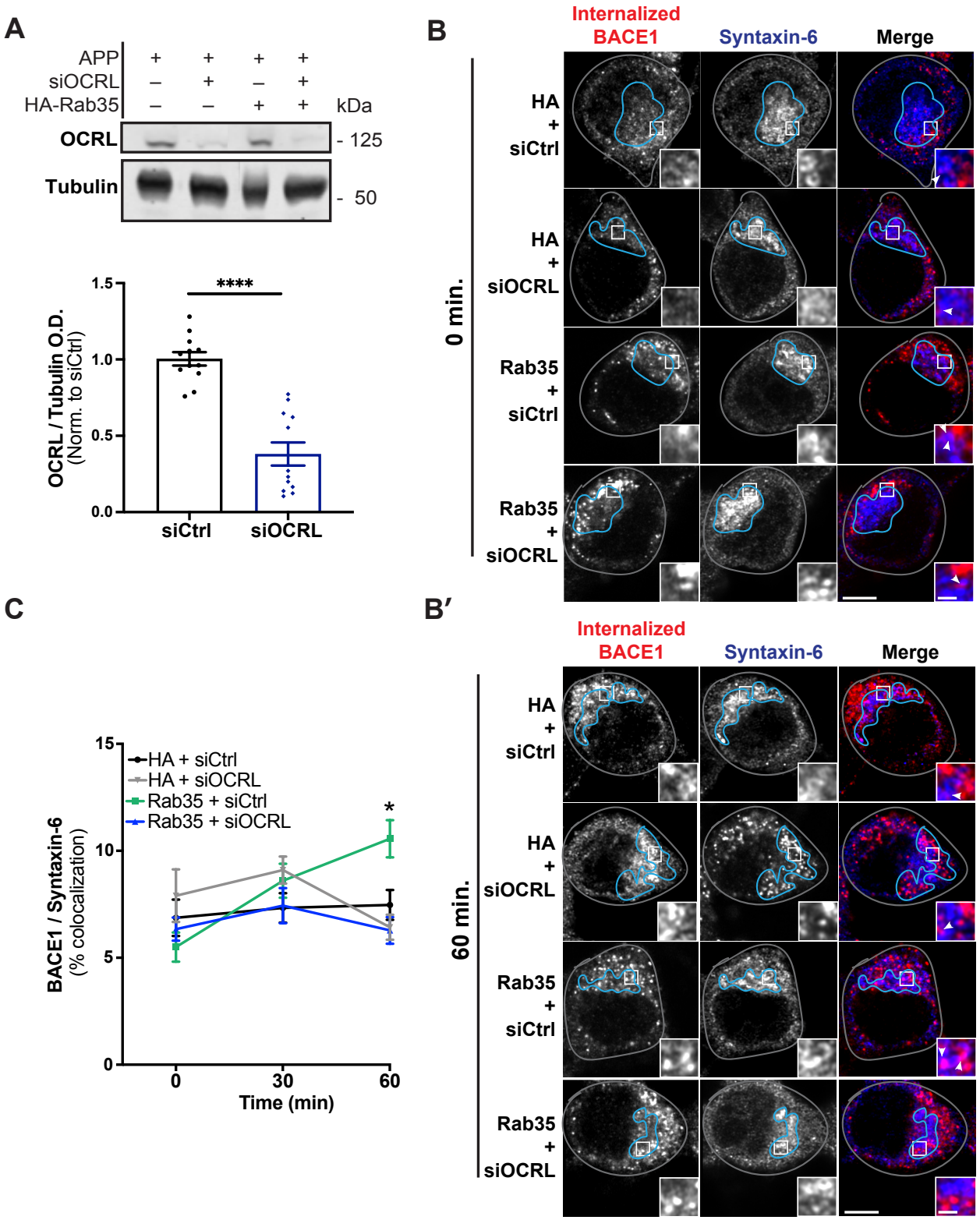

Figure 20. Rab35-mediated retrograde trafficking of BACE1 is mediated by the effector OCRL. A) Representative immunoblots and quantification of OCRL knockdown in N2a cells expressing APP-GFP and either HA control or HA-Rab35, together with control siRNA (siCtrl) or siRNA against OCRL (siOCRL). Immunoblots were probed for OCRL and tubulin. OCRL levels normalized to tubulin are expressed as a ratio of the siCtrl condition.

Cells transfected with siOCRL show a ~60% reduction in OCRL, regardless of whether they co-express HA control or HA-Rab35 (****P<0.0001; unpaired, two-tailed t-test, n=12 samples/condition). **B-C)** Representative images and quantification of BACE1 internalization in N2a cells expressing FLAG-BACE1 and HA or HA-Rab35 together with siCtrl or siOCRL. Internalized BACE1 (red) and syntaxin-6 (blue) are shown at 0 and 60 min timepoints post-labeling. Compared to control, overexpression of Rab35 increases colocalization of internalized BACE1 with syntaxin-6 at the 60 min timepoint, and knockdown of OCRL blocks this effect (**$P_{HA + siCtrl \text{ vs. } Rab35 + siCtrl}$=0.0151, 2-way ANOVA and Tukey's multiple comparisons test, n=50-61 cells per condition/timepoint, 2 experiments. *Time* × *Condition* interaction $F_{6,635}$=3.861, P=0.009, overall *Condition* effect $F_{2,635}$=2.446, P=0.0629). Scale bars: 5 μm; 1 μm for zoomed insets. All numeric data represent mean ± SEM.

To investigate whether Rab35 similarly alters BACE1 trafficking in hippocampal neurons, my colleague Mei Zhu measured endogenous APP and BACE1 colocalization with syntaxin-6 following Rab35 overexpression and knockdown. Consistent with my data in N2a cells, APP colocalization with syntaxin-6 was not affected by these manipulations (**Fig. 21A-B**), while BACE1/syntaxin-6 colocalization was significantly increased by Rab35 overexpression (**Fig. 21C-D**). This increase was not caused by Rab35-mediated alterations in TGN morphology, as the density and size of syntaxin-6 puncta were unchanged by Rab35 overexpression and knockdown (**Fig. 21E-F**).

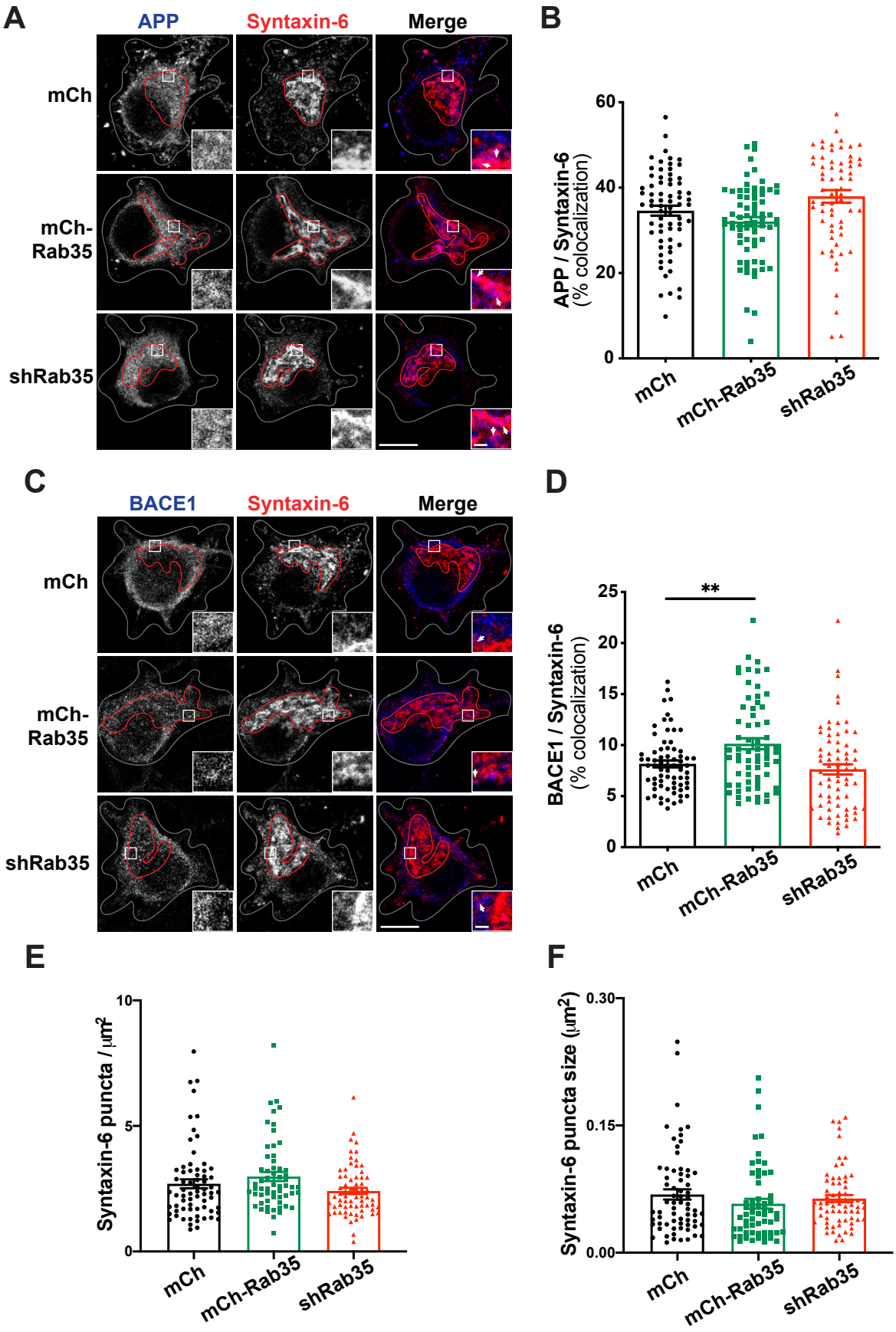
A
APP
Syntaxin-6
Merge
mCh
mCh-Rab35
shRab35
B
APP / Syntaxin-6 (% colocalization)
60
40
20
0
mCh
mCh-Rab35
shRab35
C
BACE1
Syntaxin-6
Merge
mCh
mCh-Rab35
shRab35
D
BACE1 / Syntaxin-6 (% colocalization)
**
25
20
15
10
5
0
mCh
mCh-Rab35
shRab35
E
Syntaxin-6 puncta / μm²
10
5
0
mCh
mCh-Rab35
shRab35
F
Syntaxin-6 puncta size (μm²)
0.30
0.15
0.00
mCh
mCh-Rab35
shRab35

Figure 21. Rab35 regulates BACE1 endosomal distribution in hippocampal neurons. A-B) Representative images and quantification of APP colocalization with syntaxin-6 in 14 DIV hippocampal neurons expressing mCh, mCh-Rab35, or shRab35. Rab35 overexpression or knockdown does not significantly alter APP colocalization with syntaxin-6, compared to the control condition (n=64-70 cells/condition, 3 independent cultures). **C-D)** Representative images and quantification of BACE1 colocalization with syntaxin-6 in hippocampal neurons expressing mCh, mCh-Rab35, or shRab35. Overexpression of Rab35 increases BACE1 colocalization with syntaxin-6, while Rab35 knockdown does not significantly alter this value (**P=0.006, one-way ANOVA, Dunnet post-hoc analysis, n=66-69 cells/condition, 3 independent cultures). Scale bars: 10 μm; 1 μm for zoomed insets. **E-F)** Quantification of syntaxin-6 puncta density **(E)** and size **(F)** in hippocampal neurons expressing mCh, mCh-Rab35, or shRab35. Rab35 overexpression or knockdown does not affect either value (n=56-68 cells/condition, 3 independent cultures). All numeric data represent mean ± SEM.

4.2.2. Rab35 stimulates APP recycling to the plasma membrane

Rab35's ability to promote the retrograde trafficking of BACE1 to the TGN could be sufficient for reducing APP-BACE1 interaction in the endosomal network. However, Rab35 also facilitates the fast endocytic recycling of proteins (*i.e.* T-cell receptors, β1 integrin) to the plasma membrane (PM) in a pathway that operates in parallel with Rab11-mediated endosomal recycling (Allaire *et al.*, 2013; Argenzio *et al.*, 2014; Kobayashi *et al.*, 2014; Kouranti *et al.*, 2006; Patino-Lopez *et al.*, 2008). Stimulating APP and/or BACE1 trafficking into this pathway could also reduce APP-BACE1 interactions in Rab11-positive endosomes. To determine whether Rab35 promotes the fast recycling of APP and/or BACE1, I used another antibody feeding assay *(*Ubelmann *et al.*, 2017) to monitor the internalization and PM recycling of APP-GFP and FLAG-BACE1 at several timepoints post-labeling (**Fig. 22, 23A**). Intriguingly, I found that Rab35 overexpression stimulated both APP internalization and recycling to the PM at nearly all timepoints compared to the control condition (**Fig. 23B-D**).

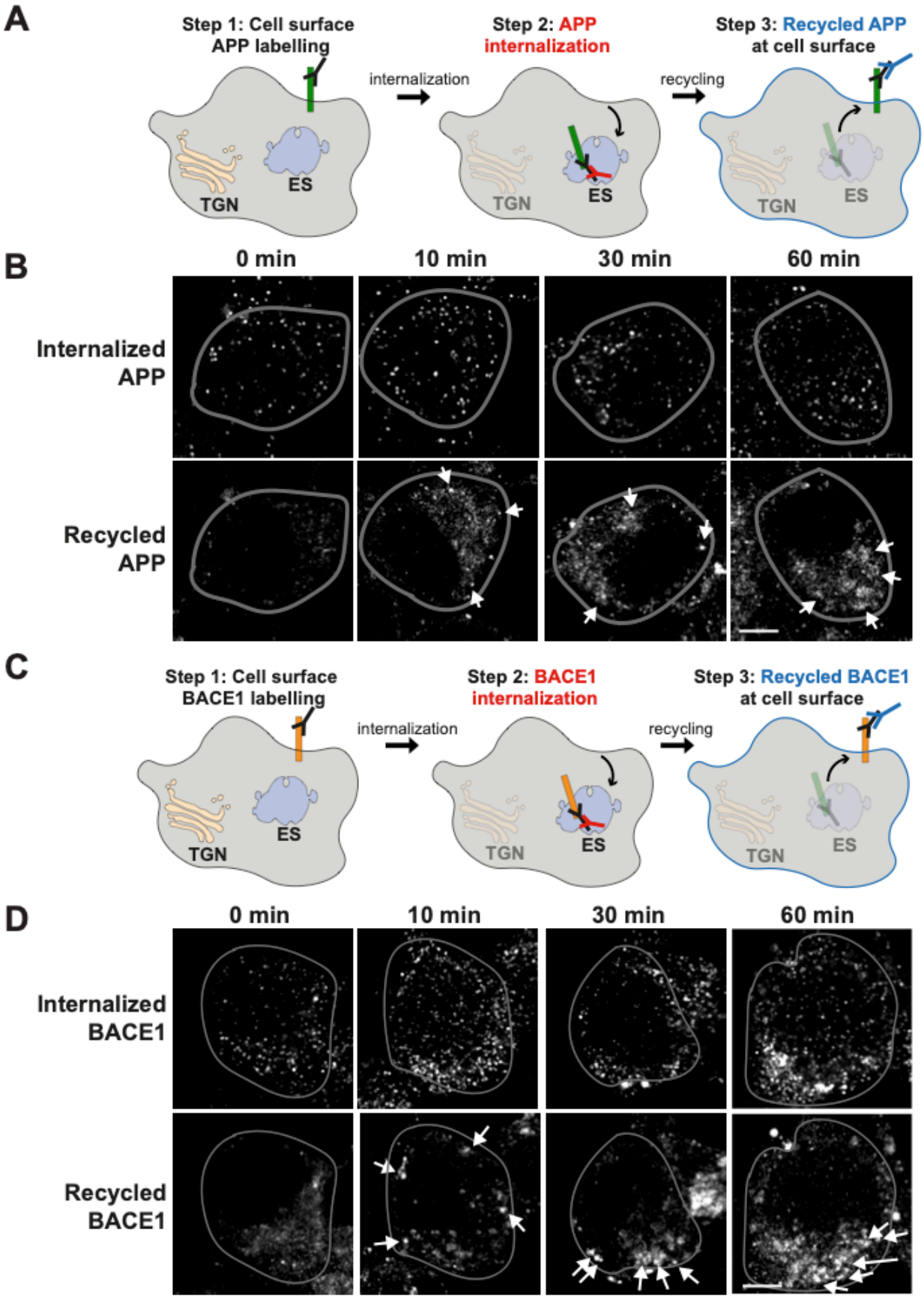
A
Step 1: Cell surface APP labelling
internalization
Step 2: APP internalization
recycling
Step 3: Recycled APP at cell surface
TGN
ES
B
0 min
10 min
30 min
60 min
Internalized APP
Recycled APP
C
Step 1: Cell surface BACE1 labelling
internalization
Step 2: BACE1 internalization
recycling
Step 3: Recycled BACE1 at cell surface
D
Internalized BACE1
Recycled BACE1

Figure 22. Recycling assay timecourse for APP and BACE1. A) Schematic representation of APP recycling assay, in which APP internalization and recycling were assessed by labeling cell-surface APP with 22C11 antibody followed by cell incubation for 0, 10, 30, or 60 minutes, and fixation and immunostaining with secondary antibodies to detect recycled or internalized APP. **B)** Representative images of APP recycling assay timecourse in control cells. Cells are outlined in gray, and white arrows point to recycled 22C11 antibody at the cell surface. **C)** Schematic representation of BACE1 recycling assay, in which BACE1 internalization and recycling were assessed by labeling cell-surface BACE1 with FLAG antibody followed by cell incubation for 0, 10, 30, or 60 minutes, and fixation and immunostaining with secondary antibodies to detect recycled or internalized BACE1. **D)** Representative images of BACE1 recycling assay timecourse, with cells outlined in gray and white arrows pointing to recycled FLAG antibody around the cell surface. Scale bars: 5 μm. ES: Endosomal structure; TGN: trans-Golgi network.

To determine whether APP internalization and recycling steps were dependent on Rab35 activation, I also performed this assay in the presence of DN Rab35. As anticipated, expression of DN Rab35 did not stimulate APP recycling relative to the control condition (**Fig. 23B, D**), indicating the dependence of this trafficking step on Rab35 activation. Surprisingly, the DN construct stimulated APP internalization at the 30 and 60 min timepoints to a similar degree as WT Rab35 (**Fig. 23B-C**), suggesting that Rab35 mediates APP internalization independently of its activation state.

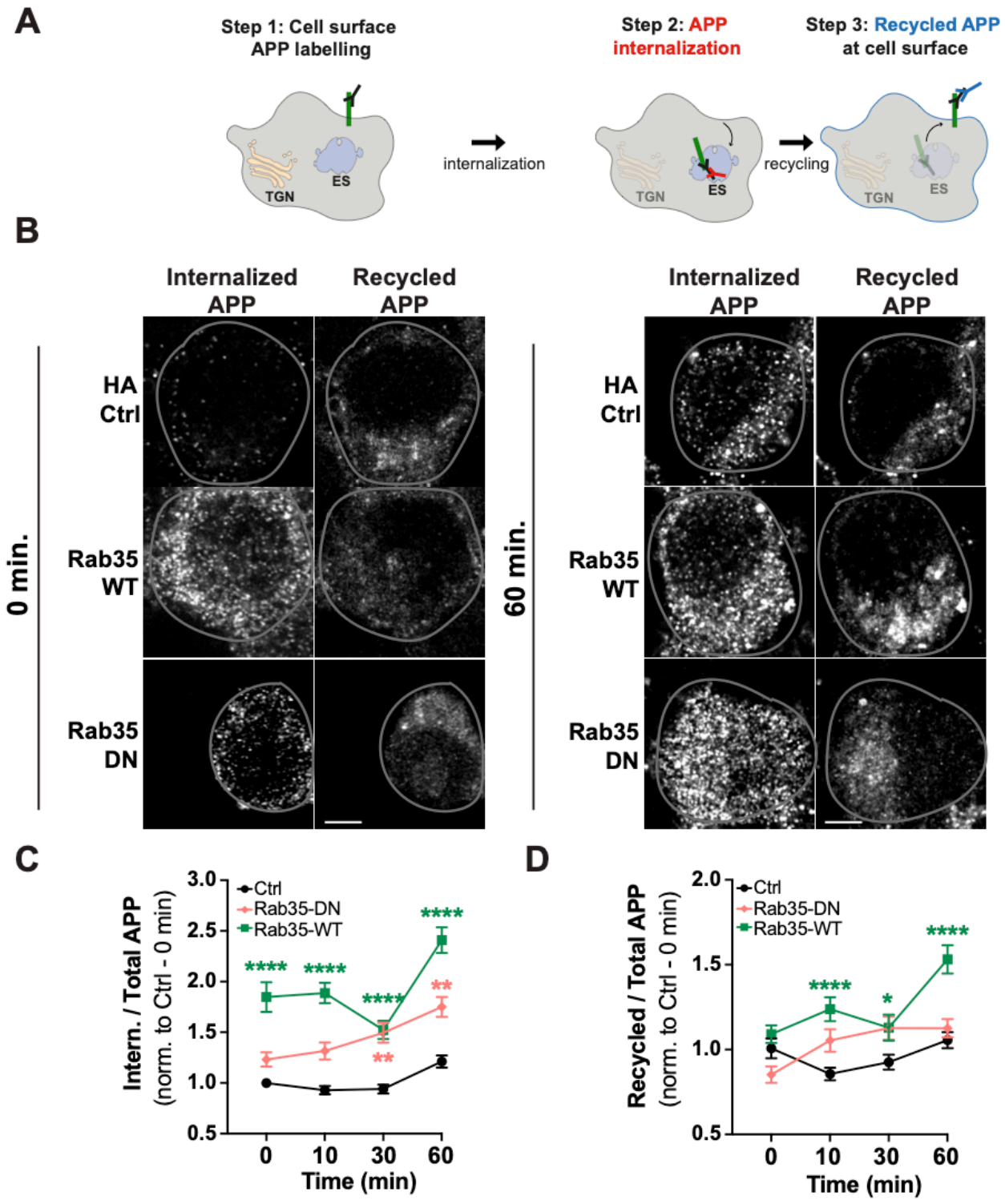

Figure 23. Rab35 stimulates APP recycling to the plasma membrane. A) Schematic of APP recycling assay, in which APP internalization and recycling were assessed by labeling cell-surface APP with 22C11 antibody, incubating cells for 0, 10, 30 or 60 minutes, and finally fixing and immunostaining cells with secondary antibodies to detect recycled or internalized APP. **B-D)** Representative images and quantification of APP internalization and recycling in N2a cells expressing APP-GFP and either HA control, HA-Rab35 WT, or HA-Rab35 DN. Internalized and recycled APP are shown at 0 and 60 min timepoints post-labeling. Compared to control, Rab35 overexpression increases the ratio of internalized **(C)** and recycled **(D)** APP over total APP-GFP at multiple timepoints (*$P_{WT\text{-}30\ min}$=0.0299, **$P_{DN\text{-}}$

$_{30\ min}$=0.0027, **$P_{DN\text{-}60\ min}$=0.0017, ****P<0.0001, 2-way ANOVA and Sidak post-hoc analysis, n=53-269 cells per condition/timepoint, 3 experiments. **For C:** *Time* × *Rab35* interaction $F_{6,1897}$=3.002, P=0.0064, overall *Rab35* effect $F_{2,1897}$=118.9. **For D:** *Time* × *Rab35* interaction $F_{6,1897}$=3.443, P=0.0022, overall *Rab35* effect $F_{2,1897}$=26.03). Scale bars: 5 µm. All numeric data represent mean ± SEM. ES: Endosomal structure; TGN: trans-Golgi network.

Rab35 also stimulated BACE1 internalization at the earliest timepoint post-labeling (0 min; **Fig. 24A-C**), but did not alter BACE1 internalization at later timepoints, nor its recycling to the PM (**Fig. 24B, D**). Consistent with these findings, I observed higher cell-surface levels of APP, but not BACE1, in N2a cells expressing Rab35 compared to the control condition (**Fig. 24E-H**).

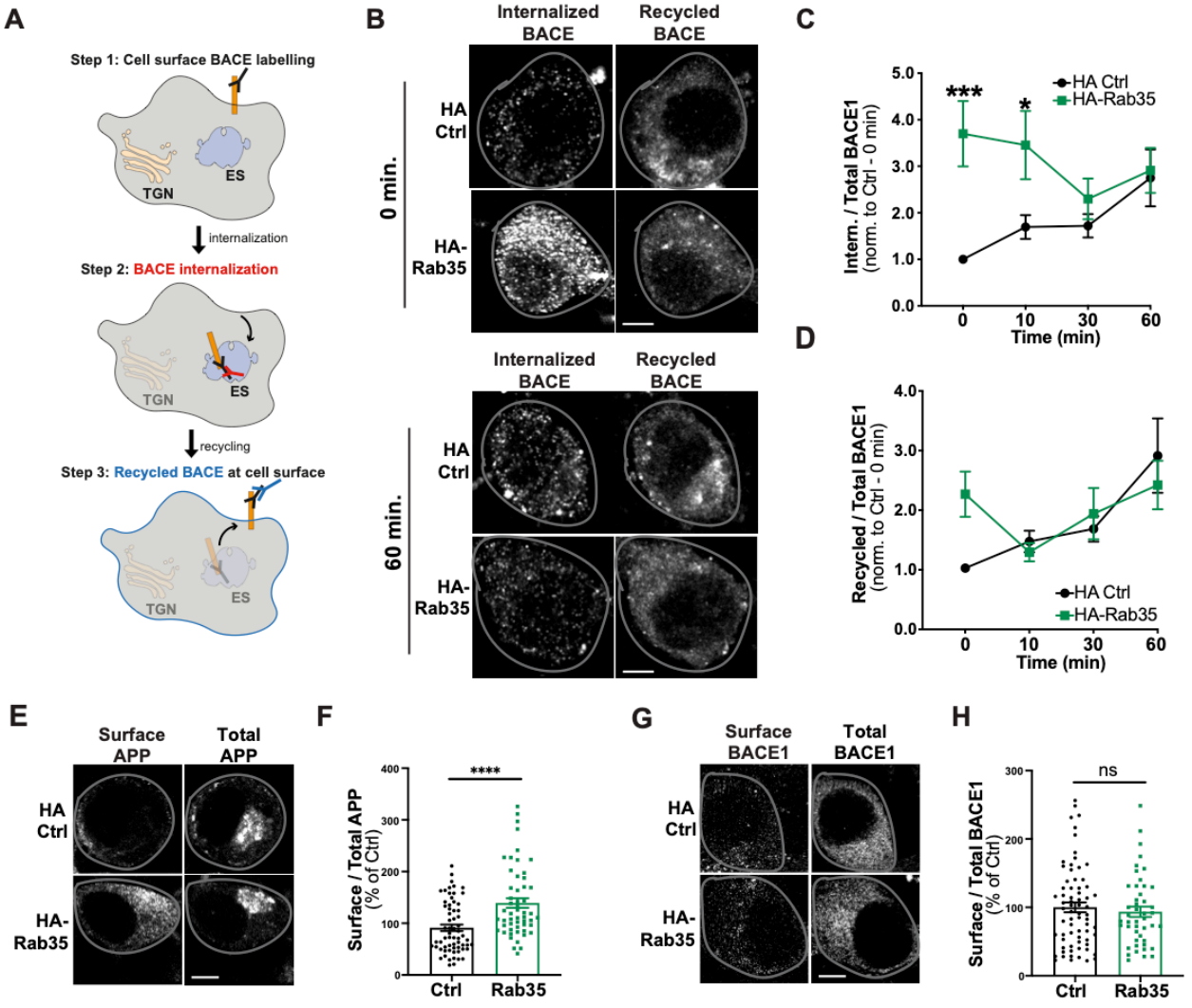

Figure 24. Rab35 does not mediate BACE1 recycling. A) Schematic representation of BACE1 recycling assay, in which BACE1 internalization and recycling were assessed by labeling cell-surface BACE1 with FLAG antibody,

incubating cells for 0, 10, 30 or 60 minutes, and finally fixing and immunostaining cells with secondary antibodies to detect recycled or internalized BACE1. **B-D)** Representative images and quantification of BACE1 internalization and recycling in N2a cells expressing FLAG-BACE1 and either HA or HA-Rab35. Internalized and recycled BACE1 are shown at 0 and 60 min timepoints post-labeling **(B)**, and are expressed in graphs as ratios of total BACE1, normalized to the 0 min timepoint **(C-D)**. Rab35 overexpression increases BACE1 internalization at early timepoints, but has no effect on BACE1 recycling dynamics (***P=0.0004, *P=0.0494 (internalization); 2-way ANOVA with Sidak post hoc analysis, n=127-143 cells per condition/timepoint, 3 experiments). **E-F)** Representative images and quantification of steady-state cell-surface levels of APP in N2a cells transfected with APP-GFP and HA control or HA-Rab35. Rab35 increases cell-surface APP, expressed as a ratio of cell surface to total protein (****P<0.0001; unpaired two-tailed t-test, n=54-64 cells/condition, 3 experiments). **G-H)** Representative images and quantification of steady-state cell-surface levels of BACE1 in N2a cells transfected with FLAG-BACE1 and HA control or HA-Rab35. Rab35 does not alter cell-surface BACE1 levels (n=46-70 cells/condition, 3 experiments). Scale bars: 5 µm. All numeric data represent mean ± SEM. ES: Endosomal structure; TGN: trans-Golgi network.

Fast endocytic recycling has been shown to occur through two distinct pathways, mediated by the Rab35 effectors OCRL and ACAP2 (Mrozowska & Fukuda, 2016). I first tested whether Rab35-mediated APP recycling to the PM relies on OCRL, using the internalization/recycling assay in N2a cells transfected with siRNAs against OCRL (see **Fig. 20A**). Interestingly, I found that while OCRL knockdown did not alter Rab35-induced APP internalization, it further increased Rab35-induced APP recycling at the 60 min timepoint (by ~50%; **Fig. 25A, C**). These data suggest that Rab35-mediated APP recycling does not occur through OCRL, but that OCRL knockdown frees Rab35 to interact with the effector responsible for APP recycling, thereby enhancing this trafficking event.

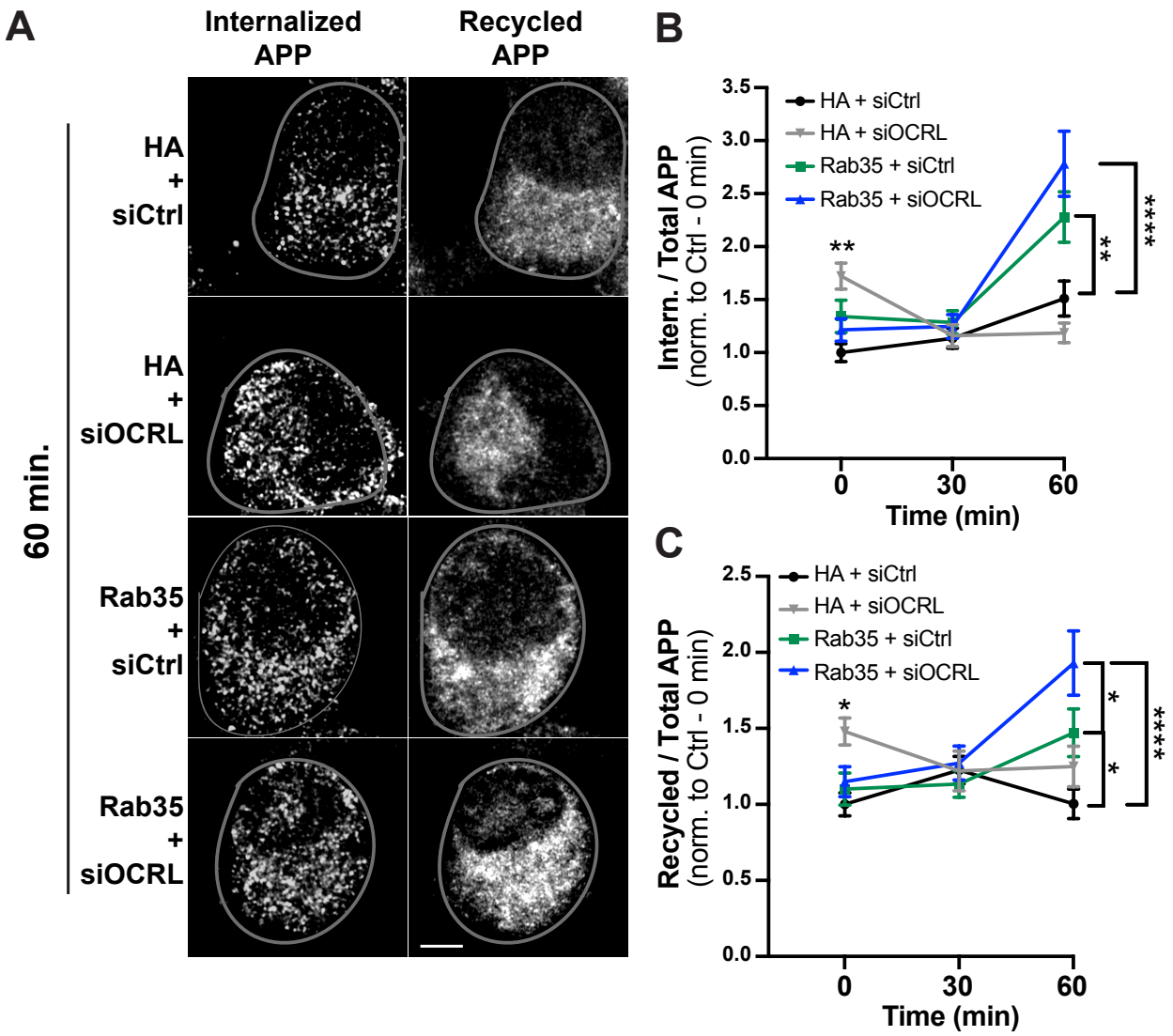

Figure 25. Rab35 effector OCRL does not mediate APP recycling. A-C) Representative images and quantification of APP internalization and recycling in N2a cells expressing APP-GFP and either HA or HA-Rab35, together with control siRNA (siCtrl) or siRNA to knockdown OCRL (siOCRL). **B)** Compared to control, overexpression of Rab35 increases APP internalization at the 60 min timepoint, and OCRL knockdown does not alter this effect (**$P_{HA+siCtrl\ vs.\ Rab35+siCtrl}$=0.0069, ****$P_{HA+siCtrl\ vs.\ Rab35+siOCRL}$<0.0001; 2-way ANOVA with Sidak's post-hoc test, n=33-47 cells per condition/timepoint, 2 experiments. *Time* × *Condition* interaction $F_{6,460}$=9.453, P<0.0001, overall *Condition* effect $F_{3,460}$=8.431, P<0.0001). **C)** Compared to control, overexpression of Rab35 increases APP recycling at 60 min, and OCRL knockdown further increases this effect (*$P_{HA+siCtrl\ vs.\ Rab35+siCtrl}$=0.0152, ****$P_{HA+siCtrl\ vs.\ Rab35+siOCRL}$<0.0001, *$P_{Rab35+siCtrl\ vs.\ Rab35+siOCRL}$=0.0400; 2-way ANOVA and Tukey's multiple comparisons test, n=33-47 cells per condition/timepoint, 2 experiments. *Time* × *Condition* interaction $F_{6,460}$=4.537, P=0.0002, overall *Condition* effect $F_{3,460}$=5.606, P=0.0009). Scale bar: 5 µm. All numeric data represent mean ± SEM.

I next tested whether ACAP2 (ArfGAP with Coiled-coil, Ankyrin repeat and PH domains 2) is the effector mediating APP recycling, again using our antibody feeding assay in the presence of siRNAs against ACAP2 (**Fig. 27A**). Here, I found that knockdown of ACAP2 did

not alter APP internalization compared to siRNA control, nor lessen the effect of Rab35 on APP internalization (**Fig. 26A-B**), as expected if this sorting step is a GTP-independent function of Rab35. However, ACAP2 knockdown completely abolished Rab35-enhanced APP recycling to the PM at the 60 min time point (**Fig. 26A, C**). These data demonstrate that Rab35 stimulates the sorting of APP into the fast recycling pathway, via GTP-independent stimulation of APP internalization and ACAP2-dependent stimulation of APP recycling to the PM. Together, these actions increase APP sorting out of endosomes and promote its accumulation at the PM, thereby decreasing its amyloidogenic processing.

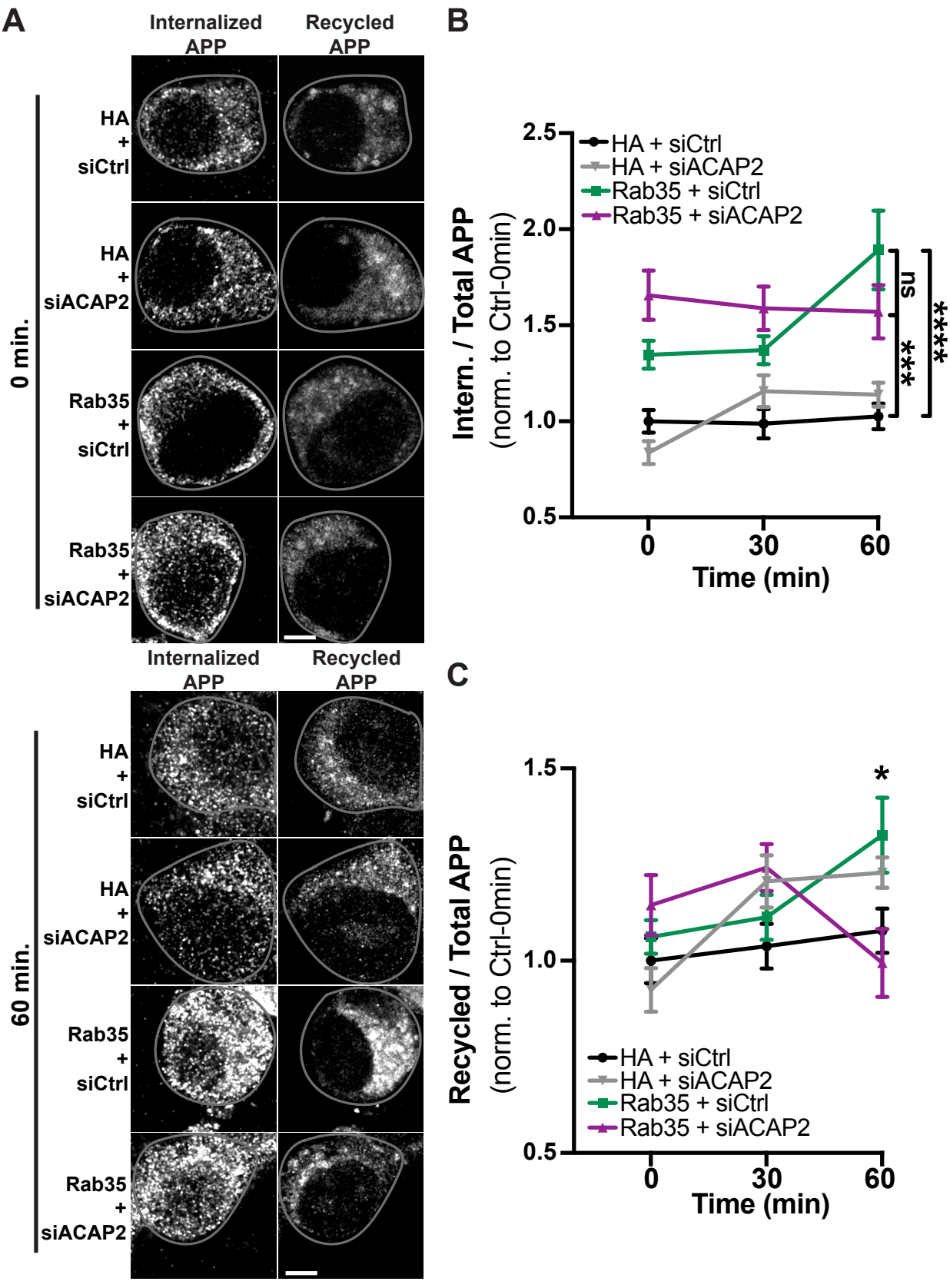
A
Internalized APP
Recycled APP
0 min.
HA + siCtrl
HA + siACAP2
Rab35 + siCtrl
Rab35 + siACAP2
60 min.
B
Intern. / Total APP
(norm. to Ctrl-0min)
HA + siCtrl
HA + siACAP2
Rab35 + siCtrl
Rab35 + siACAP2
ns
***
****
Time (min)
C
Recycled / Total APP
(norm. to Ctrl-0min)
*
Time (min)

Figure 26. Rab35 effector ACAP2 mediates APP recycling to the plasma membrane. A-C) Representative images and quantification of APP internalization and recycling in N2a cells expressing APP-GFP and either HA or HA-Rab35, together with control siRNA (siCtrl) or siRNA to knockdown ACAP2 (siACAP2). Internalized and recycled APP are shown at 0 and 60 min timepoints post-labeling. **B)** Compared to control, overexpression of Rab35 increases APP internalization, and ACAP2 knockdown does not alter this effect (***$P_{HA + siCtrl\ vs.\ Rab35 + siACAP2}$=0.0003, ****$P_{HA + siCtrl\ vs.\ Rab35 + siCtrl}$<0.0001, 2-way ANOVA and Tukey's multiple comparisons test, n=20-48 cells per condition/timepoint, 3 experiments. *Time* × *Rab35* interaction $F_{4,310}$=2.843, P=0.0244, overall *Rab35/ACAP2* effect $F_{2,310}$=39.12, P<0.0001). **C)** Compared to control, overexpression of Rab35 increases APP recycling, and ACAP2 knockdown blocks this effect (*$P_{HA + siCtrl\ vs.\ Rab35 + siCtrl}$=0.0457, 2-way ANOVA and Tukey's multiple comparisons test, n=20-48 cells per condition/timepoint, 3 experiments. *Time* × *Condition* interaction $F_{4,310}$=2.877, P=0.023, overall *Condition* effect $F_{2,310}$=3.279, P=0.039). Scale bars: 5 μm. All numeric data represent mean ± SEM.

Finally, I tested whether ACAP2, like OCRL, mediates Rab35-regulated BACE1 retrograde trafficking. Using our antibody feeding/syntaxin-6 colocalization assay to monitor BACE1 retrograde trafficking, I found that knockdown of ACAP2 (siACAP2; **Fig 27A**) did not alter the Rab35-mediated increase in BACE1/syntaxin-6 colocalization (**Fig. 27B-C**). These findings reveal that Rab35 regulates APP and BACE1 trafficking via distinct mechanisms, stimulating the retrograde trafficking of BACE1 to the TGN through OCRL, and the fast recycling of APP to the PM through ACAP2.

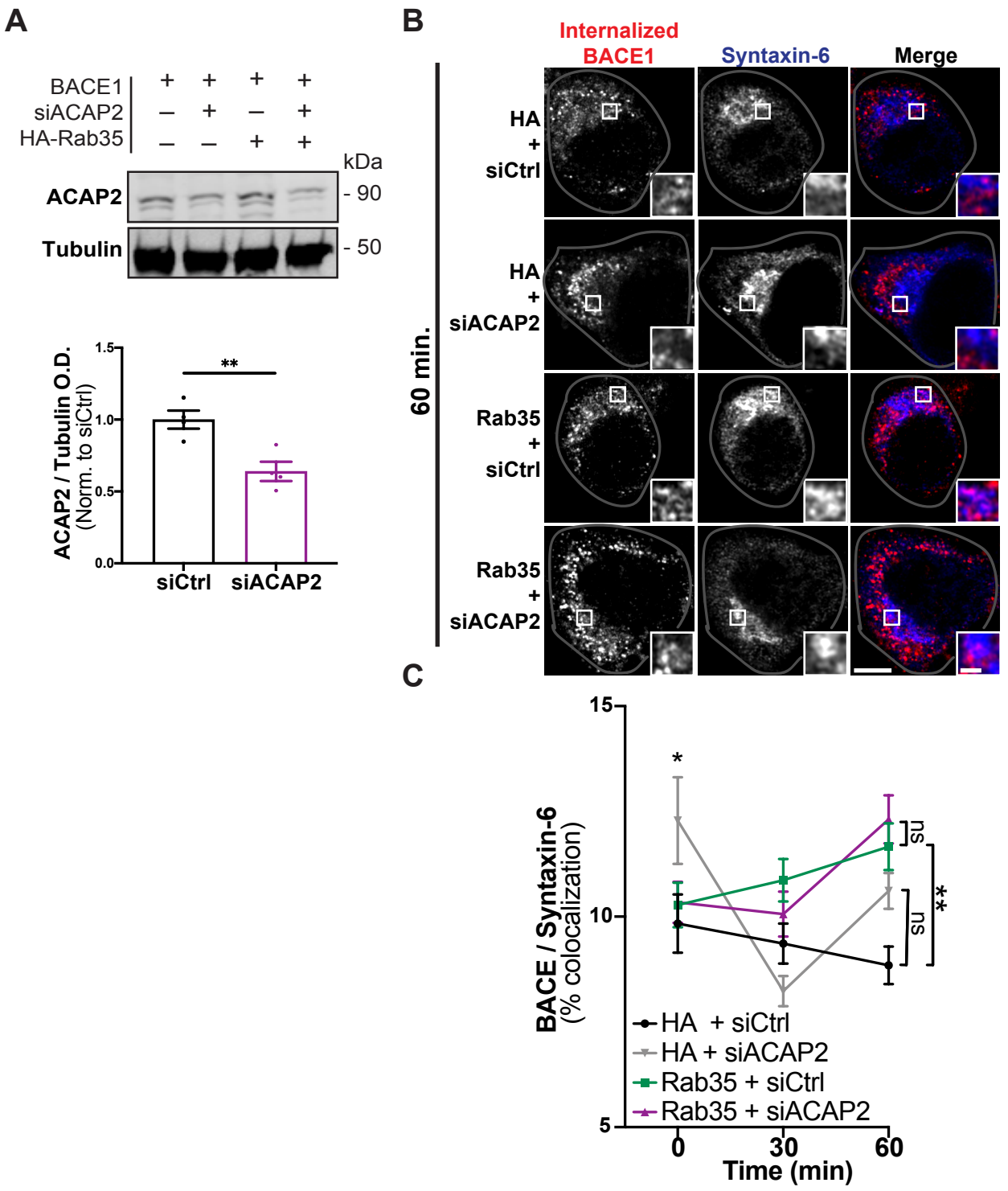

Figure 27. ACAP2 does not mediate the retrograde trafficking of BACE1. A) Representative immunoblots and quantification of ACAP2 knockdown in N2a cells expressing FLAG-BACE1 and either HA control or HA-Rab35, with control siRNA (siCtrl) or siRNAs against ACAP2 (siACAP2). Immunoblots were probed for ACAP2 and tubulin, and represented as a ratio of the control condition. Cells expressing siACAP2 show reduced levels of ACAP2, regardless of whether they co-express HA control or HA-Rab35 (**P=0.0078; un-paired, two-tailed t-test. n=4 samples/condition). **B-C)** Representative images and quantification of BACE1 retrograde trafficking in N2a cells expressing FLAG-BACE1 and either HA or HA-Rab35, with control siCtrl or siACAP2. Internalized BACE1 (red)

and syntaxin-6 (blue) are shown at 60 min post-labeling. Rab35 overexpression increases BACE1 colocalization with syntaxin-6 at 60 min, and ACAP2 knockdown does not alter this effect (**$P_{HA+siCtrl\ vs\ HA-Rab35+siCtrl}$=0.0056; 2-way ANOVA with Tukey's multiple comparison's test, n=50-66 cells per condition/timepoint, 3 experiments. *Time* × *Condition* interaction $F_{6,702}$=4.665, P=0.0001, overall *Condition* effect $F_{3,702}$=4.417, P=0.0044). Scale bars: 5 μm; 1 μm for zoomed insets. All numeric data represent mean ± SEM.

4.2.3. Rab35 counteracts GC-induced pro-amyloidogenic trafficking of APP and BACE1

Although GCs are known to stimulate Aβ production both *in vitro* and *in vivo*, their effects on APP and BACE1 trafficking are largely unexplored. I therefore examined whether GCs alter the interaction between APP and BACE1 within the endosomal network, again using the Venus BiFC assay in N2a cells (see **Fig. 11**). Here, I found that 24-hour treatment with the synthetic GC dexamethasone significantly increased Venus intensity, indicating that GCs promote APP-BACE1 interaction (**Fig. 28**). I next examined whether overexpression of Rab35 could block this effect, as predicted if GC-induced downregulation of Rab35 underlies the increased APP-BACE1 interaction. Indeed, Rab35 overexpression blocked the GC-induced increase in Venus intensity (**Fig. 28**), suggesting that Rab35 prevents this pro-amyloidogenic interaction under stress conditions.

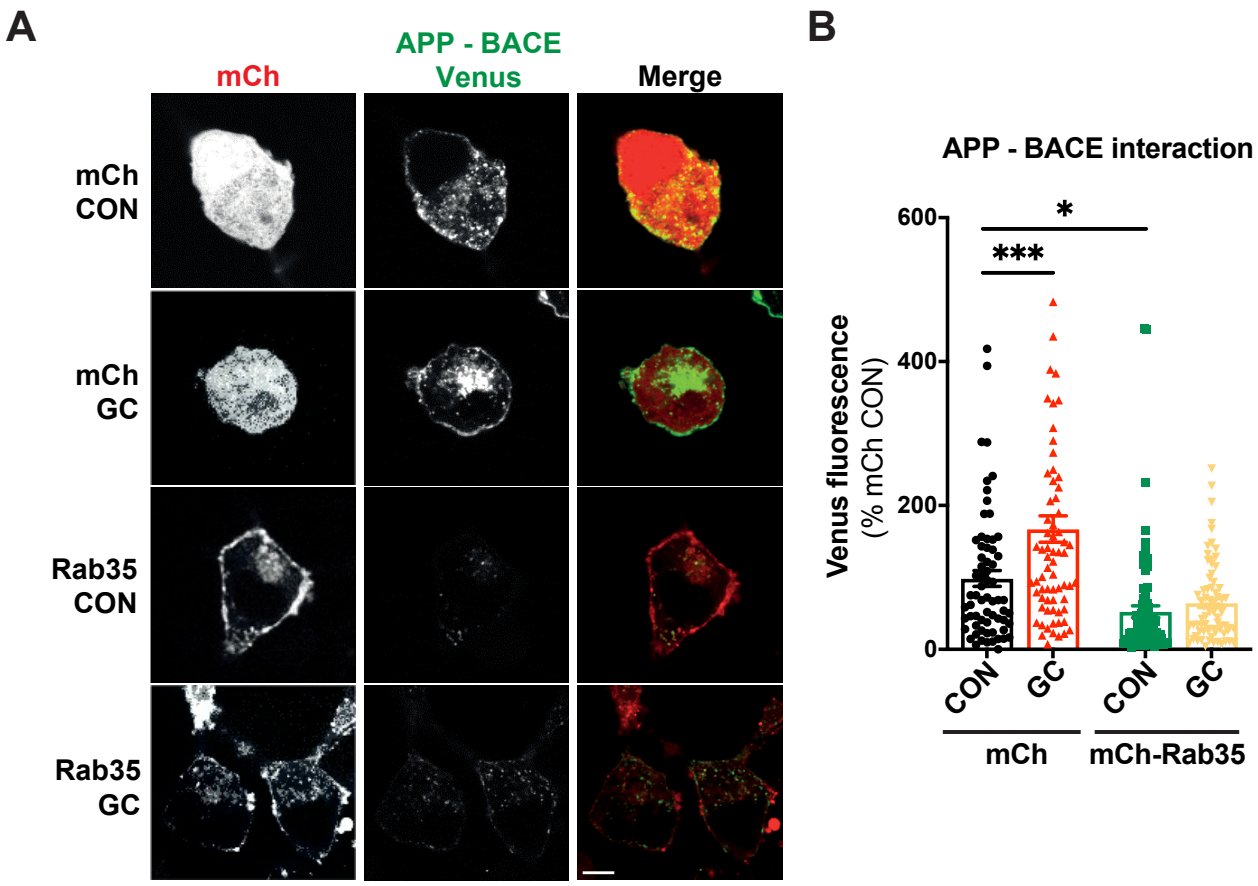

Figure 28. GC-induced APP-BACE1 interaction is blocked by Rab35 overexpression. A-B) Representative images and quantification of Venus fluorescence intensity in N2a cells expressing APP:VN, BACE:VC, and either mCh or mCh-Rab35, treated with GCs or vehicle control (CON). GCs increase Venus intensity in control cells, but have no effect in Rab35-expressing cells, which exhibit an overall decrease in Venus fluorescence (***$P_{mCh\ CON\ vs\ mCh\ GC}$=0.0004, *$P_{mCh\ CON\ vs\ mCh\text{-}Rab35\ CON}$=0.028, two-way ANOVA, Tukey's post-hoc analysis, n=3 experiments. *Rab35* x *GC* interaction $F_{1,291}$=5.989, P=0.015, overall *Rab35* effect $F_{1,291}$=41.35, P<0.0001, overall *GC* effect $F_{1,291}$=12.19, P=0.0006). Scale bar: 10 µm. All numeric data represent mean ± SEM.

I next tested whether GCs impact the APP and BACE1 trafficking pathways mediated by Rab35. Using the aforementioned antibody feeding/syntaxin-6 colocalization assay, I found that 24h treatment with GCs did not alter BACE1 retrograde trafficking compared to vehicle control (**Fig. 29**).

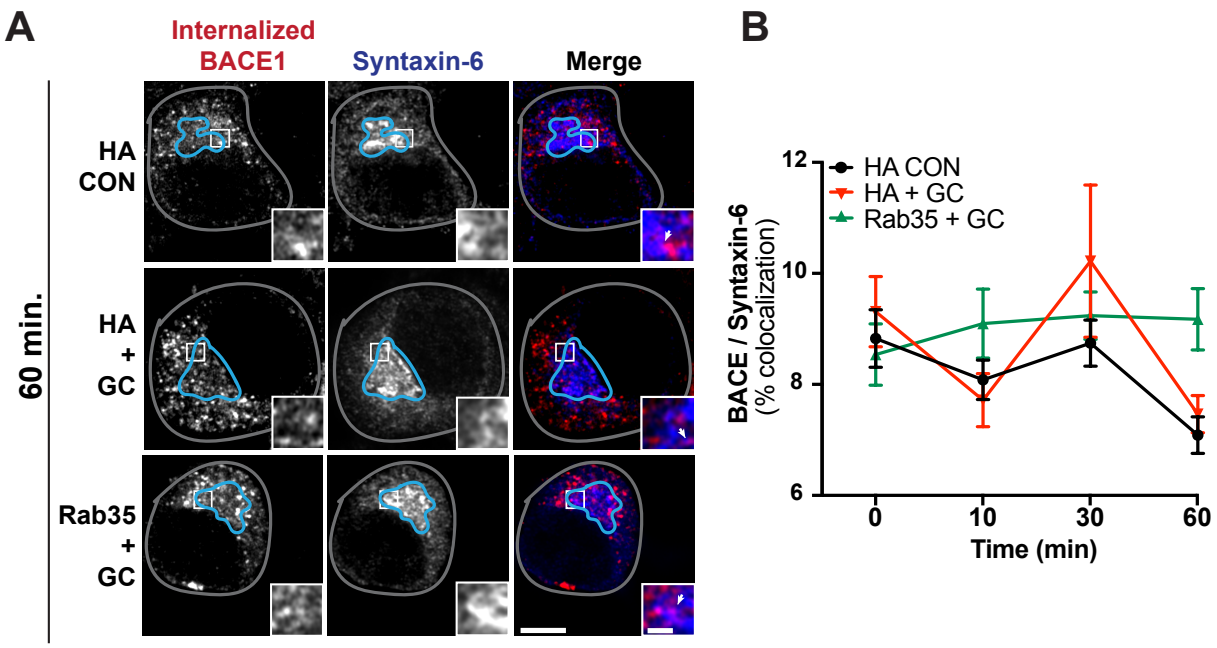

Figure 29. GCs do not affect BACE1 retrograde trafficking in N2a cells. A-B) Representative images and quantification of BACE1 retrograde trafficking in N2a cells expressing FLAG-BACE1 and either HA or HA-Rab35, treated with GCs or vehicle control (CON). Internalized BACE1 (red) and syntaxin-6 (blue) are shown at the 60 min timepoint post-labeling. GC treatment does not alter BACE1 colocalization with the TGN at any timepoint (n=43-65 cells per condition/timepoint, 3 experiments). Scale bars: 5 µm; 1 µm for zoomed insets. All numeric data represent mean ± SEM.

However, GC treatment significantly altered the kinetics of APP and BACE1 fast endocytic recycling as revealed by the antibody internalization/recycling assay. In particular, GCs stimulated APP internalization at the 0 min timepoint post-labeling, and decreased its recycling back to the PM at the 30 min timepoint compared to vehicle control (**Fig. 30A-C**). Remarkably, Rab35 further enhanced APP recycling compared to the control condition (**Fig. 30A, C**), similar to its actions in the absence of GCs (see **Fig. 23**). Additionally, GCs decreased BACE1 internalization at multiple timepoints, as well as BACE1 recycling to the PM, and Rab35 blocked these effects (**Fig. 31A-C**). Together, these findings demonstrate that GCs disrupt the endocytic trafficking of APP and BACE1, resulting in their increased colocalization in endosomes, and that Rab35 gain-of-function can rescue these effects.

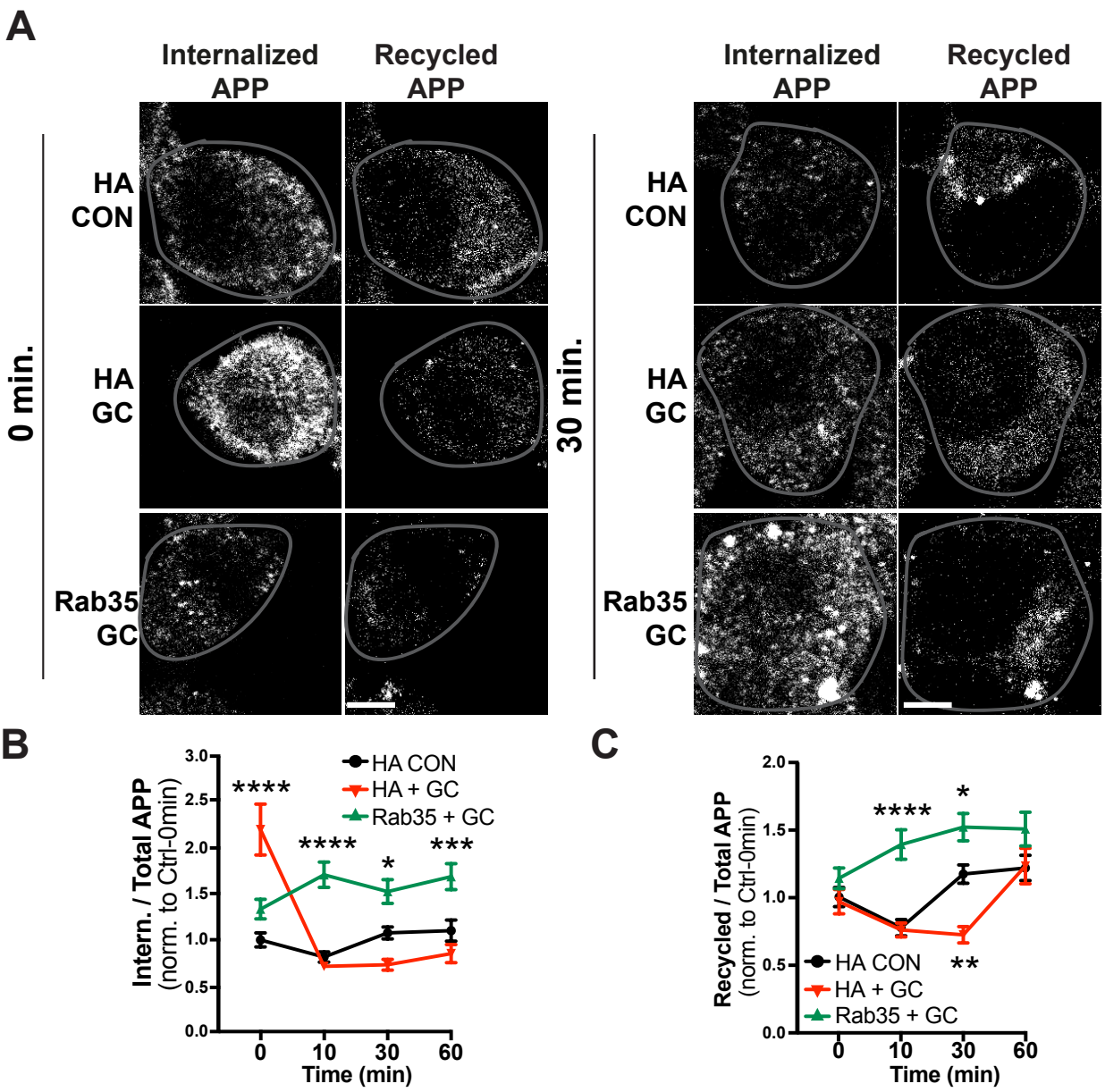

Figure 30. GC-induced pro-amyloidogenic APP trafficking is reversed by Rab35 overexpression. A-C) Representative images and quantification of APP internalization and recycling in N2a cells expressing APP-GFP and either HA or HA-Rab35, treated with GC or vehicle control (CON). GCs alter APP internalization **(B)** and recycling **(C)** kinetics, while Rab35 overexpression prevents these effects (**For B:** *$P_{HA+DMSO\ vs\ HA\text{-}Rab35+GC}$=0.0119, ***$P_{HA+DMSO\ vs\ HA\text{-}Rab35+GC}$=0.0009, ****P<0.0001; 2-way ANOVA with Tukey's post hoc analysis, n=47-77 cells per condition/timepoint, 3 experiments. For APP internalization: *Time* × *Condition* interaction $F_{6,780}$=15.81, P<0.0001. **For C:** ****$P_{HA+DMSO\ vs\ HA\text{-}Rab35+GC}$<0.0001, *$P_{HA+DMSO\ vs\ HA\text{-}Rab35+GC}$=0.0136, **$P_{HA+DMSO\ vs\ HA+GC}$=0.0011; two-way ANOVA with Tukey's post hoc analysis, n=47-77 cells per condition/timepoint, 3 experiments. For APP recycling: *Time* × *Condition* interaction $F_{6,759}$=3.556, P=0.0013). Scale bars: 5 µm. All numeric data represent mean ± SEM.

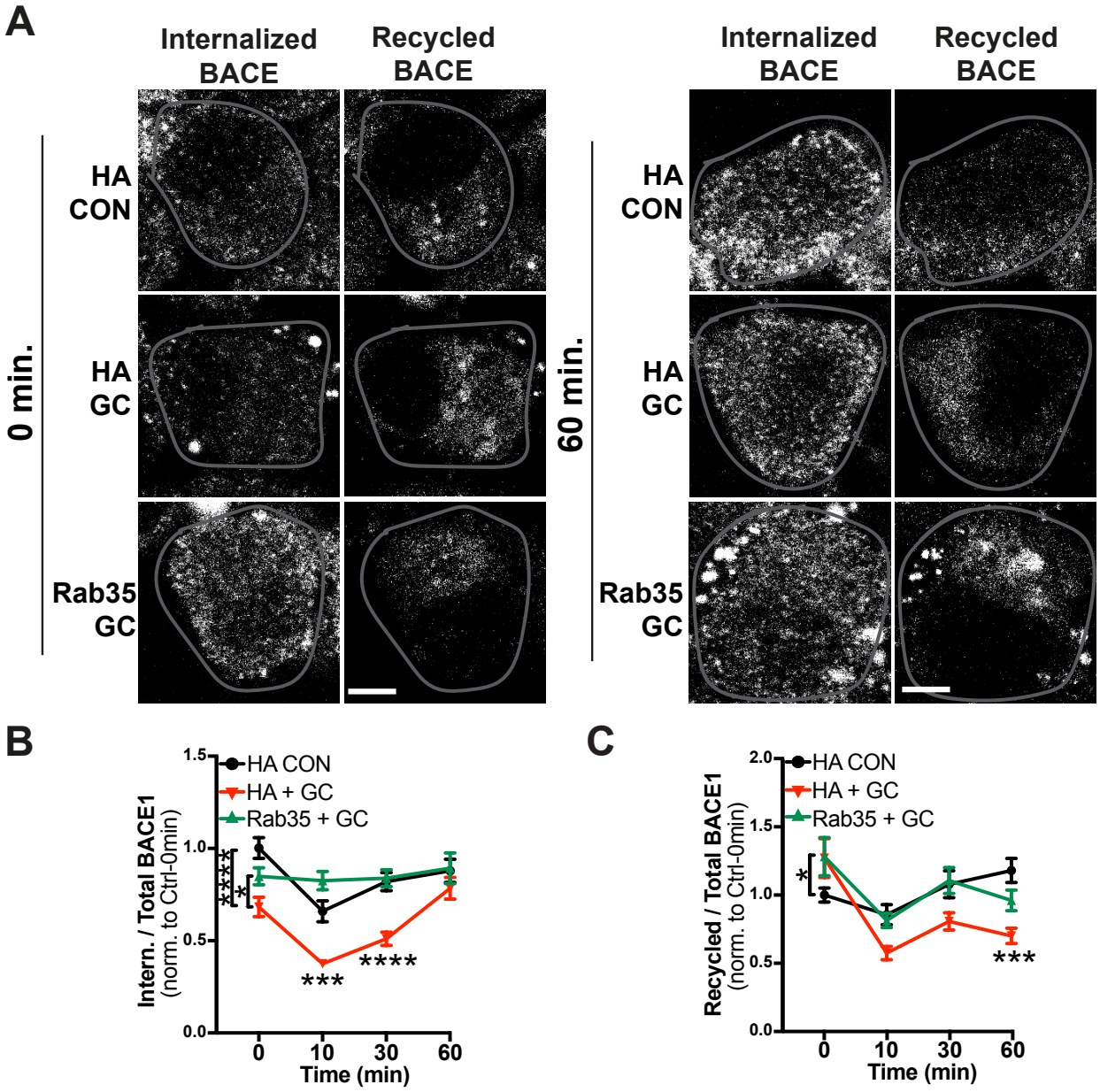

Figure 31. GC-induced pro-amyloidogenic BACE1 trafficking is blocked by Rab35 overexpression. A-C) Representative images and quantification of BACE1 internalization and recycling in N2a cells expressing FLAG-BACE1 and either HA or HA-Rab35, treated with GCs or vehicle control (CON). GC treatment decreases BACE1 internalization **(B)** and recycling **(C)**, and these effects are blocked by Rab35 overexpression (**For B:** *$P_{HA+GC\ vs\ HA-Rab35+GC}$=0.0491, ***$P_{HA+DMSO\ vs\ HA-+GC}$=0.0003, ****P<0.0001; two-way ANOVA with Tukey's multiple comparisons test, n=54-76 cells per condition/timepoint, 3 experiments. For BACE1 internalization: *Time* × *Condition* interaction $F_{6,765}$=3.385, P=0.0027. **For C:** *$P_{HA+DMSO\ vs\ HA-Rab35+GC}$=0.0487, ***$P_{HA+DMSO\ vs\ HA+GC}$=0.0009; two-way ANOVA with Tukey's multiple comparisons test, n=54-76 cells per condition/timepoint, 3 experiments. For BACE1 recycling: *Time* × *Condition* interaction $F_{6,762}$=3.504, P=0.0020). Scale bars: 5 µm. All numeric data represent mean ± SEM.

4.3. Summary

Endocytic and lysosomal abnormalities are among the earliest features of AD (Nixon, 2005), indicating that dysfunctional endosomal trafficking can trigger APP misprocessing and the accumulation of AD-associated proteins. Rab35 regulates the degradation, retrograde trafficking, and fast recycling of several membrane proteins through the endosomal network (Cauvin *et al.*, 2016; Kouranti *et al.*, 2006; Sheehan *et al.*, 2016; Vaz-Silva *et al.*, 2018), and this study is the first to investigate the role of Rab35 on APP and BACE1 trafficking pathways.

In this chapter, I demonstrate that Rab35 does not mediate the degradation of APP, APP-CTFs, or BACE1, but that it promotes BACE1 retrograde trafficking and APP recycling to the plasma membrane. I show that Rab35 overexpression increases BACE1 colocalization with the trans-Golgi network, and that this is mediated by the effector OCRL, similar to Rab35-mediated retrograde trafficking of the mannose-6-phosphate receptor (Cauvin *et al.*, 2016; Van Rahden *et al.*, 2012). Additionally, I show that APP internalization and recycling are increased by Rab35 overexpression, and that APP recycling is mediated by the effector ACAP2, an effector previously documented in Rab35-mediated recycling pathways (Mrozowska & Fukuda, 2016). These data indicate that Rab35 decreases APP-BACE1 interactions in endocytic compartments by sorting them into separate pathways that are dependent on distinct effectors.

Furthermore, the effects of chronic stress and GCs on the progression of AD and AD-related pathology in human patients and rodent models suggest that stress/GCs affect the molecular pathways underlying AD. Here, I provide more definitive evidence that GCs impact APP and BACE1 trafficking pathways. I show that GCs increase APP-BACE1 interaction and slow APP and BACE1 recycling to the cell surface, and that Rab35 overexpression blocks these effects, suggesting that Rab35-mediated trafficking pathways are disrupted by GCs. Collectively,

these data support my hypothesis that stress/GCs promote conditions for Aβ production by reducing Rab35 levels, thereby disrupting the sorting of APP and BACE1 out of the endosomal network and into their distinct trafficking pathways. Under these conditions, APP and BACE1 remain in endosomal compartments for longer time periods, enabling BACE1 to cleave APP and create Aβ.

Chapter 5: Methods for isolating and measuring exosomes

5.1. Rationale

5.1.1. Aβ and Tau spread during AD progression

The accumulation of Aβ peptides and hyperphosphorylated Tau are the hallmarks of AD, and stress/glucocorticoids (GCs) have been shown to promote both APP amyloidogenic processing and Tau hyperphosphorylation (Catania *et al.*, 2009; Green *et al.*, 2006; Jeong *et al.*, 2006; Sotiropoulos *et al.*, 2011, 2019; Srivareerat *et al.*, 2009). Furthermore, there is considerable evidence that Aβ and Tau enhance one other's accumulation to exacerbate AD pathology. For instance, secreted Tau has been shown to increase levels of Aβ peptides (Bright *et al.*, 2015), while oligomeric and fibrillar forms of Aβ promote Tau phosphorylation (Busciglio *et al.*, 1995; Ferreira *et al.*, 1997; Sackmann & Hallbeck, 2020). Aβ oligomers have also been shown to increase cellular uptake of Tau "seeds" (Shin *et al.*, 2019) that spread Tau pathology in a prion-like manner (Clavaguera *et al.*, 2020). Although AD is characterized by the combination of Aβ and Tau's degenerative effects, Tau appears to be the 'final executor' of AD progression and pathology. Intriguingly, Tau knockout has been shown to prevent Aβ-induced excitotoxicity and behavioral deficits in transgenic mice expressing human APP (hAPP) with a mutation that causes familial AD (Roberson *et al.*, 2007), and to block Aβ-induced axonal transport defects in hippocampal neurons (Vossel *et al.*, 2010). Furthermore, Tau knockout prevented stress-induced dendritic and synaptic loss in mouse hippocampus and prefrontal cortex, as well as accompanying behavioral deficits (Lopes *et al.*, 2017, 2016). These studies reveal that Tau knockout is protective against both Aβ- and stress-induced synaptotoxicity and indicate its essential role in AD- and stress-induced brain pathology.

A key characteristic of neurodegenerative diseases such as AD is their progression over time, driven by neuronal dysfunction that spreads throughout the brain (Przedborski *et al.*, 2003). Indeed, analysis of post-mortem brains from AD patients reveals that the spreading of Tau and amyloid pathology between interconnected brain areas correlates with disease severity (Braak & Braak, 1991). Amyloid plaques and Tau tangles are observed in the hippocampus during early-stage AD, and spread to the entorhinal cortex and frontal cortex in later disease stages. However, the mechanisms by which pathogenic Aβ and Tau spread between cells and across brain regions are unclear, and little is known about how stress/GCs affect these processes.

5.1.2. Astrocytes and microglia impact AD pathology

Though neurodegenerative disease research has historically focused on neuronal pathology, more recent studies have begun to uncover the contributions of glial cells in the progression of AD. Astrocytes and microglia support and protect neurons, often reacting quickly to disturbances, including injury, infection, and neurodegenerative disease (Gleichman & Carmichael, 2020; Jauregui-Huerta *et al.*, 2010). Astrocytes are the most common glial cell type in the brain, regulating functions such as blood-brain barrier maintenance and extracellular homeostasis, and their dysfunction has been linked to many types of brain pathology (Siracusa *et al.*, 2019). Astrocytes have been shown to take up and degrade Aβ (Mohamed & Posse De Chaves, 2011; Ries & Sastre, 2016), and their loss of function is linked to AD. However, astrocytes may also drive AD progression by promoting neuroinflammation (Garwood *et al.*, 2017) and potentially by producing Aβ, given that they express APP and its secretases (Frost & Li, 2017). Furthermore, Aβ synaptotoxicity and Tau phosphorylation in cell culture were reduced by the inhibition of astrocyte activation (Garwood *et al.*, 2011), suggesting that astrocytes are

drivers of neuronal damage initiated by Aβ and Tau. Astrocytes may also contribute to the intercellular spreading of amyloid and Tau pathology through the secretion of exosomes, extracellular vesicles ~40-150 nm in size that mediate intercellular communication. Exosomes released by astrocytes have been shown to selectively target neurons (Venturini *et al.*, 2019), and to carry Aβ (Winston *et al.*, 2019). It is currently unclear whether astrocytes contribute to or protect from Aβ-induced neuronal deficits, and they may behave differently depending on the stage of disease progression.

Microglia are the immune cells of the central nervous system, active and motile, patrolling the brain for pathogens, misfolded proteins, or unhealthy cells (Benarroch 2013; Bilbo & Stevens, 2017; Rock *et al.*, 2004). Microglia are important for neurogenesis, trophic support of neurons, and response to illness and injury (Paolicelli *et al.*, 2019). However, they can drive neuroinflammation when the brain is subject to chronic homeostatic perturbations (e.g. repeated injury, chronic stress, neurodegenerative disease), as they are the primary producers of cytokines and other inflammatory mediators (Hanisch, 2002; Li & Barres, 2018). Because of this feature, researchers have focused on neuroinflammation as the main contribution of microglia to AD progression. Indeed, there is ample evidence that activated microglia correlate with reduced functional brain activity and cognitive performance in AD patients, and that microglia activated by Aβ cause neuronal dysfunction and death through their release of cytokines (Leng & Edison, 2021). However, recent research indicates that in addition to neuroinflammation, microglia play a more direct role in AD by internalizing and secreting Aβ and Tau. Microglia may be protective early in AD by phagocytosing Aβ (Gratuze *et al.*, 2018), and detrimental in the later stages of AD through the spreading of Aβ or Tau pathology. Microglia have been shown to internalize aggregated Aβ and secrete it in a more synaptotoxic soluble form through extracellular vesicles

(Joshi *et al.*, 2014), suggesting that they promote the intercellular transmission of Aβ. Furthermore, microglia may also spread Tau pathology through extracellular vesicles (Fruhbeis *et al.*, 2013; Paolicelli *et al.*, 2019; Vogels *et al.*, 2019). In fact, depletion of either microglia or exosome production was found to reduce the spread of mutant Tau linked to human tauopathy (Asai *et al.*, 2015), indicating that both microglia and exosomes drive the spreading of pathogenic Tau between cells. Collectively, these studies suggest that astrocytes and microglia are important players in the progression of AD, and likely contribute to the spreading of Aβ and Tau pathology via exosomes.

Exosomes, small extracellular vesicles ~40-150nm in size, are released by most cell types (Deatherage & Cookson, 2012; Schorey *et al.*, 2015), and were initially thought to be a method of waste disposal (Johnstone, 1991; Johnstone *et al.*, 1987; Pan *et al.*, 1985; Rashed *et al.*, 2017). Currently, exosomes are known to function in intercellular communication, exchanging nucleic acids (Simpson *et al.*, 2009; Valadi *et al.*, 2007; Waldenstrom *et al.*, 2012), lipids (Vidal *et al.*, 1989), and proteins (Simpson *et al.*, 2009) between cells to maintain homeostasis, or as a response to pathological processes (Colombo *et al.*, 2014; Lo Cicero *et al.*, 2015; Van Niel *et al.*, 2018; Yanez-Mo *et al.*, 2015). Due to their role in sharing components between cells, exosomes are a means by which AD pathology can spread intercellularly. Exosomal proteins have been shown to accumulate in amyloid plaques of AD patients (Rajendran *et al.*, 2006), and prefibrillar Aβ preferentially binds to exosomes (Lim *et al.*, 2019), linking these vesicles to AD pathology. Moreover, brain-derived exosomes from AD patients carry oligomeric Aβ, which can be taken up by cells in culture (Sinha *et al.*, 2018). Interestingly, blocking the formation, secretion, and uptake of exosomes reduced the spread of Aβ oligomers (Sinha *et al.*, 2018), indicating that they are an important component in the spread of Aβ.

Tau has also been found in purified exosomes from cerebrospinal fluid (CSF) of AD patients, and from Tau transgenic (P301L) mouse brain and neuroblastoma cells (Brunello *et al.*, 2020). Neuron-derived exosomes from AD patients promote Tau phosphorylation in wild-type mice (Winston *et al.*, 2016), indicating that exosomes can spread Tau pathology. Furthermore, Tau-containing exosomes released by neurons can be taken up by neighboring neurons and microglia (Wang *et al.*, 2017), indicating that they may spread AD pathology intercellularly, and that this can occur between different cell types. Together, these studies suggest that exosomes are important mediators of the intercellular spread of Aβ and Tau.

5.1.3. Exosome generation and secretion

Exosomes play an important role in cellular homeostasis and intercellular communication, by removing misfolded proteins and transferring proteins, lipids, and RNAs from cell to cell. Exosomes are generated through the endosomal pathway: originating as the intraluminal vesicles (ILVs) of multivesicular bodies (MVBs), they become exosomes when MVBs fuse with the plasma membrane (Luarte *et al.*, 2017; Van Niel *et al.*, 2006). The endosomal sorting complex required for transport (ESCRT) pathway is critical for the formation of MVBs, and the first ESCRT component, Hrs, has been shown to regulate exosome secretion (Tamai *et al.*, 2010). ILVs are generated at MVB membranes through several pathways: in the canonical ESCRT-dependent pathway, Hrs recruits downstream ESCRT components, controlling the initiation and completion of membrane budding. In the non-canonical ESCRT-dependent pathway, the proteins syntenin, syndecan, and ALIX cluster cargoes and initiate membrane budding, but ESCRT-III and VPS-4 are still required for the completion of membrane budding to form ILVs (Teng & Fussenegger, 2021). Additionally, exosomes can form at MVB membranes

through two ESCRT-independent pathways: tetraspanin clustering and ceramide-induced ILV formation (Blanc & Vidal, 2018; Escola *et al.*, 1998; Perez-Hernandez *et al.*, 2013; Teng & Fussenegger, 2021; Trajkovic *et al.*, 2008; Van Niel *et al.*, 2018). Tetraspanins are transmembrane proteins that cluster cargo for ILV loading, and whose shape facilitates the budding of membranes to form ILVs (Blanc & Vidal, 2018). Ceramide can form lipid raft domains that induce membrane invagination to create ILVs (Teng & Fussenegger, 2021). All of these pathways facilitate cargo loading and the generation of exosomes from MVBs (**Fig. 32**).

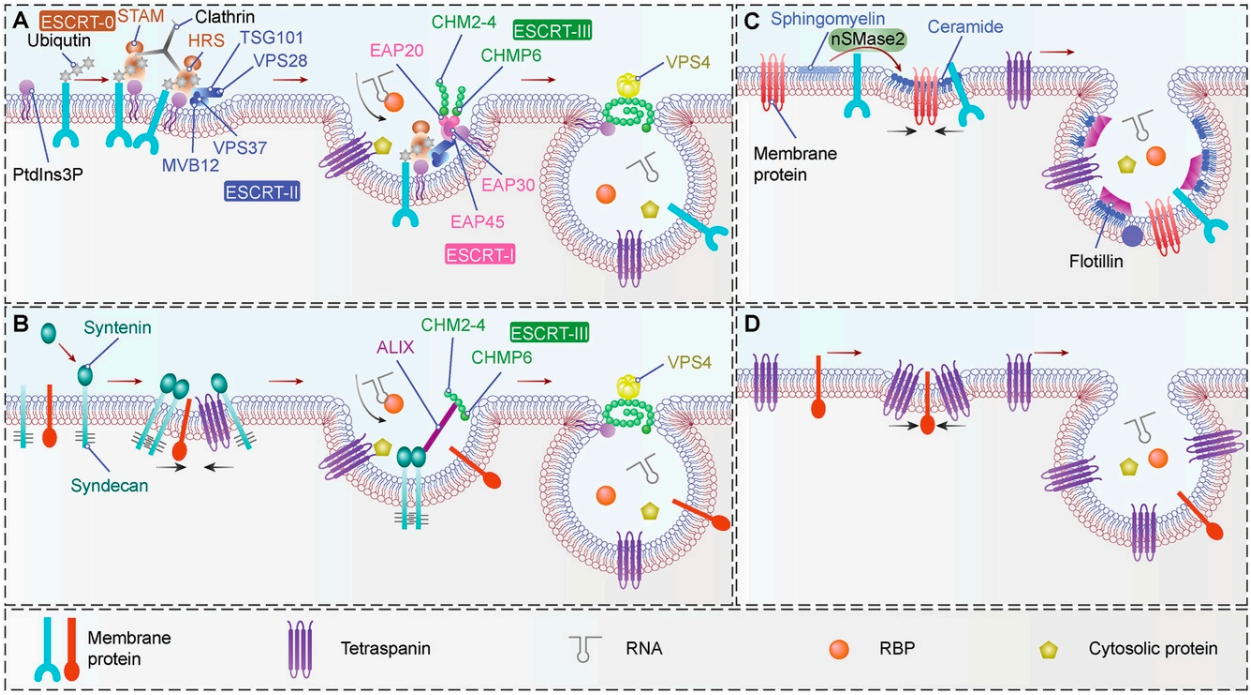

Figure 32. MVB biogenesis machineries. Multiple molecular mechanisms of ILV generation in MVB have been revealed. A) In the canonical ESCRT-dependent pathway, ubiquitinated proteins in the endosomal membrane are recognized by ESCRT-0, which is recruited to the endosomal membrane by PtdIns3P binding and subsequently clustered into microdomains via clathrin binding. Then ESCRT-0 recruits ESCRT-I, and ESCRT-I recruits ESCRT-II. ESCRT-I and ESCRT-II coordinately induce the budding of the endosomal membrane and confine cargos within the buds. ESCRT-III components are dynamically recruited for membrane scission of the ILV necks and disassembled after ILV scission via VPS4. In a non-canonical ESCRT-dependent pathway, HD-PTP binds to ESCRT-0 and coordinately recruits ESCRT-I and ESCRT-III, bypassing the need for ESCRT-II. **B)** In the syndecan-syntenin-ALIX pathway, membrane budding and cargo clustering can occur independently of ubiquitin and ESCRT-0, but ESCRT-III and VPS4 are required for the scission step. **C)** Ceramide, generated from sphingomyelin by mSMase2, plays a key role in the ESCRT-independent pathway of ILV biogenesis. Ceramide can form lipid raft microdomains, which might trigger the conversion of ILVs into MVBs. **D)** CD63 plays a vital role in the ESCRT-independent pathway of ILV biogenesis. CD63 can form tetraspanin-enriched microdomains, which might trigger the conversion of ILVs into MVBs. Abbreviations: MVB, multivesicular body; ILV, intraluminal vesicle; ESCRT, endosome sorting complex

required for transport; PdtIns3P, phosphatidylinositol 3-phosphate; STAM, signal transducing adaptor molecule; HRS, hepatocyte growth factor-regulated tyrosine kinase substrate; TSG101, tumor susceptibility gene 101 protein; VPS, vacuolar protein sorting; MVB12, multivesicular body subunit 12; CHMP, charged multivesicular body protein; HD-PTP, His domain protein tyrosine phosphatase; ALIX, ALG-2 interacting protein X; nSMase2, neutral sphingomyelinase 2. Copyright © 2021 The Authors, published by John Wiley & Sons, reprinted from Teng & Fussenegger, 2021, with permission under the terms of the Open Access Creative Commons CC BY license, provided as-is with no warranties or liabilities concerning this material.

Previous studies indicate that Rab35 regulates exosome secretion in specific cell types (Abrami *et al.*, 2013; Fruhbeis *et al.*, 2013; Gauthier *et al.*, 2017; Hsu *et al.*, 2010; Yang *et al.*, 2019). Rab35 plays an important role in the endolysosomal sorting of proteins (Sheehan & Waites, 2019; Sheehan *et al.*, 2016; Uytterhoeven *et al.*, 2011), as well as in protein endocytosis and recycling with the plasma membrane (Allaire *et al.*, 2013; Dutta & Donaldson, 2015; Klinkert & Echard, 2016; Kobayashi & Fukuda, 2012; Kobayashi *et al.*, 2014; Kobayashi & Fukuda, 2013; Patino-Lopez *et al.*, 2008), indicating that it could regulate both the formation and secretion of exosomes. Indeed, inhibition of Rab35 activity has been shown to impair exosome secretion (Abrami *et al.*, 2013; Hsu *et al.*, 2010), and the upregulation of Rab35 expression by the non-coding RNA HOTAIR enhances exosome secretion by promoting MVB docking (Yang *et al.*, 2019). While studies to date have only examined Rab35's role in exosome release (Abrami *et al.*, 2013; Fruhbeis *et al.*, 2013; Hsu *et al.*, 2010), it is conceivable that Rab35 contributes to the ESCRT-mediated formation of MVB-derived exosomes via its recruitment of ESCRT-0 component Hrs (Sheehan *et al.*, 2016; Vaz-Silva *et al.*, 2018). Our future studies will examine the role of Rab35 in exosome formation, cargo loading, and secretion in different brain cell types (neurons, microglia, and astrocytes), and in the context of Aβ and Tau intercellular transmission (**Fig. 33**). Additionally, by testing for the presence of ESCRT components, tetraspanins, and ceramide on Rab35-mediated exosomes, we can determine whether these exosomes are generated through ESCRT-dependent or -independent processes.

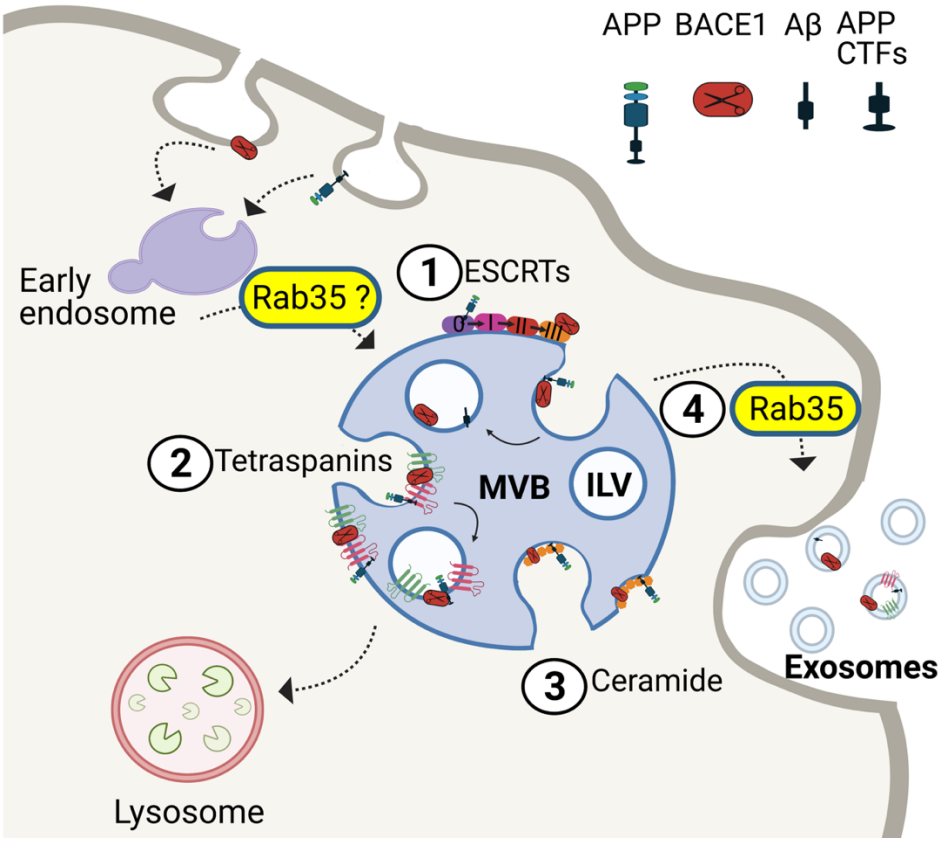

Figure 33. Putative role of Rab35 in exosome formation and secretion. Endocytosed proteins travel through the early endosome, where they can be sorted to multivesicular bodies (MVB), and loaded into intraluminal vesicles (ILV). Exosomes are generated when MVBs fuse with the plasma membrane and release ILVs into the extracellular space instead of fusing with a lysosome for degradation. ILVs can form at MVB membranes through the endosomal sorting complex required for transport (ESCRT) pathway (1), tetraspanin clustering (2), or ceramide-mediated ILV budding (3). It is unclear if Rab35 regulates the ESCRT-mediated generation of ILVs, but studies show that Rab35 promotes MVB docking and exosome secretion (4).

Exosome secretion is also modulated by stress in cells. Endoplasmic reticulum stress has been shown to promote MVB formation and extracellular vesicle release (Kanemoto *et al.*, 2016; O'Neill *et al.*, 2019). Furthermore, cellular stress can alter the protein and microRNA cargo of exosomes (Chen *et al.*, 2018; De Jong *et al.*, 2012; Harmati *et al.*, 2019), indicating that stressors have an impact on both exosome secretion and on their contents. Interestingly, stress-regulated exosome release by astrocytes has been shown to reduce neuronal dendritic complexity (Luarte *et al.*, 2020), providing a link between cellular stress, glial exosome secretion, and dendritic

damage. However, the effects of chronic stress and glucocorticoids on exosome secretion in cell types of the brain are not yet clear. Moreover, the connection between stress/GCs and APP amyloidogenic processing, Tau hyperphosphorylation and mislocalization, and their potential spread through exosomes remains largely unexplored.

In the previous chapters, I described the role of Rab35 in reducing APP-BACE1 interaction, which produces Aβ**,** and the impact of stress on Rab35-mediated APP and BACE1 trafficking pathways. These data, in combination with our previous work showing that Rab35 promotes Tau degradation, indicate that Rab35 regulates the intracellular trafficking of these major AD-associated proteins. In this chapter, I describe methods for investigating the roles of stress/GCs and Rab35 in exosome secretion, which can spread Aβ or Tau between cells.

5.2. Results

5.2.1. Size-exclusion chromatography yields more EVs than serial ultracentrifugation

To begin our investigations, we first established and compared two techniques for extracellular vesicle (EV) purification from various cell types. We purified EVs from mouse neuroblastoma (N2a) and immortalized microglial (IMG) cells, as well as primary rodent astrocytes and neurons using serial ultracentrifugation (Perez-Gonzalez *et al.*, 2017; Thery *et al.*, 2006) or size exclusion chromatography (Koh *et al.*, 2018; Lobb & Moller, 2017) (**Fig. 34A-C**). Nanoparticle tracking analysis (NTA) was used to determine particle counts and sizes, which were calculated by ParticleMetrix ZetaView by measuring the Brownian motion of each particle (**Fig. 34D**).

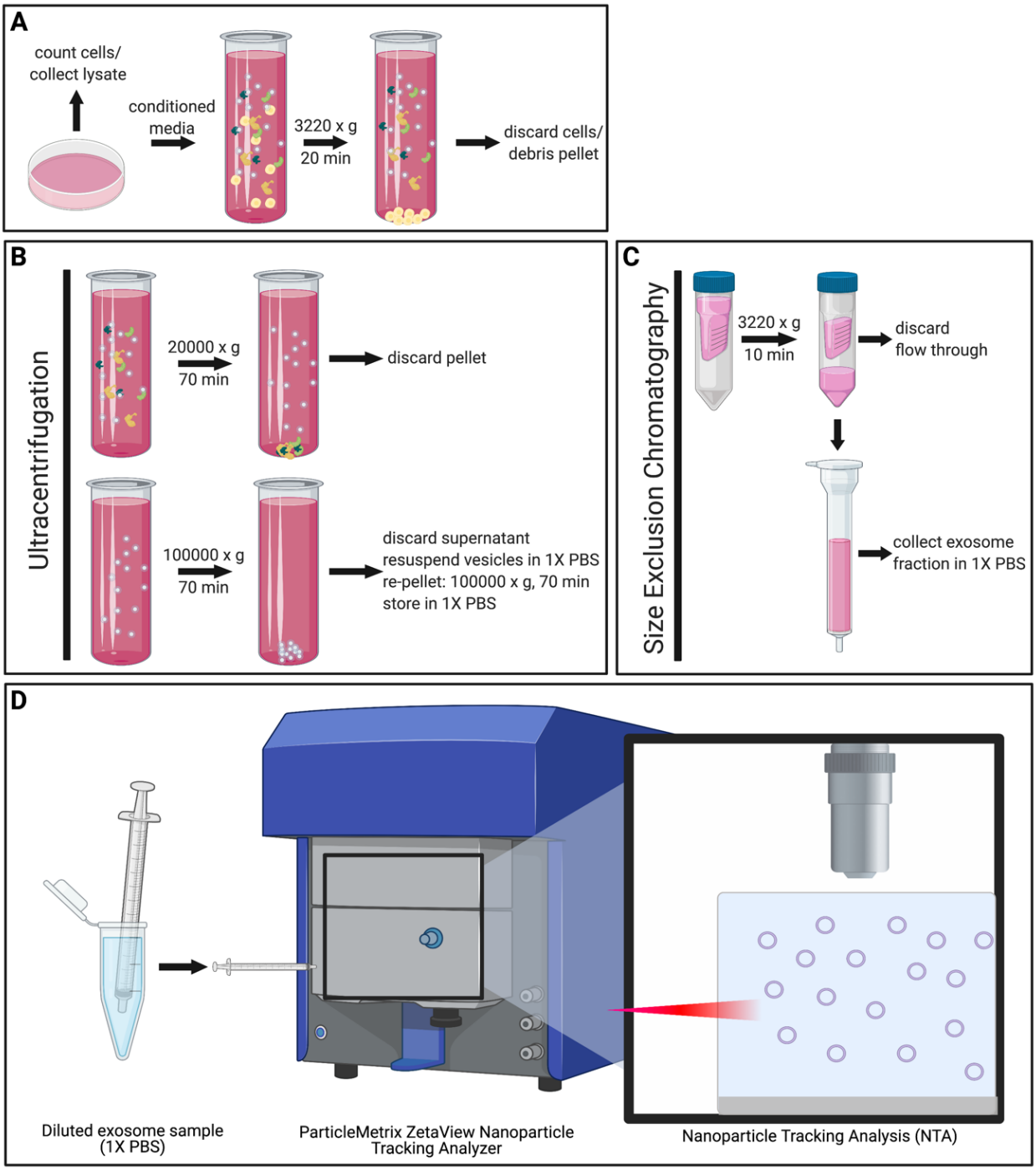

Figure 34. Techniques used for purifying and measuring EVs. A) Conditioned medium is centrifuged to remove cell debris, and cells are collected for counting and western blot analysis. **B)** Ultracentrifugation at 20000 x g (70 min) and 100000 x g (70 min, 2 times) is used to isolate EVs in the serial ultracentrifugation protocol. **C)** Size exclusion chromatography requires a conditioned medium concentration step (3220 x g, 10 min) prior to EV isolation and is a faster purification process. **D)** EV samples are diluted in 1X PBS and analyzed using Nanoparticle Tracking Analysis, which determines particle count and size by measuring Brownian motion using a laser and camera.

Following EV purification, we verified that our samples contained exosomes by immunoblotting for the commonly-used exosome markers ALIX and TSG101 (Willms *et al.*, 2016). Indeed, we found that our purified samples contained both markers and were enriched in ALIX compared to cell lysate (**Fig. 35A**). We then compared ultracentrifugation (UC) to size exclusion chromatography (SEC) by isolating EVs from primary mouse cortical neurons. By SEC, we were able to recover more EVs relative to the number of cells, and the particles measured were smaller in size than those isolated by UC, indicating a purer EV sample (**Fig. 35B-C**). We concluded that SEC provides more efficient EV purification than UC, and we will use this technique for future experiments requiring EV isolation.

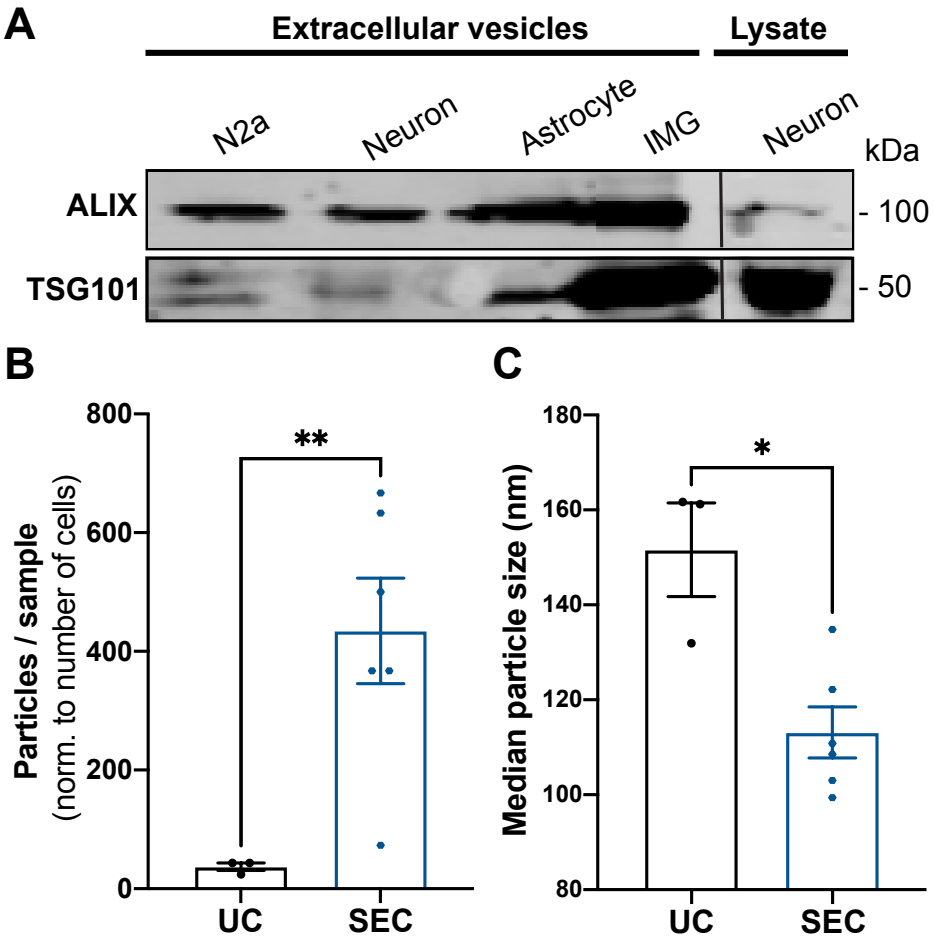

Figure 35. Verification of exosome purification and comparison of ultracentrifugation versus size exclusion chromatography techniques. A) EVs isolated by ultracentrifugation from N2a cells, rat primary cortical neurons and astrocytes, and IMG cells were probed for the exosome markers ALIX and TSG101, and showed enriched expression of ALIX compared to cell lysate. **B-C)** Comparison of particle counts and particle sizes detected by NTA from mouse primary cortical neuron EV samples, purified using ultracentrifugation (UC) and size exclusion chromatography (SEC). The number of detected particles were divided by the number of cells for each collected sample, and the median particle sizes were recorded. SEC yields more EVs relative to the number of cells (**P=0.0065, *P=0.0367, unpaired, two-tailed Welch's t-test, n=3-6 independent samples/technique), and the EVs are smaller in size, indicating purer EV isolation. All numeric data represent mean ± SEM.

5.2.2. On-chip interferometry counts EVs and antibody binding reveals tetraspanin profiles

Both ultracentrifugation and size exclusion chromatography isolate EVs based on size, but exosome identity must still be verified via immunoblot using exosome-enriched markers and via electron microscopy to visualize vesicle size and morphology. On-chip exosome analysis (ExoView R100, NanoView Biosciences) bypasses these steps by capturing EVs expressing CD9 and CD81, tetraspanin proteins enriched on exosome membranes (Andreu & Yanez-Mo, 2014). With this method, conditioned medium or purified EV samples are incubated on chips containing antibodies against CD9 and CD81, which serve as capture probes (**Fig. 36A**). Following incubation, particle sizes are measured by interferometric imaging with an infrared wavelength of 405 nm, detecting extracellular vesicles in the 50-200nm range (**Fig. 36B**). The captured vesicles are also incubated with fluorescent antibodies against CD81, CD9, and CD63 (**Fig. 36C**), and colocalization of these markers is measured by fluorescence on the chip (**Fig. 36D**) to provide a readout of the tetraspanin profiles of each sample.

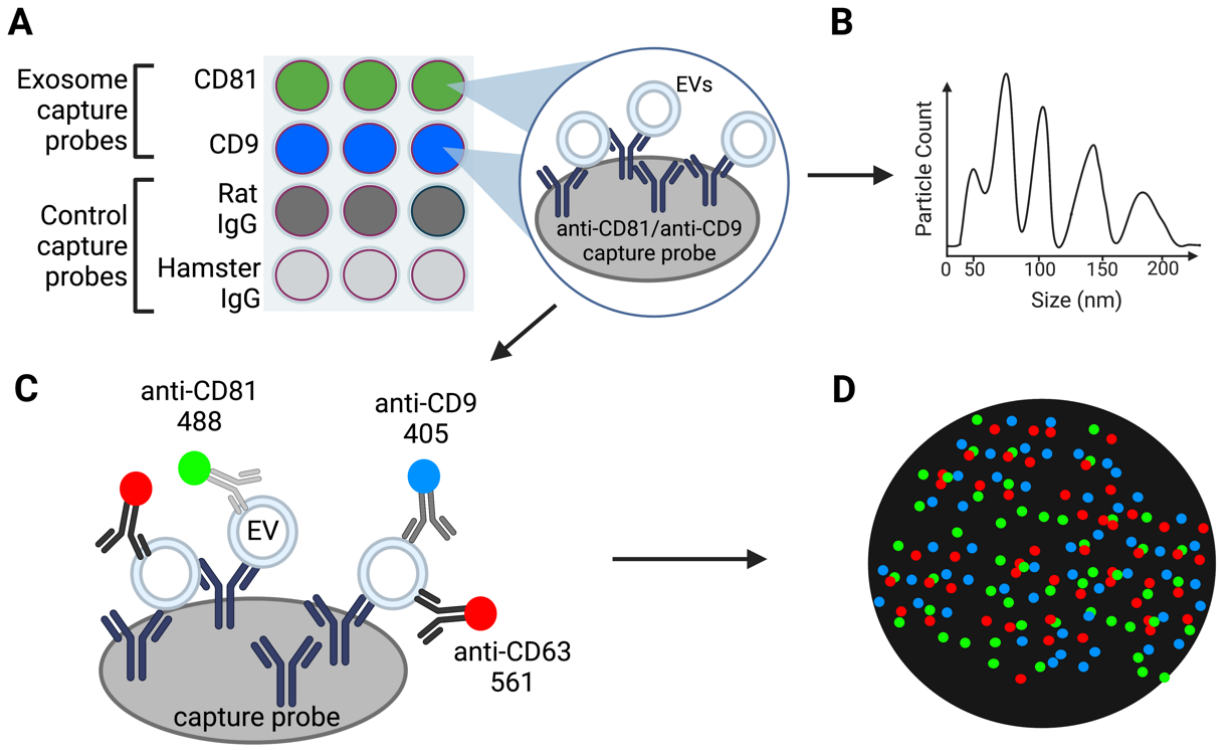

Figure 36. ExoView on-chip interferometry and tetraspanin colocalization workflow. A) Samples are loaded onto chips containing antibodies against the exosome markers CD81 and CD9, along with two isotype controls. CD81-positive and CD9-positive EVs bind to the antibodies on these capture probes. **B)** Vesicle sizes between 50-200 nm are determined using infrared interferometry. **C)** EVs bound to chip capture probes are incubated with fluorophore-conjugated antibodies against CD81, CD9, and CD63. **D)** Tetraspanin profiles of each sample are determined by fluorescence imaging measuring the colocalization between tetraspanin antibodies.

5.2.3. Microglia may secrete more exosomes than other cell types

Microglia and astrocytes have been shown to take up Aβ and Tau from their surrounding environments (Asai *et al.*, 2015; Gratuze *et al.*, 2018; Joshi *et al.*, 2014; Mohamed & Posse De Chaves, 2011; Perea *et al.*, 2019; Wang *et al.*, 2017), and contribute to the spread of AD pathology (Garwood *et al.*, 2011; Venturini *et al.*, 2019; Vogels *et al.*, 2019; Winston *et al.*, 2019), suggesting that they may take up extracellular Tau or Aβ and secrete them through exosomes. To determine which brain cell types are the primary producers of exosomes, we used NTA to compare the number of EVs released by neurons, astrocytes, and microglial cells, normalized to the number of cells in each sample. Our preliminary data show that immortalized

microglial cells (IMG) produce more EVs than primary rodent neurons and astrocytes (**Fig. 37A-B**), indicating that microglia may play a large role in exosome-mediated transmission of AD-related proteins. Because this effect could be due to the immortalized nature of the IMG cells, we compared purified EV samples from IMG cells with those of another immortalized cell line, neuronal-derived N2a cells. We used ExoView on-chip interferometry to compare the number of EVs captured on CD9 and CD81 capture probes, and found that that IMG cells secreted more total CD9+ and CD81+ particles than N2a cells (**Fig. 37C-D**). These results indicate that microglial cells may produce substantially more exosomes than neuronal cells, and potentially contribute to the spread of Tau and Aβ through exosomes.

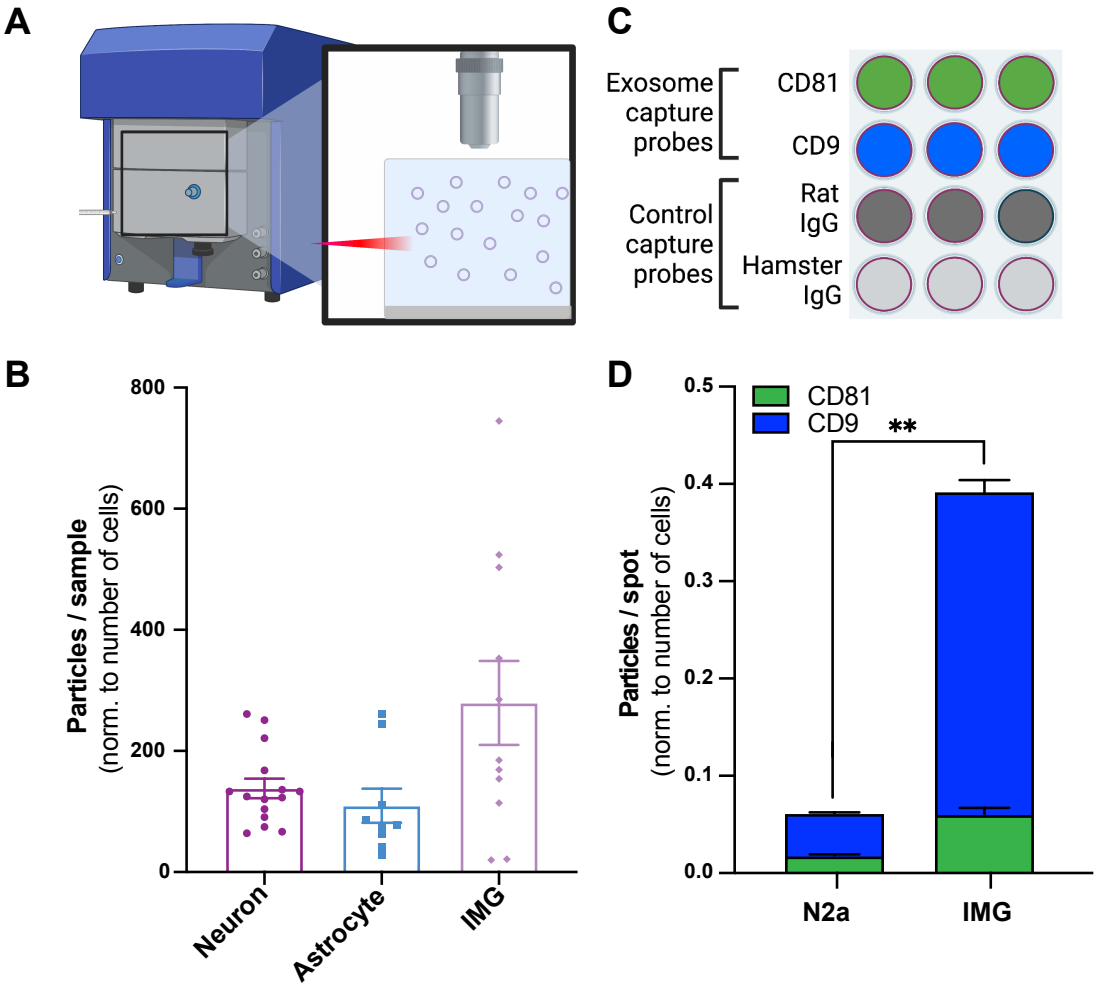

Figure 37. IMG cells produce more EVs than primary cortical neurons, astrocytes, and N2a cells. A) Schematic of nanoparticle tracking analysis (NTA) to count the number of particles per sample. **B)** EVs produced by primary rat cortical neurons and astrocytes, as well as mouse immortalized microglial cells (IMG) were collected by serial ultracentrifugation, counted by NTA, and normalized to the number of cells in the sample. IMG cells trend toward increased particles relative to the number of cells ($P_{Neuron\ vs.\ IMG}$=0.1924, $P_{Astrocyte\ vs.\ IMG}$=0.1132, Brown-Forsythe ANOVA with Dunnett's correction, n=9-15 samples/condition, 4-6 independent cultures). **C)** Schematic of ExoView chips with exosome capture probes containing anti-CD81 and anti-CD9 antibodies, along with isotype control capture probes against rat and hamster IgG. **D)** ExoView interferometry analysis of particles captured by CD81 and CD9 probes, measuring the amount of CD81+ and CD9+ particles. Compared to the N2a sample, the IMG sample contained significantly more particles relative to the number of cells (**P=0.0079, Mann-Whitney test, n=5 capture probe spots/sample; 1 sample/cell type). ExoView samples in D were run by NanoView Biosciences. All numeric data represent mean ± SEM.

Furthermore, we characterized the tetraspanin profiles of exosomes captured by CD81 and CD9 chip capture probes (**Fig. 38A).** The IMG sample was enriched for CD9 compared to the N2a sample (**Fig. 38B-E**), suggesting that different cell types release exosomes with distinct tetraspanin profiles. In upcoming experiments, we will characterize the tetraspanin profiles of primary neurons, astrocytes, and microglia, which could allow us to determine which cell types release the majority of exosomes in mixed-cell cultures and samples from intact brain.

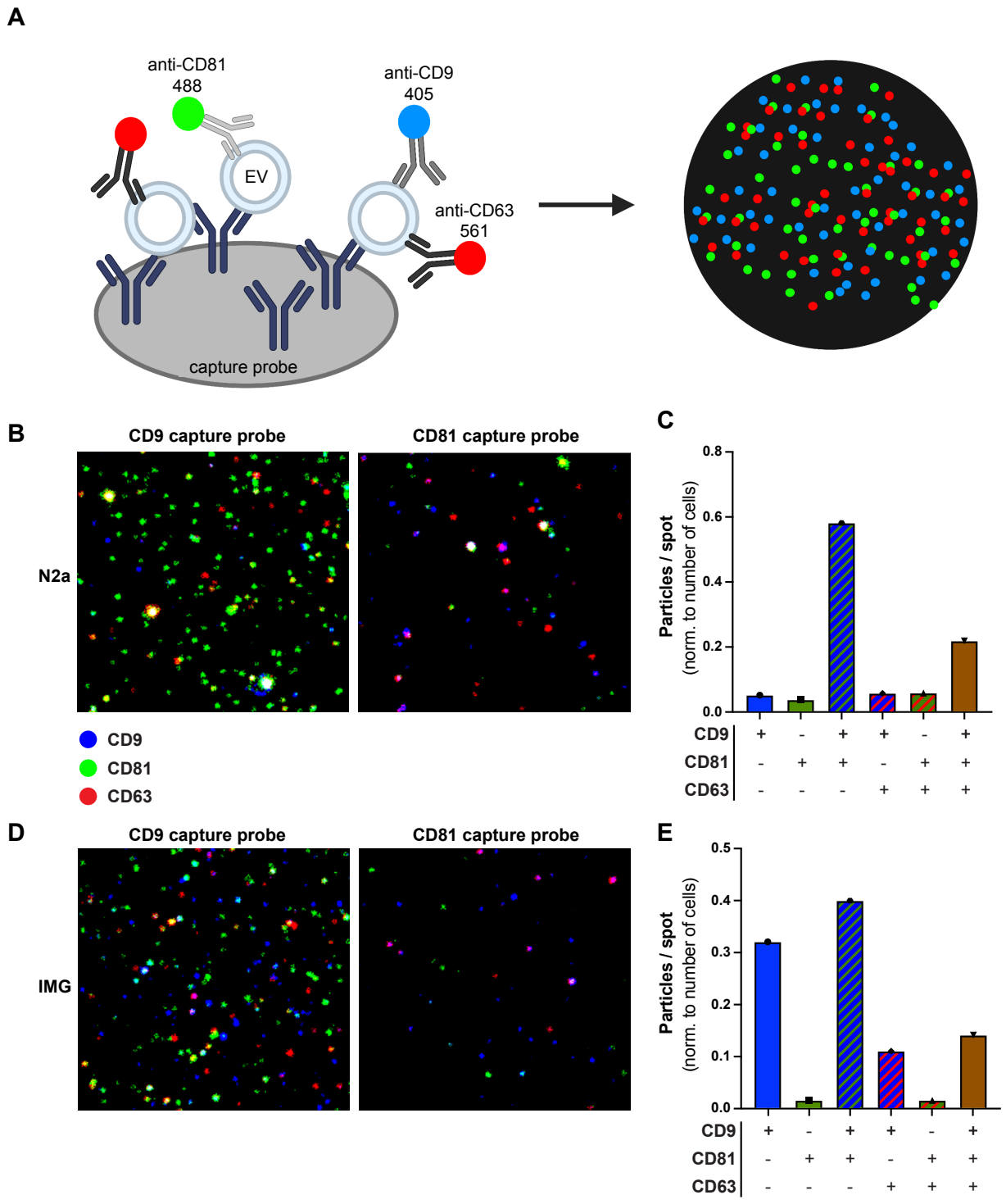

Figure 38. Exosomes from IMG cells are enriched in CD9. A) Schematic of exosomes incubated with tetraspanin antibodies after binding to ExoView capture probes, followed by fluorescence imaging for tetraspanin colocalization. **B)** Representative images of capture probe spots with CD9+ (blue), CD81+ (green), and CD63+ (red) vesicles. EVs were purified from N2a cell conditioned media by ultracentrifugation. **C)** Quantification of CD9+, CD81+, and CD63+ EVs. The number of single-, double-, and triple-positive EVs were normalized to the number of cells and averaged for both CD9 and CD81 capture spots. N2a cells produce more CD9+/CD81+ and CD9+/CD81+/CD63+ vesicles than any other tetraspanin combination. **D)** Representative images of capture probe spots with CD9+ (blue), CD81+ (green), and CD63+ (red) vesicles. EVs were purified from IMG cell conditioned media by ultracentrifugation. **E)**

Quantification of CD9+, CD81+, and CD63+ EVs, normalized to the number of cells and averaged for both CD9 and CD81 capture spots. The IMG cell sample was enriched for CD9+ and CD9+/CD63+ EVs compared to the N2a cell sample. ExoView samples in B-E were run by NanoView Biosciences. All numeric data represent mean ± SEM.

5.2.4. pHluorin-tagged CD63 and CD81 allow for the monitoring of exosome release in real time

Our EV purifications from conditioned media provide bulk data about exosome secretion and tetraspanin profiles of exosomes from specific cell types, but they cannot be used to study exosome release dynamics at the single-cell level. Thus, in addition to NTA and on-chip analysis methods of measuring EV secretion, we are employing a live imaging-based approach to measure exosome secretion from individual cells, using the pH-sensitive GFP variant pHluorin fused to CD63 or CD81 (Lee *et al.*, 2019; Pols & Klumperman, 2009). The fluorescence of these pHluorin-tagged exosomes is quenched in the acidic environment of MVBs, and activated when exosomes are released into the extracellular space (**Fig. 39A**). CD63-pHluorin has been used in a series of studies to visualize exosome secretion *in vitro* and *in vivo* with high spatial and temporal resolution (Messenger *et al.*, 2018; Sinha *et al.*, 2016; Sung *et al.*, 2015; Sung *et al.*, 2020; Verweij *et al.*, 2019; Verweij *et al.*, 2018). In my preliminary experiments, I readily visualized exosome release events in N2a cells expressing mCherry-pHluorin-CD63 and mCherry-pHluorin-CD81 by total internal reflection fluorescence (TIRF) microscopy (**Fig. 39B-C**), supporting the utility of this method. Exosome secretion was measured by timelapse image capture at 500 ms intervals over a period of 3 minutes. N2a cells on glass-bottom dishes were maintained in Normal Tyrode's solution and a humidity chamber at 37°C with 5% CO_2 for the entirety of imaging, ensuring that exosome dynamics mimic those occurring under physiological conditions.

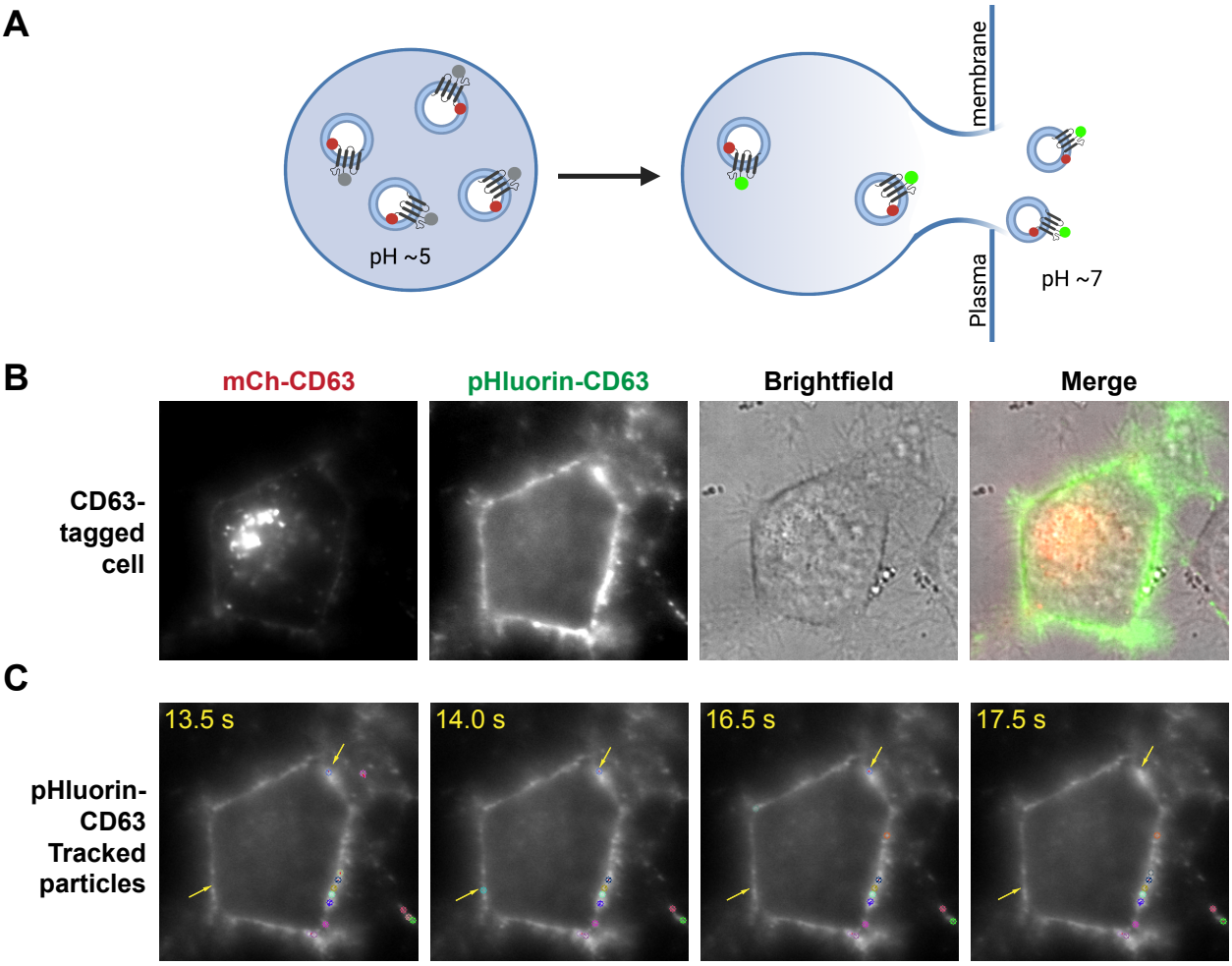

Figure 39. Total Internal Reflection Fluorescence imaging of N2a cells expressing mCherry-pHluorin-CD63. **A)** Schematic of a multivesicular body (MVB) containing exosomes expressing a tetraspanin protein tagged with mCherry and pHluorin. At the lower MVB pH (~5), pHluorin fluorescence is quenched (gray dot) while mCherry fluorescence persists (red dot). When the MVB fuses with the plasma membrane, the neutral pH (~7) of the extracellular space causes exosomes expressing the pHluorin-tagged tetraspanin to fluoresce (green dot). **B)** Representative images of an N2a cell expressing mCh-pHluorin-CD63. mCherry fluorescence is seen most brightly in the center of the cell where proteins are synthesized; pHluorin fluorescence is around the cell periphery where vesicles fuse. Brightfield images are used to visualize the cell perimeter. The merged image provides a full view of the cell expressing both mCh (red) and pHluorin (green). **C)** Example images of EV tracking in the pHluorin channel during timelapse imaging. Images were acquired every 500 ms for 3 min and analyzed using ImageJ Fiji 2D/3D Particle Tracker, which circles any moving particles. Here, transient EV release is marked by the lower left arrow. The software tracks a vesicle appearing at 14 s and disappearing at 16.5 s. More sustained vesicle release is marked by the top right arrow, where the software tracks a vesicle appearing at 13.5 s and disappearing at 17.5 s.

5.2.5. GCs may increase exosome secretion

Stress/GCs have been shown to modulate exosome secretion and contents in cancer cells as well as microglia (Chen *et al.*, 2018; Harmati *et al.*, 2019; Vulpis *et al.*, 2019). We aim to

determine how GCs affect exosome secretion in neurons, astrocytes, and microglia, and whether this contributes to the transmission of Aβ or Tau. Using ExoView on-chip exosome analysis in preliminary experiments, we found that treating mouse primary cortical neurons with dexamethasone, a synthetic glucocorticoid (GC), did not affect particle capture on CD9+ and CD81+ capture probes (**Fig. 40A-B**) or their tetraspanin profiles (**Fig. 40C-F**).

Interestingly, visualization of exosome secretion by live imaging using pHluorin-tagged tetraspanins in N2a cells revealed that GC treatment increased the total number of CD63-positive exosomes released (**Fig. 41A-B**). Surprisingly, CD81-positive exosomes did not show the same trend (**Fig. 41C-D**). This may be due to the smaller size of CD81+ exosomes (as reported by Lee *et al.*, 2019) and lower observed fluorescence of pHluorin-CD81, leading to reduced recognition of release events by the particle tracking software. Alternatively, GCs may have differential effects on specific tetraspanin-expressing exosomes, though this is contrary to our preliminary results on tetraspanin profiles of control and GC-treated primary cortical neurons, which showed no differences in exosomal CD9, CD81, and CD63 expression between conditions (see **Fig. 40**). In upcoming experiments, we will resolve this question by using primary neurons, astrocytes, and microglia to determine the effects of GCs on exosome secretion using both techniques: ExoView interferometry and tetraspanin profiling, as well as live cell imaging. In the future, our lab will also use proteomics and miRNAomics on purified EV samples to determine how GCs impact EV cargo in neurons and glia.

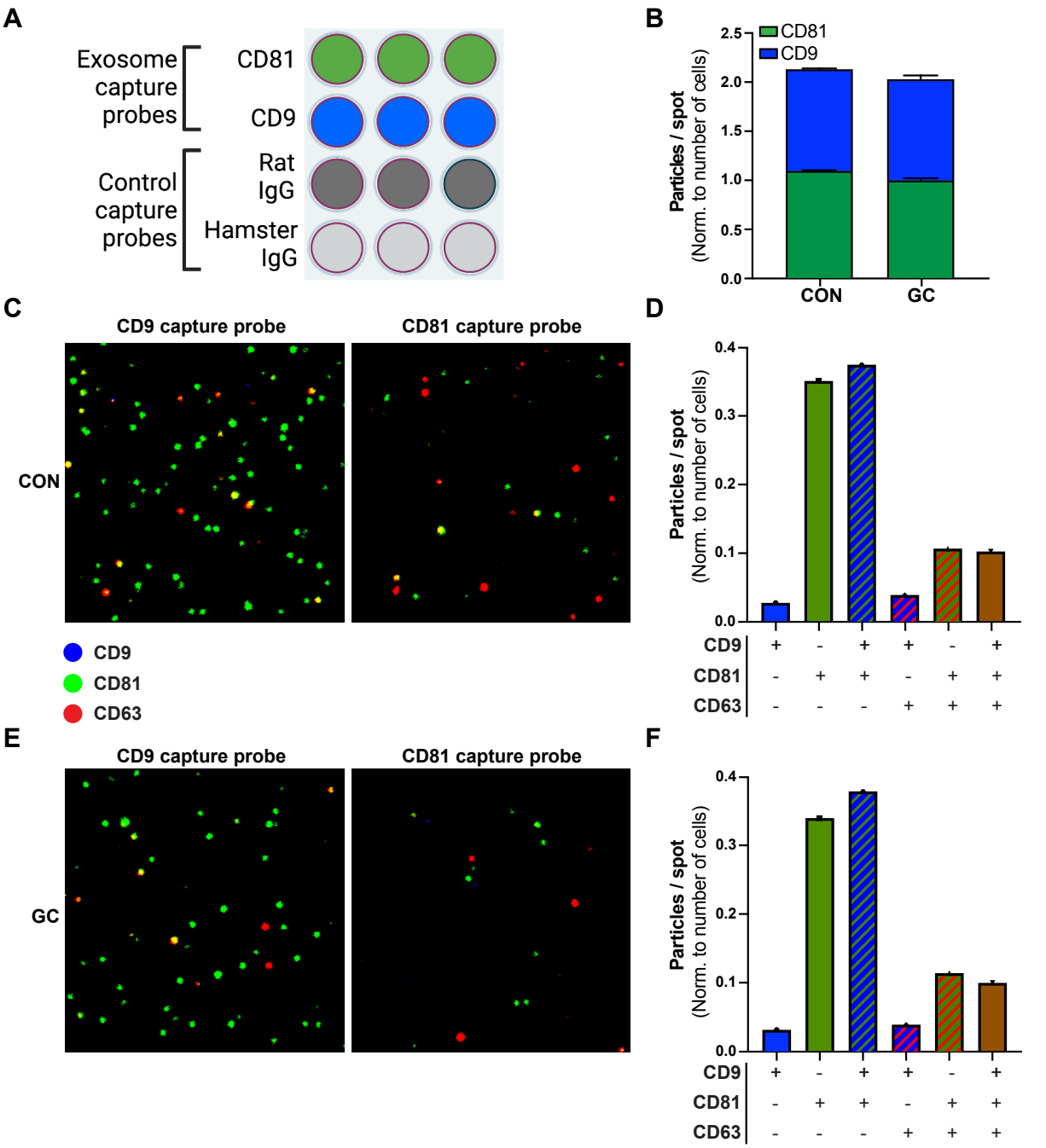

Figure 40. GC treatment does not affect total CD9+ and CD81+ exosome secretion or tetraspanin profiles in primary mouse cortical neurons. A) Schematic of ExoView chips with exosome capture probes containing anti-CD81 and anti-CD9 antibodies, along with isotype control capture probes against rat and hamster IgG. **B)** ExoView interferometry analysis of particles captured by CD81 and CD9 probes, measuring the amount of CD81+ and CD9+ positive particles in SEC-purified EV samples from primary mouse cortical neurons treated with glucocorticoids (GC) or vehicle control (CON). **C-D)** Representative images and quantification of capture probe spots with CD9+ (blue), CD81+ (green), and CD63+ (red) EVs from control neurons. The number of single-, double-, and triple-positive EVs were normalized to the number of cells and averaged for both CD9 and CD81 capture spots. **E-F)** Representative images and quantification of single-, double-, and triple-positive EVs on capture probe spots from GC-treated neurons. The number of EVs were normalized to the number of cells and averaged for both CD9 and CD81 capture spots. Exosomes captured by the probes had the same tetraspanin profiles regardless of GC treatment. All numeric data represent mean ± SEM.

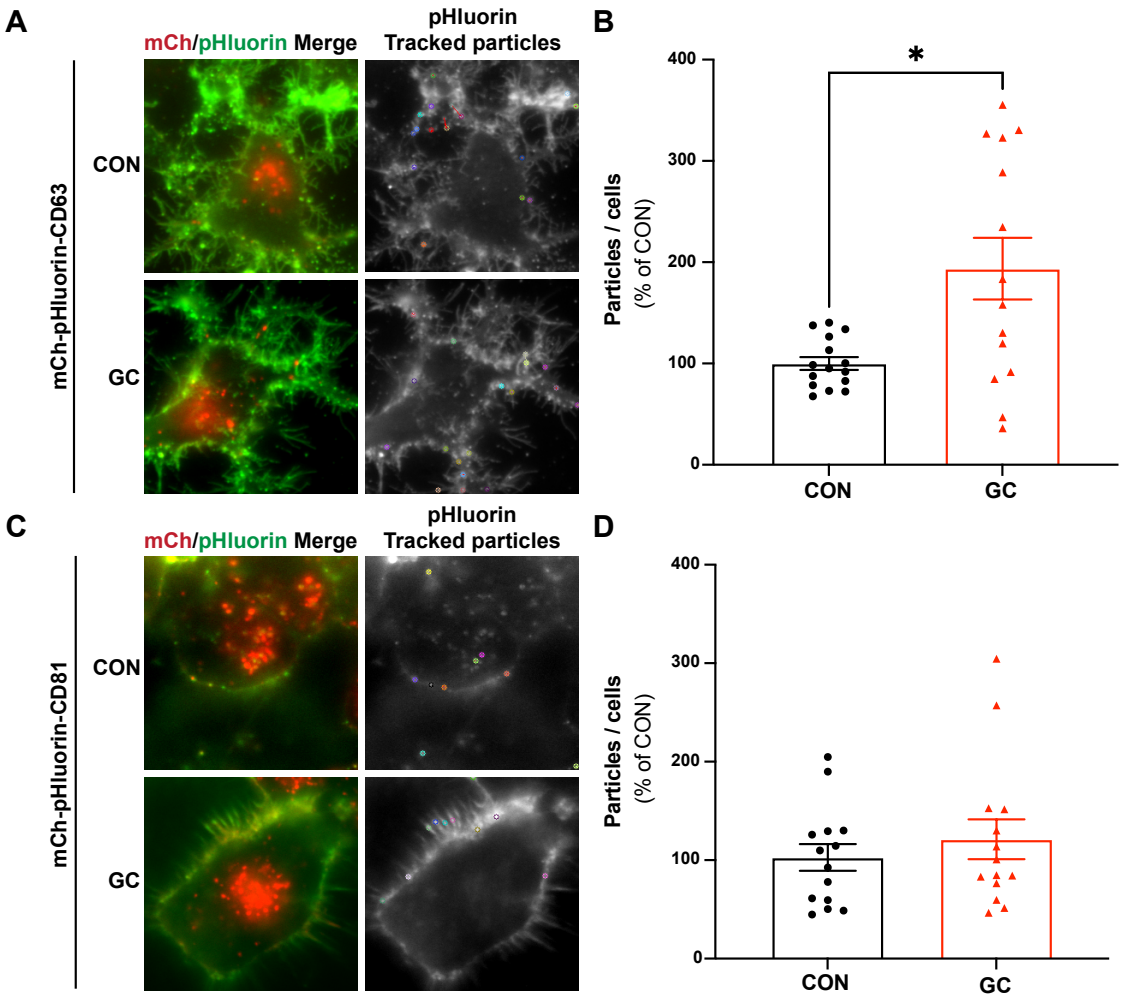

Figure 41. GCs may impact CD63-positive but not CD81-positive exosome secretion. A) Representative images of N2a cells treated with GCs or vehicle control, expressing the tetraspanin protein CD63 tagged with mCherry (red) and pHluorin (green). Grayscale images show Fiji/ImageJ 2D/3D Particle Tracker detection of moving particles in the pHluorin channel. Colored circles mark each detected particle. **B)** Quantification of total particles detected per 3 min timelapse image, normalized to the number of cells in the frame, and displayed as a percent of the control condition. GC-treated N2a cells expressing mCh-pHluorin-CD63 produce more tracked particles relative to the number of cells (*P=0.0328, Mann-Whitney test, n=15 images/condition, 4 independent cultures/condition). **C)** Representative images of N2a cells treated with GCs or vehicle control, expressing mCh-pHluorin-CD81 (red/green), and Fiji/ImageJ 2D/3D Particle Tracker detection of moving particles (grayscale, with circles). **D)** Quantification of total particles detected per 3 min timelapse image, displayed as a percent of the control condition. GC treatment in N2a cells expressing mCh-pHluorin-CD81 does not affect the total number of tracked particles (n=14 images/condition, 2 independent cultures/condition). All numeric data represent mean ± SEM.

5.3. Summary

Stress/GCs accelerate the progression of AD and the propagation of Tau and Aβ throughout brain regions, suggesting that stress can promote the spread of Tau and Aβ pathology. Nearly all brain cells release exosomes for intercellular communication (Fruhbeis *et al.*, 2013), providing a mechanism by which AD proteins could spread from cell to cell. Indeed, exosomes have been shown to carry Tau and Aβ, which can be released and taken up by neurons, astrocytes, and microglia (Guix *et al.*, 2018; Lim *et al.*, 2019; Perez-Gonzalez et al., 2012; Rajendran *et al.*, 2006; Saman *et al.*, 2012). Both stress/GCs and Rab35 have been shown to modulate exosome secretion and contents (Abrami *et al.*, 2013; Chen *et al.*, 2018; Fruhbeis *et al.*, 2013; Gauthier *et al.*, 2017; Harmati *et al.*, 2019; Hsu *et al.*, 2010; Yang *et al.*, 2019), suggesting yet another avenue by which stress may exacerbate AD. This chapter describes methods for isolating extracellular vesicles (EVs) by ultracentrifugation and size exclusion chromatography, and measuring their release by nanoparticle tracking analysis (NTA), ExoView on-chip interferometry and tetraspanin profiling, as well as live cell imaging.

Here, we learn that size exclusion chromatography (SEC) is a more precise method for isolating EVs than ultracentrifugation, in agreement with Sidhom, *et al.*, who reviewed several exosome purification techniques and concluded that SEC is the most accessible, reproducible, and easy to use. All of our future experiments will utilize SEC instead of ultracentrifugation. Using NTA in combination with ExoView interferometry and tetraspanin profiling, we find that IMG cells produce more EVs than primary neurons, astrocytes, and N2a cells, and that IMG cell exosomes are enriched in the tetraspanin protein CD9. These data indicate that microglia may be the most prolific producers of exosomes among brain cell types, with the potential to significantly influence exosome-mediated Tau and Aβ intercellular transmission.

ExoView interferometry and tetraspanin profiling allow the measurement of particle number, size, and tetraspanin colocalization using only a small amount of conditioned medium or purified EV sample. This technique will allow us to characterize the tetraspanin profiles of neurons, astrocytes, and microglia, from which we can develop a method to determine which cell types dominate exosome secretion in samples from mixed-cell cultures or brain tissues. Most intriguingly, the on-chip technology can be modified to capture EVs expressing other markers, by coating the capture probes with antibodies other than CD9 and CD81. Moreover, the ExoView workflow can be used to study the contents of exosomes pulled down by the capture probes. For this analysis, the EVs can be incubated with antibodies against proteins of interest (e.g. Tau, APP). We plan to use this technique for unraveling the complex interplay between GCs, Rab35, exosomes, and the spread of AD-related proteins in the brain.

Finally, we observe that GC treatment in primary mouse cortical neurons does not affect total exosome secretion or tetraspanin profiles in purified exosome samples analyzed by ExoView, but that GC treatment in N2a cells increases the number of pHluorin-tagged CD63-positive exosomes secreted. Together, these results suggest that GCs may differentially affect exosome secretion based on cell type and perhaps based on the tetraspanins present on these exosomes. Live imaging with pHluorin-tagged tetraspanins will allow us to measure how GCs and Rab35 expression affect exosome secretion at the single cell level. The techniques described in this chapter will be used to measure how stress/GCs, Rab35, and molecular pathways of intraluminal vesicle formation (i.e. ESCRT-mediated and ESCRT-independent ILV budding) impact exosome secretion and cargo in neurons, astrocytes, and microglia, and will allow our lab to pioneer investigations on how stress/GCs impact the intercellular spreading of AD pathology in the brain.

Chapter 6: Discussion and Future Directions

6.1. Discussion

Epidemiological and clinical studies indicate that lifetime stress accelerates Alzheimer's Disease (AD) onset and progression (Csernansky *et al.*, 2006; Elgh *et al.*, 2006; Silva *et al.*, 2019; Vyas *et al.*, 2016). Although stress activates cellular responses that ultimately return cells to homeostasis, chronic stress dysregulates these cellular mechanisms and may exacerbate protein trafficking deficits in neurodegenerative disease (De Kloet *et al.*, 2005; Farley & Watkins, 2018). In this thesis, I demonstrate that chronic stress reduces Rab35 expression in the hippocampus, impacting amyloid-beta (Aβ) production via Rab35-mediated regulation of amyloid precursor protein (APP) endocytic recycling and the retrograde trafficking of its secretase BACE1 (**Fig. 42**). Furthermore, I show that glucocorticoids (GCs), the major stress hormones, disrupt Rab35-mediated APP and BACE1 trafficking pathways, and that Rab35 overexpression blocks these effects (**Fig. 42**). Finally, I describe methods for measuring the effects of GCs and Rab35 on exosome secretion, which may contribute to AD progression by spreading pathogenic Aβ and Tau between cells.

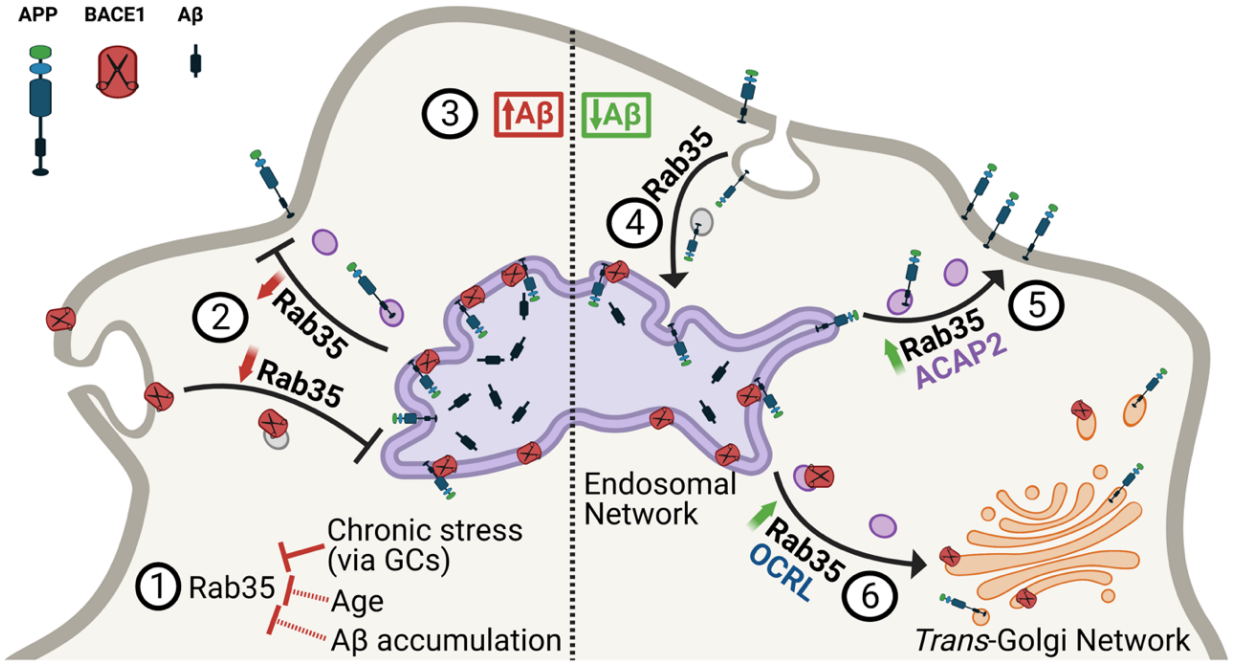

Figure 42. Model of how stress/GCs and Rab35 regulate APP processing. Stress/glucocorticoids (GCs) induce glucocorticoid receptor (GR)-mediated transcriptional downregulation of Rab35 (1). Rab35 expression also appears to be downregulated by aging and Aβ exposure. Our studies suggest that GCs reduce Rab35-mediated APP and BACE1 recycling with the plasma membrane (2), thereby increasing APP-BACE1 association in the endosomal network, leading to Aβ overproduction (3). On the other hand, higher levels of Rab35 expression promote APP internalization in a manner independent of Rab35 activation state (4) and APP recycling to the plasma membrane via the effector ACAP2 (5), as well as BACE1 retrograde trafficking to the trans-Golgi network via the effector OCRL (6). These actions decrease APP-BACE1 interaction within the endosomal network, thus reducing the production of Aβ and CTFs.

6.1.1. Rab35 expression is reduced by stress and conditions associated with AD

Our previous study identified 14 distinct glucocorticoid response elements (GREs) in the *RAB35* gene, and showed that treatment with glucocorticoids (GCs) reduced hippocampal Rab35 levels *in vitro* and *in vivo* (Vaz-Silva *et al.*, 2018). In this study, I found that chronic unpredictable stress also reduced Rab35 protein expression in the rat hippocampus, suggesting that the effects of chronic stress are GC- and glucocorticoid receptor (GR)-mediated. This finding is supported by research showing that GRs are the primary receptors involved in the chronic stress response (De Kloet *et al.*, 2008). The existence of glucocorticoid response elements in the *RAB35* gene suggests a mechanism by which stress reduces the expression of

Rab35 in the hippocampus: GCs activate the GR, which either binds directly to the *RAB35* gene at one or more of the 14 GRE sites, or interacts with other transcription factors that bind *RAB35* to block or slow its transcription. Future studies can determine whether the GR directly regulates *RAB35* through *in vitro* studies, by systematically mutating the 14 GREs in a cell line via CRISPR/Cas9 and assessing whether subsequent GC treatment affects *RAB35* mRNA levels. Additionally, ChIP-seq and luciferase transcription assays could be used to determine which sequences are bound by GRs, and whether this binding causes activation or repression of these target genes.

Since Rab35 mediates pathways involved in protein degradation and endosomal trafficking, as well as cell adhesion and migration, neurite outgrowth, and synapse formation, it is likely that Rab35 is target for regulation by acute stress. For instance, reducing Rab35-mediated synaptic vesicle protein turnover might conserve cellular energy while maintaining synaptic function under stressful conditions. Though a brief reduction in Rab35 expression could allow cells to maintain their essential functions, this thesis describes how chronic stress downregulates Rab35 in ways that are maladaptive, leading to increased Aβ production and Tau accumulation. Future studies should address whether acute stress similarly downregulates Rab35 in order to illuminate how acute versus chronic stress alter Rab35-mediated cellular processes. To study this, Rab35 mRNA and protein expression could be assessed following short-term GC treatment, and the effects of acute and chronic GC treatment on Rab35-mediated processes (e.g. cell cytokinesis, endocytic recycling, neuron outgrowth, and antigen cross-presentation) could be measured (as in Fuchs *et al.*, 2007; Kobayashi *et al.*, 2014; Kobayashi & Fukuda, 2013; Kouranti *et al.*, 2006; Zou *et al.*, 2009) to determine if these Rab35-mediated pathways are sensitive to either type of stress. If Rab35 expression and Rab35-mediated pathways are affected by acute

and chronic GC treatment, it is likely that Rab35's downregulation under acute stress benefits cells in the short term, or helps to return them to homeostasis, while its downregulation under chronic stress does not. To test this concept, Rab35-mediated pathways (e.g. protein recycling and degradation, antigen presentation, cell division) and general cell health can be measured in rescue experiments wherein Rab35 is overexpressed during short- and long-term GC treatment. I hypothesize that Rab35 overexpression in the short term would result in disruptions to cellular function by blocking 'beneficial' acute GC effects, whereas Rab35 overexpression in the long term would help return the cell to homeostasis. These investigations would reveal how acute and chronic stress affect Rab35 expression and Rab35-mediated cellular pathways, and whether blocking these effects is beneficial or detrimental to cells.

Because GR binding to DNA, and therefore gene regulation, can vary between cell types (Meijsing, 2015), additional investigations should determine if Rab35 is similarly downregulated across cell types and brain regions. Rab35 mRNA and protein levels could be measured in astrocyte, oligodendrocyte, and microglial cultures following treatment with GCs, as well as in various brain regions in GC-treated or stressed animals to determine how stress/GCs affect Rab35 expression across brain regions. Both neurons and astrocytes are capable of producing Aβ, and cellular stress has been shown to increase APP and BACE1 levels in astrocytes (Frost & Li, 2017). However, it is not yet known whether Rab35 controls APP and BACE1 trafficking pathways in astrocytes, or how stress affects Rab35 expression in these cells. Elucidating the effects of GCs in a cell type-specific manner will lead to a more complete understanding of how stress accelerates and exacerbates AD.

An intriguing finding of this study is that Rab35 levels are decreased under conditions linked to APP misprocessing and AD; namely advanced age, Aβ accumulation, and exposure to

chronic stress and/or high levels of GCs. Aging is the greatest risk factor for AD (Querfurth & LaFerla, 2010), and has been linked to increased amyloidogenic APP processing (Cisternas *et al.*, 2018; Jiang *et al.*, 2010; Kimura *et al.*, 2016), although the underlying mechanism(s) of APP misprocessing in the aged brain remain unknown. Here, I find that Rab35 protein levels are reduced in hippocampi of older vs younger rats, and that Rab35 overexpression protects against APP cleavage in aged animals. These results are in line with the human data, showing that Rab35 mRNA transcripts are reduced in hippocampi and cortices from older (60-79 year old) compared to younger (20-39 year old) individuals, indicating a similar decrease in expression over time. Importantly, my findings also show that *in vivo* infusion of the rat brain with Aβ peptides, an experimental procedure that mimics early AD neuropathology and further stimulates amyloidogenic APP processing (Catania *et al.*, 2009; Davis-salinas *et al.*, 1995; Heredia *et al.*, 2004; Lorenzo *et al.*, 2000), also reduces Rab35 levels. These findings are again in agreement with data from the human brain showing reduced Rab35 mRNA levels in hippocampi of AD patients compared to age-matched controls. Decreased Rab35 levels have also been observed in the brains of mice expressing the human ApoE4 allele (Alldred *et al.*, 2018), the strongest genetic risk factor for late-onset AD (LOAD). Human studies show that ApoE4 carriers have a significantly increased probability of developing AD and exhibit greater accumulation of Aβ in their brains compared to carriers of other ApoE alleles (Huang *et al.*, 2017). Another recent human study reported decreased Rab35 levels in brain-derived exosomes from athletes following mild traumatic brain injury (TBI) (Goetzl *et al.*, 2019), which is known to elicit AD-like neuropathology and predispose individuals to AD. Together, these studies support a role for Rab35 in APP misprocessing precipitated by stress, aging, and AD-related conditions.

Interestingly, TBI and Aβ overproduction lead to the dysregulation of neural circuits, resulting in neuronal hyperactivity (Almeida-Suhett *et al.*, 2015; Biegon *et al.*, 2004; Busche & Konnerth, 2015; Kamenetz *et al.*, 2003). Paradoxically, Rab35 activation also increases with neuronal activity (Sheehan *et al.*, 2016), and perhaps with GC treatment (unpublished preliminary experiments), suggesting that Aβ generation should be downregulated by neuronal activity-induced activation of Rab35. However, it is unclear which effectors interact with Rab35 under these conditions, potentially influencing specific trafficking events. For instance, trafficking pathways that reduce Aβ formation may not be increased by neuronal activity. Future experiments should explore the interplay between neuronal activity, Rab35 activation and downstream trafficking pathways. First, the effectors that bind Rab35 under conditions of increased neuronal activity can be determined by co-immunoprecipitation and mass spectrometry analyses. Second, the downstream targets of these effectors can be investigated to determine which trafficking pathways are likely impacted under these conditions. Finally, the effects of Aβ overproduction on these pathways could be assessed. These experiments would reveal the links between neuronal activity, which is enhanced by Aβ, and Rab35-mediated pathways, which tend to decrease Aβ generation. Together, these experiments would further elucidate the proposed negative feedback loop between Aβ and neuronal activity (Kamenetz *et al.*, 2003).

6.1.2. Rab GTPases are associated with AD and amyloidogenic APP cleavage

Amyloidogenic APP processing and overproduction of Aβ are widely accepted as triggering events for AD pathogenesis (Mucke & Selkoe, 2012), underscoring the urgent need to elucidate cellular and molecular mechanisms of APP misprocessing. Importantly, previous studies show that Aβ is not the only pathogenic component of the amyloidogenic pathway, as

APP β-CTFs (the intracellular product of BACE1 cleavage), have intrinsic synaptotoxic properties and can promote Tau hyperphosphorylation and accumulation independently of Aβ, leading to synaptic degeneration and impaired cognition (Moore *et al.*, 2015; Vaillant-Beuchot *et al.*, 2021). Accordingly, and in light of the failures of clinical trials that specifically target Aβ or molecules involved in its cleavage (*e.g.* presenilin) (Huang *et al.*, 2020), the focus of more recent studies has shifted to illuminating mechanisms of APP and BACE1 trafficking/interaction in the endosomal network (Bera et al., 2020; Tan & Gleeson, 2019), constituting the rate-limiting step for cleavage of APP into β-CTFs and Aβ peptides (Haass *et al.*, 2012). Targeting the molecular modulators of APP and/or BACE1 intracellular trafficking could serve as a promising therapeutic approach against amyloidogenesis (Sun & Roy, 2017).

Here, we show that Rab35 reduced APP cleavage and the production of Aβ40 and Aβ42 peptides. APP amyloidogenic vs. non-amyloidogenic cleavage is determined by the intracellular localization of APP and its secretases (Haass *et al.*, 2012; Yan *et al.*, 2013), whose trafficking pathways are controlled by a series of Rab GTPases (Stenmark, 2009). In my screen for Rab GTPases that regulate APP-BACE1 interaction, I identified Rabs 6, 15 and 26 as positive regulators of this interaction, and Rab35 as a negative regulator. Interestingly, Rab6 levels are reportedly increased in brain tissue from AD patients (Scheper *et al.*, 2007), and Rab6 was previously demonstrated to positively regulate Aβ but not sAPPβ production, suggesting that its influence on APP processing occurs via γ-secretase rather than β-secretase regulation (Udayar *et al.*, 2013). However, our findings indicate a potential role for Rab6 in stimulating APP-BACE1 interaction, indicating that it may influence more than one step of APP processing. In contrast to Rab6, little is known about the roles of Rabs 15 and 26 in AD etiology, although both have been implicated in endocytic trafficking (Chan *et al.*, 2011; Zuk & Elferink, 2000) and Rab26 is

linked to autophagy (Binotti *et al.*, 2015; Dong *et al.*, 2018), suggesting the potential importance of these pathways for APP and BACE1 trafficking or interaction.

A limitation of my approach is that overexpression of wild-type or dominant-negative Rab35 can act as a sink for GAPs (Rab inactivators) and GEFs (Rab activators), which are shared with other Rabs, thereby leading to the dysregulation of other trafficking pathways in the cell. However, the GC-induced decrease in Rab35 expression could also perturb these pathways by freeing shared GAPs, GEFs, and effectors (facilitators of trafficking events) to interact with other Rabs (Chaineau, *et al.*, 2013). For instance, Rab35 shares GAPs with several Rabs, i.e. TBC1D13 is shared with Rabs 1, 3a and 10 (Davey *et al.*, 2012), and TBC1D10A is shared with Rabs 8a and 27a (Chaineau *et al.*, 2013; Hokanson & Bretscher, 2012; Itoh & Fukuda, 2006). Intriguingly, all of these Rabs have been associated with AD (Zhang *et al.*, 2018). Rab1, which controls ER-to-Golgi trafficking, was shown to reduce Tau secretion in neurons (Mohamed *et al.*, 2017), suggesting that Rab1-mediated trafficking pathways may be disrupted in AD. Hippocampal tissue from AD patients shows reduced Rab3 levels (Sze *et al.*, 2000), suggesting that this Rab may function in AD-relevant trafficking pathways. Intriguingly, synaptic protein levels may serve as a predictor of cognitive decline (Bereczki *et al.*, 2016), and Rab3a promotes synaptic vesicle transport to the active zone of neurons (Leenders *et al.*, 2001), indicating the possible importance of this trafficking pathway in AD. Like Rab35, Rab8a has been shown to reduce amyloidogenic APP processing (Udayar *et al.*, 2013). Investigators found that reduced expression of Rab8a disrupted trafficking between the trans-Golgi Network and the plasma membrane (Kametani *et al.*, 2004), highlighting another protein trafficking step that may be important in AD. Rab8a also promotes the recycling of endocytic vesicles in concert with Arf6 (Rahajeng, *et al.*, 2012), a GTPase that can inhibit Rab35 activity (and reciprocally, be inhibited

by Rab35) (Allaire *et al.*, 2013; Kobayashi & Fukuda, 2012; Sheehan & Waites, 2019). It is possible that GC/stress-mediated downregulation of Rab35 expression could lead to reduced Rab8a activity because their shared GAP is more available to interact with Rab8a. Simultaneously, Arf6 activity may be enhanced through a decrease in its Rab35-mediated inhibition. These modifications could result in APP misprocessing through the dysregulation of TGN-plasma membrane trafficking or Arf6/Rab8a-mediated endosomal recycling. Overall, these studies suggest that Rab35 reduction could lead to the inactivation of Rabs 1, 3, or 8 through a shared Rab GAP, thereby disrupting pathways mediated by these GTPases and contributing to endosomal protein trafficking defects in AD.

Conversely, Rab10 protein levels were shown to be elevated in AD brains (Ridge *et al.*, 2018; Zhao *et al.*, 2016), and Rab10 silencing was found to reduce Aβ secretion and Aβ42 generation (Ridge *et al.*, 2018; Udayar *et al.*, 2013), indicating that Rab10 is a driver of amyloidogenesis. Additionally, phosphorylated Rab10 was present in hippocampal neurofibrillary tangles of AD patients (Yan *et al.*, 2018), suggesting that Rab10 may regulate both Aβ generation and Tau trafficking. Rab10 localizes to the plasma membrane, where it mediates steps of the secretory pathway, possibly including neurotransmitter release (Mitra *et al.*, 2011), implicating these processes in AD pathomechanisms. It is conceivable that GC-induced downregulation of Rab35 could reduce Rab10 activation through the previously mentioned effect on Rab GAPs, thereby decreasing Rab10-mediated Aβ and Tau pathology. However, this effect is likely minimal, as loss of Rab35 has been shown to increase Aβ production (Udayar *et al.*, 2013), and GCs have been shown to increase Tau accumulation by disrupting Rab35-mediated Tau degradation (Vaz-Silva *et al.*, 2018).

Together, these data suggest that numerous trafficking pathways, controlled by distinct Rab GTPases, are disrupted during AD. Future studies should address whether and how stress/GCs impact the activation of Rab GTPases linked to AD pathology, as well as those that share Rab35 GEFs, GAPs, or effectors. Though there are currently few assays to measure Rab activation, antibodies are available to detect the active/GTP-bound forms of several Rabs. Additionally, our lab has developed a Venus bimolecular fluorescence complementation (BiFC) assay for measuring Rab activation (unpublished data). In this assay, individual Rabs are tagged with an N-terminal fragment of Venus fluorescent protein (Rab:VN), and an effector Rab binding domain (RBD) is tagged with the complementary C-terminal fragment (RBD:VC). Using flow cytometry or fluorescence imaging to analyze the Venus fluorescence intensity in cells co-expressing Rab:VN and RBD:VC, we would be able to measure how GCs or Rab35 reduction affects the activation of Rab GTPases that share GAPs, GEFs, and effectors with Rab35. Further analysis of the activation, expression, and localization of these Rabs in AD will clarify their roles in the mechanisms of amyloidogenesis and Tau pathology.

6.1.3. Rab35 sorts APP and BACE1 into distinct trafficking pathways, respectively mediated by the effectors ACAP2 and OCRL

Defects in the endolysosomal pathway are among the earliest cellular features of AD (Nixon, 2005; Orr & Oddo, 2013), suggesting that dysfunction of endosomal trafficking underlies AD pathogenesis. Indeed, the endosomal network is the major site of Aβ production (Haass *et al.*, 2012), and Aβ accumulation is associated with enlarged multi-vesicular bodies (MVBs) (Willen *et al.*, 2017), implying that amyloidogenic conditions drive APP and BACE1 interactions in the endosomal system. Furthermore, conditions associated with decreased

residence of APP or BACE1 in this subcellular compartment typically inhibit Aβ generation (Small *et al.*, 2017). Here, I demonstrate that Rab35 gain-of-function decreases the localization of both APP and BACE1 in endosomal compartments.

For APP, this decrease occurs via Rab35-mediated stimulation of APP recycling to the plasma membrane (PM) through the effector ACAP2, similar to Rab35-induced fast endocytic recycling of other PM-associated proteins, *e.g.* T-cell receptors and β1 integrin (Allaire *et al.*, 2013; Kobayashi & Fukuda, 2013; Patino-Lopez *et al.*, 2008). Not only does this fast recycling pathway decrease APP colocalization with BACE1 in endosomes, but it also boosts levels of APP at the PM, likely promoting cleavage by α-secretase and thus preventing amyloidogenic processing.

A particularly interesting result in my experiments is that APP endocytosis from the plasma membrane appears to be driven by Rab35 independently of its activation state and of the effector ACAP2, since both wild-type (WT) and dominant-negative (DN) Rab35 increased APP internalization, and ACAP2 knockdown did not attenuate this effect. It is likely that the observed Rab35-induced APP internalization occurs via clathrin-mediated endocytosis because Rab35 sorts proteins internalized through this pathway (Donaldson *et al.*, 2016). DN Rab35 has been shown to inhibit the clathrin-dependent pathway (Dutta & Donaldson, 2015), suggesting that DN Rab35 might shift APP internalization to the clathrin-independent pathway without affecting the total rate of APP endocytosis. Follow up studies could test this concept by measuring the dependence of APP endocytosis on clathrin in cells expressing WT Rab35 or DN Rab35. If clathrin knockdown decreases APP internalization in the presence of WT Rab35 but not DN Rab35, this finding would indicate that APP internalization occurs through a clathrin-dependent pathway under conditions of increased Rab35 activation, and a clathrin-independent pathway

under conditions of reduced Rab35 activation. In this case, the dependence of APP internalization on dynamin could be tested, as dynamin-mediated endocytosis has been proposed as a clathrin-independent APP internalization pathway (Mayor *et al.*, 2014; Saavedra *et al.*, 2007).

Alternatively, Rab35 may be driving APP internalization in both its GTP- and GDP-bound states. In some instances, effectors have been found to interact with GDP-bound Rabs (Shirane & Nakayama, 2006), suggesting that it is possible for 'inactive' Rabs to drive trafficking events. Identifying binding partners of DN Rab35 vs. WT Rab35 by co-immunoprecipitation and mass spectrometry would help determine if there is an effector or other interacting protein that binds with similar affinity to active and inactive forms of Rab35. Follow-up experiments could test whether any such protein regulates APP internalization. These studies would reveal not only how Rab35 controls APP internalization, but also whether inactive Rab35 can facilitate cellular trafficking events.

For BACE1, the decrease in endosomal localization results from its Rab35-mediated retrograde trafficking to the TGN through the effector OCRL, similar to Rab35/OCRL-mediated mannose-6-phosphate receptor retrograde trafficking (Cauvin *et al.*, 2016). Interestingly, two genes identified as risk factors for LOAD, namely *VPS35* and *VPS26*, encode protein components of the retromer complex that regulates the retrograde trafficking of proteins from the endosomal network to the TGN. Mutation of these genes is hypothesized to disrupt the retrograde trafficking of APP (Zhang *et al.*, 2016), and potentially BACE1 (Wang *et al.*, 2012), increasing APP-BACE1 interaction in endosomes and therefore stimulating Aβ production. Although I did not see any effect of Rab35 gain-of-function on the retrograde trafficking of APP, I did observe a significant stimulation of BACE1 retrograde trafficking, thus reducing BACE1

residence time within endosomes as well as its exposure to APP. Rab35 may be acting in concert with the retromer to promote BACE1 retrograde trafficking, or it may be mediating a parallel pathway. To address this question, BACE1 retrograde trafficking could be measured under conditions of retromer knockdown with Rab35 overexpression. If Rab35 overexpression counteracts the effects of retromer knockdown, then Rab35-mediated BACE1 retrograde trafficking likely occurs through a separate pathway. Additionally, if Rab35 mediates a parallel retrograde trafficking pathway, then knocking down both Rab35 and components of the retromer should have additive effects on blocking BACE1 retrograde trafficking compared to Rab35 or retromer knockdown alone.

My finding that Rab35 sorts APP and BACE1 into separate pathways through its interaction with distinct effectors, ACAP2 and OCRL, encourages future examination to determine at which step of intracellular trafficking this Rab35 sorting occurs (e. g. protein internalization, exit from early/recycling/late endosomes). Since efficient recycling from endosomes typically requires Rab35 (Allaire *et al.*, 2010; Marat & McPherson, 2010), and we provide evidence that Rab35 drives both APP and BACE1 internalization but only APP recycling (via ACAP2), it is likely that this sorting of APP and BACE1 occurs at the endosomal level. The differential intracellular localizations of ACAP2 and OCRL further support this concept, as ACAP2 primarily localizes to the cell periphery (Allaire *et al.*, 2013; Jackson *et al.*, 2000), while OCRL localizes to the plasma membrane as well as to endosomes and the TGN, where it regulates receptor recycling through its hydrolysis of the lipid phosphatidylinositol 4,5-biphosphate (PtdIns(4,5)P_2) (Cauvin *et al.*, 2016; Festa *et al.*, 2019; Mondin *et al.*, 2019; Sharma *et al.*, 2015; Vicinanza *et al.*, 2011). Although Rab35 typically recruits OCRL after clathrin-coated vesicle scission (Cauvin *et al.*, 2016), suggesting that Rab35/OCRL-mediated protein

sorting could occur immediately upon protein internalization, Rab35 and OCRL have been shown to colocalize at several endosome types (Cauvin *et al.*, 2016), suggesting that OCRL may initiate BACE1 sorting into the retrograde pathway from early or recycling endosomes. Future experiments can utilize super-resolution microscopy to investigate where in the cell ACAP2 and OCRL colocalize with APP and BACE1, together with gain- and loss-of-function experiments to determine which distinct steps of APP and BACE1 trafficking involve Rab35-mediated sorting through these effectors. Together, these investigations would reveal where along these pathways Rab35 downregulation by GCs or other stimuli could disrupt APP and BACE1 trafficking.

6.1.4. Rab35-mediated APP and BACE1 trafficking – implications for Arf6-mediated pathways

Another important trafficking molecule that acts in concert with Rab35 is the small GTPase Arf6. Rab35 and Arf6 have been shown to reciprocally inhibit one another's activation in a variety of cellular processes, including cell migration, vesicle secretion, and cytokinesis (Allaire *et al.*, 2013; Kobayashi & Fukuda, 2012; Sheehan & Waites, 2019). Further, Rab35 and Arf6 have been shown to regulate clathrin-mediated and clathrin-independent endocytosis, respectively (Donaldson *et al.*, 2016), suggesting that the observed effects of Rab35 on APP and BACE1 internalization may result from Rab35-mediated inactivation of Arf6.

In the studies described in this thesis, I show that Rab35-regulated APP recycling is dependent on ACAP2, an Arf6 GAP that Rab35 recruits to the plasma membrane to facilitate Arf6 inactivation and reduce clathrin-independent endocytosis (Allaire *et al.*, 2013; Donaldson *et al.*, 2016; Egami *et al.*, 2011; Jackson *et al.*, 2000; Kobayashi & Fukuda, 2012, 2013; Mayor *et al.*, 2014). Overexpression of Rab35 in my experiments may thus reduce Arf6-mediated internalization and recycling pathways by recruiting ACAP2 to Arf6-positive endosomes and

deactivating Arf6 (Allaire *et al.*, 2013). However, to date, a role for Arf6 in APP internalization or recycling has not been reported, though it has been implicated in APP macropinocytosis, which sends APP directly to the lysosome, bypassing early and late endosomes (Tang *et al.*, 2015). Dominant-negative Arf6 has been shown to reduce Aβ generation by blocking lysosomal transport, indicating that Arf6 promotes APP amyloidogenic processing occurring in lysosomes. Furthermore, immunostaining for Arf6 in hippocampi of AD patients and age-matched controls showed that its expression increases with AD (Tang *et al.*, 2015), providing further correlation between Arf6 activity and amyloidogenesis. Since Arf6 inhibits Rab35 activation, it is possible that increased Arf6 expression promotes amyloidogenic trafficking pathways by reducing Rab35 activity. Manipulating Arf6 expression or activity and monitoring APP fast recycling and BACE1 retrograde trafficking would reveal whether Arf6 disrupts these Rab35-mediated trafficking pathways. Moreover, using the techniques described in Tang, *et al.*, future studies can measure whether altering Rab35 expression affects APP macropinocytosis and investigate whether Rab35/ACAP2-mediated APP trafficking reduces Arf6-controlled macropinocytosis, providing an additional mechanism for reducing Aβ generation.

It is conceivable that Rab35 also regulates BACE1 trafficking through Arf6, which has been reported to facilitate BACE1 endocytosis from the PM into the endosomal network (Sannerud *et al.*, 2011). Thus, Rab35 overexpression could reduce BACE1 endocytosis via Arf6 inhibition, preventing BACE1 interaction with APP in endosomes. To test this, Arf6 activation can be compared under our control and Rab35 overexpression conditions using an Arf6-GTP-specific antibody. Additionally, BACE1-Arf6 colocalization could be measured when Rab35 is overexpressed or knocked down to determine whether Rab35 influences Arf6-mediated BACE1 trafficking pathways. Reducing BACE1-Arf6 interactions should reduce Arf6-mediated BACE1

internalization, but in the current study, I found that steady-state cell-surface BACE1 levels remained unchanged upon Rab35 overexpression, indicating that Rab35 does not inhibit BACE1 endocytosis. This finding suggests that Rab35 drives BACE1 retrograde trafficking without interfering with Arf6-mediated endocytosis. My studies show that Rab35 regulates distinct trafficking pathways of APP and BACE1, and studying the interplay between Rab35 and Arf6 in these trafficking pathways would further illuminate how these cellular mechanisms are impacted by conditions associated with AD.

6.1.5. Stress/GCs disrupt Rab35-mediated trafficking pathways

The studies in this thesis show that exposure to chronic stress and high levels of GCs reduces Rab35 levels and stimulates the pro-amyloidogenic trafficking of APP and BACE1, while Rab35 overexpression attenuates these effects. These findings are in line with previous studies demonstrating that stress and GCs trigger APP misprocessing and Aβ production (Catania *et al.*, 2009; Green *et al.*, 2006; Jeong *et al.*, 2006; Srivareerat *et al.*, 2009), and offer a novel, Rab35-driven mechanism for how stress/GCs precipitate amyloidogenesis. Combined with our previous work showing the critical role of Rab35 in Tau sorting and degradation (Vaz-Silva *et al.*, 2018), these findings suggest that Rab35 serves as a molecular link through which chronic stress/GCs trigger both major AD pathomechanisms: Aβ production and accumulation of hyperphosphorylated Tau (Carroll *et al.*, 2011; Catania *et al.*, 2009; Green *et al.*, 2006; Sotiropoulos *et al.*, 2008). Interestingly, the effects of Rab35 on APP and Tau are through distinct mechanisms, as Rab35 stimulates Tau degradation via the endolysosomal pathway (Vaz-Silva *et al.*, 2018), whereas it modulates the fast endocytic recycling and retrograde trafficking of APP and BACE1, respectively.

A substantial limitation of my studies is that they capture one hour of cellular trafficking events that occur after 24 hours of treatment with a high dose of glucocorticoids. In the human brain, chronic stress occurs on the timeline of months or years, suggesting that these effects may be more pronounced because the cellular pathways are disrupted for much longer periods of time. Nevertheless, these results provide a mechanism by which high levels of GCs/stress can lead to the generation of excess Aβ, and they provide the groundwork for investigating how stress/GCs affect the intercellular spread of Aβ and Tau. Recently, Rab35 and ACAP2 were implicated in the formation of tunneling nanotubes that connect distant cells and enable passage of vesicles, organelles, and molecules (Bhat *et al.*, 2020). Tunneling nanotubes may be involved in the cell-to-cell spread of proteins such as APP, Aβ, or Tau, though it is unclear whether this would have a pathogenic or protective effect on neurons. Investigations exploring how GC-induced changes in Rab35- and ACAP2-mediated trafficking affect neuronal health and the spread of these proteins could lead the way to studying the role that tunneling nanotubes play in the intercellular spread of AD proteins.

6.2. Future Directions

6.2.1. Stress/GCs and Rab35 in glial contributions to AD

My studies motivate investigations of intra- and inter-cellular trafficking pathways for APP, BACE1, and Tau proteins in glia, which are responsible for maintaining brain homeostasis. Astrocytes, microglia, and oligodendrocytes express glucocorticoid receptors, and GCs have been shown to reduce astrocyte density and function, increase microglial activation, and modulate oligodendrocyte proliferation (Jauregui-Huerta *et al.*, 2010). Glia quickly react to changes in the brain, including stress, infection, and injury (Jauregui-Huerta *et al.*, 2010); and

there is mounting evidence that microglia, astrocytes, and oligodendrocytes undergo morphological and functional changes in AD (Alibhai *et al.*, 2018; Dzamba *et al.*, 2016), making them a prime suspect for accelerating and exacerbating AD in response to homeostatic perturbations. Indeed, microglia and astrocytes can internalize Aβ (Mohamed & Posse De Chaves, 2011; Wang *et al.*, 2017) and facilitate the endolysosomal clearance of AD proteins (Ries & Sastre, 2016; Wong, 2020), a process that could be disrupted by stress. Furthermore, astrocytes may secrete Aβ (Frost & Li, 2017), increasing the spread of AD pathology. To determine how stress affects the endocytosis and possible clearance or spread of Aβ and Tau, future studies should measure Aβ production in GC-treated vs. control astrocytes; as well as Aβ and Tau internalization, degradation, and potential secretion by glial cells treated with GCs. Investigating how stress affects glial function in AD will provide a more complete understanding of this complex disease. Though Rab35 is not expressed at high enough levels for consistent detection in glial cells of the hippocampus (Thul *et al.*, 2017; Uhlen *et al.*, 2015; http://www.proteinatlas.org), its role in several glial processes has been documented. Namely, Rab35 regulates the integrity of glial morphology (Coutinho-Budd *et al.*, 2017), oligodendrocyte differentiation and myelination (Miyamoto *et al.*, 2014; Sawade *et al.*, 2020), and glial exosome secretion (Blanc & Vidal, 2018; Hsu *et al.*, 2010). These studies suggest that Rab35 controls intracellular pathways in glia, and future studies should explore Rab35's role in Aβ clearance or generation pathways in glial cells.

6.2.2. Stress/GC effects on exosome secretion

Stress/GCs promote the spread of amyloid and Tau pathology (Dong & Csernansky, 2009; Sotiropoulos *et al.*, 2019; Vyas *et al.*, 2016), but it is unclear which mechanisms drive this.

Exosomes, small extracellular vesicles (EVs), function in intercellular communication and have been linked to AD (Lim *et al.*, 2019; Perez-Gonzalez *et al.*, 2012; Rajendran *et al.*, 2006; Saman *et al.*, 2012), suggesting a method for the intercellular transmission of AD-associated proteins. Indeed, *BIN1*, a risk gene associated with late-onset AD, is involved in the spread of Tau through exosomes (Crotti *et al.*, 2019). Rab35 and GCs impact exosome secretion and cargo (Abrami *et al.*, 2013; Chen *et al.*, 2018; De Jong *et al.*, 2012; Fruhbeis *et al.*, 2013; Gauthier *et al.*, 2017; Harmati *et al.*, 2019; Hsu *et al.*, 2010; Luarte *et al.*, 2020; Yang *et al.*, 2019), and our lab plans to uncover how GCs and/or Rab35 influence exosome secretion and contents in brain cell types (neurons, astrocytes, microglia), and whether they are a means for intercellular Aβ and Tau transmission.

In this thesis, I describe methods for biochemically isolating and measuring exosome secretion in neurons, microglial cells, and astrocytes to investigate the effects of stress/GCs on exosome release and the spread of AD pathology. We conclude that size exclusion chromatography isolates extracellular vesicles from conditioned medium more efficiently than ultracentrifugation, and we show the feasibility of three exosome measurement techniques: nanoparticle tracking analysis, ExoView on-chip interferomentry and tetraspanin profiling, and live cell imaging of exosome secretion using pHluorin reporters. Using these techniques in our preliminary data, we show that tetraspanin profiles vary among cell types, and that microglia may be the primary producers of extracellular vesicles among cell types of the brain. Furthermore, I show that GC treatment does not affect exosome production in primary cortical neurons, but that it increases the number pHluorin-CD63-tagged exosomes secreted by N2a cells. These results provide preliminary evidence that GCs may alter exosome release in a cell-type specific and/or tetraspanin-marker specific manner, but additional studies are needed to

determine how GCs affect exosome secretion in different cell types, and whether GCs differentially affect exosomes generated by different pathways (e.g. ESCRT-, tetraspanin-, ceramide-mediated).

Our result showing that microglial cells produce more EVs than primary neurons, astrocytes, and N2a cells suggest that microglia may be essential in exosome-mediated transmission of AD pathology. Recent studies show that microglia phagocytose Tau and release non-degradable forms of the protein in exosomes, playing an important role in Tau propagation (Asai *et al.*, 2015; Spanic *et al.*, 2019; Vogels *et al.*, 2019; Wang *et al.*, 2017). Furthermore, microglia are capable of endocytosing Aβ, though it is unclear whether this degrades Aβ or packages it for transmission (Mohamed & Posse De Chaves, 2011). There is conflicting evidence showing both increased and decreased Aβ load with deficiency of complement proteins (Hemonnot *et al.*, 2019), which signal microglia to phagocytose Aβ (Fu *et al.*, 2012). Furthermore, microglia are among the first responders to homeostatic changes in the brain (Bilbo & Stevens, 2017), making them a particularly important target for our research on stress and AD.

Though GCs are anti-inflammatory in many contexts (Cain & Cidlowski, 2017), stress and GCs can prime the brain for inflammation, leading to enhanced microglial activation and phagocytosis in response to immune challenges (Fonken *et al.*, 2018). Tau and Aβ aggregates can serve as such challenges, activating microglia and provoking pro-inflammatory cytokine production (Guillot-Sestier & Town, 2013; Stancu *et al.*, 2019). Thus, stress/GCs could precipitate a vicious cycle of Aβ and Tau secretion, microglial activation, and Aβ/Tau phagocytosis and exosomal release by microglia, accelerating the propagation of AD pathology. Interestingly, Rab35, ACAP2, and Arf6 are involved in protein endocytosis by microglia through their mutual activation/inhibition cycles (Egami *et al.*, 2015), suggesting that stress/GC-induced

reduction of Rab35 could dysregulate microglial phagocytic properties. Astrocytes can also internalize Tau and Aβ (Mohamed & Posse De Chaves, 2011; Perea *et al.*, 2019), and chronic stress has been found to alter their morphology in the hippocampus (Jauregui-Huerta *et al.*, 2010; Naskar & Chattarji, 2019), suggesting that astrocytes may also play a role in AD pathology propagation under stress.

In future experiments, we will characterize how GCs affect the potential spread of AD-related proteins through exosomes by measuring the concentration of secreted exosomes from GC-treated neurons, astrocytes, and microglia. To delve deeper into exosome characterization, we will use loss-of-function and/or inhibitors against ESCRT components, nSmase2, and tetraspanins to determine which pathways of exosome cargo loading are most important for GC-induced spread of AD proteins. Furthermore, we will address whether glial Tau and Aβ endocytosis lead to the intercellular spread of these proteins by identifying exosome contents using ExoView on-chip technology to probe for Aβ and Tau, and proteomics and microRNomics to determine other exosome cargo. Finally, we will measure Aβ and Tau concentrations in exosome-purified samples and exosome-depleted media to determine whether transmission of pathological proteins occurs through both exosomal and non-exosomal pathways, and whether GCs affect which pathways dominate. These experiments will reveal the contributions of neurons and glial cells to the intercellular propagation of Aβ and Tau, and further uncover the effects of stress on AD-associated protein trafficking pathways.

6.2.3. Exosomes as biomarkers

Exosomes are a prime biomarker candidate because they can carry proteins, lipids, and RNAs indicative of neurodegenerative diseases, are able to cross the blood-brain-barrier, are

resistant to proteases and RNases, and can be detected in cerebrospinal fluid, blood, and urine (DeLeo & Ikezu, 2018; Quek & Hill, 2017; Saman *et al.*, 2012; Xiao *et al.*, 2017). Indeed, investigators were recently able to detect AD 10 years prior to clinical onset by measuring Tau and Aβ levels in brain-derived exosomes isolated from plasma of AD patients (Fiandaca *et al.*, 2015). In another study using brain-derived exosomes isolated from plasma, the levels of Aβ and phosphorylated Tau in exosomes could predict the progression from mild cognitive impairment to AD (Winston *et al.*, 2016). Because exosomes were recently implicated in the propagation of Tau and Aβ pathology in animal models (Asai *et al.*, 2015; Sardar Sinha *et al.*, 2018), we hypothesize that exosomes carrying AD proteins may reflect stress-induced brain pathology, offering prognostic potential. Neuron-derived exosomes have also been shown to carry RNA-binding proteins (RBPs) and microRNAs (miRNAs) (Quek & Hill, 2017; Xiao *et al.*, 2017; You & Ikezu, 2019), which are increasingly linked to neurodegenerative mechanisms (Apicco *et al.*, 2019; Xiao *et al.*, 2017). Recently, a panel of 7 miRNAs from plasma exosomes has been found to predict AD diagnostic status with 83-89% accuracy (Lugli *et al.*, 2015). Intriguingly, recent work from our collaborator's lab indicates that stress/GCs alter the cellular machinery for RNA metabolism, leading to the accumulation of RBPs and the formation of stress granules (Silva *et al.*, 2019). These findings suggest that chronic stress and elevated GCs may impact the composition of miRNAs and RBPs in exosomes. By using proteomics and microRNomics in our isolated EVs to address whether exosome cargo (e.g. proteins and miRNAs) reflect brain pathology driven by stress/GCs, and which cell types (neurons, astrocytes, microglia) contribute to these differences, our studies will provide a more complete picture of how stress/GCs affect trafficking pathways of Aβ and Tau secretion and propagation in neurons, microglia, and

astrocytes, and promote further investigation of exosomes as biomarkers of neurodegenerative disease.

Conclusion

Collectively, the studies described in this thesis identify Rab35 as a molecular link between chronic stress/high levels of GCs and Aβ generation. I show that Rab35 controls APP and BACE1 intracellular trafficking pathways, reducing their interaction in endosomal compartments and subsequent Aβ production. Stress/glucocorticoids (GCs) disrupt these pathways, promoting amyloidogenesis, and Rab35 overexpression blocks this. Finally, I describe methods for studying how stress/GCs and Rab35 affect exosome secretion and intercellular transmission of Aβ and Tau in neurons, astrocytes, and microglia. Altogether, these findings support multiple roles for Rab35 in the intracellular trafficking of AD-relevant proteins and suggest that downregulation of Rab35 may precipitate amyloidogenesis. These studies highlight Rab35's potential relevance for AD brain pathology and suggest that additional work investigating its roles in AD and aging-related intracellular pathways could open novel therapeutic avenues for treating AD brain pathology.

References

Abrami, L., Brandi, L., Moayeri, M., Brown, M. J., Krantz, B. A., Leppla, S. H., & VanderGoot, F. G. (2013). Hijacking Multivesicular Bodies Enables Long-Term and Exosome-Mediated Long-Distance Action of Anthrax Toxin. *Cell Reports*, *5*(4), 986–996. https://doi.org/10.1016/j.celrep.2013.10.019

Alibhai, J. D., Diack, A. B., & Manson, J. C. (2018). Unravelling the glial response in the pathogenesis of Alzheimer's disease. *FASEB Journal*, *32*(11), 5766–5777. https://doi.org/10.1096/fj.201801360R

Allaire, P. D., Marat, A. L., Armi, C. D., Paolo, G. Di, S, P., & Ritter, B. (2010). The connecdenn DENN domain: a GEF for Rab35 mediating cargo- specific exit from early endosomes. *Molecular and Cellular Neuroscience*, *37*(3), 370–382. https://doi.org/10.1016/j.molcel.2009.12.037.The

Allaire, P. D., Seyed Sadr, M., Chaineau, M., Seyed Sadr, E., Konefal, S., Fotouhi, M., … McPherson, P. S. (2013). Interplay between Rab35 and Arf6 controls cargo recycling to coordinate cell adhesion and migration. *Journal of Cell Science*, *126*(3), 722–731. https://doi.org/10.1242/jcs.112375

Alldred, M. J., Goulbourne, C. N., Peng, K. Y., Morales-corraliza, J., Saito, M., Saito, M., & Ginsberg, S. D. (2018). Apolipoprotein E4 genotype compromises brain exosome production. *Brain*, 1–13. https://doi.org/10.1093/brain/awy289

Almeida-Suhett, C. P., Prager, E. M., Pidoplichko, V., Figueiredo, T. H., Marini, A. M., Li, Z., … Braga, M. F. M. (2015). GABAergic interneuronal loss and reduced inhibitory synaptic transmission in the hippocampal CA1 region after mild traumatic brain injury. *Experimental Neurology*, *273*, 11–23. https://doi.org/10.1016/j.expneurol.2015.07.028

Almeida, C. G., Takahashi, R. H., & Gouras, G. K. (2006). B-Amyloid Accumulation Impairs Multivesicular Body Sorting By Inhibiting the Ubiquitin-Proteasome System. *Journal of Neuroscience*, *26*(16), 4277–4288. https://doi.org/10.1523/JNEUROSCI.5078-05.2006

Andreu, Z., & Yanez-Mo, M. (2014). Tetraspanins in extracellular vesicle formation and function. *Frontiers in Immunology*, *5*(SEP), 1–12. https://doi.org/10.3389/fimmu.2014.00442

Andrew, R. J., De Rossi, P., Nguyen, P., Kowalski, H. R., Recupero, A. J., Guerbette, T., … Thinakaran, G. (2019). Reduction of the expression of the late-onset Alzheimer's disease (AD) risk-factor BIN1 does not affect amyloid pathology in an AD mouse model. *Journal of Biological Chemistry*, *294*(12), 4477–4487. https://doi.org/10.1074/jbc.RA118.006379

Apicco, D. J., Zhang, C., Maziuk, B., Jiang, L., Ballance, H. I., Boudeau, S., … Wolozin, B. (2019). Dysregulation of RNA Splicing in Tauopathies. *Cell Reports*, *29*(13), 4377-4388.e4. https://doi.org/10.1016/j.celrep.2019.11.093

Argenzio, E., Margadant, C., Leyton-Puig, D., Janssen, H., Jalink, K., Sonnenberg, A., & Moolenaar, W. H. (2014). CLIC4 regulates cell adhesion and β1 integrin trafficking. *Journal of Cell Science*, *127*(24), 5189–5203. https://doi.org/10.1242/jcs.150623

Asai, H., Ikezu, S., Tsunoda, S., Medalla, M., Luebke, J., Haydar, T., … Ikezu, T. (2015). Depletion of microglia and inhibition of exosome synthesis halt tau propagation. *Nature Neuroscience*, *18*(11), 1584–1593. https://doi.org/10.1038/nn.4132

Baglietto-Vargas, D., Chen, Y., Suh, D., Ager, R. R., Rodriguez-Ortiz, C. J., Medeiros, R., … LaFerla, F. M. (2015). Short-term modern life-like stress exacerbates Aβ-pathology and synapse loss in 3xTg-AD mice. *Journal of Neurochemistry*, *134*(5), 915–926. https://doi.org/10.1111/jnc.13195

Banker, G., & Goslin, K. (1998). *Culturing Nerve Cells* (2nd ed.). Cambridge, MA: Massachusetts Institute ofTechnology.

Bellezza, I., Grottelli, S., Mierla, A. L., Cacciatore, I., Fornasari, E., Roscini, L., … Minelli, A. (2014). Neuroinflammation and endoplasmic reticulum stress are coregulated by cyclo(His-Pro) to prevent LPS neurotoxicity. *International Journal of Biochemistry and Cell Biology*, *51*(1), 159–169. https://doi.org/10.1016/j.biocel.2014.03.023

Benarroch, E. E. (2013). Microglia: Multiple roles in surveillance, circuit shaping, and response to injury. *Neurology*, *81*, 1079–1088. https://doi.org/10.1212/WNL.0000000000000399

Bera, S., Camblor-Perujo, S., Calleja Barca, E., Negrete-Hurtado, A., Racho, J., De Bruyckere, E., … Kononenko, N. L. (2020). AP-2 reduces amyloidogenesis by promoting BACE 1 trafficking and degradation in neurons. *EMBO Reports*, *21*(6), 1–21. https://doi.org/10.15252/embr.201947954

Bereczki, E., Francis, P. T., Howlett, D., Pereira, J. B., Höglund, K., Bogstedt, A., … Aarsland, D. (2016). Synaptic proteins predict cognitive decline in Alzheimer's disease and Lewy body dementia. *Alzheimer's and Dementia*, *12*(11), 1149–1158. https://doi.org/10.1016/j.jalz.2016.04.005

Bhat, S., Ljubojevic, N., Zhu, S., Fukuda, M., Echard, A., & Zurzolo, C. (2020). Rab35 and its effectors promote formation of tunneling nanotubes in neuronal cells. *Scientific Reports*, *10*(1), 1–14. https://doi.org/10.1038/s41598-020-74013-z

Bi, C., Bi, S., & Li, B. (2019). Processing of mutant β-amyloid precursor protein and the clinicopathological features of familial alzheimer's disease. *Aging and Disease*, *10*(2), 383–403. https://doi.org/10.14336/AD.2018.0425

Biegon, A., Fry, P. A., Paden, C. M., Alexandrovich, A., Tsenter, J., & Shohami, E. (2004). Dynamic changes in N-methyl-D-aspartate receptors after closed head injury in mice: Implications for treatment of neurological and cognitive deficits. *Proceedings of the National Academy of Sciences of the United States of America*, *101*(14), 5117–5122. https://doi.org/10.1073/pnas.0305741101

Bilbo, S., & Stevens, B. (2017). Microglia: The Brain's First Responders. *Cerebrum*, (November), 1–14.

Binotti, B., Pavlos, N. J., Riedel, D., Wenzel, D., Vorbruggen, G., Schalk, A. M., … Jahn, R. (2015). The GTPase Rab26 links synaptic vesicles to the autophagy pathway. *ELife*, *4*, e05597. https://doi.org/10.7554/eLife.05597

Blanc, L., & Vidal, M. (2018). New insights into the function of Rab GTPases in the context of exosomal secretion. *Small GTPases*, *9*(1–2), 95–106. https://doi.org/10.1080/21541248.2016.1264352

Bloss, E. B., Janssen, W. G., McEwen, B. S., & Morrison, J. H. (2010). Interactive effects of stress and aging on structural plasticity in the prefrontal cortex. *Journal of Neuroscience*, *30*(19), 6726–6731. https://doi.org/10.1523/jneurosci.0759-10.2010

Braak, H., & Braak, E. (1991). Neuropathological stageing of Alzheimer-related changes. *Acta Neuropathologica*, *82*, 239–259.

Braak, H., & Del Tredici, K. (2016). Potential Pathways of Abnormal Tau and alpha-Synuclein Dissemination in Sporadic Alzheimer's and Parkinson's Diseases. *Cold Spring Harbor Perspectives in Biology*, *8*(11), 1–24. https://doi.org/10.1101/cshperspect.a023630

Breijyeh, Z., & Karaman, R. (2020). Comprehensive Review on Alzheimer's Disease. *Molecules*, *25*(24), 5789.

Bright, J., Hussain, S., Dang, V., Wright, S., Cooper, B., Byun, T., … Griswold-Prenner, I. (2015). Human secreted tau increases amyloid-beta production. *Neurobiology of Aging*, *36*(2), 693–709. https://doi.org/10.1016/j.neurobiolaging.2014.09.007

Brunello, C. A., Merezhko, M., Uronen, R. L., & Huttunen, H. J. (2020). Mechanisms of secretion and spreading of pathological tau protein. *Cellular and Molecular Life Sciences*, *77*(9), 1721–1744. https://doi.org/10.1007/s00018-019-03349-1

Brunson, K. L., Kramar, E., Lin, B., Chen, Y., Colgin, L. L., Yanagihara, T. K., … Baram, T. Z. (2005). Mechanisms of late-onset cognitive decline after early-life stress. *Journal of Neuroscience*, *25*(41), 9328–9338. https://doi.org/10.1523/jneurosci.2281-05.2005

Buggia-Prevot, V., Fernandez, C. G., Riordan, S., Vetrivel, K. S., Roseman, J., Waters, J., … Thinakaran, G. (2014). Axonal BACE1 dynamics and targeting in hippocampal neurons: A role for Rab11 GTPase. *Molecular Neurodegeneration*, *9*(1). https://doi.org/10.1186/1750-1326-9-1

Burke, S. L., Cadet, T., Alcide, A., O'Driscoll, J., & Maramaldi, P. (2018). Psychosocial risk factors and Alzheimer's disease: the associative effect of depression, sleep disturbance, and anxiety. *Aging Mental Health*, *22*(12), 1577–1584. https://doi.org/doi:10.1080/13607863.2017.1387760

Busche, M. A., & Konnerth, A. (2015). Neuronal hyperactivity - A key defect in Alzheimer's

disease? *BioEssays*, *37*(6), 624–632. https://doi.org/10.1002/bies.201500004

Busciglio, J., Lorenzo, A., Yeh, J., & Yankner, B. A. (1995). β-Amyloid fibrils induce tau phosphorylation and loss of microtubule binding. *Neuron*, *14*(4), 879–888. https://doi.org/10.1016/0896-6273(95)90232-5

Caballero, B., Bourdenx, M., Luengo, E., Diaz, A., Sohn, P. D., Chen, X., … Cuervo, A. M. (2021). Acetylated tau inhibits chaperone-mediated autophagy and promotes tau pathology propagation in mice. *Nature Communications*, *12*(1), 1–18. https://doi.org/10.1038/s41467-021-22501-9

Cain, D. W., & Cidlowski, J. A. (2017). Immune regulation by glucocorticoids. *Nature Reviews Immunology*, *17*(4), 233–247. https://doi.org/10.1038/nri.2017.1

Carey, R. M., Balcz, B. A., Lopez-Coviella, I., & Slack, B. E. (2005). Inhibition of dynamin-dependent endocytosis increases shedding of the amyloid precursor protein ectodomain and reduces generation of amyloid β protein. *BMC Cell Biology*, *6*, 1–10. https://doi.org/10.1186/1471-2121-6-30

Carroll, J. C., Iba, M., Bangasser, D. A., Valentino, R. J., James, M. J., Brunden, K. R., … Trojanowski, J. Q. (2011). Chronic Stress Exacerbates Tau Pathology, Neurodegeneration, and Cognitive Performance through a Corticotropin-Releasing Factor Receptor-Dependent Mechanism in a Transgenic Mouse Model of Tauopathy. *Journal of Neuroscience*, *31*(40), 14436–14449. https://doi.org/10.1523/JNEUROSCI.3836-11.2011

Catania, C., Sotiropoulos, I., Silva, R., Onofri, C., Breen, K. C., Sousa, N., & Almeida, O. F. X. (2009). The amyloidogenic potential and behavioral correlates of stress. *Molecular Psychiatry*, *14*(1), 95–105. https://doi.org/10.1038/sj.mp.4002101

Cauvin, C., Rosendale, M., Gupta-Rossi, N., Rocancourt, M., Larraufie, P., Salomon, R., … Echard, A. (2016). Rab35 GTPase Triggers Switch-like Recruitment of the Lowe Syndrome Lipid Phosphatase OCRL on Newborn Endosomes. *Current Biology*, *26*(1), 120–128. https://doi.org/10.1016/j.cub.2015.11.040

Chaineau, M., Ioannou, M. S., & Mcpherson, P. S. (2013). Rab35: GEFs, GAPs and Effectors. *Traffic*, *14*(11), 1109–1117. https://doi.org/10.1111/tra.12096

Chan, C. C., Scoggin, S., Wang, D., Cherry, S., Dembo, T., Greenberg, B., … Hiesinger, P. R. (2011). Systematic discovery of Rab GTPases with synaptic functions in Drosophila. *Current Biology*, *21*(20), 1704–1715. https://doi.org/10.1016/j.cub.2011.08.058

Chen, F., Swartzlander, D. B., Ghosh, A., Fryer, J. D., Wang, B., & Zheng, H. (2021). Clusterin secreted from astrocyte promotes excitatory synaptic transmission and ameliorates Alzheimer's disease neuropathology. *Molecular Neurodegeneration*, *16*(1), 1–16. https://doi.org/10.1186/s13024-021-00426-7

Chen, Y., Zhang, M., & Zheng, Y. (2018). Glucocorticoids inhibit production of exosomes containing inflammatory microRNA-155 in lipopolysaccharide-induced macrophage

inflammatory responses. *Int J Clin Exp Pathol*, *11*(7), 3391–3397. Retrieved from www.ijcep.com/

Chia, P. Z. C., Toh, W. H., Sharples, R., Gasnereau, I., Hill, A. F., & Gleeson, P. A. (2013). Intracellular itinerary of internalised β-secretase, BACE1, and its potential impact on β-amyloid peptide biogenesis. *Traffic*, *14*(9), 997–1013. https://doi.org/10.1111/tra.12088

Cirrito, J. R., Kang, J. E., Lee, J., Stewart, F. R., Verges, D. K., Silverio, L. M., … Holtzman, D. M. (2008). Endocytosis Is Required for Synaptic Activity-Dependent Release of Amyloid-β In Vivo. *Neuron*, *58*(1), 42–51. https://doi.org/10.1016/j.neuron.2008.02.003

Cirrito, J. R., May, P. C., O'Dell, M. A., Taylor, J. W., Parsadanian, M., Cramer, J. W., … Holtzman, D. M. (2003). In vivo assessment of brain interstitial fluid with microdialysis reveals plaque-associated changes in amyloid-β metabolism and half-life. *Journal of Neuroscience*, *23*(26), 8844–8853. https://doi.org/10.1523/jneurosci.23-26-08844.2003

Cirrito, J. R., Yamada, K. A., Finn, M. B., Sloviter, R. S., Bales, K. R., May, P. C., … Holtzman, D. M. (2005). Synaptic activity regulates interstitial fluid amyloid-beta levels in vivo. *Neuron*, *48*(6), 913–922. https://doi.org/10.1016/j.neuron.2005.10.028

Cisternas, P., Zolezzi, J. M., Lindsay, C., Rivera, D. S., & Martinez, A. (2018). New Insights into the Spontaneous Human Alzheimer's Disease-Like Model Octodon degus : Unraveling Amyloid-beta Peptide Aggregation and Age-Related Amyloid Pathology. *Journal of Alzheimer's Disease*, *66*, 1145–1163. https://doi.org/10.3233/JAD-180729

Clavaguera, F., Duyckaerts, C., & Haïk, S. (2020). Prion-like properties of Tau assemblies. *Current Opinion in Neurobiology*, *61*, 49–57. https://doi.org/10.1016/j.conb.2019.11.022

Colombo, M., Raposo, G., & Thery, C. (2014). Biogenesis, secretion, and intercellular interactions of exosomes and other extracellular vesicles. *Annual Review of Cell and Developmental Biology*, *30*, 255–289. https://doi.org/10.1146/annurev-cellbio-101512-122326

Cook, S. C., & Wellman, C. L. (2004). Chronic stress alters dendritic morphology in rat medial prefrontal cortex. *Journal of Neurobiology*, *60*(2), 236–248. https://doi.org/10.1002/neu.20025

Coutinho-Budd, J. C., Sheehan, A. E., & Freeman, M. R. (2017). The secreted neurotrophin spätzle 3 promotes glial morphogenesis and supports neuronal survival and function. *Genes and Development*, *31*(20), 2023–2038. https://doi.org/10.1101/gad.305888.117

Crotti, A., Sait, H. R., McAvoy, K. M., Estrada, K., Ergun, A., Szak, S., … Ransohoff, R. M. (2019). BIN1 favors the spreading of Tau via extracellular vesicles. *Scientific Reports*, *9*(1), 1–20. https://doi.org/10.1038/s41598-019-45676-0

Csernansky, J. G., Dong, H., Fagan, A. M., Wang, L., Xiong, C., Holtzman, D. M., & Morris, J. C. (2006). Plasma cortisol and progression of dementia in subjects with Alzheimer-type dementia. *American Journal of Psychiatry*, *163*(12), 2164–2169.

https://doi.org/10.1176/ajp.2006.163.12.2164

Dai, M. H., Zheng, H., Zeng, L. D., & Zhang, Y. (2018). The genes associated with early-onset Alzheimer's disease. *Oncotarget*, *9*(19), 15132–15143. https://doi.org/10.18632/oncotarget.23738

Das, U., Wang, L., Ganguly, A., Saikia, J. M., Wagner, S. L., Koo, E. H., & Roy, S. (2015). Visualizing APP and BACE-1 approximation in neurons yields insight into the amyloidogenic pathway. *Nature Neuroscience*, *19*(1), 55–64. https://doi.org/10.1038/nn.4188

Datson, N. A., Morsink, M. C., Meijer, O. C., & De Kloet, E. R. (2008). Central corticosteroid actions: Search for gene targets. *European Journal of Pharmacology*, *583*(2–3), 272–289. https://doi.org/10.1016/j.ejphar.2007.11.070

Davey, J. R., Humphrey, S. J., Junutula, J. R., Mishra, A. K., Lambright, D. G., James, D. E., & Stöckli, J. (2012). TBC1D13 is a RAB35 Specific GAP that Plays an Important Role in GLUT4 Trafficking in Adipocytes. *Traffic*, *13*(10), 1429–1441. https://doi.org/10.1111/j.1600-0854.2012.01397.x

Davis-salinas, J., Saporito-irwin, S. M., Cotman, C. W., & Nostrand, W. E. Van. (1995). Amyloid b-Protein Induces Its Own Production in Cultured Degenerating Cerebrovascular Smooth Muscle Cells. *Journal of Neurochemistry*, 8–11.

Dawson, G. R., Seabrook, G. R., Zheng, H., Smith, D. W., Graham, S., O'Dowd, G., … Sirinathsinghji, D. J. S. (1999). Age-related cognitive deficits, impaired long-term potentiation and reduction in synaptic marker density in mice lacking the β-amyloid precursor protein. *Neuroscience*, *90*(1), 1–13. https://doi.org/10.1016/S0306-4522(98)00410-2

De Jong, O. G., Verhaar, M. C., Chen, Y., Vader, P., Gremmels, H., Posthuma, G., … van Balkom, B. W. M. (2012). Cellular stress conditions are reflected in the protein and RNA content of endothelial cell-derived exosomes. *Journal of Extracellular Vesicles*, *1*(1). https://doi.org/10.3402/jev.v1i0.18396

De Kloet, E. R., Joels, M., & Holsboer, F. (2005). Stress and the brain: From adaptation to disease. *Nature Reviews Neuroscience*, *6*(6), 463–475. https://doi.org/10.1038/nrn1683

De Kloet, E. R., Karst, H., & Joels, M. (2008). Corticosteroid hormones in the central stress response: Quick-and-slow. *Frontiers in Neuroendocrinology*, *29*(2), 268–272. https://doi.org/10.1016/j.yfrne.2007.10.002

Deatherage, B. L., & Cookson, B. T. (2012). Membrane vesicle release in bacteria, eukaryotes, and archaea: A conserved yet underappreciated aspect of microbial life. *Infection and Immunity*, *80*(6), 1948–1957. https://doi.org/10.1128/IAI.06014-11

DeLeo, A. M., & Ikezu, T. (2018). Extracellular Vesicle Biology in Alzheimer's Disease and Related Tauopathy. *Journal of Neuroimmune Pharmacology*, *13*(3), 292–308.

https://doi.org/10.1007/s11481-017-9768-z

Donaldson, J. G., Johnson, D. L., & Dutta, D. (2016). Rab and Arf G proteins in endosomal trafficking and cell surface homeostasis. *Small GTPases*, *7*(4), 247–251. https://doi.org/10.1080/21541248.2016.1212687

Dong, H., & Csernansky, J. G. (2009). Effects of stress and stress hormones on amyloid-beta protein and plaque deposition. *Journal of Alzheimer's Disease*, *18*(2), 459–469. https://doi.org/10.3233/JAD-2009-1152

Dong, W., He, B., Qian, H., Liu, Q., Wang, D., Li, J., … Wang, G. (2018). RAB26-dependent autophagy protects adherens junctional integrity in acute lung injury. *Autophagy*, *14*(10), 1677–1692. https://doi.org/10.1080/15548627.2018.1476811

Drake, T. M. (2015). Unfolding the Promise of Translational Targeting in Neurodegenerative Disease. *NeuroMolecular Medicine*, *17*(2), 147–157. https://doi.org/10.1007/s12017-015-8346-x

Dutta, D., & Donaldson, J. G. (2015). Sorting of Clathrin-Independent Cargo Proteins Depends on Rab35 Delivered by Clathrin-Mediated Endocytosis. *Traffic*, *16*(9), 994–1009. https://doi.org/10.1111/tra.12302

Dzamba, D., Harantova, L., Butenko, O., & Anderova, M. (2016). Glial Cells - The Key Elements of Alzheimers Disease. *Current Alzheimer Research*, *13*(8), 894–911. https://doi.org/10.2174/1567205013666160129095924

Egami, Y., Fujii, M., Kawai, K., Ishikawa, Y., Fukuda, M., & Araki, N. (2015). Activation-inactivation cycling of Rab35 and ARF6 is required for phagocytosis of zymosan in RAW264 macrophages. *Journal of Immunology Research*, *2015*. https://doi.org/10.1155/2015/429439

Egami, Y., Fukuda, M., & Araki, N. (2011). Rab35 regulates phagosome formation through recruitment of ACAP2 in macrophages during FcγR-mediated phagocytosis. *Journal of Cell Science*, *124*(21), 3557–3567. https://doi.org/10.1242/jcs.083881

Elgh, E., Lindqvist Åstot, A., Fagerlund, M., Eriksson, S., Olsson, T., & Näsman, B. (2006). Cognitive dysfunction, hippocampal atrophy and glucocorticoid feedback in Alzheimer's disease. *Biological Psychiatry*, *59*(2), 155–161. https://doi.org/10.1016/j.biopsych.2005.06.017

Escola, J. M., Kleijmeer, M. J., Stoorvogel, W., Griffith, J. M., Yoshie, O., & Geuze, H. J. (1998). Selective enrichment of tetraspan proteins on the internal vesicles of multivesicular endosomes and on exosomes secreted by human B-lymphocytes. *Journal of Biological Chemistry*, *273*(32), 20121–20127. https://doi.org/10.1074/jbc.273.32.20121

Farley, M. M., & Watkins, T. A. (2018). Intrinsic Neuronal Stress Response Pathways in Injury and Disease. *Annual Review of Pathology: Mechanisms of Disease*, *13*, 93–116. https://doi.org/10.1146/annurev-pathol-012414-040354

Feng, Q., Luo, Y., Zhang, X. N., Yang, X. F., Hong, X. Y., Sun, D. S., … Wang, J. Z. (2020). MAPT/Tau accumulation represses autophagy flux by disrupting IST1-regulated ESCRT-III complex formation: a vicious cycle in Alzheimer neurodegeneration. *Autophagy*, *16*(4), 641–658. https://doi.org/10.1080/15548627.2019.1633862

Ferreira, A., Lu, Q., Orecchio, L., & Kosik, K. S. (1997). Selective phosphorylation of adult tau isoforms in mature hippocampal neurons exposed to fibrillar aβ. *Molecular and Cellular Neurosciences*, *9*(3), 220–234. https://doi.org/10.1006/mcne.1997.0615

Festa, B. P., Berquez, M., Gassama, A., Amrein, I., Ismail, H. M., Samardzija, M., … Devuyst, O. (2019). OCRL deficiency impairs endolysosomal function in a humanized mouse model for Lowe syndrome and Dent disease. *Human Molecular Genetics*, *28*(12), 1931–1946. https://doi.org/10.1093/hmg/ddy449

Fiandaca, M. S., Kapogiannis, D., Mapstone, M., Boxer, A., Eitan, E., Schwartz, J. B., … Goetzl, E. J. (2015). Identification of preclinical Alzheimer's disease by a profile of pathogenic proteins in neurally derived blood exosomes: A case-control study. *Alzheimer's and Dementia*, *11*(6), 600-607.e1. https://doi.org/10.1016/j.jalz.2014.06.008

Finnie, P. S. B., & Nader, K. (2020). Amyloid Beta Secreted during Consolidation Prevents Memory Malleability. *Current Biology*, *30*(10), 1934-1940.e4. https://doi.org/10.1016/j.cub.2020.02.083

Fjell, A. M., McEvoy, L., Holland, D., Dale, A. M., & Walhovd, K. B. (2014). What is normal in normal aging? Effects of aging, amyloid and Alzheimer's disease on the cerebral cortex and the hippocampus. *Progress in Neurobiology*, *117*, 20–40. https://doi.org/10.1016/j.pneurobio.2014.02.004

Fonken, L. K., Frank, M. G., Gaudet, A. D., & Maier, S. F. (2018). Stress and aging act through common mechanisms to elicit neuroinflammatory priming. *Brain, Behavior, and Immunity*, *73*(July), 133–148. https://doi.org/10.1016/j.bbi.2018.07.012

Foster, E. M., Dangla-Valls, A., Lovestone, S., Ribe, E. M., & Buckley, N. J. (2019). Clusterin in Alzheimer's disease: Mechanisms, genetics, and lessons from other pathologies. *Frontiers in Neuroscience*, *13*(FEB), 1–27. https://doi.org/10.3389/fnins.2019.00164

Fraustchy, S. A., Yang, F., Calderon, L., & Cole, G. M. (1996). Rodent Models of Alzheimer's Disease: Rat Abeta Infusion Approaches to Amyloid Deposits. *Neurobiology of Aging*, *17*(2), 311–321.

Frost, G. R., & Li, Y. M. (2017). The role of astrocytes in amyloid production and Alzheimer's disease. *Open Biology*, *7*(12), 1–14. https://doi.org/10.1098/rsob.170228

Fruhbeis, C., Frohlich, D., Kuo, W. P., Amphornrat, J., Thilemann, S., Saab, A. S., … Kramer-Albers, E. M. (2013). Neurotransmitter-Triggered Transfer of Exosomes Mediates Oligodendrocyte-Neuron Communication. *PLoS Biology*, *11*(7). https://doi.org/10.1371/journal.pbio.1001604

Fruhbeis, C., Frohlich, D., Kuo, W. P., & Kramer-Albers, E. M. (2013). Extracellular vesicles as mediators of neuron-glia communication. *Frontiers in Cellular Neuroscience*, *7*(OCT), 1–6. https://doi.org/10.3389/fncel.2013.00182

Fu, H., Liu, B., Frost, J. L., Hong, S., Jin, M., Ostaszewski, B., … Lemere, C. A. (2012). Complement component C3 and complement receptor type 3 contribute to the phagocytosis and clearance of fibrillar Aβ by microglia. *Glia*, *60*(6), 993–1003. https://doi.org/10.1002/glia.22331

Fuchs, E., Haas, A. K., Spooner, R. A., Yoshimura, S. I., Lord, J. M., & Barr, F. A. (2007). Specific Rab GTPase-activating proteins define the Shiga toxin and epidermal growth factor uptake pathways. *Journal of Cell Biology*, *177*(6), 1133–1143. https://doi.org/10.1083/jcb.200612068

Garcia-Osta, A., & Alberini, C. M. (2009). Amyloid beta mediates memory formation. *Learning and Memory*, *16*(4), 267–272. https://doi.org/10.1101/lm.1310209

Garwood, C. J., Pooler, A. M., Atherton, J., Hanger, D. P., & Noble, W. (2011). Astrocytes are important mediators of Aβ-induced neurotoxicity and tau phosphorylation in primary culture. *Cell Death and Disease*, *2*(6), 1–9. https://doi.org/10.1038/cddis.2011.50

Garwood, C. J., Ratcliffe, L. E., Simpson, J. E., Heath, P. R., Ince, P. G., & Wharton, S. B. (2017). Review: Astrocytes in Alzheimer's disease and other age-associated dementias: a supporting player with a central role. *Neuropathology and Applied Neurobiology*, *43*(4), 281–298. https://doi.org/10.1111/nan.12338

Gauthier, S. A., Perez-Gonzalez, R., Sharma, A., Huang, F. K., Alldred, M. J., Pawlik, M., … Levy, E. (2017). Enhanced exosome secretion in Down syndrome brain - a protective mechanism to alleviate neuronal endosomal abnormalities. *Acta Neuropathologica Communications*, *5*(1), 65. https://doi.org/10.1186/s40478-017-0466-0

Geula, C., Wu, C., Saroff, D., Lorenzo, A., Yuan, M., & Yankner, B. (1998). Aging renders the brain vulnerable to amyloid beta-protein neurotoxicity. *Nature Medicine*.

Giuffrida, M. L., Caraci, F., Pignataro, B., Cataldo, S., De Bona, P., Bruno, V., … Copani, A. (2009). B-Amyloid Monomers Are Neuroprotective. *Journal of Neuroscience*, *29*(34), 10582–10587. https://doi.org/10.1523/JNEUROSCI.1736-09.2009

Gleichman, A. J., & Carmichael, S. T. (2020). Glia in neurodegeneration: Drivers of disease or along for the ride? *Neurobiology of Disease*, *142*(May), 104957. https://doi.org/10.1016/j.nbd.2020.104957

Goedert, M., & Jakes, R. (2005). Mutations causing neurodegenerative tauopathies. *Biochimica et Biophysica Acta - Molecular Basis of Disease*, *1739*(2), 240–250. https://doi.org/10.1016/j.bbadis.2004.08.007

Goetzl, E. J., Ledreux, A., Granholm, A. C., Elahi, F. M., Goetzl, L., Hiramoto, J., & Kapogiannis, D. (2019). Neuron-derived exosome proteins may contribute to progression

from repetitive mild traumatic brain injuries to chronic traumatic encephalopathy. *Frontiers in Neuroscience*, *13*(May), 1–8. https://doi.org/10.3389/fnins.2019.00452

Gosztyla, M. L., Brothers, H. M., & Robinson, S. R. (2018). Alzheimer's Amyloid-β is an Antimicrobial Peptide: A Review of the Evidence. *Journal of Alzheimer's Disease*, *62*(4), 1495–1506. https://doi.org/10.3233/JAD-171133

Gratuze, M., Leyns, C. E. G., & Holtzman, D. M. (2018). New insights into the role of TREM2 in Alzheimer's disease. *Molecular Neurodegeneration*, *13*(1), 1–16. https://doi.org/10.1186/s13024-018-0298-9

Green, K. N., Billings, L. M., Roozendaal, B., McGaugh, J. L., & LaFerla, F. M. (2006). Glucocorticoids Increase Amyloid-beta and Tau Pathology in a Mouse Model ofAlzheimer's Disease. *Journal of Neuroscience*, *26*(35), 9047–9056. https://doi.org/10.1523/jneurosci.2797-06.2006

Guillot-Sestier, M.-V., & Town, T. (2013). Innate Immunity in Alzheimer's Disease: A Complex Affair. *CNS & Neurological Disorders - Drug Targets*, *12*(5), 593–607. https://doi.org/10.2174/18715273113120500 08

Guix, F. X., Corbett, G. T., Cha, D. J., Mustapic, M., Liu, W., Mengel, D., … Walsh, D. M. (2018). Detection of aggregation-competent tau in neuron-derived extracellular vesicles. *International Journal of Molecular Sciences*, *19*(3), 1–23. https://doi.org/10.3390/ijms19030663

Gulisano, W., Melone, M., Li Puma, D. D., Tropea, M. R., Palmeri, A., Arancio, O., … Puzzo, D. (2018). The effect of amyloid-β peptide on synaptic plasticity and memory is influenced by different isoforms, concentrations, and aggregation status. *Neurobiology of Aging*, *71*, 51–60. https://doi.org/10.1016/j.neurobiolaging.2018.06.025

Gundamaraju, R., Vemuri, R., Chong, W. C., Geraghty, D. P., & Eri, R. (2018). Cell Stress Signaling Cascades Regulating Cell Fate. *Current Pharmaceutical Design*, *24*(27), 3176–3183. https://doi.org/10.2174/1381612824666180711122753

Guo, J. L., & Lee, V. M. Y. (2011). Seeding of normal tau by pathological tau conformers drives pathogenesis of Alzheimer-like tangles. *Journal of Biological Chemistry*, *286*(17), 15317–15331. https://doi.org/10.1074/jbc.M110.209296

Haass, C., Kaether, C., Thinakaran, G., & Sisodia, S. (2012). Trafficking and proteolytic processing of APP. *Cold Spring Harbor Perspectives in Medicine*, *2*(5), 1–26. https://doi.org/10.1101/cshperspect.a006270

Hanisch, U. K. (2002). Microglia as a source and target of cytokines. *Glia*, *40*(2), 140–155. https://doi.org/10.1002/glia.10161

Harmati, M., Gyukity-Sebestyen, E., Dobra, G., Janovak, L., Dekany, I., Saydam, O., … Buzas, K. (2019). Small extracellular vesicles convey the stress-induced adaptive responses of melanoma cells. *Scientific Reports*, *9*(1), 1–19. https://doi.org/10.1038/s41598-019-51778-6

Harris, A., & Seckl, J. (2011). Glucocorticoids, prenatal stress and the programming of disease. *Hormones and Behavior*, *59*(3), 279–289. https://doi.org/10.1016/j.yhbeh.2010.06.007

Hemonnot, A. L., Hua, J., Ulmann, L., & Hirbec, H. (2019). Microglia in Alzheimer disease: Well-known targets and new opportunities. *Frontiers in Cellular and Infection Microbiology*, *9*(JUL), 1–20. https://doi.org/10.3389/fnagi.2019.00233

Heredia, L., Lin, R., Sola, F., Kedikian, G., Busciglio, J., & Lorenzo, A. (2004). Deposition of amyloid fibrils promotes cell-surface accumulation of amyloid B precursor protein. *Neurobiology of Disease*, *16*, 617–629. https://doi.org/10.1016/j.nbd.2004.04.015

Hoe, H. S., Lee, H. K., & Pak, D. T. S. (2012). The upside of APP at synapses. *CNS Neuroscience and Therapeutics*, *18*(1), 47–56. https://doi.org/10.1111/j.1755-5949.2010.00221.x

Hokanson, D. E., & Bretscher, A. P. (2012). EPI64 interacts with Slp1/JFC1 to coordinate Rab8a and Arf6 membrane trafficking. *Molecular Biology of the Cell*, *23*(4), 701–715. https://doi.org/10.1091/mbc.E11-06-0521

Holler, C. J., Davis, P. R., Beckett, T. L., Platt, T. L., Webb, R. L., Head, E., & Murphy, M. P. (2014). Bridging integrator 1 (BIN1) protein expression increases in the alzheimer's disease brain and correlates with neurofibrillary tangle pathology. *Journal of Alzheimer's Disease*, *42*(4), 1221–1227. https://doi.org/10.3233/JAD-132450

Hoover, B. R., Reed, M. N., Su, J., Penrod, R. D., Kotilinek, L. A., Grant, M. K., … Liao, D. (2010). Tau Mislocalization to Dendritic Spines Mediates Synaptic Dysfunction Independently of Neurodegeneration. *Neuron*, *68*(6), 1067–1081. https://doi.org/10.1016/j.neuron.2010.11.030

Hsu, C., Morohashi, Y., Yoshimura, S. I., Manrique-Hoyos, N., Jung, S. Y., Lauterbach, M. A., … Simons, M. (2010). Regulation of exosome secretion by Rab35 and its GTPase-activating proteins TBC1D10A-C. *Journal of Cell Biology*, *189*(2), 223–232. https://doi.org/10.1083/jcb.200911018

Huang, L. K., Chao, S. P., & Hu, C. J. (2020). Clinical trials of new drugs for Alzheimer disease. *Journal of Biomedical Science*, *27*(1), 1–13. https://doi.org/10.1186/s12929-019-0609-7

Huang, Y. A., Zhou, B., Wernig, M., Su, T. C., Huang, Y. A., Zhou, B., … Su, T. C. (2017). ApoE2, ApoE3, and ApoE4 Differentially Stimulate APP Transcription and Aβ Secretion. *Cell*, 427–441. https://doi.org/10.1016/j.cell.2016.12.044

Humphreys, D. T., Carver, J. A., Easterbrook-Smith, S. B., & Wilson, M. R. (1999). Clusterin has chaperone-like activity similar to that of small heat shock proteins. *Journal of Biological Chemistry*, *274*(11), 6875–6881. https://doi.org/10.1074/jbc.274.11.6875

Hung, C. O. Y., & Livesey, F. J. (2018). Altered γ-Secretase Processing of APP Disrupts Lysosome and Autophagosome Function in Monogenic Alzheimer's Disease. *Cell Reports*, *25*(13), 3647-3660.e2. https://doi.org/10.1016/j.celrep.2018.11.095

Itoh, T., & Fukuda, M. (2006). Identification of EPI64 as a GTPase-activating Protein Specific for Rab27A. *Journal of Biological Chemistry*, *281*(42), 31823–31831. https://doi.org/10.1016/s0021-9258(19)84097-8

Ittner, L. M., Ke, Y. D., Delerue, F., Bi, M., Gladbach, A., van Eersel, J., … Gotz, J. (2010). Dendritic function of tau mediates amyloid-β toxicity in alzheimer's disease mouse models. *Cell*, *142*(3), 387–397. https://doi.org/10.1016/j.cell.2010.06.036

Jackson, T. R., Brown, F. D., Nie, Z., Miura, K., Foroni, L., Sun, J., … Randazzo, P. A. (2000). ACAPs are Arf6 GTPase-activating proteins that function in the cell periphery. *Journal of Cell Biology*, *151*(3), 627–638. https://doi.org/10.1083/jcb.151.3.627

Jauregui-Huerta, F., Ruvalcaba-Delgadillo, Y., Gonzalez-Perez, O., Gonzalez-Castaneda, R., Garcia-Estrada, J., & Luquin, S. (2010). Responses of Glial Cells to Stress and Glucocorticoids. *Current Immunology Reviews*, *6*(3), 195–204. https://doi.org/10.2174/157339510791823790

Jeong, Y. H., Park, C. H., Yoo, J., Shin, K. Y., Ahn, S.-M., Kim, H.-S., … Suh, Y.-H. (2006). Chronic stress accelerates learning and memory impairments and increases amyloid deposition in APPV717I-CT100 transgenic mice, an Alzheimer's disease model. *The FASEB Journal*, *22*, 1–22. https://doi.org/10.1096/fj.05-4265fje

Jiang, Y., Mullaney, K. A., Peterhoff, C. M., Che, S., Schmidt, S. D., & Boyer-boiteau, A. (2010). Alzheimer 's-related endosome dysfunction in Down syndrome is Aβ -independent but requires APP and is reversed by BACE-1 inhibition. *Proceedings of the National Academy of Sciences*, *107*(4), 1630–1635. https://doi.org/10.1073/pnas.0908953107

Joels, M., & Baram, T. Z. (2009). The neurosymphony of stress. *Nature Reviews Neuroscience*, *10*(June), 459–466.

Johansson, L., Guo, X., Waern, M., Ostling, S. O., Gustafson, D., Bengtsson, C., & Skoog, I. (2010). Midlife psychological stress and risk of dementia: A 35-year longitudinal population study. *Brain*, *133*(8), 2217–2224. https://doi.org/10.1093/brain/awq116

Johnstone, R. M. (1991). Maturation of reticulocytes: formation of exosomes as a mechanism for shedding membrane proteins. *Biochemistry and Cell Biology*, *70*, 179–190.

Johnstone, R. M., Adam, M., Hammond, J. R., Orr, L., & Turbide, C. (1987). Vesicle formation during reticulocyte maturation. Association of plasma membrane activities with released vesicles (exosomes). *Journal of Biological Chemistry*, *262*(19), 9412–9420. https://doi.org/10.1016/s0021-9258(18)48095-7

Joshi, P., Turola, E., Ruiz, A., Bergami, A., Libera, D. D., Benussi, L., … Verderio, C. (2014). Microglia convert aggregated amyloid-β into neurotoxic forms through the shedding of microvesicles. *Cell Death and Differentiation*, *21*(4), 582–593. https://doi.org/10.1038/cdd.2013.180

Kamenetz, F., Tomita, T., Hsieh, H., Seabrook, G., Borchelt, D., Iwatsubo, T., … Malinow, R.

(2003). APP Processing and Synaptic Function. *Neuron*, *37*(6), 925–937. https://doi.org/10.1016/S0896-6273(03)00124-7

Kametani, F., Usami, M., Tanaka, K., Kume, H., & Mori, H. (2004). Mutant presenilin (A260V) affects Rab8 in PC12D cell. *Neurochemistry International*, *44*(5), 313–320. https://doi.org/10.1016/S0197-0186(03)00176-1

Kanemoto, S., Nitani, R., Murakami, T., Kaneko, M., Asada, R., Matsuhisa, K., … Imaizumi, K. (2016). Multivesicular body formation enhancement and exosome release during endoplasmic reticulum stress. *Biochemical and Biophysical Research Communications*, *480*(2), 166–172. https://doi.org/10.1016/j.bbrc.2016.10.019

Kashyap, G., Bapat, D., Das, D., Gowaikar, R., Amritkar, R. E., Rangarajan, G., … Ambika, G. (2019). Synapse loss and progress of Alzheimer's disease -A network model. *Scientific Reports*, *9*(1), 1–9. https://doi.org/10.1038/s41598-019-43076-y

Killick, R., Ribe, E. M., Al-Shawi, R., Malik, B., Hooper, C., Fernandes, C., … Lovestone, S. (2014). Clusterin regulates β-amyloid toxicity via Dickkopf-1-driven induction of the wnt-PCP-JNK pathway. *Molecular Psychiatry*, *19*(1), 88–98. https://doi.org/10.1038/mp.2012.163

Kim, J., Basak, J. M., & Holtzman, D. M. (2009). The Role of Apolipoprotein E in Alzheimer's Disease. *Neuron*, *63*(3), 287–303. https://doi.org/10.1016/j.neuron.2009.06.026.The

Kimura, N., Samura, E., Suzuki, K., Okabayashi, S., Shimozawa, N., & Yasutomi, Y. (2016). Dynein Dysfunction Reproduces Age-Dependent Retromer Deficiency: Concomitant Disruption of Retrograde Trafficking Is Required for Alteration in β-Amyloid Precursor Protein Metabolism. *American Journal of Pathology*, *186*(7), 1952–1966. https://doi.org/10.1016/j.ajpath.2016.03.006

Kinney, J. W., Bemiller, S. M., Murtishaw, A. S., Leisgang, A. M., Salazar, A. M., & Lamb, B. T. (2018). Inflammation as a central mechanism in Alzheimer's disease. *Alzheimer's and Dementia: Translational Research and Clinical Interventions*, *4*, 575–590. https://doi.org/10.1016/j.trci.2018.06.014

Klinkert, K., & Echard, A. (2016). Rab35 GTPase: A Central Regulator of Phosphoinositides and F-actin in Endocytic Recycling and Beyond. *Traffic*, *17*(10), 1063–1077. https://doi.org/10.1111/tra.12422

Kobayashi, H., Etoh, K., Ohbayashi, N., & Fukuda, M. (2014). Rab35 promotes the recruitment of Rab8, Rab13 and Rab36 to recycling endosomes through MICAL-L1 during neurite outgrowth. *Biology Open*, *3*(9), 803–814. https://doi.org/10.1242/bio.20148771

Kobayashi, H., & Fukuda, M. (2012). Rab35 regulates Arf6 activity through centaurin- 2 (ACAP2) during neurite outgrowth. *Journal of Cell Science*, *125*(9), 2235–2243. https://doi.org/10.1242/jcs.098657

Kobayashi, H., & Fukuda, M. (2013). Rab35 establishes the EHD1-association site by

coordinating two distinct effectors during neurite outgrowth. *Journal of Cell Science*, *126*(11), 2424–2435. https://doi.org/10.1242/jcs.117846

Koffie, R. M., Meyer-Luehmann, M., Hashimoto, T., Adams, K. W., Mielke, M. L., Garcia-Alloza, M., … Spires-Jones, T. L. (2009). Oligomeric amyloid β associates with postsynaptic densities and correlates with excitatory synapse loss near senile plaques. *Proceedings of the National Academy of Sciences of the United States of America*, *106*(10), 4012–4017. https://doi.org/10.1073/pnas.0811698106

Koh, Y. Q., Almughlliq, F. B., Vaswani, K., Peiris, H. N., & Mitchell, M. D. (2018). Exosome enrichment by ultracentrifugation and size exclusion chromatography. *Frontiers in Bioscience*, *23*(5), 865–874. https://doi.org/10.2741/4621

Koolhaas, J. M., Bartolomucci, A., Buwalda, B., De Boer, S. F., Flugge, G., Korte, S. M., … Fuchs, E. (2011). Stress revisited: A critical evaluation of the stress concept. *Neuroscience and Biobehavioral Reviews*, *35*(5), 1291–1301. https://doi.org/10.1016/j.neubiorev.2011.02.003

Kouranti, I., Sachse, M., Arouche, N., Goud, B., & Echard, A. (2006). Rab35 Regulates an Endocytic Recycling Pathway Essential for the Terminal Steps of Cytokinesis. *Current Biology*, *16*(17), 1719–1725. https://doi.org/10.1016/j.cub.2006.07.020

Lacor, P. N., Buniel, M. C., Furlow, P. W., Clemente, A. S., Velasco, P. T., Wood, M., … Klein, W. L. (2007). Aβ oligomer-induced aberrations in synapse composition, shape, and density provide a molecular basis for loss of connectivity in Alzheimer's disease. *Journal of Neuroscience*, *27*(4), 796–807. https://doi.org/10.1523/jneurosci.3501-06.2007

Laird, F. M., Cai, H., Savonenko, A. V., Farah, M. H., He, K., Melnikova, T., … Wong, P. C. (2005). BACE1, a major determinant of selective vulnerability of the brain to amyloid-β amyloidogenesis, is essential for cognitive, emotional, and synaptic functions. *Journal of Neuroscience*, *25*(50), 11693–11709. https://doi.org/10.1523/JNEUROSCI.2766-05.2005

Largo-Barrientos, P., Apóstolo, N., Creemers, E., Callaerts-Vegh, Z., Swerts, J., Davies, C., … Verstreken, P. (2021). Lowering Synaptogyrin-3 expression rescues Tau-induced memory defects and synaptic loss in the presence of microglial activation. *Neuron*, *109*(5), 767-777.e5. https://doi.org/10.1016/j.neuron.2020.12.016

Lazarevic, V., Fieńko, S., Andres-Alonso, M., Anni, D., Ivanova, D., Montenegro-Venegas, C., … Fejtova, A. (2017). Physiological concentrations of amyloid beta regulate recycling of synaptic vesicles via alpha7 acetylcholine receptor and CDK5/calcineurin signaling. *Frontiers in Molecular Neuroscience*, *10*(July), 1–14. https://doi.org/10.3389/fnmol.2017.00221

Ledreux, A., Thomas, S., Hamlett, E. D., Trautman, C., Gilmore, A., Hager, E. R., … Granholm, A.-C. (2021). Small Neuron-Derived Extracellular Vesicles from Individuals with Down Syndrome Propagate Tau Pathology in the Wildtype Mouse Brain. *Journal of Clinical Medicine*, *10*(3931), 1–23.

Lee, S. S., Won, J. H., Lim, G. J., Han, J., Lee, J. Y., Cho, K. O., & Bae, Y. K. (2019). A novel population of extracellular vesicles smaller than exosomes promotes cell proliferation. *Cell Communication and Signaling*, *17*(1), 1–15. https://doi.org/10.1186/s12964-019-0401-z

Leenders, A. G. M., Lopes da Silva, F. H., Ghijsen, W. E. J. M., & Verhage, M. (2001). Rab3A is involved in transport of synaptic vesicles to the active zone in mouse brain nerve terminals. *Molecular Biology of the Cell*, *12*(10), 3095–3102. https://doi.org/10.1091/mbc.12.10.3095

Leng, F., & Edison, P. (2021). Neuroinflammation and microglial activation in Alzheimer disease: where do we go from here? *Nature Reviews Neurology*, *17*(3), 157–172. https://doi.org/10.1038/s41582-020-00435-y

Lesuis, S. L., Weggen, S., Baches, S., Lucassen, P. J., & Krugers, H. J. (2018). Targeting glucocorticoid receptors prevents the effects of early life stress on amyloid pathology and cognitive performance in APP/PS1 mice. *Translational Psychiatry*, *8*(1). https://doi.org/10.1038/s41398-018-0101-2

Li, N. M., Liu, K. F., Qiu, Y. J., Zhang, H. H., Nakanishi, H., & Qing, H. (2019). Mutations of beta-amyloid precursor protein alter the consequence of Alzheimer's disease pathogenesis. *Neural Regeneration Research*, *14*(4), 658–665. https://doi.org/10.4103/1673-5374.247469

Li, Q., & Barres, B. A. (2018). Microglia and macrophages in brain homeostasis and disease. *Nature Reviews Immunology*, *18*(4), 225–242. https://doi.org/10.1038/nri.2017.125

Li, S., Hong, S., Shepardson, N. E., Walsh, D. M., Shankar, G. M., & Selkoe, D. (2009). Soluble Oligomers of Amyloid β Protein Facilitate Hippocampal Long-Term Depression by Disrupting Neuronal Glutamate Uptake. *Neuron*, *62*(6), 788–801. https://doi.org/10.1016/j.neuron.2009.05.012

Li, X., Hong, X., Wang, Y., Zhang, S., Zhang, J., Li, X., … Wang, J. (2019). Tau accumulation triggers STAT 1-dependent memory deficits by suppressing NMDA receptor expression . *EMBO Reports*, *20*(6), 1–18. https://doi.org/10.15252/embr.201847202

Liao, D., Miller, E. C., & Teravskis, P. J. (2014). Tau acts as a mediator for Alzheimer's disease-related synaptic deficits. *European Journal of Neuroscience*, *39*(7), 1202–1213. https://doi.org/10.1111/ejn.12504

Lichtenthaler, S. F. (2006). Ectodomain shedding of the amyloid precursor protein: Cellular control mechanisms and novel modifiers. *Neurodegenerative Diseases*, *3*(4–5), 262–269. https://doi.org/10.1159/000095265

Lim, C. Z. J., Zhang, Y., Chen, U., Chung, J., Reilhac, A., Loh, T. P., … Shao, H. (2019). Subtyping of circulating exosome-bound amyloid β reflects brain plaque deposition. *Nature Communications*, *10*(1), 1–11. https://doi.org/10.1038/s41467-019-09030-2

Liston, C., Miller, M. M., Goldwater, D. S., Radley, J. J., Rocher, A. B., Hof, P. R., … McEwen, B. S. (2006). Stress-induced alterations in prefrontal cortical dendritic morphology predict

selective impairments in perceptual attentional set-shifting. *Journal of Neuroscience*, *26*(30), 7870–7874. https://doi.org/10.1523/JNEUROSCI.1184-06.2006

Liu, C. C., Kanekiyo, T., Xu, H., & Bu, G. (2013). Apolipoprotein e and Alzheimer disease: Risk, mechanisms and therapy. *Nature Reviews Neurology*, *9*(2), 106–118. https://doi.org/10.1038/nrneurol.2012.263

Livingston, G., Huntley, J., Sommerlad, A., Ames, D., Ballard, C., Banerjee, S., … Mukadam, N. (2020). Dementia prevention, intervention, and care: 2020 report of the Lancet Commission. *The Lancet Commissions*, *396*(August), 413–446.

Lo Cicero, A., Stahl, P. D., & Raposo, G. (2015). Extracellular vesicles shuffling intercellular messages: For good or for bad. *Current Opinion in Cell Biology*, *35*, 69–77. https://doi.org/10.1016/j.ceb.2015.04.013

Lobb, R., & Moller, A. (2017). Size Exclusion Chromatography: A Simple and Reliable Method for Exosome Purification. In W. P. Kuo & S. Jia (Eds.), *Extracellular Vesicles: Methods and Protocols* (pp. 105–110). New York, NY: Springer New York. https://doi.org/10.1007/978-1-4939-7253-1_9

Logsdon, A. F., Lucke-Wold, B. P., Nguyen, L., Matsumoto, R. R., Turner, R. C., Rosen, C. L., & Huber, J. D. (2016). Salubrinal reduces oxidative stress, neuroinflammation and impulsive-like behavior in a rodent model of traumatic brain injury. *Brain Research*, *1643*, 140–151. https://doi.org/10.1016/j.brainres.2016.04.063

Lopes, S., Teplytska, L., Vaz-Silva, J., Dioli, C., Trindade, R., Morais, M., … Filiou, M. D. (2017). Tau deletion prevents stress-induced dendritic atrophy in prefrontal cortex: Role of synaptic mitochondria. *Cerebral Cortex*, *27*(4), 2580–2591. https://doi.org/10.1093/cercor/bhw057

Lopes, S., Vaz-Silva, J., Pinto, V., Dalla, C., Kokras, N., Bedenk, B., … Sotiropoulos, I. (2016). Tau protein is essential for stress-induced brain pathology. *Proceedings of the National Academy of Sciences*, *113*(26), E3755–E3763. https://doi.org/10.1073/pnas.1600953113

Lorenzo, A., Yuan, M., Zhang, Z., Paganetti, P. A., Sturchler-pierrat, C., Staufenbiel, M., … Yankner, B. A. (2000). Amyloid β interacts with the amyloid precursor protein: a potential toxic mechanism in Alzheimer's disease. *Nature Neuroscience*, *3*(5), 1–5.

Luarte, A., Cisternas, P., Caviedes, A., Batiz, L. F., Lafourcade, C., Wyneken, U., & Henzi, R. (2017). Astrocytes at the Hub of the Stress Response: Potential Modulation of Neurogenesis by miRNAs in Astrocyte-Derived Exosomes. *Stem Cells International*, *2017*. https://doi.org/10.1155/2017/1719050

Luarte, A., Henzi, R., Fern, A., Gaete, D., Cisternas, P., Pizarro, M., … Wyneken, U. (2020). Astrocyte-Derived Small Extracellular Vesicles miR-26a-5p Activity. *Cells*, *9*, 930.

Lugli, G., Cohen, A. M., Bennett, D. A., Shah, R. C., Fields, C. J., Hernandez, A. G., & Smalheiser, N. R. (2015). Plasma exosomal miRNAs in persons with and without

Alzheimer disease: Altered expression and prospects for biomarkers. *PLoS ONE*, *10*(10), 1–18. https://doi.org/10.1371/journal.pone.0139233

Lupien, S. J., McEwen, B. S., Gunnar, M. R., & Heim, C. (2009). Effects of stress throughout the lifespan on the brain, behaviour and cognition. *Nature Reviews Neuroscience*, *10*(6), 434–445. https://doi.org/10.1038/nrn2639

Marat, A. L., & McPherson, P. S. (2010). The connecdenn family, Rab35 guanine nucleotide exchange factors interfacing with the clathrin machinery. *Journal of Biological Chemistry*, *285*(14), 10627–10637. https://doi.org/10.1074/jbc.M109.050930

Mayor, S., Parton, R. G., & Donaldson, J. G. (2014). Clathrin-independent pathways of endocytosis. *Cold Spring Harbor Perspectives in Biology*, *6*(6), 1–20. https://doi.org/10.1101/cshperspect.a016758

McEwen, B. S. (1999). Stress and hippocampal plasticity. *Annual Review of Neuroscience*, *22*, 105–122. https://doi.org/10.1146/annurev.neuro.22.1.105

McEwen, B. S. (2007). Physiology and neurobiology of stress and adaptation: Central role of the brain. *Physiological Reviews*, *87*(3), 873–904. https://doi.org/10.1152/physrev.00041.2006

McEwen, B. S., De Kloet, E. R., & Rostene, W. (1986). Adrenal steroid receptors and actions in the nervous system. *Physiological Reviews*, *66*(4), 1121–1188. https://doi.org/10.1152/physrev.1986.66.4.1121

McEwen, B. S., Nasca, C., & Gray, J. D. (2016). Stress Effects on Neuronal Structure: Hippocampus, Amygdala, and Prefrontal Cortex. *Neuropsychopharmacology*, *41*(1), 3–23. https://doi.org/10.1038/npp.2015.171

McInnes, J., Wierda, K., Snellinx, A., Bounti, L., Wang, Y. C., Stancu, I. C., … Verstreken, P. (2018). Synaptogyrin-3 Mediates Presynaptic Dysfunction Induced by Tau. *Neuron*, *97*(4), 823-835.e8. https://doi.org/10.1016/j.neuron.2018.01.022

Mckee, A. C., & Daneshvar, D. H. (2015). *The neuropathology of traumatic brain injury*. *Handbook of Clinical Neurology* (1st ed., Vol. 127). Elsevier B.V. https://doi.org/10.1016/B978-0-444-52892-6.00004-0

Meijsing, S. H. (2015). Mechanisms of glucocorticoid-regulated gene transcription. *Advances in Experimental Medicine and Biology*, *872*, 59–81. https://doi.org/10.1007/978-1-4939-2895-8_3

Mejia, S., Giraldo, M., Pineda, D., Ardila, A., & Lopera, F. (2003). Nongenetic Factors as Modifiers of the Age of Onset of Familial Alzheimer's Disease. *International Psychogeriatrics*, *15*(4), 337–349. https://doi.org/10.1017/S1041610203009591

Messenger, S. W., Woo, S. S., Sun, Z., & Martin, T. F. J. (2018). A Ca2+-stimulated exosome release pathway in cancer cells is regulated by Munc13-4. *Journal of Cell Biology*, *217*(8), 2877–2890. https://doi.org/10.1083/jcb.201710132

Miranda, A. M., Lasiecka, Z. M., Xu, Y., Neufeld, J., Shahriar, S., Simoes, S., … Di Paolo, G. (2018). Neuronal lysosomal dysfunction releases exosomes harboring APP C-terminal fragments and unique lipid signatures. *Nature Communications*, *9*(1). https://doi.org/10.1038/s41467-017-02533-w

Mitra, S., Cheng, K. W., & Mills, G. B. (2011). Rab GTPases implicated in inherited and acquired disorders. *Seminars in Cell and Developmental Biology*, *22*(1), 57–68. https://doi.org/10.1016/j.semcdb.2010.12.005

Miyamoto, T., Stein, L., Thomas, R., Djukic, B., Taneja, P., Knox, J., … Mucke, L. (2017). Phosphorylation of tau at Y18, but not tau-fyn binding, is required for tau to modulate NMDA receptor-dependent excitotoxicity in primary neuronal culture. *Molecular Neurodegeneration*, *12*(1), 1–19. https://doi.org/10.1186/s13024-017-0176-x

Miyamoto, Y., Yamamori, N., Torii, T., Tanoue, A., & Yamauchi, J. (2014). Rab35, acting through ACAP2 switching off Arf6, negatively regulates oligodendrocyte differentiation and myelination. *Molecular Biology of the Cell*, *25*(9), 1532–1542. https://doi.org/10.1091/mbc.E13-10-0600

Mohamed, A., & Posse De Chaves, E. (2011). Aß internalization by neurons and glia. *International Journal of Alzheimer's Disease*. https://doi.org/10.4061/2011/127984

Mohamed, N. V., Desjardins, A., & Leclerc, N. (2017). Tau secretion is correlated to an increase of Golgi dynamics. *PLoS ONE*, *12*(5), 1–23. https://doi.org/10.1371/journal.pone.0178288

Molteni, R., Calabrese, F., Chourbaji, S., Brandwein, C., Racagni, G., Gass, P., & Riva, M. A. (2010). Depression-prone mice with reduced glucocorticoid receptor expression display an altered stress-dependent regulation of brain-derived neurotrophic factor and activity-regulated cytoskeleton-associated protein. *Journal of Psychopharmacology*, *24*(4), 595–603. https://doi.org/10.1177/0269881108099815

Mondin, V. E., El Kadhi, K. Ben, Cauvin, C., Jackson-Crawford, A., Bélanger, E., Decelle, B., … Carréno, S. (2019). PTEN reduces endosomal PtdIns(4,5)P2 in a phosphatase-independent manner via a PLC pathway. *Journal of Cell Biology*, *218*(7), 2198–2214. https://doi.org/10.1083/jcb.201805155

Moore, S., Evans, L. D. B., Andersson, T., Portelius, E., Smith, J., Dias, T. B., … Livesey, F. J. (2015). APP Metabolism Regulates Tau Proteostasis in Human Cerebral Cortex Neurons. *Cell Reports*, *11*(5), 689–696. https://doi.org/10.1016/j.celrep.2015.03.068

Mrozowska, P. S., & Fukuda, M. (2016). Regulation of podocalyxin trafficking by Rab small GTPases in 2D and 3D epithelial cell cultures. *Journal of Cell Biology*, *213*(3), 355–369. https://doi.org/10.1083/jcb.201512024

Mucke, L., & Selkoe, D. J. (2012). Neurotoxicity of amyloid β-protein: Synaptic and network dysfunction. *Cold Spring Harbor Perspectives in Medicine*, *2*(7), 1–18. https://doi.org/10.1101/cshperspect.a006338

Mufson, E. J., Ward, S., & Binder, L. (2014). Prefibrillar tau oligomers in mild cognitive impairment and Alzheimer's disease. *Neurodegenerative Diseases*, *13*(2–3), 151–153. https://doi.org/10.1159/000353687

Myeku, N., Clelland, C. L., Emrani, S., Kukushkin, N. V., Yu, W. H., Goldberg, A. L., & Duff, K. E. (2016). Tau-driven 26S proteasome impairment and cognitive dysfunction can be prevented early in disease by activating cAMP-PKA signaling. *Nature Medicine*, *22*(1), 46–53. https://doi.org/10.1038/nm.4011

Naskar, S., & Chattarji, S. (2019). Stress elicits contrasting effects on the structure and number of astrocytes in the amygdala versus hippocampus. *ENeuro*, *6*(1), 1–14. https://doi.org/10.1523/ENEURO.0338-18.2019

Nativio, R., Lan, Y., Donahue, G., Sidoli, S., Berson, A., Srinivasan, A. R., … Berger, S. L. (2020). An integrated multi-omics approach identifies epigenetic alterations associated with Alzheimer's disease. *Nature Genetics*, *52*(10), 1024–1035. https://doi.org/10.1038/s41588-020-0696-0

Nelson, P. T., Alafuzoff, I., Bigio, E. H., Bouras, C., Braak, H., Cairns, N. J., … Beach, T. G. (2012). Correlation of alzheimer disease neuropathologic changes with cognitive status: A review of the literature. *Journal of Neuropathology and Experimental Neurology*, *71*(5), 362–381. https://doi.org/10.1097/NEN.0b013e31825018f7

Newcombe, E. A., Camats-Perna, J., Silva, M. L., Valmas, N., Huat, T. J., & Medeiros, R. (2018). Inflammation: the link between comorbidities, genetics, and Alzheimer's disease. *Journal of Neuroinflammation*, *15*(1), 1–26. https://doi.org/10.1186/s12974-018-1313-3

Ni Chasaide, C., & Lynch, M. A. (2020). The role of the immune system in driving neuroinflammation. *Brain and Neuroscience Advances*, *4*, 239821281990108. https://doi.org/10.1177/2398212819901082

nia.nih.gov. (2019). What Causes Alzheimer's Disease.

Nixon, R. A. (2005). Endosome function and dysfunction in Alzheimer's disease and other neurodegenerative diseases. *Neurobiology of Aging*, *26*(3), 373–382. https://doi.org/10.1016/j.neurobiolaging.2004.09.018

Nizard, P., Tetley, S., Le Dréan, Y., Watrin, T., Le Goff, P., Wilson, M. R., & Michel, D. (2007). Stress-induced retrotranslocation of clusterin/ApoJ into the cytosol. *Traffic*, *8*(5), 554–565. https://doi.org/10.1111/j.1600-0854.2007.00549.x

O'Neill, C. P., Gilligan, K. E., & Dwyer, R. M. (2019). Role of extracellular vesicles (EVs) in cell stress response and resistance to cancer therapy. *Cancers*, *11*(2), 1–14. https://doi.org/10.3390/cancers11020136

Orr, M. E., & Oddo, S. (2013). Autophagic/lysosomal dysfunction in Alzheimer's disease. *Alzheimer's Research & Therapy*.

Pallas-Bazarra, N., Draffin, J., Cuadros, R., Antonio Esteban, J., & Avila, J. (2019). Tau is required for the function of extrasynaptic NMDA receptors. *Scientific Reports*, *9*(1), 1–10. https://doi.org/10.1038/s41598-019-45547-8

Pan, B. T., Teng, K., Wu, C., Adam, M., & Johnstone, R. M. (1985). Electron microscopic evidence for externalization of the transferrin receptor in vesicular form in sheep reticulocytes. *Journal of Cell Biology*, *101*(3), 942–948. https://doi.org/10.1083/jcb.101.3.942

Paolicelli, R. C., Bergamini, G., & Rajendran, L. (2019). Cell-to-cell Communication by Extracellular Vesicles: Focus on Microglia. *Neuroscience*, *405*, 148–157. https://doi.org/10.1016/j.neuroscience.2018.04.003

Parihar, M., & Brewer, G. J. (2010). *Amyloid Beta as a Modulator of Synaptic Plasticity*. *Journal of Alzheimer's Disease* (Vol. 22). https://doi.org/doi:10.3233/JAD-2010-101020. Amyloid

Park, J., Jang, M., & Chang, S. (2013). Deleterious effects of soluble amyloid-β oligomers on multiple steps of synaptic vesicle trafficking. *Neurobiology of Disease*, *55*, 129–139. https://doi.org/10.1016/j.nbd.2013.03.004

Patino-Lopez, G., Dong, X., Ben-Aissa, K., Bernot, K. M., Itoh, T., Fukuda, M., … Shaw, S. (2008). Rab35 and its GAP EPI64C in T cells regulate receptor recycling and immunological synapse formation. *Journal of Biological Chemistry*, *283*(26), 18323–18330. https://doi.org/10.1074/jbc.M800056200

Paxinos, G., & Watson, C. (1986). *The Rat Brain in Stereotaxic Coordinates*. New York: Academic Press.

Perea, J. R., Lopez, E., Diez-Ballesteros, J. C., Avila, J., Hernandez, F., & Bolos, M. (2019). Extracellular monomeric tau is internalized by astrocytes. *Frontiers in Neuroscience*, *13*(May), 1–7. https://doi.org/10.3389/fnins.2019.00442

Perez-Gonzalez, R., Gauthier, S. A., Kumar, A., & Levy, E. (2012). The exosome secretory pathway transports amyloid precursor protein carboxyl-terminal fragments from the cell into the brain extracellular space. *Journal of Biological Chemistry*, *287*(51), 43108–43115. https://doi.org/10.1074/jbc.M112.404467

Perez-Gonzalez, R., Gauthier, S. A., Kumar, A., Saito, M., Saito, M., & Levy, E. (2017). A Method for Isolation of Extracellular Vesicles and Characterization of Exosomes from Brain Extracellular Space. *Methods in Molecular Biology*, *1545*, 139–151. https://doi.org/10.1007/978-1-4939-6728-5

Perez-Hernandez, D., Gutierrez-Vazquez, C., Jorge, I., Lopez-Martin, S., Ursa, A., Sanchez-Madrid, F., … Yanez-Mo, M. (2013). The intracellular interactome of tetraspanin-enriched microdomains reveals their function as sorting machineries toward exosomes. *Journal of Biological Chemistry*, *288*(17), 11649–11661. https://doi.org/10.1074/jbc.M112.445304

Perez, M., Avila, J., & Hernandez, F. (2019). Propagation of tau via extracellular vesicles.

Frontiers in Neuroscience, *13*(JUL), 1–7. https://doi.org/10.3389/fnins.2019.00698

Pols, M. S., & Klumperman, J. (2009). Trafficking and function of the tetraspanin CD63. *Experimental Cell Research*, *315*(9), 1584–1592. https://doi.org/10.1016/j.yexcr.2008.09.020

Prediger, R. D. S., Franco, J. L., Pandolfo, P., Medeiros, R., Duarte, F. S., Di, G., … Dafre, A. L. (2007). Differential susceptibility following β-amyloid peptide-(1–40) administration in C57BL/6 and Swiss albino mice: Evidence for a dissociation between cognitive deficits and the glutathione system response. *Behavioural Brain Research*, *177*, 205–213. https://doi.org/10.1016/j.bbr.2006.11.032

Przedborski, S., Vila, M., & Jackson-Lewis, V. (2003). Neurodegeneration: What is it and where are we? *Journal of Clinical Investigation*, *111*(1), 3–10. https://doi.org/10.1172/JCI200317522

Puzzo, D., Privitera, L., Fa', M., Staniszewski, A., Hashimoto, G., Aziz, F., … Arancio, O. (2011). Endogenous amyloid-β is necessary for hippocampal synaptic plasticity and memory. *Annals of Neurology*, *69*(5), 819–830. https://doi.org/10.1002/ana.22313

Puzzo, D., Privitera, L., Leznik, E., Fà, M., Staniszewski, A., Palmeri, A., & Arancio, O. (2008). Picomolar amyloid-β positively modulates synaptic plasticity and memory in hippocampus. *Journal of Neuroscience*, *28*(53), 14537–14545. https://doi.org/10.1523/JNEUROSCI.2692-08.2008

Quek, C., & Hill, A. F. (2017). The role of extracellular vesicles in neurodegenerative diseases. *Biochemical and Biophysical Research Communications*, *483*(4), 1178–1186. https://doi.org/10.1016/j.bbrc.2016.09.090

Querfurth, H. W., & LaFerla, F. M. (2010). Alzheimer's disease. *The New England Journal of Medicine*, *362*(4), 329–344. https://doi.org/10.1056/NEJMra0909142

Radley, J. J., Sisti, H. M., Hao, J., Rocher, A. B., McCall, T., Hof, P. R., … Morrison, J. H. (2004). Chronic behavioral stress induces apical dendritic reorganization in pyramidal neurons of the medial prefrontal cortex. *Neuroscience*, *125*(1), 1–6. https://doi.org/10.1016/j.neuroscience.2004.01.006

Radley, Jason J., Rocher, A. B., Janssen, W. G. M., Hof, P. R., McEwen, B. S., & Morrison, J. H. (2005). Reversibility of apical dendritic retraction in the rat medial prefrontal cortex following repeated stress. *Experimental Neurology*, *196*(1), 199–203. https://doi.org/10.1016/j.expneurol.2005.07.008

Rahajeng, J., Panapakkam Giridharan, S. S., Cai, B., Naslavsky, N., & Caplan, S. (2012). MICAL-L1 is a tubular endosomal membrane hub that connects Rab35 and Arf6 with Rab8a. *Traffic*, *13*(1), 82–93. https://doi.org/10.1111/j.1600-0854.2011.01294.x

Rajendran, L., Honsho, M., Zahn, T. R., Keller, P., Geiger, K. D., Verkade, P., & Simons, K. (2006). Alzheimer's disease β-amyloid peptides are released in association with exosomes.

Proceedings of the National Academy of Sciences of the United States of America, *103*(30), 11172–11177. https://doi.org/10.1073/pnas.0603838103

Rajmohan, R., & Reddy, P. H. (2017). Amyloid-Beta and Phosphorylated Tau Accumulations Cause Abnormalities at Synapses of Alzheimer's disease Neurons. *Journal of Alzheimer's Disease*, *57*(4), 975–999. https://doi.org/10.3233/JAD-160612

Rashed, M. H., Bayraktar, E., Helal, G. K., Abd-Ellah, M. F., Amero, P., Chavez-Reyes, A., & Rodriguez-Aguayo, C. (2017). Exosomes: From garbage bins to promising therapeutic targets. *International Journal of Molecular Sciences*, *18*(3). https://doi.org/10.3390/ijms18030538

Reddy, P. H., Mani, G., Park, B. S., Jacques, J., Murdoch, G., Whetsell, W., … Manczak, M. (2005). Differential loss of synaptic proteins in Alzheimer's disease: Implications for synaptic dysfunction. *Journal of Alzheimer's Disease*, *7*(2), 103–117. https://doi.org/10.3233/JAD-2005-7203

Rice, H. C., De Malmazet, D., Schreurs, A., Frere, S., Van Molle, I., Volkov, A. N., … De Wit, J. (2019). Secreted amyloid-b precursor protein functions as a GABA B R1a ligand to modulate synaptic transmission. *Science*, *363*(6423). https://doi.org/10.1126/science.aao4827

Ridder, S., Chourbaji, S., Hellweg, R., Urani, A., Zacher, C., Schmid, W., … Gass, P. (2005). Mice with genetically altered glucocorticoid receptor expression show altered sensitivity for stress-induced depressive reactions. *Journal of Neuroscience*, *25*(26), 6243–6250. https://doi.org/10.1523/JNEUROSCI.0736-05.2005

Ridge, P. G., Karch, C. M., Hsu, S., Arano, I., Teerlink, C. C., Ebbert, M. T. W., … Kauwe, J. S. K. (2018). Linkage, whole genome sequence, and biological data implicate variants in RAB10 in Alzheimer's disease resilience. *Genome Medicine*, *10*(1), 1–14. https://doi.org/10.1186/s13073-018-0516-7

Ries, M., & Sastre, M. (2016). Mechanisms of Aβ clearance and degradation by glial cells. *Frontiers in Aging Neuroscience*, *8*(June), 1–9. https://doi.org/10.3389/fnagi.2016.00160

Roberson, E. D., Scearce-Levie, K., Palop, J. J., Yan, F., Cheng, I. H., Wu, T., … Mucke, L. (2007). Reducing Endogenous Tau Ameliorates Amyloid b–Induced Deficits in an Alzheimer's Disease Mouse Model. *Science*, *316*(May), 750–754.

Rock, R. B., Gekker, G., Hu, S., Sheng, W. S., Cheeran, M., Lokensgard, J. R., & Peterson, P. K. (2004). Role of microglia in central nervous system infections. *Clinical Microbiology Reviews*, *17*(4), 942–964. https://doi.org/10.1128/CMR.17.4.942-964.2004

Rodrigue, K. M., Kennedy, K. M., & Park, D. C. (2009). Beta-amyloid deposition and the aging brain. *Neuropsychology Review*, *19*(4), 436–450. https://doi.org/10.1007/s11065-009-9118-x

Ruan, Z., Pathak, D., Venkatesan Kalavai, S., Yoshii-Kitahara, A., Muraoka, S., Bhatt, N., …

Ikezu, T. (2021). Alzheimer's disease brain-derived extracellular vesicles spread tau pathology in interneurons. *Brain*, *144*(1), 288–309. https://doi.org/10.1093/brain/awaa376

Ruel, J., & De Kloet, E. R. (1985). Two receptor systems for corticosterone in Rat Brain: Microdistribution and differential occupation. *Endocrinology*, *117*(6), 2505–2511. https://doi.org/doi: 10.1210/endo-117-6-2505

Saavedra, L., Mohamed, A., Ma, V., Kar, S., & De Chaves, E. P. (2007). Internalization of β-amyloid peptide by primary neurons in the absence of apolipoprotein E. *Journal of Biological Chemistry*, *282*(49), 35722–35732. https://doi.org/10.1074/jbc.M701823200

Sackmann, C., & Hallbeck, M. (2020). Oligomeric amyloid-β induces early and widespread changes to the proteome in human iPSC-derived neurons. *Scientific Reports*, *10*(1), 1–12. https://doi.org/10.1038/s41598-020-63398-6

Saman, S., Kim, W. H., Raya, M., Visnick, Y., Miro, S., Saman, S., … Hall, G. F. (2012). Exosome-associated tau is secreted in tauopathy models and is selectively phosphorylated in cerebrospinal fluid in early Alzheimer disease. *Journal of Biological Chemistry*, *287*(6), 3842–3849. https://doi.org/10.1074/jbc.M111.277061

Sannerud, R., Declerck, I., Peric, A., Raemaekers, T., Menendez, G., & Zhou, L. (2011). ADP ribosylation factor 6 (ARF6) controls amyloid precursor protein (APP) processing by mediating the endosomal sorting of BACE1. *Proceedings of the National Academy of Sciences*, *108*(34). https://doi.org/10.1073/pnas.1100745108

Sardar Sinha, M., Ansell-Schultz, A., Civitelli, L., Hildesjo, C., Larsson, M., Lannfelt, L., … Hallbeck, M. (2018). Alzheimer's disease pathology propagation by exosomes containing toxic amyloid-beta oligomers. *Acta Neuropathologica*, *136*(1), 41–56. https://doi.org/10.1007/s00401-018-1868-1

Sawade, L., Grandi, F., Mignanelli, M., Patiño-López, G., Klinkert, K., Langa-Vives, F., … Haucke, V. (2020). Rab35-regulated lipid turnover by myotubularins represses mTORC1 activity and controls myelin growth. *Nature Communications*, *11*(1), 25–28. https://doi.org/10.1038/s41467-020-16696-6

Scheff, S. W., Price, D. A., Schmitt, F. A., & Mufson, E. J. (2006). Hippocampal synaptic loss in early Alzheimer's disease and mild cognitive impairment. *Neurobiology of Aging*, *27*(10), 1372–1384. https://doi.org/10.1016/j.neurobiolaging.2005.09.012

Scheper, W., Hoozemans, J. J. M., Hoogenraad, C. C., Rozemuller, A. J. M., Eikelenboom, P., & Baas, F. (2007). Rab6 is increased in Alzheimer's disease brain and correlates with endoplasmic reticulum stress. *Neuropathology and Applied Neurobiology*, *33*(5), 523–532. https://doi.org/10.1111/j.1365-2990.2007.00846.x

Schorey, J. S., Cheng, Y., Singh, P. P., & Smith, V. L. (2015). Exosomes and other extracellular vesicles in host–pathogen interactions. *EMBO Reports*, *16*(1), 24–43. https://doi.org/10.15252/embr.201439363

Selkoe, D. J. (2002). Alzheimer's disease is a synaptic failure. *Science*, *298*(5594), 789–791. https://doi.org/10.1126/science.1074069

Seubert, P., Vigo-Pelfrey, C., Esch, F., Lee, M., Dovey, H., Davis, D., … Schenk, D. (1992). Isolation and quantification of soluble Alzheimer's β-peptide from biological fluids. *Nature*, *359*(September), 325–327.

Shankar, G. M., Li, S., Mehta, T. H., Garcia-Munoz, A., Shepardson, N. E., Smith, I., … Selkoe, D. J. (2008). Amyloid-β protein dimers isolated directly from Alzheimer's brains impair synaptic plasticity and memory. *Nature Medicine*, *14*(8), 837–842. https://doi.org/10.1038/nm1782

Sharma, S., Skowronek, A., & Erdmann, K. S. (2015). The role of the Lowe syndrome protein OCRL in the endocytic pathway. *Biological Chemistry*, *396*(12), 1293–1300. https://doi.org/10.1515/hsz-2015-0180

Sheehan, P., & Waites, C. L. (2019). Coordination of synaptic vesicle trafficking and turnover by the Rab35 signaling network. *Small GTPases*, *0*(0), 1–10. https://doi.org/10.1080/21541248.2016.1270392

Sheehan, P., Zhu, M., Beskow, A., Vollmer, C., & Waites, C. L. (2016). Activity-Dependent Degradation of Synaptic Vesicle Proteins Requires Rab35 and the ESCRT Pathway. *The Journal of Neuroscience*, *36*(33), 8668–8686. https://doi.org/10.1523/JNEUROSCI.0725-16.2016

Shin, W. S., Di, J., Cao, Q., Li, B., Seidler, P. M., Murray, K. A., … Jiang, L. (2019). Amyloid β-protein oligomers promote the uptake of tau fibril seeds potentiating intracellular tau aggregation. *Alzheimer's Research and Therapy*, *11*(1), 1–13. https://doi.org/10.1186/s13195-019-0541-9

Shirane, M., & Nakayama, K. I. (2006). Protrudin induces neurite formation by directional membrane trafficking. *Science*, *314*(5800), 818–821. https://doi.org/10.1126/science.1134027

Sidhom, K., Obi, P. O., & Saleem, A. (2020). A review of exosomal isolation methods: Is size exclusion chromatography the best option? *International Journal of Molecular Sciences*, *21*(18), 1–19. https://doi.org/10.3390/ijms21186466

Silva, J. M., Rodrigues, S., Sampaio-marques, B., Gomes, P., Neves-carvalho, A., Dioli, C., … Sotiropoulos, I. (2019). Dysregulation of autophagy and stress granule-related proteins in stress-driven Tau pathology. *Cell Death & Differentiation*, 1411–1427. https://doi.org/10.1038/s41418-018-0217-1

Simpson, R. J., Lim, J. W. E., Moritz, R. L., & Mathivanan, S. (2009). Exosomes: Proteomic insights and diagnostic potential. *Expert Review of Proteomics*, *6*(3), 267–283. https://doi.org/10.1586/epr.09.17

Sinha, S., Hoshino, D., Hong, N. H., Kirkbride, K. C., Grega-Larson, N. E., Seiki, M., …

Weaver, A. M. (2016). Cortactin promotes exosome secretion by controlling branched actin dynamics. *Journal of Cell Biology*, *214*(2), 197–213. https://doi.org/10.1083/jcb.201601025

Siracusa, R., Fusco, R., & Cuzzocrea, S. (2019). Astrocytes: Role and functions in brain pathologies. *Frontiers in Pharmacology*, *10*(SEP), 1–10. https://doi.org/10.3389/fphar.2019.01114

Small, S. A., Simoes-Spassov, S., Mayeux, R., & Petsko, G. A. (2017). Endosomal Traffic Jams Represent a Pathogenic Hub and Therapeutic Target in Alzheimer's Disease. *Trends in Neurosciences*, *40*(10), 592–602. https://doi.org/10.1016/j.tins.2017.08.003

Sochocka, M., Zwolinska, K., & Leszek, J. (2017). The Infectious Etiology of Alzheimer's Disease. *Current Neuropharmacology*, *15*(7), 996–1009. https://doi.org/10.2174/1570159x15666170313122937

Sotiropoulos, I., Catania, C., Pinto, L. G., Silva, R., Pollerberg, G. E., Takashima, A., … Almeida, O. F. X. (2011). Stress Acts Cumulatively To Precipitate Alzheimer's Disease-Like Tau Pathology and Cognitive Deficits. *Journal of Neuroscience*, *31*(21), 7840–7847. https://doi.org/10.1523/JNEUROSCI.0730-11.2011

Sotiropoulos, I., Catania, C., Riedemann, T., Fry, J. P., Breen, K. C., Michaelidis, T. M., & Almeida, O. F. X. (2008). Glucocorticoids trigger Alzheimer disease-like pathobiochemistry in rat neuronal cells expressing human tau. *Journal of Neurochemistry*, *107*(2), 385–397. https://doi.org/10.1111/j.1471-4159.2008.05613.x

Sotiropoulos, I., Cerqueira, J. J., Catania, C., Takashima, A., Sousa, N., & Almeida, O. F. X. (2008). Stress and glucocorticoid footprints in the brain-The path from depression to Alzheimer's disease. *Neuroscience and Biobehavioral Reviews*, *32*(6), 1161–1173. https://doi.org/10.1016/j.neubiorev.2008.05.007

Sotiropoulos, I., Silva, J. M., Gomes, P., Sousa, N., & Almeida, O. F. X. (2019). Stress and the Etiopathogenesis of Alzheimer's Disease and Depression. In *Advances in Experimental Medicine and Biology* (Vol. 1184, pp. 241–257). https://doi.org/10.1007/978-981-32-9358-8_20

Sousa, N., & Almeida, O. F. X. (2012). Disconnection and reconnection: The morphological basis of (mal)adaptation to stress. *Trends in Neurosciences*, *35*(12), 742–751. https://doi.org/10.1016/j.tins.2012.08.006

Spanic, E., Langer Horvat, L., Hof, P. R., & Simic, G. (2019). Role of Microglial Cells in Alzheimer's Disease Tau Propagation. *Frontiers in Aging Neuroscience*, *11*(October), 1–10. https://doi.org/10.3389/fnagi.2019.00271

Spires-Jones, T. L., Meyer-Luehmann, M., Osetek, J. D., Jones, P. B., Stern, E. A., Bacskai, B. J., & Hyman, B. T. (2007). Impaired spine stability underlies plaque-related spine loss in an Alzheimer's disease mouse model. *American Journal of Pathology*, *171*(4), 1304–1311. https://doi.org/10.2353/ajpath.2007.070055

Sprenkle, N. T., Sims, S. G., Sánchez, C. L., & Meares, G. P. (2017). Endoplasmic reticulum stress and inflammation in the central nervous system. *Molecular Neurodegeneration*, *12*(1), 1–18. https://doi.org/10.1186/s13024-017-0183-y

Srivareerat, M., Tran, T. T., Alzoubi, K. H., & Alkadhi, K. A. (2009). Chronic Psychosocial Stress Exacerbates Impairment of Cognition and Long-Term Potentiation in β-Amyloid Rat Model of Alzheimer's Disease. *Biological Psychiatry*, *65*(11), 918–926. https://doi.org/10.1016/j.biopsych.2008.08.021

Stancu, I. C., Cremers, N., Vanrusselt, H., Couturier, J., Vanoosthuyse, A., Kessels, S., … Dewachter, I. (2019). Aggregated Tau activates NLRP3–ASC inflammasome exacerbating exogenously seeded and non-exogenously seeded Tau pathology in vivo. *Acta Neuropathologica*, *137*(4), 599–617. https://doi.org/10.1007/s00401-018-01957-y

Stenmark, H. (2009). Rab GTPases as coordinators of vesicle traffic. *Nature Reviews. Molecular Cell Biology*, *10*(8), 513–525. https://doi.org/10.1038/nrm2728

Stephan, A., & Phillips, A. G. (2005). A case for a non-transgenic animal model of Alzheimer's disease. *Genes, Brain and Behavior*, 157–172. https://doi.org/10.1111/j.1601-183X.2004.00113.x

Sun, J., & Roy, S. (2017). The Physical Approximation of APP and BACE-1 : A Key Event in Alzheimer's Disease Pathogenesis. *Developmental Neurobiology*, 340–347. https://doi.org/10.1002/dneu.22556

Sung, B. H., Ketova, T., Hoshino, D., Zijlstra, A., & Weaver, A. M. (2015). Directional cell movement through tissues is controlled by exosome secretion. *Nature Communications*, *6*(May). https://doi.org/10.1038/ncomms8164

Sung, B. H., von Lersner, A., Guerrero, J., Krystofiak, E. S., Inman, D., Pelletier, R., … Weaver, A. M. (2020). A live cell reporter of exosome secretion and uptake reveals pathfinding behavior of migrating cells. *Nature Communications*, *11*(1), 1–15. https://doi.org/10.1038/s41467-020-15747-2

Sze, C. I., Bi, H., Kleinschmidt-Demasters, B. K., Filley, C. M., & Martin, L. J. (2000). Selective regional loss of exocytotic presynaptic vesicle proteins in Alzheimer's disease brains. *Journal of the Neurological Sciences*, *175*(2), 81–90. https://doi.org/10.1016/S0022-510X(00)00285-9

Taira, K., Bujo, H., Hirayama, S., Yamazaki, H., Kanaki, T., Takahashi, K., … Saito, Y. (2001). of ApoE-Rich Lipoproteins In Vitro. *Arteriosclerosis, Thrombosis, and Vascular Biology*, *21*, 1501–1506.

Tamai, K., Tanaka, N., Nakano, T., Kakazu, E., Kondo, Y., Inoue, J., … Sugamura, K. (2010). Exosome secretion of dendritic cells is regulated by Hrs, an ESCRT-0 protein. *Biochemical and Biophysical Research Communications*, *399*(3), 384–390. https://doi.org/10.1016/j.bbrc.2010.07.083

Tan, J. Z. A., & Gleeson, P. A. (2019). The role of membrane trafficking in the processing of amyloid precursor protein and production of amyloid peptides in Alzheimer's disease. *Biochimica et Biophysica Acta - Biomembranes*, *1861*(4), 697–712. https://doi.org/10.1016/j.bbamem.2018.11.013

Tang, W., Tam, J. H. K., Seah, C., Chiu, J., Tyrer, A., Cregan, S. P., … Pasternak, S. H. (2015). Arf6 controls beta-amyloid production by regulating macropinocytosis of the Amyloid Precursor Protein to lysosomes. *Molecular Brain*, *8*(1). https://doi.org/10.1186/s13041-015-0129-7

Tcw, J., & Goate, A. M. (2017). Genetics of β-Amyloid Precursor Protein in Alzheimer's Disease. *Cold Spring Harbor Perspectives in Medicine*, *7*(6), 1–12. https://doi.org/10.1101/cshperspect.a024539

Teng, F., & Fussenegger, M. (2021). Shedding Light on Extracellular Vesicle Biogenesis and Bioengineering. *Advanced Science*, *8*(1), 1–17. https://doi.org/10.1002/advs.202003505

Thery, C., Amigorena, S., Raposo, G., & Clayton, A. (2006). Isolation and Characterization of Exosomes from Cell Culture Supernatants and Biological Fluids. *Current Protocols in Cell Biology*, *30*(1), 1–29. https://doi.org/10.1002/0471143030.cb0322s30

Thul, P. J., Akesson, L., Wiking, M., Mahdessian, D., Geladaki, A., Ait Blal, H., … Lundberg, E. (2017). A subcellular map of the human proteome. *Science*, *356*(6340). https://doi.org/10.1126/science.aal3321

Topol, A., Tran, N. N., & Brennand, K. J. (2015). A Guide to Generating and Using hiPSC Derived NPCs for the Study of Neurological Diseases. *Journal of Visualized Experiments*, 2015. https://doi.org/10.3791/52495

Trajkovic, K., Hsu, C., Chiantia, S., Rajendran, L., Wenzel, D., Wieland, F., … Simons, M. (2008). Ceramide triggers budding of exosome vesicles into multivesicular endosomes. *Science*, *319*, 1244–1247. https://doi.org/10.1126/science.1153124

Ubelmann, F., Burrinha, T., Salavessa, L., Gomes, R., Ferreira, C., Moreno, N., & Guimas Almeida, C. (2017). Bin1 and CD2AP polarise the endocytic generation of beta-amyloid. *EMBO Reports*, *18*(1), 102–122. https://doi.org/10.15252/embr.201642738

Udayar, V., Buggia-Prevot, V., Guerreiro, R. L., Siegel, G., Rambabu, N., Soohoo, A. L., … Rajendran, L. (2013). A Paired RNAi and RabGAP overexpression screen identifies Rab11 as a regulator of beta-amyloid production. *Cell Reports*, *5*(6), 1536–1551. https://doi.org/10.1016/j.celrep.2013.12.005

Uhlen, M., Fagerberg, L., Hallstrom, B. M., Lindskog, C., Oksvold, P., Mardinoglu, A., … Ponten, F. (2015). Tissue-based map of the human proteome. *Science*, *347*(6220). https://doi.org/10.1126/science.1260419

Uytterhoeven, V., Kuenen, S., Kasprowicz, J., Miskiewicz, K., & Verstreken, P. (2011). Loss of Skywalker reveals synaptic endosomes as sorting stations for synaptic vesicle proteins. *Cell*,

145(1), 117–132. https://doi.org/10.1016/j.cell.2011.02.039

Vaillant-Beuchot, L., Mary, A., Pardossi-Piquard, R., Bourgeois, A., Lauritzen, I., Eysert, F., … Chami, M. (2021). Accumulation of amyloid precursor protein C-terminal fragments triggers mitochondrial structure, function, and mitophagy defects in Alzheimer's disease models and human brains. *Acta Neuropathologica*, *141*(1), 39–65. https://doi.org/10.1007/s00401-020-02234-7

Valadi, H., Ekström, K., Bossios, A., Sjöstrand, M., Lee, J. J., & Lötvall, J. O. (2007). Exosome-mediated transfer of mRNAs and microRNAs is a novel mechanism of genetic exchange between cells. *Nature Cell Biology*, *9*(6), 654–659. https://doi.org/10.1038/ncb1596

Van Niel, G., D'Angelo, G., & Raposo, G. (2018). Shedding light on the cell biology of extracellular vesicles. *Nature Reviews Molecular Cell Biology*, *19*(4), 213–228. https://doi.org/10.1038/nrm.2017.125

Van Niel, G., Porto-Carreiro, I., Simoes, S., & Raposo, G. (2006). Exosomes: A common pathway for a specialized function. *Journal of Biochemistry*, *140*(1), 13–21. https://doi.org/10.1093/jb/mvj128

Van Rahden, V. A., Brand, K., Najm, J., Heeren, J., Pfeffer, S. R., Braulke, T., & Kutsche, K. (2012). The 5-phosphatase OCRL mediates retrograde transport of the mannose 6-phosphate receptor by regulating a Rac1-cofilin signalling module. *Human Molecular Genetics*, *21*(23), 5019–5038. https://doi.org/10.1093/hmg/dds343

Vana, L., Kanaan, N. M., Ugwu, I. C., Wuu, J., Mufson, E. J., & Binder, L. I. (2011). Progression of tau pathology in cholinergic basal forebrain neurons in mild cognitive impairment and Alzheimer's disease. *American Journal of Pathology*, *179*(5), 2533–2550. https://doi.org/10.1016/j.ajpath.2011.07.044

Vaz-Silva, J., Gomes, P., Jin, Q., Zhu, M., Zhuravleva, V., Quintremil, S., … Waites, C. L. (2018). Endo-lysosomal sorting and degradation of Tau and its role in glucocorticoid-driven hippocampal malfunction. *Embo*, 1–16. https://doi.org/10.15252/embj.201899084

Veldhuis, H. D., Van Koppen, C., Van Ittersum, M., & De Kloet, E. R. (1982). Specificity of the adrenal steroid receptor system in rat hippocampus. *Endocrinology*, *110*(6), 2044–2051. https://doi.org/10.1210/endo-110-6-2044

Venturini, A., Passalacqua, M., Pelassa, S., Pastorino, F., Tedesco, M., Cortese, K., … Cervetto, C. (2019). Exosomes from astrocyte processes: Signaling to neurons. *Frontiers in Pharmacology*, *10*(December), 1–11. https://doi.org/10.3389/fphar.2019.01452

Verweij, Frederik J., Revenu, C., Arras, G., Dingli, F., Loew, D., Pegtel, D. M., … van Niel, G. (2019). Live Tracking of Inter-organ Communication by Endogenous Exosomes In Vivo. *Developmental Cell*, *48*(4), 573-589.e4. https://doi.org/10.1016/j.devcel.2019.01.004

Verweij, Frederik Johannes, Bebelman, M. P., Jimenez, C. R., Garcia-Vallejo, J. J., Janssen, H., Neefjes, J., … Pegtel, D. M. (2018). Quantifying exosome secretion from single cells

reveals a modulatory role for GPCR signaling. *Journal of Cell Biology*, *217*(3), 1129–1142. https://doi.org/10.1083/jcb.201703206

Vicinanza, M., Di Campli, A., Polishchuk, E., Santoro, M., Di Tullio, G., Godi, A., … De Matteis, M. A. (2011). OCRL controls trafficking through early endosomes via PtdIns4,5P 2-dependent regulation of endosomal actin. *EMBO Journal*, *30*(24), 4970–4985. https://doi.org/10.1038/emboj.2011.354

Vidal, M., Sainte-Marie, J., Philippot, J. R., & Bienvenue, A. (1989). Asymmetric distribution of phospholipids in the membrane of vesicles released during in vitro maturation of guinea pig reticulocytes: Evidence precluding a role for "aminophospholipid translocase." *Journal of Cellular Physiology*, *140*(3), 455–462. https://doi.org/10.1002/jcp.1041400308

Vieira, S. I., Rebelo, S., Esselmann, H., Wiltfang, J., Lah, J., Lane, R., … Da Cruz E Silva, O. A. B. (2010). Retrieval of the Alzheimer's amyloid precursor protein from the endosome to the TGN is S655 phosphorylation state-dependent and retromer-mediated. *Molecular Neurodegeneration*, *5*(1), 1–21. https://doi.org/10.1186/1750-1326-5-40

Vijayan, M., & Reddy, P. H. (2016). Stroke, Vascular Dementia, and Alzheimer's Disease: Molecular Links. *Journal of Alzheimer's Disease*, *54*(2), 427–443. https://doi.org/10.3233/JAD-160527

Vogels, T., Murgoci, A. N., & Hromadka, T. (2019). Intersection of pathological tau and microglia at the synapse. *Acta Neuropathologica Communications*, *7*(1), 109. https://doi.org/10.1186/s40478-019-0754-y

Vossel, K. A., Zhang, K., Brodbeck, J., Daub, A. C., Sharma, P., Finkbeiner, S., … Mucke, L. (2010). Tau reduction prevents Aβ-induced defects in axonal transport. *Science*, *330*(6001), 8–10. https://doi.org/10.1126/science.1194653

Vulpis, E., Soriani, A., Cerboni, C., Santoni, A., & Zingoni, A. (2019). Cancer exosomes as conveyors of stress-induced molecules: New players in the modulation of NK cell response. *International Journal of Molecular Sciences*, *20*(3). https://doi.org/10.3390/ijms20030611

Vyas, S., Rodrigues, A. J., Silva, J. M., Tronche, F., Almeida, O. F. X., Sousa, N., & Sotiropoulos, I. (2016). Chronic stress and glucocorticoids: From neuronal plasticity to neurodegeneration. *Neural Plasticity*, *2016*. https://doi.org/10.1155/2016/6391686

Waldenstrom, A., Genneback, N., Hellman, U., & Ronquist, G. (2012). Cardiomyocyte microvesicles contain DNA/RNA and convey biological messages to target cells. *PLoS ONE*, *7*(4), 1–7. https://doi.org/10.1371/journal.pone.0034653

Wang, C. L., Tang, F. L., Peng, Y., Shen, C. Y., Mei, L., & Xiong, W. C. (2012). VPS35 regulates developing mouse hippocampal neuronal morphogenesis by promoting retrograde trafficking of BACE1. *Biology Open*, *1*(12), 1248–1257. https://doi.org/10.1242/bio.20122451

Wang, Y., Balaji, V., Kaniyappan, S., Krüger, L., Irsen, S., Tepper, K., … Mandelkow, E. M.

(2017). The release and trans-synaptic transmission of Tau via exosomes. *Molecular Neurodegeneration*, *12*(1), 1–25. https://doi.org/10.1186/s13024-016-0143-y

Willen, K., Edgar, J. R., Hasegawa, T., Tanaka, N., Futter, C. E., & Gouras, G. K. (2017). Aβ accumulation causes MVB enlargement and is modelled by dominant negative VPS4A. *Molecular Neurodegeneration*, *12*(1), 1–18. https://doi.org/10.1186/s13024-017-0203-y

Willms, E., Johansson, H. J., Mager, I., Lee, Y., Blomberg, K. E. M., Sadik, M., … Vader, P. (2016). Cells release subpopulations of exosomes with distinct molecular and biological properties. *Scientific Reports*, *6*(March), 1–12. https://doi.org/10.1038/srep22519

Winston, C. N., Goetzl, E. J., Akers, J. C., Carter, B. S., Rockenstein, E. M., Galasko, D., … Rissman, R. A. (2016). Prediction of conversion from mild cognitive impairment to dementia with neuronally derived blood exosome protein profile. *Alzheimer's and Dementia: Diagnosis, Assessment and Disease Monitoring*, *3*, 63–72. https://doi.org/10.1016/j.dadm.2016.04.001

Winston, C. N., Romero, H. K., Ellisman, M., Nauss, S., Julovich, D. A., Conger, T., … Rissman, R. A. (2019). Assessing Neuronal and Astrocyte Derived Exosomes From Individuals With Mild Traumatic Brain Injury for Markers of Neurodegeneration and Cytotoxic Activity. *Frontiers in Neuroscience*, *13*(October), 1–14. https://doi.org/10.3389/fnins.2019.01005

Wong, C. O. (2020). Endosomal-Lysosomal Processing of Neurodegeneration-Associated Proteins in Astrocytes. *International Journal of Molecular Sciences*, *21*(14), 1–17. https://doi.org/10.3390/ijms21145149

www.who.int. (2020). Dementia. Retrieved May 24, 2021, from https://www.who.int/news-room/fact-sheets/detail/dementia

Xiao, T., Zhang, W., Jiao, B., Pan, C. Z., Liu, X., & Shen, L. (2017). The role of exosomes in the pathogenesis of Alzheimer's disease. *Translational Neurodegeneration*, *6*(1), 1–6. https://doi.org/10.1186/s40035-017-0072-x

Xie, F., Xiao, P., Chen, D., Xu, L., & Zhang, B. (2012). miRDeepFinder: A miRNA analysis tool for deep sequencing of plant small RNAs. *Plant Molecular Biology*, *80*(1), 75–84. https://doi.org/10.1007/s11103-012-9885-2

Xu, W., Tan, L., & Yu, J. T. (2015). The Role of PICALM in Alzheimer's Disease. *Molecular Neurobiology*, *52*(1), 399–413. https://doi.org/10.1007/s12035-014-8878-3

Xu, W., Weissmiller, A. M., White, J. A., Fang, F., Wang, X., Wu, Y., … Wu, C. (2016). Amyloid precursor protein-mediated endocytic pathway disruption induces axonal dysfunction and neurodegeneration. *Journal of Clinical Investigation*, *126*(5), 1815–1833. https://doi.org/10.1172/JCI82409

Yan, T., Wang, L., Gao, J., Siedlak, S. L., Huntley, M. L., Termsarasab, P., … Wang, X. (2018). Rab10 Phosphorylation is a Prominent Pathological Feature in Alzheimer's Disease.

Journal of Alzheimer's Disease, *63*(1), 157–165. https://doi.org/10.1126/science.1249098.Sleep

Yan, T., Wang, L. L., Gao, J., Siedlak, S. L., Huntley, M. L., Perry, G., … Ichikawa, T. (2013). Amyloid precursor protein trafficking, processing, and function. *Journal of Biological Chemistry*, *6*(1), 1–23. https://doi.org/10.1074/jbc.R800019200

Yanez-Mo, M., Siljander, P. R. M., Andreu, Z., Zavec, A. B., Borras, F. E., Buzas, E. I., … De Wever, O. (2015). Biological properties of extracellular vesicles and their physiological functions. *Journal of Extracellular Vesicles*, *4*(2015), 1–60. https://doi.org/10.3402/jev.v4.27066

Yang, L., Peng, X., Li, Y., Zhang, X., Ma, Y., Wu, C., … Liu, J. (2019). Long non-coding RNA HOTAIR promotes exosome secretion by regulating RAB35 and SNAP23 in hepatocellular carcinoma. *Molecular Cancer*, *18*(1), 1–12. https://doi.org/10.1186/s12943-019-0990-6

Yerbury, J. J., Poon, S., Meehan, S., Thompson, B., Kumita, J. R., Dobson, C. M., & Wilson, M. R. (2007). The extracellular chaperone clusterin influences amyloid formation and toxicity by interacting with prefibrillar structures. *The FASEB Journal*, *21*(10), 2312–2322. https://doi.org/10.1096/fj.06-7986com

Yiannopoulou, K. G., & Papageorgiou, S. G. (2020). Current and Future Treatments in Alzheimer Disease: An Update. *Journal of Central Nervous System Disease*, *12*, 117957352090739. https://doi.org/10.1177/1179573520907397

Yin, R. H., Yu, J. T., & Tan, L. (2015). The Role of SORL1 in Alzheimer's Disease. *Molecular Neurobiology*, *51*(3), 909–918. https://doi.org/10.1007/s12035-014-8742-5

You, Y., & Ikezu, T. (2019). Emerging roles of extracellular vesicles in neurodegenerative disorders. *Neurobiology of Disease*, *130*(May), 104512. https://doi.org/10.1016/j.nbd.2019.104512

Yuen, E. Y., Liu, W., Karatsoreos, I. N., Ren, Y., Feng, J., McEwen, B. S., & Yan, Z. (2011). Mechanisms for acute stress-induced enhancement of glutamatergic transmission and working memory. *Molecular Psychiatry*, *16*(2), 156–170. https://doi.org/10.1038/mp.2010.50

Zhang, H., Wu, L., Pchitskaya, E., Zakharova, O., Saito, T., Saido, T., & Bezprozvanny, I. (2015). Neuronal store-operated calcium entry and mushroom spine loss in amyloid precursor protein knock-in mouse model of Alzheimer's disease. *Journal of Neuroscience*, *35*(39), 13275–13286. https://doi.org/10.1523/JNEUROSCI.1034-15.2015

Zhang, Q. Y., Tan, M. S., Yu, J. T., & Tan, L. (2016). The Role of Retromer in Alzheimer's Disease. *Molecular Neurobiology*, *53*(6), 4201–4209. https://doi.org/10.1007/s12035-015-9366-0

Zhang, X., Huang, T. Y., Yancey, J., Luo, H., & Zhang, Y. W. (2018). Role of Rab GTPases in Alzheimer's Disease. *ACS Chemical Neuroscience*.

https://doi.org/10.1021/acschemneuro.8b00387

Zhao, J., Liu, X., Xia, W., Zhang, Y., & Wang, C. (2020). Targeting Amyloidogenic Processing of APP in Alzheimer's Disease. *Frontiers in Molecular Neuroscience*, *13*(August). https://doi.org/10.3389/fnmol.2020.00137

Zhao, Y., Tan, W., Sheng, W., & Li, X. (2016). Identification of Biomarkers Associated with Alzheimer's Disease by Bioinformatics Analysis. *American Journal of Alzheimer's Disease and Other Dementias*, *31*(2), 163–168. https://doi.org/10.1177/1533317515588181

Zhou, L., McInnes, J., Wierda, K., Holt, M., Herrmann, A. G., Jackson, R. J., … Verstreken, P. (2017). Tau association with synaptic vesicles causes presynaptic dysfunction. *Nature Communications*, *8*(May), 1–13. https://doi.org/10.1038/ncomms15295

Zou, Lin, Zou, L., Wang, Z., Shen, L., Bao, G. Bin, Wang, T., … Pei, G. (2007). Receptor tyrosine kinases positively regulate BACE activity and Amyloid-β production through enhancing BACE internalization. *Cell Research*, 389–401. https://doi.org/10.1038/cr.2007.5

Zou, Liyun, Zhou, J., Zhang, J., Li, J., Liu, N., Chai, L., … Wu, Y. (2009). The GTPase Rab3b/3c-positive recycling vesicles are involved in cross-presentation in dendritic cells. *Proceedings of the National Academy of Sciences of the United States of America*, *106*(37), 15801–15806. https://doi.org/10.1073/pnas.0905684106

Zuk, P. A., & Elferink, L. A. (2000). Rab15 differentially regulates early endocytic trafficking. *Journal of Biological Chemistry*, *275*(35), 26754–26764. https://doi.org/10.1074/jbc.M000344200